Involvement of the host RNA N^6-adenosine methylation (m^6A) pathway in the infection cycle of *Alfalfa mosaic virus*

Mireya Martínez Pérez

September 2020

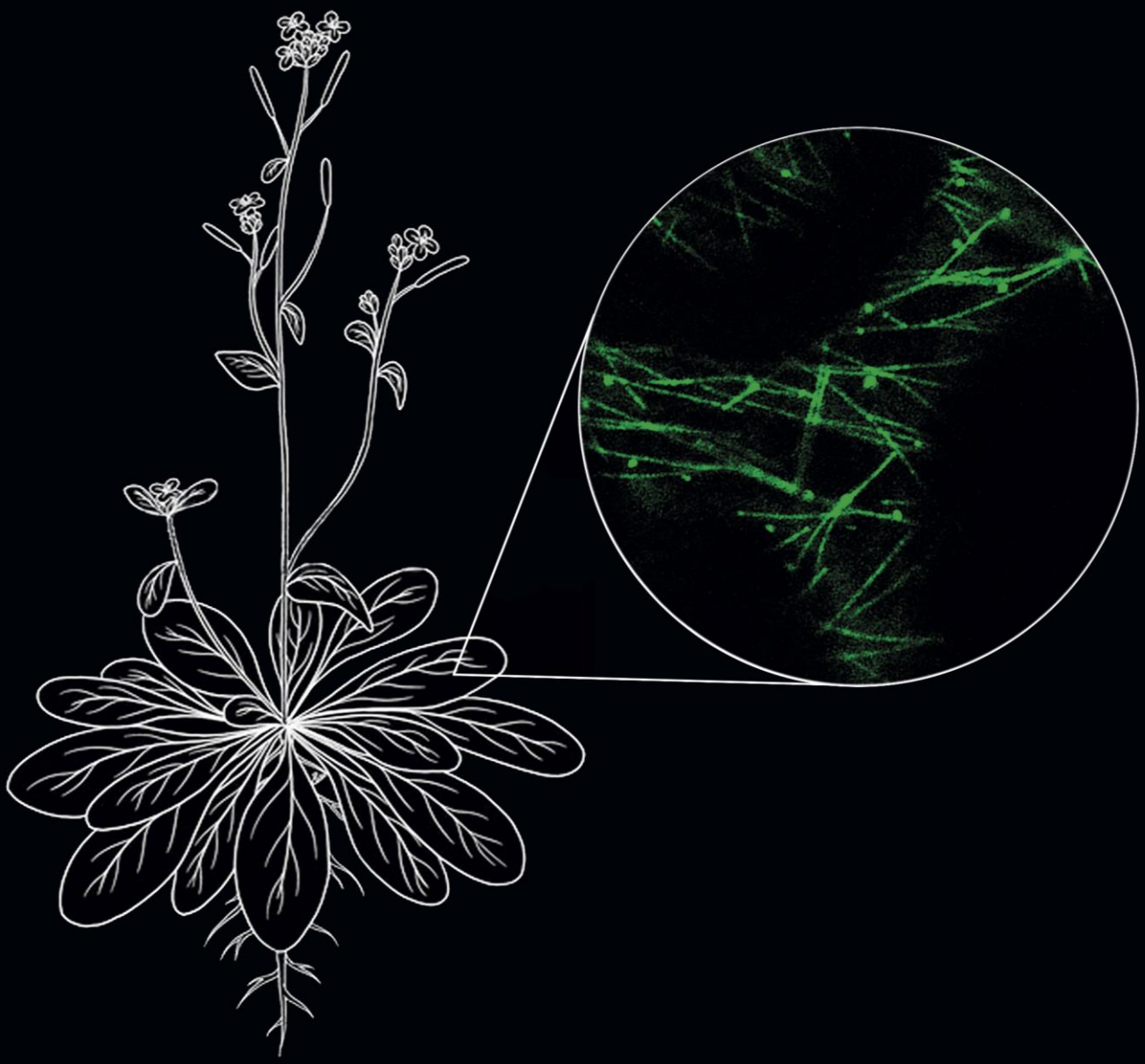

UNIVERSITAT POLITÈCNICA DE VALÈNCIA

Directors:

Prof. Vicente Pallás Benet

Dr. Frederic Aparicio Herrero

Dr. Jesús Ángel Sánchez Navarro

UNIVERSITAT POLITÈCNICA DE VALÈNCIA

CSIC

CONSEJO SUPERIOR DE INVESTIGACIONES CIENTÍFICAS
DELEGACIÓN DE GALICIA

Involvement of the host RNA N^6-adenosine methylation (m^6A) pathway in the infection cycle of *Alfalfa mosaic virus*

Mireya Martínez Pérez

September 2020

Directors:

Prof. Vicente Pallás Benet

Dr. Frederic Aparicio Herrero

Dr. Jesús Ángel Sánchez Navarro

UNIVERSITAT POLITÈCNICA DE VALÈNCIA

Don Vicente Pallás Benet, Doctor en Ciencias Biológicas, Profesor de Investigación del Consejo Superior de Investigaciones Científicas del Instituto de Biología Molecular y Celular de Plantas (Universidad Politécnica de Valencia-Consejo Superior de Investigaciones Científicas) de Valencia.

Don Frederic Aparicio Herrero, Doctor en Biología, Profesor Contratado Doctor (Universidad Politécnica de Valencia) de Valencia.

Don Jesús Ángel Sánchez Navarro, Doctor en Biología, Científico Titular del Consejo Superior de Investigaciones Científicas del Instituto de Biología Molecular y Celular de Plantas (Universidad Politécnica de Valencia-Consejo Superior de Investigaciones Científicas) de Valencia.

CERTIFICAN:

Que Doña Mireya Martínez Pérez, Licenciada en Biotecnología por la Universidad Politécnica de Valencia, ha realizado bajo su dirección el trabajo que con título "Involvement of the host RNA N^6-adenosine methylation (m^6A) pathway in the infection cycle of *Alfalfa mosaic virus*" presenta para optar al grado de Doctor en Biotecnología por la Universidad Politécnica de Valencia.

Y para que así conste a los efectos oportunos, firman el presente certificado en Valencia a ____ de _____ de 2020.

Vicente Pallás Benet **Frederic Aparicio Herrero** **Jesús Ángel Sánchez Navarro**

Table of contents

Summary

Alfalfa mosaic virus (AMV) affects the global production of alfalfa and other important economical crops, e.g. potato (*Solanum tuberosum),* tomato (*Solanum lycopersicum*) or soybean (*Glycine max*). This virus is the only member of *Alfamovirus* genus, belonging to the *Bromoviridae* family, and its genome consists of three positive-sense single-stranded RNA molecules. AMV RNAs are capped (m^7GG) at the 5'UTR and present a homologous sequence at the 3'UTR that adopts two mutually exclusive conformations, which were proposed to act as a molecular switch from translation to replication. The two subunits of the viral replicase, P1 and P2, are encoded from the RNA 1 and RNA 2, respectively. RNA 3 encodes the movement protein (MP) and the capsid protein (CP), although the latest is translated from a subgenomic RNA (sgRNA 4). Many studies show that viral CPs are multifunctional proteins implied in diverse steps of the infection cycle and, additionally, AMV and ilarvirus CPs acquire a special relevance, since the presence of CP or sgRNA 4 molecules are required to onset the infection. Therefore, the identification of host CP-interactors is a prevalent strategy to shed light on the molecular mechanisms governing viral infections. Post-transcriptional chemical modifications can affect intramolecular interactions or the RNA recognition by different RNA-binding proteins and, thus, entail a new level of gene expression modulation. N^6-methylation of adenosine (m^6A) is the most abundant internal modification of mRNA across eukaryotes. Proteins known as m^6A *writers* and *erasers* define the methylation state of an mRNA, whereas m^6A *readers* recognize this modified nucleotide and drive the fate of methylated mRNAs. In mammals, *erasers* belong to the AlkB (2-oxoglutarate- and Fe(II)-dependent oxygenase) protein family, which in *Escherichia coli* protects nucleic acids against methylation damage, whereas m^6A *readers* comprise RNA-binding proteins with a so-called YT521-B homology (YTH) domain.

At the beginning of this Thesis, some components of the methylation complex had been characterized in plants, whereas 13 homologs of AlkB (atALKBH1-10B) and 13 proteins of the YTH family (EVOLUTIONARILY CONSERVED C-TERMINAL REGION proteins 1-11, ECT1-11, At4g11970 and Cleavage and Polyadenylation Specificity Factor 30 (CPSF30)) had been identified in the Arabidopsis genome. However, unlike mammals and yeast, no functional roles had been described for any of these proteins. Besides, since the early 70s, several reports have brought to light the presence of m^6A residues in viral RNAs from mammalian viruses with RNA and DNA genomes, and the critical roles that this modification and the m^6A host machinery play regulating viral infections. However, no m^6A-containing plant virus had been reported so far and the

potential relevance of this molecular mechanism on plant viral infections remained fully unexplored.

The discovery of the interaction between the AMV CP and an Arabidopsis protein with similarity to a human RNA demethylase belonging to AlkB family was the starting point of this Thesis. Thereby, a yeast two-hybrid screening of an Arabidopsis leaf-specific cDNA library using the CP as bait revealed the interaction between this protein and the Arabidopsis ALKBH9B protein (atALKBH9B; At2g17970). Here, a Bimolecular Fluorescence Complementation (BiFC) analysis and an *in vitro* coimmunoprecipitation confirm this interaction, and a north-western blot assay demonstrates that atALKBH9B can also recognize the viral RNAs. Furthermore, the obtained results prove that atALKBH9B has the capability of demethylating m^6A from single-stranded RNA molecules *in vitro*. This protein was observed to accumulate in cytoplasmic granules that colocalize with siRNA-bodies and associate to P-bodies, suggesting that atALKBH9B activity could be related to mRNA silencing and/or decay processes. On the other hand, preliminary assays consisting of anti-m^6A inmunoprecipitation and viral detection show that viral RNAs of AMV, *Cucumber mosaic virus* (CMV), *Turnip crinkle virus* (TCV) and *Cauliflower mosaic virus* (CaMV), but not *Tobacco rattle virus* (TRV), become m^6A methylated during infection in Arabidopsis. Besides, for AMV and CMV, the results were corroborated by UPLC-PDA-Tof-MS analysis and m^6A sites along the three RNAs of AMV were identified through MeRIP-seq approach. According to the *in vitro* demethylation capability of atALKBH9B, the results presented here confirm that m^6A/A ratio along viral RNAs is increased in *atalkbh9b* plants compared to wild type, whereas translation and/or replication are impaired and systemic movement to the floral stems is practically blocked. In contrast to AMV, CMV CP does not interact with atALKBH9B by Y2H and, as it occurs with the rest of the assayed viruses (CMV, TCV and CaMV), its infection cycle is not affected in *atalkbh9b* plants compared to wild type. Thus, while m^6A methylation of viral RNAs during infection process may be a widespread mechanism among DNA and RNA plants infections, atALKBH9B-dependent viral modulation seems to be specific for AMV. During the course of this Thesis, atALKBH10B was reported to remove m^6A from mRNAs, both *in vitro* and *in vivo,* and to be required for proper flowering and vegetative growth.

On the other hand, several studies reported that viral infections in mammals are regulated in some cases in a *reader*-dependent manner. Furthermore, ECT2, ECT3 and ECT4 were recently characterized as cytoplasmic m^6A readers playing a key role in controlling plant development. In line with these discoveries, the mRNA-seq analysis performed in this Thesis reveals that some Arabidopsis factors belonging to the m^6A machinery, MTA, MTB, VIR and ECT5 genes, are

upregulated upon AMV infection. Consistent with the m^{6}A-dependent antiviral effect for AMV, mutations of ECT2/ECT3/ECT5 Arabidopsis module significantly increase AMV and CMV systemic titers. Furthermore, the antiviral effect of ECT2 on AMV seems to be modulated via its direct binding to the m^{6}A residues presented in the viral RNAs, since an ECT2 mutant defective in m^{6}A recognition loses wild type antiviral activity and is not able to pull down viral RNAs *in vivo*. On the other hand, according to the previous subcellular localization described for ECT2 and ECT4 and the ability of ECT2 to undergo gel-like phase *in vitro*, the transitory expression of ECT5 in *Nicotiana benthamiana* displays a cytoplasmic pattern with the formation of some granules and aggregates. Thus, it is proposed that, as found for mammal YTH proteins, the interaction between ECTs and poly-methylated RNA (in this case viral RNA) would promote the formation of stress granules and, consequently, reduce viral translation and replication rates. Furthermore, the observation that ECT2 and ECT5 associate with atALKBH9B might be an evidence of a potential auto-regulatory mechanism through a crosstalk between *readers* and *erasers*, although further analyses are needed to undoubtedly confirm these interactions and to disclose their biological meaning.

In summary, in this work, atALKBH9B is reported as the first m^{6}A *eraser* identified in plants and, for the first time, it is described the influence of m^{6}A methylation mechanism in plant viral infections. In this way, the present Thesis provides new observations about the vast repertoire of molecular pathways that plants exploit to control viral infections.

Resumen

El virus del mosaico de la alfalfa (AMV) afecta a la producción global de alfalfa y a otros cultivos económicamente importantes, como patata (*Solanum tuberosum*), tomate (*Solanum lycopersicum*) o soja (*Glycine max*). Este virus es el único miembro del género *Alfamovirus*, perteneciente a la familia *Bromoviridae*, y su genoma consta de tres moléculas de RNA monocatenario de polaridad positiva. Los RNAs de AMV presentan una estructura de tipo cap (m7GG) en el 5'UTR y una secuencia homóloga en el 3'UTR que adopta dos conformaciones mutuamente excluyentes. Se ha propuesto que este cambio conformacional podría actuar como un interruptor molecular entre traducción y replicación. Las dos subunidades de la replicasa viral, P1 y P2, se codifican a partir del RNA 1 y el RNA 2, respectivamente. El RNA 3 codifica la proteína de movimiento (MP) y la proteína de la cápside (CP), aunque esta última se traduce a partir de un RNA subgenómico (sgRNA 4). Muchos estudios han demostrado que las CPs son

proteínas multifuncionales implicadas en diversas etapas del ciclo viral y, además, en el caso del AMV y los ilarvirus, estas adquieren una relevancia especial, ya que, para iniciar la infección, se requiere la presencia de moléculas de CP o sgRNA 4. Por lo tanto, la identificación de proteínas del huésped que interaccionan con la CP es una estrategia frecuente para desentrañar los mecanismos moleculares que rigen las infecciones virales. Las modificaciones químicas post-transcripcionales pueden afectar a las interacciones intramoleculares del RNA o a su reconocimiento por parte de diferentes proteínas de unión a RNA y, por lo tanto, implican un nuevo nivel de modulación de la expresión génica. La metilación del nitrógeno en posición 6 de la adenosina (m^6A) es la modificación interna más abundante de mRNAs en eucariotas. Las proteínas conocidas como m^6A *writers* y *erasers* definen el estado de metilación de un mRNA, mientras que las m^6A *readers* reconocen este nucleótido modificado y controlan el destino de los mRNAs metilados. En mamíferos, las *erasers* pertenecen a la familia de proteínas AlkB (2-oxoglutarato y Fe (II) dependiente de la oxigenasa), que en *Escherichia coli* protege los ácidos nucleicos contra el daño por metilación, mientras que las *readers* son proteínas de unión al RNA que contienen un dominio llamado YT521-B homolog (YTH).

Al comienzo de esta Tesis, se habían caracterizado algunos componentes del complejo de metilación en plantas. Sin embargo, a diferencia de mamíferos y levadura, ninguno de los 13 homólogos de AlkB (atALKBH1-10B) y las 13 proteínas de la familia YTH (proteínas EVOLUTIONARILY CONSERVED C-TERMINAL REGION 1-11, ECT1- 11, AT4G11970 y CPSF30) identificadas en el genoma de Arabidopsis se habían caracterizado funcionalmente. Además, desde principios de los años 70, varios estudios han descrito la presencia de residuos m^6A en RNAs de virus de mamíferos con genomas de RNA y DNA, así como las diferentes funciones que desempeña esta modificación y la maquinaria m^6A del huésped en la regulación de las infecciones virales. Sin embargo, hasta la fecha, no se conoce ningún virus en plantas que contenga nucleótidos m^6A, ni se ha estudiado la posible implicación de este mecanismo molecular en las infecciones virales de plantas.

El descubrimiento de la interacción entre la CP de AMV y una proteína de Arabidopsis con homología a una RNA desmetilasa humana perteneciente a la familia AlkB fue el punto de partida de esta Tesis. De este modo, un ensayo de doble híbrido en levadura de una librería de cDNA específica de hoja de Arabidopsis usando la CP como cebo reveló la interacción entre esta proteína y la proteína ALKBH9B de Arabidopsis (atALKBH9B; At2g17970). En este trabajo se muestra un análisis de Complementación de Fluorescencia Bimolecular (BiFC) y una coinmunoprecipitación *in vitro* que confirman esta interacción, y, mediante un ensayo north-

western, se demuestra que atALKBH9B también puede reconocer los RNAs virales. Además, los resultados obtenidos demuestran que atALKBH9B tiene la capacidad de desmetilar m^6A a partir de moléculas de RNA monocatenario *in vitro*. Se observó que esta proteína se acumula en gránulos citoplasmáticos que se colocalizan con siRNA *bodies* y se asocian a P-*bodies*, lo que sugiere que la actividad de atALKBH9B podría estar relacionada con los procesos de silenciamiento y/o degradación de mRNA. Por otro lado, ensayos preliminares, que consisten en la inmunoprecipitación anti-m^6A y detección viral, muestran que los RNAs virales del AMV, el virus del mosaico del pepino (CMV), el virus de la arruga del nabo (TCV) y el virus del mosaico de la coliflor (CaMV), pero no el virus del cascabel del tabaco (TRV), se metilan durante la infección en Arabidopsis. Además, para AMV y CMV, los resultados fueron corroborados por análisis UPLC-PDA-Tof-MS y los sitios m^6A a lo largo de los tres RNAs del AMV fueron identificados mediante MeRIP-seq. De acuerdo con la capacidad de desmetilación *in vitro* de atALKBH9B, los resultados presentados aquí confirman que la relación m^6A/A a lo largo de los RNAs virales aumenta en las plantas *atalkbh9b* en comparación con las silvestres, mientras que la traducción y/o la replicación se ven afectadas y el movimiento sistémico a los tallos florales está prácticamente bloqueado. A diferencia de la CP de AMV, la de CMV no interacciona con atALKBH9B por Y2H y, como ocurre con el resto de los virus analizados (CMV, TCV y CaMV), su ciclo de infección no se ve afectado en plantas *atalkbh9b* en comparación con las silvestres. Por lo tanto, mientras que la metilación m^6A de RNAs virales durante el proceso de infección parece ser un mecanismo generalizado en infecciones de plantas provocadas por virus de DNA y RNA, la modulación viral dependiente de atALKBH9B podría ser específica de AMV. Cabe mencionar que, en el transcurso de esta Tesis, se describió que atALKBH10B elimina la metilación m^6A de los mRNAs, tanto *in vitro* como *in vivo*, y es necesaria para una floración y un crecimiento vegetativo adecuados.

Por otro lado, se ha descrito que, en algunos casos, las infecciones virales en mamíferos están reguladas de manera dependiente de m^6A *readers*. Además, recientemente ECT2, ECT3 y ECT4 han sido caracterizadas como *readers* citoplasmáticas que tienen un papel clave en el control del desarrollo de la planta. En consonancia con estos descubrimientos, el análisis de secuenciación de mRNA realizado en este trabajo revela que la infección por AMV induce algunos genes de Arabidopsis pertenecientes a la maquinaria m^6A, MTA, MTB, VIR y ECT5. De acuerdo con el efecto antiviral dependiente de m^6A para el AMV, la supressión del módulo ECT2/ECT3/ECT5 aumenta significativamente los títulos sistémicos de AMV y CMV. Además, el efecto antiviral de ECT2 sobre AMV parece estar modulado a través de su unión directa a los

residuos de m^{6}A presentes en los RNAs virales, ya que un mutante de la proteína ECT2 defectuoso en el reconocimiento de m^{6}A pierde la actividad antiviral que sí presenta la proteína original y no es capaz de arrastrar RNAs virales *in vivo*. Por otro lado, acorde a la localización subcelular previamente descrita para ECT2 y ECT4 y la capacidad de ECT2 para experimentar una fase similar al gel *in vitro*, la expresión transitoria de ECT5 en *Nicotiana benthamiana* muestra un patrón citoplasmático con la formación de algunos gránulos y agregados. Por lo tanto, se propone que, como se ha descrito para las proteínas YTH de mamíferos, la interacción entre las ECTs y el RNA polimetilado (en este caso, RNA viral) promovería la formación de gránulos de estrés y, en consecuencia, reduciría las tasas de traducción y replicación viral. Además, la observación de que ECT2 y ECT5 se asocian con atALKBH9B podría ser una evidencia de un posible mecanismo de autorregulación a través de la asociación entre *readers* y *erasers*, aunque se necesitan análisis adicionales para confirmar estas interacciones y revelar su significado biológico.

En resumen, en este trabajo, se caracteriza la primera m^{6}A *eraser* de plantas, atALKBH9B, y, por primera vez, se describe la influencia del mecanismo de metilación m^{6}A en las infecciones virales de plantas. Por tanto, la presente Tesis proporciona nuevas observaciones que extienden el amplio repertorio de rutas moleculares que las plantas emplean para controlar las infecciones virales.

Resum

El virus del mosaic de l'alfals (AMV) afecta a la producció global d'alfals i a altres cultius econòmicament importants, com ara la creïlla (*Solanum tuberosum*), tomata (*Solanum lycopersicon*) o soia (*Glycine max*). Este virus és l'únic membre del gènere *Alfamovirus*, pertanyent a la família *Bromoviridae*, i el seu genoma consta de tres molècules de RNA monocatenari de polaritat positiva. Els RNAs d'AMV presenten una estructura de tipus CAP (m7GG) en el 5'UTR i una seqüència homòloga en el 3'UTR que adopta dos conformacions mútuament excloents. S'ha proposat que este canvi conformacional podria actuar com un interruptor molecular de la traducció a la replicació. Les dos subunitats de la replicasa viral, P1 i P2, estan codificades a partir del RNA 1 i el RNA 2, respectivament. El RNA 3 codifica la proteïna de moviment (MP) i la proteïna de la càpsida (CP), encara que esta última es traduïx a partir d'un RNA subgenòmic (sgRNA 4). Molts estudis han demostrat que les CPs virals són proteïnes multifuncionals implicades en diversos passos del cicle d'infecció i, a més, les CPs d'AMV i

ilarvirus adquirixen una rellevància especial ja que, per a iniciar la infecció, es requerix la presència de molècules de CP o sgRNA 4. Per tant, la identificació de proteïnes de l'hoste que interaccionen amb la CP és una estratègia freqüent per a aclarir els mecanismes moleculars que regixen les infeccions virals. Les modificacions químiques post-transcripcionals poden afectar les interaccions intramoleculars o el reconeixement dels RNAs per diverses proteïnes i, per tant, impliquen un nou nivell de modulació de l'expressió gènica. La metilació del nitrogen en posició 6 de l'adenosina (m^6A) és la modificació interna més abundant de mRNAs en eucariotes. Les proteïnes conegudes com m^6A *writers* i *erasers* definixen l'estat de metilació d'un mRNA, mentre que les m^6A *readers* reconeixen este nucleòtid modificat i controlen el destí dels mRNAs metilats. En mamífers, les *erasers* pertanyen a la família de proteïnes AlkB (2-oxoglutarat i Fe(II) dependent de l'oxigenasa), que en *Escherichia coli* protegix els àcids nucleics contra els efectes perjudicials produïts per metilació, mentre que les *readers* són proteïnes d'unió al RNA que contenen un domini anomenat YT521-B homolog (YTH).

Al començament d'esta Tesi, s'havien caracteritzat alguns components del complex de metilació en plantes. No obstant això, a diferència de mamífers i llevat, cap dels 13 homòlegs d'AlkB (atALKBH1-10B) i les 13 proteïnes de la família YTH (proteïnes EVOLUTIONARILY CONSERVED C-TERMINAL REGION 1-11, ECT1-11, At4g11970 i CPSF30) identificades en el genoma d'Arabidopsis s'havien caracteritzat funcionalment. Des de principis dels anys 70, diversos estudis han descrit la presència de residus m^6A en RNAs de virus de mamífers amb genomes de RNA i DNA, així com les diferents funcions que exercix esta modificació i la maquinària m^6A de l'hoste en la regulació de les infeccions virals. No obstant això, hui dia no es coneix cap virus de plantes que continga nucleòtids m^6A, ni s'ha estudiat la possible implicació d'este mecanisme molecular en les infeccions virals de plantes.

El descobriment de la interacció entre la CP d'AMV i una proteïna d'Arabidopsis amb homologia a una RNA desmetilasa humana pertanyent a la família AlkB va ser el punt de partida d'esta Tesi. D'esta manera, un assaig de doble híbrid en llevat d'una llibreria de cDNA específica de fulla d'Arabidopsis utilitzant la CP com a esquer va revelar la interacció entre esta proteïna i la proteïna ALKBH9B d'Arabidopsis (atALKBH9B; At2g17970). En este treball es mostra una anàlisi de Complementació de Fluorescència Bimolecular (BiFC) i una coimmunoprecipitació *in vitro* que confirmen esta interacció, i, mitjançant un assaig north-western, es demostra que atALKBH9B també pot reconéixer els RNAs virals. A més, els resultats obtinguts demostren que atALKBH9B té la capacitat de desmetilar molècules de RNA monocatenari *in vitro*. Es va observar que esta proteïna s'acumulava en grànuls citoplasmàtics que es colocalitzen amb siRNA *bodies* i

s'associen a P-*bodies*, la qual cosa suggerix que l'activitat atALKBH9B podria estar relacionada amb els processos de silenciament i/o degradació de mRNAs. D'altra banda, assajos preliminars, que consistixen en la immunoprecipitació anti-m^{6}A i detecció viral, mostren que els RNAs virals de l'AMV, el virus del mosaic del cogombre (CMV), el virus de l'arruga del nap (TCV) i el virus del mosaic de la coliflor (CaMV), però no el virus del cascavell del tabac (TRV), es metilen durant la infecció en Arabidopsis. A més, per a AMV i CMV, els resultats es confirmen per anàlisi UPLC-PDA-Tof-MS i els llocs m^{6}A al llarg dels tres RNAs d'AMV s'identifiquen mitjançant MeRIP-seq. D'acord amb la capacitat de desmetilació *in vitro* d'atALKBH9B, els resultats ací presentats confirmen que la relació m^{6}A/A al llarg dels RNAs virals augmenta en les plantes *atalkbh9b* en comparació amb les silvestres, mentre que la traducció i/o la replicació es veuen afectades i el moviment sistèmic a les tiges florals està pràcticament bloquejat. A diferència de la CP d'AMV, la de CMV no interacciona amb atALKBH9B per Y2H i, com ocorre amb la resta dels virus analitzats (CMV, TCV i CaMV), el seu cicle d'infecció no es veu afectat en plantes *atalkbh9b* en comparació amb les silvestres. Per tant, mentre que la metilació m^{6}A de RNAs virals durant el procés d'infecció pot ser un mecanisme generalitzat en infeccions de plantes provocades per virus de DNA i RNA, la modulació viral dependent de atALKBH9B sembla ser específica per a AMV. Cal mencionar que en el transcurs d'esta Tesi es va descriure que atALKBH10B elimina m^{6}A dels mRNAs, tant *in vitro* com *in vivo*, i és necessària per a una floració i un creixement vegetatiu adequats.

D'altra banda, s'ha trobat que, en alguns casos, les infeccions virals en mamífers estan regulades per m^{6}A *readers*. A més, recentment s'han caracteritzat les proteïnes ECT2, ECT3 i ECT4 com *readers* citoplasmàtics que tenen un paper clau en el control del desenvolupament de la planta. En línia amb estos descobriments, l'anàlisi de seqüenciació de mRNA realitzat en este treball revela que la infecció per AMV induïx alguns gens d'Arabidopsis pertanyents a la maquinària m^{6}A, MTA, MTB, VIR i ECT5. D'acord amb l'efecte antiviral dependent de m^{6}A per a l'AMV, les mutacions del mòdul ECT2/ECT3/ECT5 augmenten significativament els títols sistèmics d'AMV i CMV. A més, l'efecte antiviral d'ECT2 sobre AMV sembla estar modulat a través de la seua unió directa als nucleòtids m^{6}A presents en els RNAs virals, ja que un mutant de la proteïna ECT2 defectuós en el reconeixement de m^{6}A perd l'activitat antiviral que sí que presenta la proteïna original i no és capaç d'arrossegar RNAs virals *in vivo*. D'altra banda, d'acord amb la localització subcel·lular descrita prèviament per a ECT2 i ECT4 i la capacitat d'ECT2 per a experimentar una fase similar al gel *in vitro*, l'expressió transitòria d'ECT5 en *Nicotiana benthamiana* mostra un patró citoplasmàtic amb la formació d'alguns grànuls i agregats. Per tant, es proposa que, com

s'ha descrit per a les proteïnes YTH de mamífers, la interacció entre les ECTs i el RNA polimetilat (en este cas, RNA viral) promouria la formació de gränuls d'estrès i, en conseqüència, reduiria les taxes de traducció i replicació viral. A més, l'observació que ECT2 i ECT5 s'associen amb atALKBH9B podria ser una evidència d'un possible mecanisme d'autoregulació a través de l'associació entre *readers* i *erasers*, encara que es necessiten anàlisis addicionals per a confirmar estes interaccions i revelar el seu significat biològic.

En resum, en este treball es caracteritza la primera m^{6}A *eraser* de plantes, atALKBH9B, i, per primera vegada, es descriu la influència del mecanisme de metilació m^{6}A en les infeccions virals de plantes. D'esta manera, la present Tesi proporciona noves observacions que estenen l'ampli repertori de rutes moleculars que les plantes utilitzen per a controlar les infeccions virals.

Abbreviations

VIRUSES

Plants	Animals	
AMV *Alfalfa mosaic virus*	**AV** *Adenovirus*	**IAV** *Influenza A virus*
BMV *Brome mosaic virus*	**DENV** *Dengue virus*	**KSHV** *Kaposi's sarcoma-associated herpesvirus*
CaMV *Cauliflower mosaic virus*	**EBV** *Epstein-Barr virus*	**MLV** *Murine leukemia virus*
CMV *Cucumber mosaic virus*	**EV71** *Enterovirus type 71*	**PV** *Poliovirus*
PNRSV *Prunus necrotic ringspot virus*	**HBV** *Hepatitis B virus*	**RSV** *Rous sarcoma virus*
TCV *Turnip crinkle virus*	**HCV** *Hepatitis C virus*	**SV40** *Simian virus 40*
TMV *Tobacco mosaic virus*	**HIV-1** *Human Immunodeficiency virus-1*	**VSV** *Vesicular stomatitis virus*
TRV *Tobacco rattle virus*	**HRSV** *Human respiratory syncytial virus*	**ZIKV** *Zika virus*
	HSV-1 *Herpes simplex virus-1*	

OTHERS

A Adenosine

aa Amino acids

AGO ARGONAUTE

AlkB Alkylation B

ALKBH AlKB homolog

AN ANGUSTIFOLIA

BiFC Bimolecular fluorescence complementation

cDNA Complementary DNA

CLSM Confocal laser-scanning microscopy

CP Coat protein

CPB CP binding

CPSF30 Cleavage and Polyadenylation Specificity Factor 30

DCP1 and DCP2 mRNA-decapping enzyme 1 and 2

DDX Nuclear DEAD-box

DNA Deoxyribonucleic acid

Dpi Days post-inoculation

dsDNA Double strand DNA

dsRNA Double strand RNA

EBNA3C EBV nuclear antigen 3C

ECT1-11 EVOLUTIONARILY CONSERVED C-TERMINAL REGION 1-11

eIF3 Eukaryotic initiation factor 3

ETI Effector-triggered immunity

FIP37 FKBP12 interacting protein 37

FTO Fat mass and obesity associated protein

G3BP Ras-GAP SH3 domain binding protein

GFP Green fluorescence protein

gRNA Genomic RNA

HA Hemagglutinin

HC-pro Viral helper component-protease

His Histidine

hnRNPA2B1 Heterogeneous nuclear RNP A2B1

HPLC-MS/MS High-performance liquid chromatography-tandem mass spectrometry

Hr Hour

ICR Internal control region

ICTV International Committee on Taxonomy of Viruses

IDR Intrinsically disordered domain

IFN Interferon

IP Inmunoprecipitation/Inmunoprecipotated

ISG Interferon-stimulated gene

Lsm1-7 Deadenylation complex or decapping activators

m^{6}A *N^6*-methyladenosine

m^{6}A$_m$ 2'-*O,N^6*-dimethyladenosine

MeRIP-seq Methylated RNA immunoprecipitation sequencing

METTL Methyltransferase-like protein

min Minutes

miRNA Micro RNA

MP Movement protein

mRNA Messenger RNA

MVB Multivesicular body

NA Neuraminidase

NMD Nonsense-mediated decay

NP Nucleoprotein

nts Nucleotides

OD Optical density

ORF Open reading frame

P Polymerase

P1 and P2 AMV polymerase subunits

PAMP Pathogen-associated molecular patterns

PAS Polyadenylation signal

P-body or PB Processing body

PD Plasmodesmata

pgRNA Pre-genomic RNA

PQN Pro-Gln-Asn-rich region

PTC Premature termination codon

PTGS Post-transcriptional gene silencing

PTI Pattern-triggered immunity

R Resistance

RdDM RNA-dependent DNA methylation

RDR RNA dependent RNA polymerase

RT Reverse transcription

RNAi RNA interference

RNA pol RNA polymerase

RNA Ribonucleic acid

RNase Ribonuclease

RNP Ribonucleoprotein

RRE Rev Response Element

rRNA Ribosomal RNA

RTA Replication transcription activator

SAM S-adenosyl-L-methionine

SG Stress granule

sgRNA Subgenomic RNA

SGS3 SUPRESSOR OF GENE SILENCING 3

siRNA Small interfering RNA

SMG Serine/threonine-protein kinase

ssDNA Single-stranded DNA

(+)ssRNA or (-)ssRNA Positive or negative-sense single-stranded RNA

TCA Citric acid cycle

TLS tRNA-like structure

tRNA Transference RNA

TSN TUDOR STAPHYLOCOCCAL NUCLEASE PROTEIN

U Uracil

UPLC-PDA-TOF-MS Ultra-performance liquid chromatography-photodiode detector quadrupole/time-of-flight–mass spectrometry

UPF Up-frameshift proteins

UTR Untranslated region

UV Ultraviolet light

VAR VARICOSE

VOZ VASCULAR PLANT ONE-ZINC FINGER

VRC Viral replication complexes/factories

vRNA Viral RNA

vsiRNAs Viral small interfering RNAs

WT Wild type

WTAP WILMS' TUMOR-ASSOCIATED PROTEIN

XRN 5'-3' exoribonuclease

Y2H Yeast two hybrid

YPQ Tyr-Pro-Gln rich region

YTH YT521-B homology

ZF Zinc-finger domains

General introduction

1. Virus concept

In 1882, Robert Koch described the criteria to assume a causative relationship between a microorganism and a disease: (i) all sick organisms must present the microorganism in a detectable level, but not the healthy one; (ii) the isolation and growth in pure culture of the microorganism from an ill organism should be viable; (iii) the introduction of the cultured microorganism into a healthy individual must provoke the disease; and (iv) it has to be possible to re-isolate the microorganism from the diseased experimental host.

These postulates set the basis for the discovery of a new infectious agent, which was named "virus" (from Latin, meaning "venom"). Virology research began in the late 19th century when Martinus Beijerinck and Dmitri Iwanowski independently described an unusual agent that caused a mosaic disease in tobacco (Iwanowski, 1892; Beijerinck, 1898), which was later named *Tobacco mosaic virus* (TMV) (for a review, see Pallás, 2007). Viruses are obligate, biotrophic parasites, which extract nutrients only from living cells and cannot live without their hosts, and are found in all living organisms, including animals, plants, fungi and bacteria (Encyclopædia Britannica, 2011). From a molecular point of view, viral genomes consist of DNA or RNA molecules that can be single or double stranded, linear or circular, segmented or non-segmented, and may have positive or negative sense. The nucleic acids are protected by a coat or capsid protein and, in some occasions, by an additional lipid bilayer, especially in the case of animal-infecting viruses.

The tenth report of the International Committee on Taxonomy of Viruses (ICTV) listed 6590 viral species grouped in 1421 genera. Among them, plant viruses comprise 118 genera and 1516 species (ICTV, 2017). While most of them possess positive-sense single-stranded RNA ((+)ssRNA) genomes, just a few comprise negative-sense single-stranded RNA ((-)ssRNA) genomes. Furthermore, viruses from the economically important family *Geminiviridae* present single-stranded DNA (ssDNA) genomes, whilst only the *Caulimoviridae* family present double-stranded DNA (dsDNA) genomes (Gergerich and Dolja, 2006). With the exception of satellite viruses, plant viral genomes range from 4 to 20 Kb – *Carmoviruses* and *Closteroviruses*, respectively – and encode 5-20 proteins that interact with host factors to accomplish every stage of their life cycle: replication, translation, cell-to-cell transport, systemic movement and plant-to-plant transmission. Moreover, in response to plant defense mechanisms, viruses have also developed counteracting molecular strategies. All these interactions trigger biochemical, metabolic and gene expression changes in the host that appear as physiological and developmental symptoms

and result in the severe loss of yield of high-value agricultural crops (Culver and Padmanabhan, 2007; Pallas and García, 2011).

Nowadays, more than 50% of the emerging plant illnesses are induced by viruses, whose economic impact is estimated in more than $30 billion annually (Jones and Naidu, 2019). Therefore, virus-induced diseases entail a worldwide threat for crop production, food security and crop cultivars diversity that, in addition, is being increased because of two main reasons. First, the variable environmental conditions caused by the climate change make the epidemics harder to manage. Second, the population growth is forcing changes in agricultural techniques (extensification, intensification and diversification) that favor inter-species transmission and, thereby, facilitate new epidemics: endemic viruses that invade new crops or traditional crops infected by new crops-infecting viruses (Jones, 2014, 2016). Understanding virus biology aspects, such as virus-host interaction mechanisms, is critical to fight against their negative impact.

2. Alfalfa mosaic virus (AMV)

Alfalfa mosaic virus (AMV) is the only member of the *Alfamovirus* genus, which belongs to the *Bromoviridae* family. *Anulavirus*, *Bromovirus*, *Cucumovirus*, *Ilarvirus* and *Oleavirus* genera complete this family (ICTV, 2017; Bujarski et al., 2019).

2.1. Origin, geographical distribution and economic impact

AMV was first described as the causative agent of an economically important disease in alfalfa (*Medicago sativa*) in the United States by J.L. Weimer (Weimer, 1931). Nowadays, practically the global production of this forage crop is affected by this pathogen. In Spain, the first identified strain of this virus was isolated from alfalfa plants in Madrid (Díaz-Ruiz and Moreno, 1972). Although several factors, as the plant age, can influence the AMV infection levels in alfalfa crops, in the producer countries – such as Spain, Great Britain, United States, Canada, Australia and New Zeeland –, the average infection levels are around 50% or above (Escriu et al., 2011). According to 2018 data, Spain is the second biggest producer of alfalfa in the world after the United States. Indeed, in the last season, the total production exceeded 13 tones and the 78% of it was destined to international export trade (*Asociación Española de fabricantes de alfalfa deshidratada*, https://www.alfalfaspain.es/). Additionally, AMV has a wide host range, considering that it infects more than 600 species belonging to 70 families (Bol, 2008). Among

the most economically important crops affected by AMV are potato (*Solanum tuberosum),* pepper *(Capsicum annuum),* pea (*Pisum sativum*), tobacco (*Nicotiana tabacum*), tomato (*Solanum lycopersicum*), broad bean (*Vicia faba*), chickpea (*Cicer arietinum*), lentil (*Lens culinaris*), soybean (*Glycine max*) and white clover (*Trifolium repens*) (Escriu et al., 2011).

2.2. Viral transmission and symptomatology

AMV is transmitted in a non-persistent manner by at least 14 aphid species, including species that frequently colonize alfalfa crops: the black legume aphid (*Aphis craccivora*), the pea aphid (*Acyrthosiphon pisum*) and the yellow clover aphid (*Therioaphis trifolii*); and species that typically infect vegetable crops, such as the black bean aphid (*Aphis fabae*) and the green peach aphid (*Myzus persicae*) (Escriu et al., 2011; Moreno and Fereres, 2012). Besides, the virus transmission may also occur by pollen and seeds (Valkonen et al., 1992). In fact, seed transmission is frequent and favors the persistence of AMV in alfalfa, soybean and pepper (He et al., 2010). In perennial crops, like alfalfa, plants of different ages grow at the same time and it collaborates in the continued presence of the virus (Escriu et al., 2011).

The typical AMV symptoms are the appearance of yellow mosaicism in leaves together with, less commonly, wrinkling, dwarfism, malformations and, in the most severe cases, necrosis of the fruits. Besides, the irregular and bright yellow mosaic known as *calico* is a characteristic symptom that was observed in young leaves of pepper and tomato plants (Fig. 1) (Knorr, 1983; Sepúlveda R et al., 2005). In alfalfa, AMV infection negatively affects root nodulation and, consequently, nitrogen fixation capacity, which overall causes a decrease in crop production and nutritional quality of the forage. Likewise, AMV increases the susceptibility of the plant to other pathogen infections and abiotic factors such as frosts (Escriu et al., 2011).

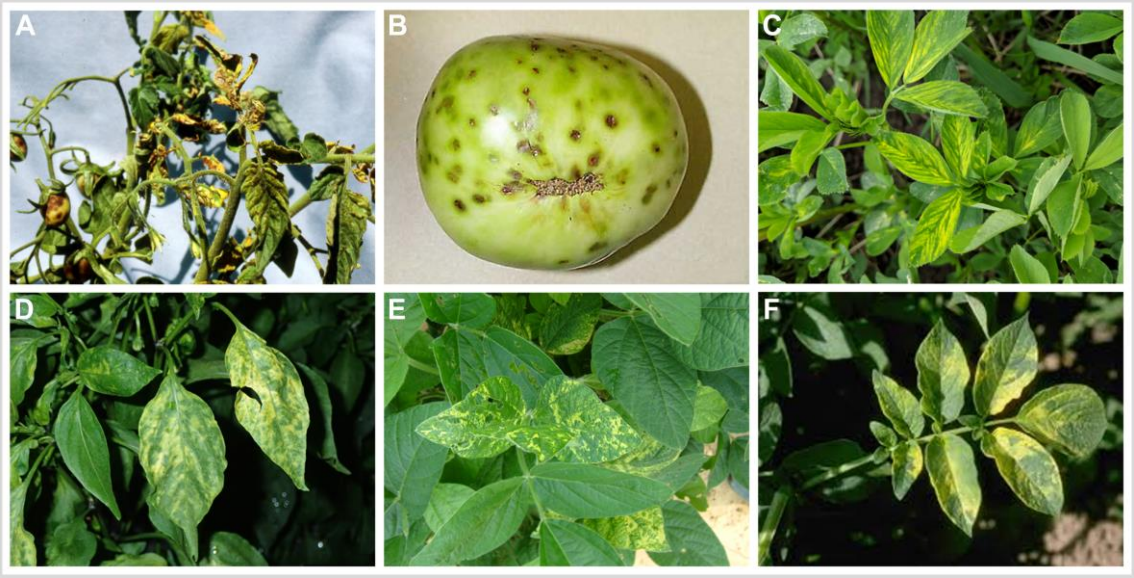

Figure 1. Symptomatology of AMV infection on different crops. (A) *Tomato plant with yellow and wrinkling leaves, and dwarf fruits.* ***(B)*** *Necrosis and dark spots in tomato fruits.* ***(C-F)*** *Yellow mosaicism on leaves of alfalfa* ***(C)****, pepper* ***(D)****, soybean* ***(E)*** *and potato* ***(F)****. Photos from: seminis-las.com (A), T.A. Zitter, Cornell University (B), extension.sdstate.edu (C), Whitney Cranshaw, Colorado State University, Bugwood.org (D), www.nexles.com (E), Howard F. Schwartz, Colorado State University, Bugwood.org (F).*

2.3. Genome organization and life cycle

The *Bromoviridae* family is characterized by a genome organization consisting of three (+)ssRNAs. AMV genomic RNAs (gRNAs) are capped (m^7GG) at the 5' end and lack of poly A tail at the 3' terminus (Fig. 2). RNA 1 (3,65 Kb) and RNA 2 (2,6 Kb) encode the two subunits of the RNA polymerase (P1 and P2). P1 contains a N-terminal methyltransferase-like domain and a C-terminal helicase-like domain, whereas P2 presents a polymerase-like domain (Bol, 2008). P1 and P2 form the replication complex that associates with the tonoplast membrane during the infection (Van Der Heijden et al., 2001; Ibrahim et al., 2012). RNA 3 (2,1 Kb) is bicistronic and encodes the movement protein (MP) and the capsid protein (CP), although the latter is expressed from a subgenomic RNA (sgRNA 4, 0,88 kb) (Fig. 2) (Bol, 2008). AMV RNAs 1, 2 and 3 are separately encapsidated into particles of bacilliform structure with a diameter of 19 nm and a length varying from 30 to 56 nm. Additionally, two copies of RNA 4 are assembled into spheroidal particles (Bol, 2003).

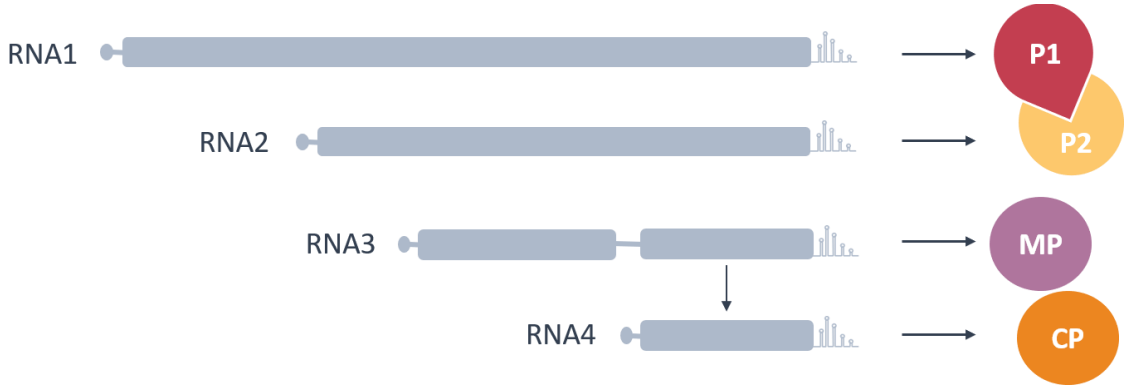

Figure 2. AMV genome organization. *Schematic representation of the four RNAs and the proteins that they encode. The cap structure in the 5'UTR is represented by small gray spheres and the hairpin structure at the 3'UTR is displayed.*

As stated, viral RNAs (vRNAs) lack polyadenylation at the 3' terminus. Instead, the 3' untranslated regions (UTR) of AMV and ilarviruses present homologous sequences that can form two mutually exclusive conformations acting like a molecular switch from translation to replication (Fig. 3A) (Aparicio et al., 2003; Chen and Olsthoorn, 2010). On one hand, 3'UTRs are predicted to fold into linear arrays of several hairpin structures (A to E). A to C are separated by AUGC-motifs constituting two overlapped CP binding (CPB) sites (Fig. 3A, upper linear stem-loop structure). The process known as "genomic activation" is distinctive of the AMV and ilarviruses infection cycles: CP or sgRNA 4 molecules must be present in the inoculum to initiate viral infection (Bol et al., 1971). CP dimers, the building blocks of AMV capsid, must bind to the 3'UTR of vRNAs (Tenllado and Bol, 2000; Choi et al., 2003). The RNA binding sequence of the CP is a basic residues-rich region located at the N-terminal part of the protein in which the arginine at position 17 is critical for this interaction (Ansel-McKinney et al., 1996). On the other hand, base pairing between the sequences UCCU and AGGG of hairpins D and A, respectively, generates a structure resembling the tRNA-like structure (TLS) described for bromo- and cucumoviruses (Fig 3A, lower pseudoknot structure). In fact, ATP(CTP):tRNA nucleotidyl transferase, an enzyme that adds CCA to the 3' end of tRNAs, can add radioactive AMP to the 3' end of AMV RNA *in vitro* (Olsthoorn et al., 1999). This TLS conformer, together with E hairpin (Fig. 3A), was found to serve as promoter for the synthesis of negative polarity vRNAs (Olsthoorn et al., 1999). Thus, according to the conformational switch model, TLS would favor the synthesis of the negative vRNAs, whereas binding of the CP to the 3'UTR would stabilize the linear stem-loop structure, favoring protein translation (Olsthoorn et al., 1999; Chen and Olsthoorn, 2010).

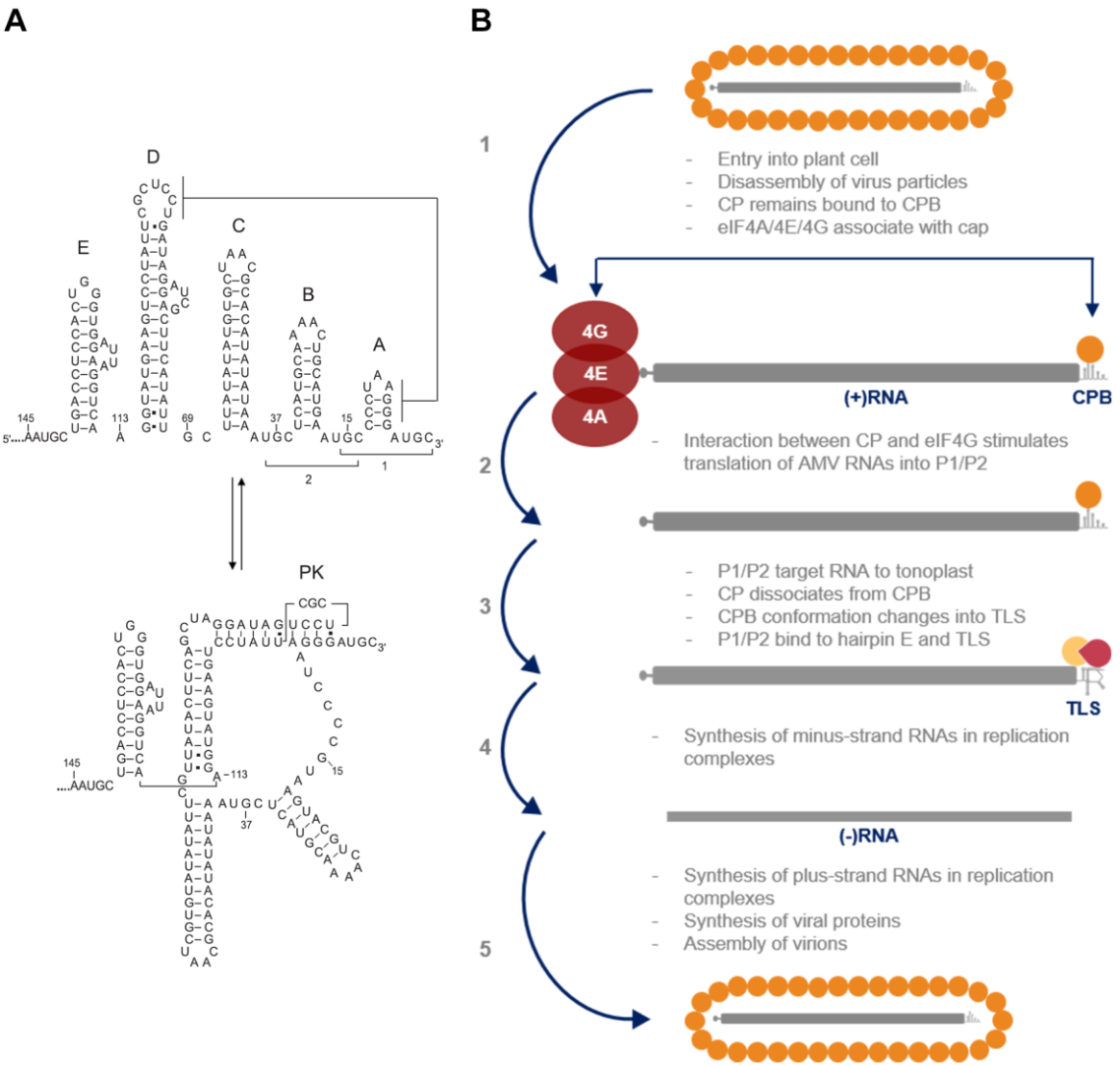

Figure 3. (A) *Molecular switch between CPB (upper panel) and TLS (bottom panel) conformations of the AMV RNA 3 3'UTR. The two conformers formed by the 145 nts of the AMV RNA 3 3'UTR are shown. The two CPB sites are indicated by brackets. Base pairing between loop D and stem A promotes TLS conformation (Chen and Olsthoorn, 2010).* ***(B)*** *Proposed model of the AMV replication cycle. The bacilliform structures represent AMV virions consisting of coat protein (CP, orange spheres) and RNA (gray bars with a reading frame indicated by a gray box). The 3' end 145 nts of AMV RNAs are represented by two different structures indicated as CPB (CP binding site) or TLS (tRNA-like structure). The complex of the replicase proteins P1 and P2 is represented by a red and yellow complex. Adapted from Bol (2003).*

2.3.1. Replication, translation and encapsidation

After viral particles have entered into the plant cell, the gRNAs are uncoated and P1 and P2 genes are translated. Then, the assembly of these viral proteins with gRNAs and host factors forms the replication complexes. Next, the virus invades neighboring cells until they reach the vascular system to spread throughout the plant (Bol, 2005).

Hence, based on the described evidence, the current model for the AMV replication cycle proposes that, after virus entry into the cell, uncoating is probably motivated by morphological variations in the viral capsid induced by changes in environmental pH. However, some CP

molecules bound to the 3'UTR would keep the CPB structure (Fig. 3B, step 1) and promote P1 and P2 translation by hijacking components of the host eIF4F initiation factor complex (or plant-specific eIFiso4F complex), which, in turn, bind to the 5'cap structure (Neeleman et al., 2002; Krab et al., 2005). In other words, the CP mimics the poly-A binding protein role to compensate for the lack of poly-A of vRNAs. It favors viral RNA translation whilst block the formation of the TLS structure (Fig. 3B, step 2). Then, replication complexes would be assembled in virus-induced vesicles that offer an adequate environment for several stages of viral life cycle and protect from the host antiviral mechanisms (Laliberté and Zheng, 2014). A pioneering study reported that AMV replication complexes were located in the tonoplast (Van Der Heijden et al., 2001). Later on, a confocal microscopy study using Arabidopsis protoplasts showed that, when expressed alone, P1 localized in multivesicular bodies (MVBs), also denominated pre-vacuolar compartments, whereas P2 alone accumulated in the cytosol but was recruited to the MVBs by P1 when co-expressed. Moreover, co-expression of both proteins together with AMV RNAs led to the formation of a replication complex containing P1, P2 and vRNAs that associated with the tonoplast (Ibrahim et al., 2012). Thus, the authors of the study proposed that P1 recruits P2 and AMV RNAs into MVBs, driving the assembly of replicase complexes. Then, MVBs would transport the complexes to the tonoplast (Fig. 3B, step 3).

After translation and assembly of the replication complexes, the synthesis of the negative vRNAs takes place. According to *in vitro* experiments, the promoter for this synthesis comprises the E hairpin and the TLS (Olsthoorn and Bol, 2002). Thus, the viral replicase would recognize and bind the E hairpin of the positive polarity vRNAs and, at the same time, the CP might be released from the 3'UTR sites to allow the formation of the TLS structure (Fig. 3B, step 3). The dissociation of the CP could be caused either by the binding between the replicase complex to the E hairpin, by the proteolytic cleavage of the N-terminal of the CP or by the insertion of RNA-CP complexes into the vacuole membrane (Bol, 2005). The TLS would accommodate the replicase complex to the 3'-terminal initiation site, allowing the negative strand synthesis (Fig. 3B, step 4) (Chen and Olsthoorn, 2010). Current evidence indicates that the CP is not required for neither AMV positive nor negative vRNAs synthesis (Houwing and Jaspars, 1986). Instead, the CP role during viral replication would be to protect the positive strand vRNAs from degradation and, thus, to promote their accumulation (Bol, 2005).

Next, for synthesis of the positive polarity vRNAs, similar to *Bromo mosaic virus* (BMV), AMV P1 might bind to the internal control region (ICR) 2 motifs that were identified in a stem-loop structure within the 5'UTR of the AMV RNA 3 (Van Der Vossen et al., 1993; Chen et al., 2001).

ICR2 sequences resemble the eukaryotic promotor recognized by the host RNA Polymerase II (Marsh et al., 1989). Both, ICR2 motifs and the stem-loop structure in which they are located seem essential for the synthesis of the positive strand (Van Der Vossen and Bol, 1996). Host transcription factors might bind to ICR2 in the minus-plus RNA duplexes, inducing structural changes in the negative strand that would favor the accessibility of the replicase complex to this region for the initiation of the positive vRNAs synthesis (Van Der Vossen and Bol, 1996). Finally, after translation of the 4 viral proteins, virion assembly takes place (Fig 3B, step 5). But the whole molecular mechanism for this step is unknown so far (Krab et al., 2005; Bol, 2005, 2008).

2.3.2. Cell-to-cell and systemic movement

Although small molecules can freely traffic between plant cells, macromolecules or complexes require an active transport through plasmodesmata (PD). Plant viruses have to use this cell-to-cell connectivity channels to invade nearby cells to reach the vascular system of the plant. Thus, they encode one or a few MPs to facilitate cell-to-cell transport of the virus. At least three different mechanisms for viral transport to adjacent cells through PD have been described so far: i) moving as mobile ribonucleoprotein (RNP) complexes through modified PD, ii) moving as complete virions through tubules formed across PD via MP (and sometimes CP) oligomerization, or iii) using host membranes to form mobile vesicular replication complexes, although the latter mechanism is much more common for animal viruses (Navarro et al., 2019; Reagan and Burch-Smith, 2020).

The MP and the CP of AMV are required for cell-to-cell movement and both can be detected in PD of infected leaf tissue (Van Der Vossen et al., 1994; Sánchez-Navarro and Bol, 2001). Moreover, the interaction between the C-terminal part of the MP and the CP is critical for this transport, and may represent a control mechanism to assure the specificity of this process (Sánchez-Navarro and Bol, 2001). The mechanism used for AMV transport to adjacent cells through PD remains unclear, although several findings point to a tubule-guided mechanism. In this sense, transient expression of the AMV MP in protoplasts led to the formation of tubular structures, which were filled with viral particles after infection (Zheng et al., 1997). Furthermore, while mutations on the MP that interfere with the tubule formation affected cell-to-cell transport of AMV (Kasteel et al., 1997), a mutant version of CP unable to encapsidate vRNAs did not produce this phenotype, suggesting that virion assembly would not be a requirement for AMV local movement (Van Der Vossen et al., 1994; Sánchez-Navarro and Bol, 2001). The formation of tubules were observed in other members of the *Bromoviridae* family, like

Cucumber mosaic virus (CMV), *Tobacco streak virus*, and *Olive latent virus* (Huang et al., 2001). Moreover, Van Der Wel et al. (1998) described that, during AMV infection, PD augment diameter and lack the desmotubule, the endomembranous structure traversing the PD to connect the endoplasmic reticulum (ER) of two adjacent cells. However, no MP-derived tubular structures traversing the cell wall were detected, which argues against a tubule-guided transport. On the other hand, some studies pointed out that the cytoskeleton has a role assisting some viruses to get to and through the PD (Laliberté and Zheng, 2014; Reagan and Burch-Smith, 2020). Nevertheless, using drug inhibitors, it was shown that neither functional microfilaments nor the actomyosin system are required for AMV tubule formation (Huang et al., 2001). The AMV MP and the closely related ilarviruses MPs belong to the 30K superfamily: they present a functional RNA-binding domain and a contiguous hydrophobic domain at the N-terminus (Pallas et al., 2013). Consistently, cell-to-cell movement of AMV can be mediated by the MPs of *Cucumo-*, *Tobamo-*, *Ilar-*, *Bromo-* and *Comoviruses* (Sánchez-Navarro et al., 2006). Herranz and colleagues (2005) demonstrated that an AMV chimeric virus that contains different mutant MP genes of the *Prunus necrotic ringspot virus* (PNRSV), either lacking the RNA-binding domain or with diverse point mutations in this region, is unable to move from cell to cell. Within the hydrophobic region, the presence of a proline and a glutamine constrains both the secondary structure of this region and its interaction with the lipid interface of the ER membrane. The mutation of this strictly conserved proline residue precludes viral cell-to-cell movement *in vivo* (Martinez-Gil et al., 2009).

To facilitate intra- and/or intercellular movement, viruses require not only viral MPs, but also the involvement of host proteins. In fact, different host proteins were identified to interact with several MPs: components of the PD transport machinery and the cytoskeleton, cell wall-associated proteins, protein kinases, calcium sensors and putative transcriptional coactivators, which, in some cases, affect viral movement (Pallas and García, 2011). In this sense, the AMV MP interacts with the Arabidopsis proteins PATELLIN 3 and 6. These proteins present a so-called Sec14 domain that was linked to membrane trafficking, cytoskeleton dynamics, lipid metabolism and lipid-mediated regulatory functions. Interestingly, the overexpression of PATELLIN 3 and/or 6 reduces viral cell-to-cell movement by interfering with the PD targeting of the AMV MP (Peiro et al., 2014).

Finally, to systemically invade the whole plant, viruses need to reach the vascular system (Pallas et al., 2011; Navarro et al., 2019). To invade the sieve elements, viruses have to overcome diverse cellular barriers: the vascular bundle, the parenchyma and the companion cells (Hipper

et al., 2013). AMV can accomplish long-distance transmission as viral particles, resembling viruses that belong to other genera: *Begomovirus, Benyvirus, Carmovirus, Closterovirus, Cucumovirus, Dianthovirus, Mastrevirus, Necrovirus, Potexvirus, Sobemovirus* and *Tobamovirus* (Seo and Kim, 2016). Nonetheless, the molecular mechanism involved in phloem load and unload of AMV is undisclosed thus far.

2.4. CP interaction proteins

The AMV CP is a multifunctional protein essential for most viral stages, from early infection to encapsidation (Bol. 2003). Thereby, several studies have been focused on understanding the molecular role of the CP during infection, including the identification of CP-binding host proteins and the purpose of these interactions in the viral life cycle.

As mentioned above, to trigger translation, the CP interacts with components of the initiation complexes eIF4F or eIFiso4F, in particular eIF4G or eIFiso4G (Krab et al., 2005). Besides, via a yeast two-hybrid screening, the CP was found to interact with the Arabidopsis PsbP protein, a nuclear-encoded component of the oxygen-evolving complex of photosystem II (Balasubramaniam et al., 2014). The study showed that overexpression of PsbP results in lower viral titer, suggesting an antiviral role for this protein. The authors proposed that the CP avoids PsbP transport to the chloroplasts through its sequestration into the cytosol, causing the inhibition of its antiviral function.

Early electron microscopy studies reported that the AMV CP accumulates not only in the cytoplasm but also in the nucleus and the nucleolus of infected cells (Van Pelt-Heerschap et al., 1987). More recently, two domains that explain the nucleocytoplasmic localization of the CP were identified: a N-terminal lysine-rich nucleolar localization signal, required for the entry and the accumulation of this protein in the nucleus/nucleolus, and a C-terminal leucine-rich domain that might act as a nuclear export signal (NES) (Herranz et al., 2012). Guogas and coworkers (2005) found that the concentration of CP may represent a mechanism to regulate AMV replication and encapsidation, since viral replication was stimulated or repressed at low and high CP levels, respectively. Thus, it was suggested that AMV may use the nucleus/nucleolus as a temporary storage site of CP, reducing CP levels in the cytoplasm to avoid viral replication decrease (Herranz et al., 2012). In line with the nuclear/nucleolar localization of the AMV CP, this viral protein was found to interact with ILR3, a transcription factor of the helix–loop–helix (bHLH) family that is implicated in diverse metabolic and developmental pathways (Samira et al., 2018). Interestingly, the AMV CP-ILR3 interaction leads to the translocation of a fraction of

ILR3 from the nucleus to the nucleolus (Aparicio and Pallás, 2017). ILR3 is known to regulate atNEET (At5g51720), a plant protein belonging to the NEET family class of proteins, which, in turn, plays a critical role for plant development, senescence, iron metabolism and reactive oxygen species homeostasis (Rampey et al., 2006; Nechushtai et al., 2012; Su et al., 2013). CP-ILR3 binding was suggested to downregulate atNEET, resulting in the activation of plant hormone responses, such as salicylic and jasmonic acid pathways, to reach a hormonal balance state. It allows the reduction of virus accumulation to levels that do not affect plant viability without hampering systemic infection (Aparicio and Pallás, 2017).

Regardless these recent observations, it is expected that many other CP-interacting host proteins modulate AMV cycle, either by promoting infection or by acting as antiviral factors.

3. RNA granules

RNA granules are membraneless cellular structures comprising RNP complexes that are part of a regulatory network to adjust RNA metabolism. They play essential roles in regulating cell development and other functions, for instance stress response. In cells, nuclear granules include Cajal bodies, the nucleolus, nuclear speckles, nuclear stress bodies or plant photobodies, while processing bodies (P-bodies), stress granules (SGs), neuronal bodies or small interfering RNA (siRNA) bodies are cytoplasmic RNA granules (Anderson and Kedersha, 2008).

P-bodies and SGs components have been extensively studied in mammals and yeast, and it is accepted that their structure and functions are conserved among eukaryotes, including plants (Fig. 4) (Zhang et al., 2019b; Xu et al., 2020). Whereas P-bodies are constitutively present in cells and are involved in RNA turnover and mRNA decay, SGs are reversible dynamic structures that appear as a consequence of stress and mostly consist of translationally blocked mRNAs aggregations (Xu et al., 2020). There are different marker proteins characteristic of each kind of granule, but others have been seen in both P-bodies and SGs, probably due to the proposed dynamically interchange of RNPs cargo between them (Anderson and Kedersha, 2008). In mammals, after stress-triggered translation inhibition, diverse mRNA-binding proteins, such as cytoplasmic polyadenylation element binding protein, Histone deacetylase 6, Tudor domain-containing protein 3 or Ras-GAP SH3 domain binding protein (G3BP), facilitate aggregation of SGs. Later, the accumulated translationally stalled RNPs may be degraded or reinitiate translation (Anderson and Kedersha, 2008). Some examples of SG components in plants are

G3BP homolog, which localizes in SGs after heat shock in Arabidopsis (Krapp et al., 2017), and ANGUSTIFOLIA (AN), which regulates SGs formation during stress (Fig. 4) (Bhasin and Hülskamp, 2017). On the other hand, P-bodies are mainly composed of proteins involved in translational repression and/or the mRNA decay pathway: mRNA-decapping enzyme 1 and 2 (DCP1 and DCP2), 5'-3' exoribonuclease 1 (XRN1), Lsm1-7 deadenylation complex or decapping activators, such as the enhancer of mRNA-decapping protein 3 (EDC3) or PAT1, and the scaffolding proteins HEDLS/GE1 (VARICOSE (VAR) in plants) (Luo et al., 2018). However, P-bodies have been proposed to play a prominent role in the accumulation of translationally repressed mRNAs, while mRNA decay events would occur in the surrounding cytoplasm, out of the P-bodies (Hubstenberger et al., 2017; Luo et al., 2018; Tutucci et al., 2018). Thus, the function of P-bodies in mRNA decay still has to be clarified. In Arabidopsis, in addition to DCP1, DCP2 and VAR, DCP5 is also involved in P-bodies formation (Fig. 4) (Xu et al., 2020). Additionally, Arabidopsis TUDOR STAPHYLOCOCCAL NUCLEASE PROTEIN (TSN1 and TSN2) and VASCULAR PLANT ONE-ZINC FINGER (VOZ) PROTEIN were found to associate with P-bodies and SGs (Fig. 4) (Gutierrez-Beltran et al., 2015; Bhasin and Hülskamp, 2017).

In addition to deadenylation and decapping, the nonsense mediated decay (NMD) mechanism targets mRNAs with premature termination codons (PTC) to P-bodies (Sheth and Parker, 2006). Components of this pathway include the ATP dependent RNA helicase up-frameshift proteins 1-3 (UPF1-3) and serine protein kinases SMG1 and SMG5-7 (Fig. 4) (Schweingruber et al., 2013). In Arabidopsis, UPF1 was found to colocalize with DCP5 to P-bodies (Chicois et al., 2018). Furthermore, RNA silencing or RNA interference (RNAi) is another mechanism that regulates gene expression and RNA stability and whose innate function in plants was proposed to be antiviral defense. In fact, most, if not all viruses, encode proteins with RNAi suppressor activity (Pumplin and Voinnet, 2013). siRNA bodies are specific plant granules associated with the amplification of secondary siRNAs by the action of RNA-dependent RNA polymerases (RDRs). siRNA bodies contain ARGONAUTE 7 (AGO7), SUPPRESSOR OF GENE SILENCING 3 (SGS3) and RDR6 (Fig. 4) (Kumakura et al., 2009; Jouannet et al., 2012). It was proposed that siRNA bodies compete with P-bodies for the same RNA substrates, since P-bodies formation is enhanced in *rdr6* knockout plants and, in turn, siRNA production dependent on RDR6 activity is increased in plants with a dysfunctional decapping pathway (Martínez de Alba et al., 2015; Tsuzuki et al., 2017).

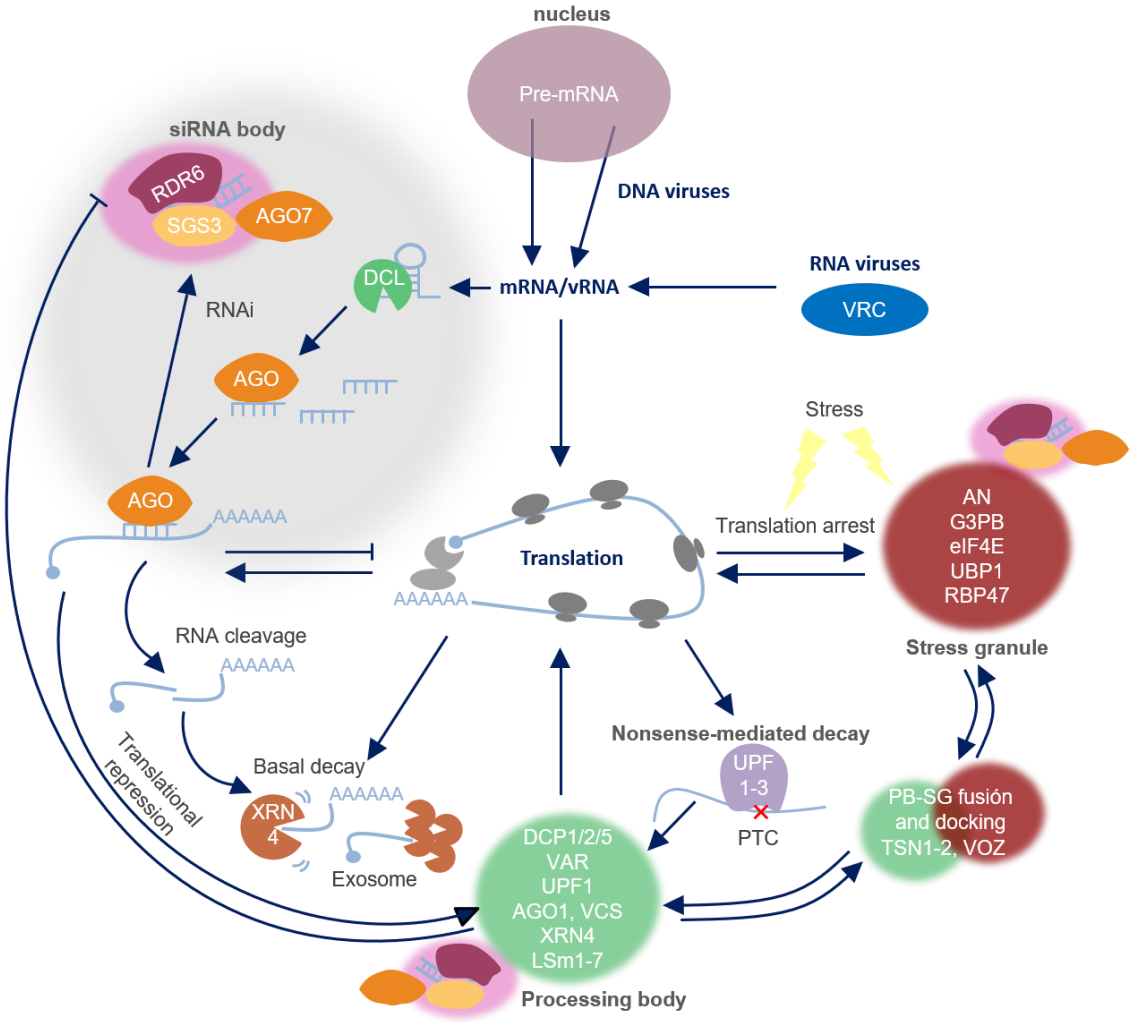

Figure 4. Main mRNA regulatory processes in plant cells. *Translation of host mRNAs is carried out in the ribosome sites. Viruses have evolved strategies to manipulate host translation. Cellular stresses, as viral infections, trigger SGs formation and increase the number and size of PBs. While stress conditions continue, translationally blocked pre-initiation complexes condense into SGs. These translationally repressed RNAs can be transmitted from PBs back to translation. PBs and SGs fuse and exchange components. Whereas decay mechanisms target aberrant RNAs – without 5'cap or polyA tail –, RNA silencing and NMD machineries can target host mRNAs and vRNAs for degradation. NMD is partially located to PBs and RNA silencing to siRNA bodies. During stress, siRNA bodies can associate with SGs and PBs. Only the main components are mentioned. PB, processing body; SG, stress granule; NMD, nonsense-mediated decay; PTC, premature termination codon; VRC, virus replication complex. Adapted from Mäkinen et al., 2017.*

3.1. Interplay between cytoplasmic RNA granules and viral infections

Host RNA metabolism plays crucial roles in the life cycle of any virus. Although there are far more examples in animals, the study of RNA granules functions in plant regulatory networks, including their implication in viral infections, has attracted more and more attention in the last years.

Viruses activate stress responses on diverse levels, including the modulation of SGs and P-bodies functions. Hence, key components of P-bodies and SGs may act in host defense, limiting viral infections (Beckham and Parker, 2008). And, in turn, viruses can manipulate the formation, composition and structure of these granules to promote infection (Lloyd, 2013; Zhang et al.,

2019b). In fact, many observations demonstrate that most human RNA viruses subvert and alter the distribution of mRNA decay factors (Jungfleisc et al., 2016). For example, the nsP3 protein from *Semliki Forest virus* and *Chickungunya virus* interacts with G3BP. This binding leads to the block of SGs assembly and the hijack of host translation components into the vicinity of viral replication complexes, enhancing the translation of viral factors (Fros et al., 2012; Panas et al., 2012). The nonstructural protein 1 of *Influenza A virus* (IAV) impedes cytoplasmic SGs formation to permit translation of viral mRNAs (Khaperskyy et al., 2012). Moreover, *Poliovirus* (PV) actively disrupts SGs and P-bodies formation by enhancing the degradation of G3BP1, DCP1 and XRN1 through their cleavage by the viral protease 3C (White et al., 2007; Dougherty et al., 2011). Likewise, the CP of *Zika Virus* (ZIKV) specifically interacts and targets UPF1 for degradation in the proteasome, leading to NMD pathway disruption (Fontaine et al., 2018).

Plant viruses have also developed strategies to circumvent and manipulate RNA surveillance and control mechanisms associated to RNA granules (Mäkinen et al., 2017; Xu et al., 2020). Studies with *Tobacco rattle virus* (TRV) (Ma et al., 2015), TMV (Conti et al., 2017) and *Turnip mosaic virus* (TuMV) (Li and Wang, 2018) demonstrated that mRNA decay is implicated in degradation of vRNAs. TuMV counterattacks by suppressing DCP1-DCP2 complex through direct interaction of the viral protein genome-linked (VPg) to DCP2 (Li and Wang, 2018). Furthermore, studies about the replication process of BMV in *Saccharomyces cerevisiae* revealed that vRNAs specifically capture the yeast decapping activators LSm1-7 complex, PAT1 and DEXD/H-BOX ATP-DEPENDENT RNA HELICASE (DHH1). These factors bind to 5’ and 3’UTR structures on vRNAs, remodeling their secondary conformation and favoring translation and replication of BMV RNAs (Jungfleisc et al., 2016). Likewise, NMD and RNAi surveillance pathways interplay during viral infection. García and colleagues (2014) found that both mechanisms are activated upon *Turnip crinkle virus* (TCV) infection, competing for the same vRNA pools, and, in Arabidopsis, TCV accumulation was enhanced in *upf1* mutants. Moreover, it was suggested that viruses using gRNAs and sgRNAs, like TCV, trigger NMD. Thus, whereas RNA silencing may target any type of vRNAs, NMD targets gRNAs that contain PTC (Garcia et al., 2014).

Further studies are needed to identify new plant components of these granules and to understand their roles as antiviral structures, as well as how plant viruses counteract these host defenses and subvert their components and functions for their own benefit.

4. RNA m^{6}A methylation

RNA modifications have been known for five decades (Holley et al., 1965; Perry and Kelley, 1974), but they had not been defined as a new level of gene expression regulation until recently. To date, around 160 post-transcriptional modifications have been described (Boccaletto et al., 2018). Chemical modifications of the canonical nucleotides can cause changes in the RNA structure that affect intramolecular interactions – making the molecules more flexible or more rigid – or influence their interaction with other factors.

In the 1970s, *N*^{6}-methyladenosine (m^{6}A) was identified in animal mRNA hydrolysates (Desrosiers et al., 1974; Perry and Kelley, 1974) and, some years later, it was also found in maize poly-A-containing RNAs (Nichols and Welder, 1981). Shortly after m^{6}A discovery, it was related to mRNA instability (Sommer et al., 1978), but it was not until almost twenty years later that the main mRNA m^{6}A methyltransferase, the methyltransferase-like protein METTL3, was characterized (Bokar et al., 1997). Thereafter, it was shown that METTL3-homologs are required for successful Arabidopsis seed germination and yeast sporulation processes (Clancy, 2002; Zhong et al., 2008).

As these indications supported putative essential roles of m^{6}A mechanism, they motivated the development of diverse methods to quantify m^{6}A levels or even map m^{6}A sites in mRNAs. Levels of m^{6}A can be analyzed by two-dimensional thin layer chromatography, high-performance liquid chromatography-tandem mass spectrometry (HPLC-MS/MS) (Zheng et al., 2013) and m^{6}A dot-blot using a specific antibody. The first m^{6}A mapping methods were based on high-throughput sequencing of immunoprecipitated methylated RNA (MeRIP-seq) (Meyer et al., 2012; Dominissini et al., 2012, 2013). Since antibody-based methods are currently known to miscalculate the number of m^{6}A sites, many other techniques to obtain robust m^{6}A mapping results have emerged during the last years, such as photo-crosslinking-assisted m^{6}A-sequencing (PA-m^{6}A-Seq), site-specific cleavage and radioactive-labelling followed by ligation-assisted extraction and thin-layer chromatography (SCARLET), m^{6}A individual nucleotide resolution crosslinking immunoprecipitation (miCLIP) (for a recent review, see Linder & Jaffrey, 2019) or MAZTER-seq, based on RNA digestion via an m^{6}A sensitive RNase (Garcia-Campos et al., 2019). Some of these methods offer nucleotide resolution, while others define intervals containing the modification, but in order to compensate the limitations of each one, recent studies highlight the importance of comparing more than one technique. Luckily, direct RNA sequencing by Oxford Nanopore Technology is being already successfully used to map m^{6}A residues in plants (Parker et al., 2020).

Nowadays, it is well established that m^6A methylation is the most prevalent internal modification in eukaryotic mRNAs and influences the fate and function of the modified transcripts. It is a selective modification that occurs in the sequence context (R)RACH (R=A/G, H=A/C/U) (Arribas-Hernández and Brodersen, 2020) and is enriched in the 3'UTRs. Two alternative motifs (URUAY, R=A/G and Y=C/U; GGAU), in addition to RRACH, were proposed to be specific for plants (Anderson et al., 2018; Wei et al., 2018b; Zhang et al., 2019a; Luo et al., 2020; Miao et al., 2020). However, Parker and coworkers (2020) excluded the possibility that these are actual methylation sites and suggested that these motifs co-occur with m^6A in the already mentioned single-nucleotide resolution study. In mammals, an average of one to three m^6A residues per mRNA are present, but, whereas most of mRNAs only have one site, others can have above twenty (Dominissini et al., 2012; Meyer et al., 2012; Schwartz et al., 2014; Linder et al., 2015). Arabidopsis transcriptome contains 0,5-0,7 m^6A peaks per 1000 nucleotides or 0,7–1,0 m^6A peaks per actively expressed transcript (Luo et al., 2014). Highly enriched m^6A genes are involved in response to environmental variation (Dominissini et al., 2012) and development (Meyer et al., 2012), whereas m^6A levels of constitutive genes are low in yeast and mammalian cell cultures (Schwartz et al., 2014; Ke et al., 2017). Distinct from mammals, housekeeping genes, like ribosomal and photosynthetic factors, are part of m^6A-enriched mRNAs in Arabidopsis (Luo et al., 2014; Wan et al., 2015; Shen et al., 2016; Wang et al., 2017; Anderson et al., 2018).

Despite the recent progress, there are important aspects of this post-transcriptional gene regulation pathway that are not defined yet: (1) the exact m^6A stoichiometry transcriptome, (2) whether it is a dynamic mechanism or not, and (3) how specific (R)RACH motifs are selected for modification, as not every A residue within this context becomes methylated (Meyer and Jaffrey, 2017; Yang et al., 2018; Shi et al., 2019). Point two has been particularly discussed, since, although the discovery of *erasers* fueled the idea of m^6A methylation as a dynamic process (Jia et al., 2011; Zheng et al., 2013; Dominissini et al., 2012; Meyer et al., 2012; Schwartz et al., 2013; Wei et al., 2018a), there is no evidence that the same mRNA molecule is subjected to methylation/demethylation cycles (Ke et al., 2017; Meyer and Jaffrey, 2017; Rosa-Mercado et al., 2017; Darnell et al., 2018). Future research will hopefully shed some light on these issues.

4.1. m^6A machinery

The presence of m^6A on a transcript depends on the action of methyltransferases (known as *writers*) and demethylases (or *erasers*), and the so-called m^6A *reader*s recognize these modified nucleotides. The best-characterized m^6A *writers*, *erasers* and *readers* in Arabidopsis are shown

in Figure 5 and their putative functions related to this mechanism are explained in the following sections.

4.1.1. m^{6}A *writers*

In agreement with the existence of a common methylation motif, the S-adenosyl-L-methionine (SAM)-dependent *writer* complex is conserved in eukaryotes. In mammals, two subcomplexes were initially identified as essential for full methyltransferase activity, MT-A and MT-B (Bokar et al., 1994). While MT-A comprises two key subunits, the catalytic enzyme METTL3 and the allosteric activator METTL14 (Bokar et al., 1997; Liu et al., 2014), the known assisting factors that compound MT-B are Wilms' tumor-associated protein (WTAP) (Ping et al., 2014), the Vir-like m^{6}A methyltransferase associated protein (VIRMA or KIAA1429) (Schwartz et al., 2014), the E3 ubiquitin-protein ligase CBLL1 or HAKAI (Horiuchi et al., 2013), the Zn finger protein ZC3H13 and the RNA binding proteins RBM15/15B (Knuckles et al., 2018). In plants, the catalytic core is formed by two MTA-70 family proteins, MTA (AT4G10760) – METTL3 homolog – and MTB (AT4G09980) – METTl14 homolog. So far, the described co-factors are FKBP12 interacting protein 37 (FIP37, AT3G54170) – WTAP homolog –, VIRILIZER (VIR, AT3G05680) – VIRMA homolog – and the E3 ubiquitin ligase HAKAI (AT5G01160) (Zhong et al., 2008; Shen et al., 2016; Růžička et al., 2017) (Fig. 5). However, other *writers* exist. In mammals, METTL5 and ZCCHC4 were identified as the responsible enzymes for m^{6}A modification of 18S and 28S rRNAs, respectively (Van Tran et al., 2019). Moreover, structured RNAs that contains the sequence UAC(A)GAGAA are methylated by METTL16, which also seem to bind the U6 small nuclear RNAs (snRNA), non-coding RNAs, long non-coding RNAs and pre-mRNAs (Pendleton et al., 2017; Warda et al., 2017). FIONA1 is the plant homolog of METLL16 (Kim et al., 2008), but, while the MTA/MTB complex is undoubtable the main responsible for m^{6}A methylation in Arabidopsis, m^{6}A methyltransferase ability of FIONA1 has not been tested (Zhong et al., 2008; Shen et al., 2016; Růžička et al., 2017; Anderson et al., 2018). Finally, neither orthologues of the mammalian ZC3H13 (Balacco and Soller, 2019) nor METLL5 and ZCCHC4 have been found in plants yet.

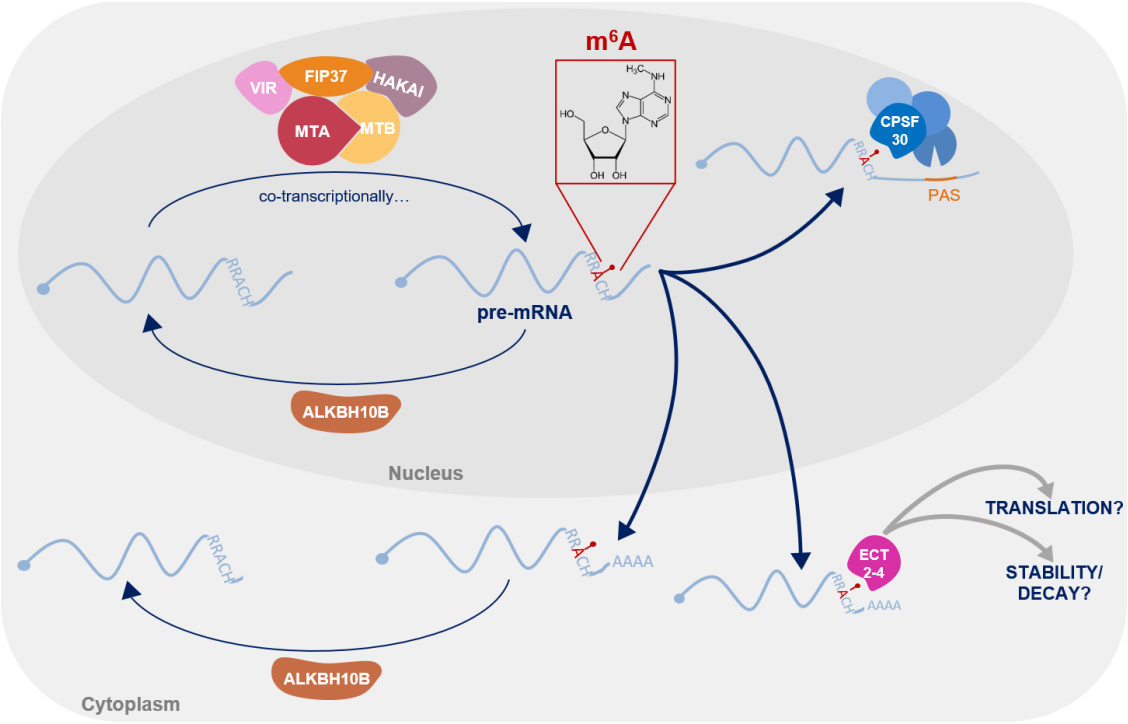

Figure 5. Schematic representation of the m⁶A pathway in Arabidopsis. *The known components of the m⁶A writer complex, the described eraser and readers and their possible molecular functions are displayed. While m⁶A methylation is thought to occur co-transcriptionally, there is no evidence about the subcellular location where the demethylation process takes place. PAS, polyadenylation signal. See main text for details.*

4.1.2. m⁶A *erasers*

Erasers described so far are homologs of the Alkylation B (AlkB) protein of *Escherichia coli* (Samson and Cairns, 1977). The AlkB protein family is conserved among all organisms except archaea and yeast, and it is part of the 2-oxoglutarate and Fe (II)-dependent dioxygenases superfamily (Aravind and Koonin, 2001). In general, these proteins revert alkylation damage on nucleic acids, but they can show preference for different substrates – RNA, DNA or proteins – and remove several alkyl groups, such as m⁶A or 5-methylcytosine (Fedeles et al., 2015). It is worth remarking that the discovery of proteins with m⁶A demethylation activity suggested a potential regulatory role for this modification (Jia et al., 2011).

In mammals, there are nine AlKB homolog proteins (AlKBH1-8 and Fat mass and obesity associated protein, FTO), but only ALKBH5 and FTO were characterized as m⁶A erasers (Jia et al., 2011; Zheng et al., 2013). ALKBH5 accumulates in nuclear speckles, so it is thought to demethylate m⁶A of nuclear RNAs during their synthesis (Zheng et al., 2013). FTO is located in both the nucleus and the cytoplasm of Human hepatoma Huh7 cells, suggesting that this protein can demethylate nuclear and cytoplasmic mRNAs (Gokhale et al., 2016). Interestingly, FTO was later found to act preferentially on 2'-*O*,*N*⁶-dimethyladenosine (m^6A_m) rather than m⁶A,

influencing m^6A_m-labelled mRNAs stability (Mauer et al., 2017). More recently, the modulation of small nuclear RNAs processing in the nucleus was the proposed prime biological role for FTO (Mauer et al., 2019).

In Arabidopsis, there are 13 AlkB homolog proteins (AtALKBH1A-D, AtALKBH2, AtALKBH6, AtALKBH8A-B, AtALKBH9A-C, AtALKBH10A-B), which, in protoplasts, were found to accumulate in six possible subcellular localizations: nucleocytoplasmic, nucleocytoplasmic with nuclear or cytoplasmic predominance, nucleocytoplasmic and chloroplast, and exclusively nuclear or cytoplasmic (Mielecki et al., 2012). During the course of this PhD Thesis, Duan and co-workers (2017) demonstrated that ALKBH10B is enriched in flowers and adult leaves, and reverts m^6A methylation in mRNA *in vitro* and *in vivo* (Fig. 5).

As it will be explained in the section 6 (*m^6A modification in plant viral infections: everything is about to be done*), AlkB domains were found in the ORFs of replicases of (+)ssRNA viruses as well (Bratlie and Drabløs, 2005; Van den Born et al., 2008; Moore and Meng, 2019).

4.1.3. m^6A *readers*

The best characterized m^6A *readers* comprise proteins that contain the so-called YT521-B homology (YTH) domain (Imai et al., 1998; Zhang et al., 2010). YTH domains conform two evolutionary groups, termed DC and DF clades. In mammals, YTH proteins that belong to the DC clade are YTHDC1 and YTHDC2 (DC1 and DC2 families), whereas the three YTHDF1-3 proteins cluster into the DF clade (DF family) (Fig. 6A) (Liao et al., 2018; Patil et al., 2018; Scutenaire et al., 2018). In these proteins, the YTH domain is responsible of m^6A-binding specificity via a highly conserved hydrophobic pocket made of aromatic amino acid residues and located internally (DC1) or at the C-terminal region of the protein (DC2 and the DF proteins) (Fig. 6B) (Theler et al., 2014; Patil et al., 2018; Scutenaire et al., 2018). Human YTHDF proteins contain an N-terminal low complexity region (LCR; regions with low diversity in amino acids composition) with several Pro-Gln-Asn-rich (PQN) patches, predicted to be an intrinsically disordered region (IDR; functional polypeptide segments without defined three-dimensional structure) (Liao et al., 2018; Patil et al., 2018). Four observations point to a regulatory function of this region: (i) the N-terminal region of YTHDF2 rich in PQN patches is required to relocate YTHDF2-m^6A-mRNA complexes into P-bodies (Wang et al., 2014). (ii) Deletion of either the YTH domain or the N-terminal from YTHDF3 prevents the binding to several endogenous target mRNAs, suggesting that both regions are required for the interaction of YTHDF3 to RNAs (Zhang et al., 2019c). (iii) YTHDF2 recruits the carbon catabolite repression–negative on TATA-less (CCR4-NOT)

deadenylase complex through a direct interaction with the YTHDF2 N-terminal region (Du et al., 2016). (iv) The N-terminal 1–100 aa of YTHDF2 are the minimal region able to bind the heat-responsive protein (HRSP)12–ribonuclease (RNase) P/mitochondrial RNA-processing (MRP) complex and are sufficient for rapid RNA endoribonucleolytic cleavage (Park et al., 2019). Additionally, YTHDC1 contains long N- and C-terminal IDRs, which are also thought to be regulatory elements (Patil et al., 2016). However, while YTHDF1-3 are cytoplasmic proteins and recognize mRNAs, YTHDC1 is mainly nuclear and interacts with mRNAs and nuclear non-coding RNAs (Hartmann et al., 1999). YTHDC2 is localized in both nucleus and cytoplasm and presents a much weaker m^{6}A binding affinity than the others (Xu et al., 2015; Wojtas et al., 2017). Moreover, YTHDC2 is specific to mammals and, in addition to the YTH domain, possesses helicase and R3H domains and ANK repeats (Fig. 6B). ANK repeats mediate in protein-protein interactions, whereas R3H domain might function as an RNA sequence-specific binding domain (Bailey et al., 2017; Hsu et al., 2017; Wojtas et al., 2017; Kretschmer et al., 2018).

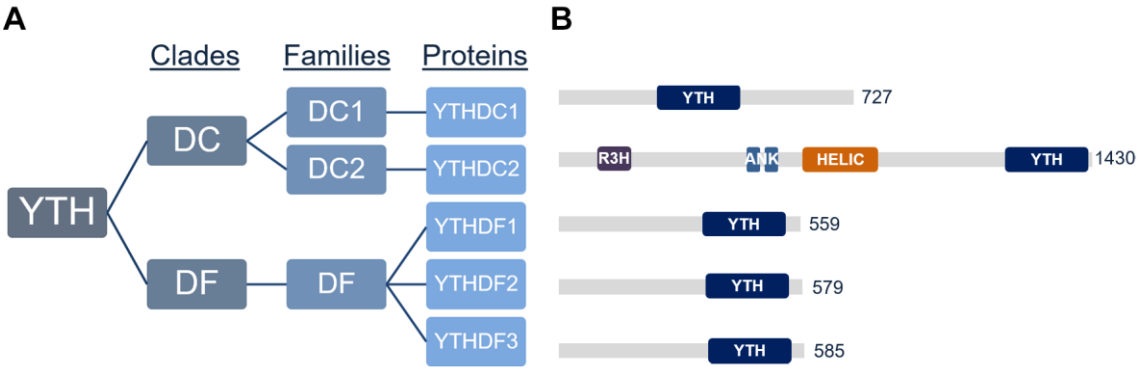

Figure 6. Human YTH proteins. (A) *Different clades and families that human YTH proteins are clustered in.* ***(B)*** *Schematic representation of the five human YTH proteins. Described domains/regions are indicated (in blue, YTH domains; in purple, R3H domain; in orange, helicase domain; and in pale blue, ANK repeats) (Patil et al., 2018).*

Several studies also proposed other proteins outside the YTH family as m^{6}A *readers* (Balacco and Soller, 2019; Berlivet et al., 2019). For example, in addition to its function in the nucleus as subunit of the m^{6}A methyltransferase complex, a fraction of METTL3 localized in the cytoplasm is recruited to m^{6}A sites on 3'UTR regions of mRNAs in human cancer cells, suggesting a role either as a direct m^{6}A *reader* or participating as a subunit of a m^{6}A *reader* complex (Lin et al., 2016). Moreover, the eukaryotic initiation factor 3 (eIF3) favors cap-independent translation of mRNAs that contains m^{6}A at their 5'UTR upon heat stress treatment (Meyer et al., 2015). In other cases, m^{6}A *readers* do not directly recognize the methylated residues, but the weak interaction between uracil (U) and m^{6}A affects RNA structures (Roost et al., 2015) and may leave a better access for certain RNA-binding proteins (Liu et al., 2015, 2017; Wu et al., 2018). For instance, Heterogeneous nuclear RNP (HnRNP) G and C preferentially bind to m^{6}A sites in hairpin

structures of long non-coding RNAs, whose structural conformation switches to a permissive binding status by the effect of m^{6}A deposition (Wu et al., 2018). On the other hand, a mass-spectrometry-based screening of m^{6}A interactors in mammalian cells identified diverse proteins, known as anti-m^{6}A *readers*, that are repelled by m^{6}A residues. One of these anti-m^{6}A *readers* is G3BP1, a protein that takes part in SGs assembly and positively regulates mRNA stability (Edupuganti et al., 2017).

In plants, the YTH family is more extensive than in animals. In particular, the Arabidopsis YTH family is composed of 11 YTHDF proteins – EVOLUTIONARILY CONSERVED C-TERMINAL REGION 1-11 (ECT1-11) – and two YTHDC proteins – AT4G11970 (of unknown function) and the CLEAVAGE AND POLYADENYLATION SPECIFICITY FACTOR 30 (CPSF30) – (Fig. 7), whereas the rice genome encodes twelve YTH proteins (OsYTH1-12). YTH domains are highly conserved between rice and Arabidopsis proteins (Li et al., 2014a; Scutenaire et al., 2018). Arabidopsis CPSF30 and OsYTH09 carry a CCCH-type zinc finger (ZF) domain, while ECT2 and ECT4-8 present a small region enriched in Tyr-Pro-Gln residues (YPQ-rich patches) similar to the PQN patches found in human YTHDFs (Fig. 7B) (Li et al., 2014a; Berlivet et al., 2019). Moreover, as in mammalian YTHDF proteins, ECT2, ECT3, and ECT4 are predicted to contain IDRs at their N-terminal sides (Arribas-Hernández et al., 2018).

Experimental analysis and public microarray data examination showed that the expression of YTH domain-containing proteins in rice and Arabidopsis depends on the specific tissue and the developmental stage (Li et al., 2014a). Furthermore, several Arabidopsis ECT proteins were found to interact with RNAs (Li et al., 2014a; Reichel et al., 2016) and, more recently, *in vitro* and *in vivo* assays demonstrated that ECT2 and ECT3 bind to m^{6}A through the aromatic residues located in the hydrophobic pocket of their YTH domains (Fig. 5) (Arribas-Hernández et al., 2018; Scutenaire et al., 2018; Wei et al., 2018b). Subcellular localization experiments reported that ECT1 has a predominant nuclear localization that might be regulated by calcium (Ok et al., 2005), while under normal growth conditions, ECT2, ECT3 and ECT4 accumulate in a cytoplasmic diffuse pattern (Arribas-Hernández et al., 2018; Scutenaire et al., 2018). Interestingly, following osmotic stress, ECT2 and ECT4 were found to aggregate into cytoplasmic foci that rarely co-localized with P-bodies (Arribas-Hernández et al., 2018), whilst, in response to heat stress, cytoplasmic ECT2 was found forming cytosolic punctate foci that were identified as SGs. Thus, it was proposed that translation initiation block induced by stress would trigger ECTs rearrangement to SGs (Scutenaire et al., 2018). The authors of this work suggested that YPQ-rich regions would be involved in this process, since ECT2 and ECT4 present these patches, but it is a feature absent in

ECT3, which did not form granular structures to the same extent after osmotic stress (Arribas-Hernández et al., 2018).

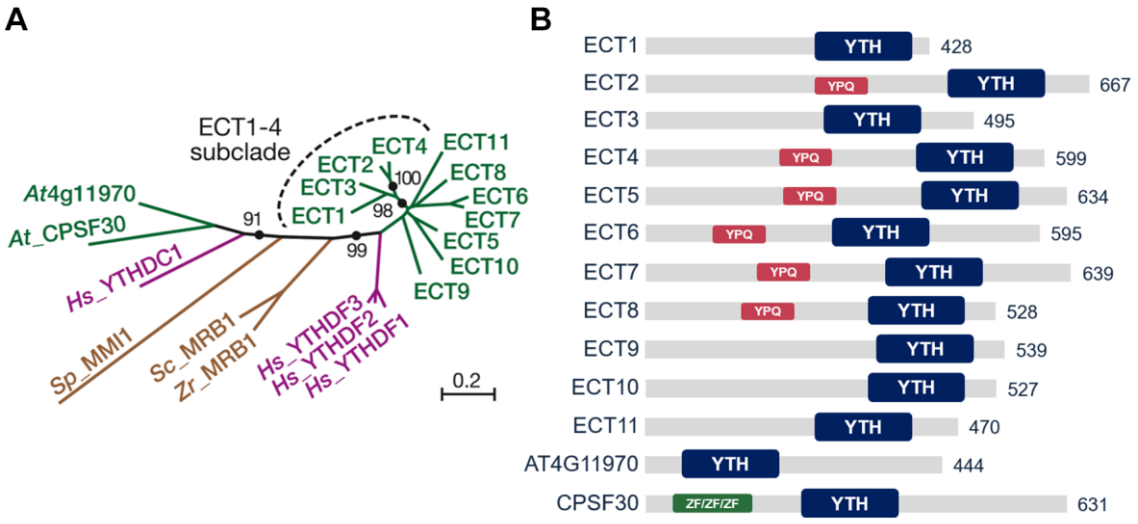

Figure 7. Arabidopsis YTH family. (A) *Phylogenetic tree including Arabidopsis YTH domain proteins (green) from Arribas et al. (2018). The ECT1-4 subclade is highlighted. In magenta, Human YTHDFs and YTHDC1 (Hs, Homo sapiens) and in brown, three yeast YTH domain proteins (Zr, Zygosaccharomyces rouxii; Sc, Saccharomyces cerevisiae; Sp, Schizo saccharomyces pombe).* ***(B)*** *Schematic representation of Arabidopsis YTH proteins. Described domains/regions are indicated (in red, YPQ-rich regions; in blue, YTH domains; in green, zinc-finger domains) (Scutenaire et al., 2018).*

4.2. Roles of m^{6}A

4.2.1. Molecular functions

In animals, the different processing fates of a m^{6}A-modified mRNA are being thoroughly investigated, and most of them are *reader*-binding dependent (for a recent review, see Zaccara et al., 2019). A recently published study revealed that chromosome-associated regulatory RNAs undergo m^{6}A modification, and loss of methylation increases the levels of these RNAs, promoting the open chromatin state and downstream transcription (Liu et al., 2020). Moreover, m^{6}A plays a role in mRNA splicing in *Drosophila melanogaster* (Haussmann et al., 2016; Lence et al., 2016; Kan et al., 2017). Accordingly, YTHDC1 interacts with several splicing factors (Imai et al., 1998; Hartmann et al., 1999; Wilkinson et al., 2003; Xiao et al., 2016) and deficiency of this protein in mice oocytes causes massive defects in alternative splicing (Kasowitz et al., 2018). In addition, m^{6}A is involved in alternative polyadenylation (APA), since deficiency of YTHDC1 or methyltransferase activity induce changes in the accumulation of transcripts subjected to APA (Ke et al., 2015; Kasowitz et al., 2018; Liu et al., 2018). Besides, m^{6}A promotes transcriptional repression via XIST (long non-coding RNA X-inactive specific transcript) (Patil et al., 2016) and participate in the ultraviolet-induced DNA damage response (Xiang et al., 2017). Moreover, since m^{6}A deposition is known to occur co-transcriptionally in the nucleus (Huang et al., 2019),

YTHDC1 was suggested to induce mRNA nuclear export by binding to SRSF3, a factor of an mRNA export pathway (Roundtree et al., 2017).

Until very recently, cytoplasmic *readers* YTHDF1-3 were thought to bind different m^{6}A-modified mRNAs and exert distinct functions. YTHDF2 was proposed to mediate m^{6}A-containing mRNA rapid degradation via two possible mechanisms: deadenylation by direct recruiting of the CCR4–NOT deadenylase complex (Wang et al., 2014; Du et al., 2016) or endoribonucleolytic cleavage through the binding to the heat-responsive protein (HRSP)12–ribonuclease (RNase) P/mitochondrial RNA-processing (MRP) complex (Park et al., 2019). On the other hand, several lines of evidence suggested that m^{6}A promotes translation through distinct mechanisms, including direct binding of YTHDF1 (Wang et al., 2015), YTHDC2 (Hsu et al., 2017), METTL3 (Lin et al., 2016; Choe et al., 2018) or eIF3 (Meyer et al., 2015). However, Zaccara and Jaffrey (2020) lately demonstrated that YTHDF1-3 recognize the same m^{6}A-modified mRNAs and act together in mRNA degradation proportionally to the number of m^{6}A residues. In this line, a mechanism to bring m^{6}A-modified mRNAs to cytoplasmic granules for their processing was proposed. It consists in a phased separation via the interaction between the low complexity domains of the YTH proteins when incubated with poly-methylated m^{6}A mRNAs (Ries et al., 2019). Similarly, in response to oxidative stress, m^{6}A levels in the 5'UTR of mRNAs increase in human cells and YTHDF3 recognizes these m^{6}A-marked mRNAs selectively accumulating them into SGs (Anders et al., 2018). Interestingly, Arabidopsis ECT2 was shown to undergo this phase-separation *in vitro* too (Arribas-Hernández et al., 2018; Scutenaire et al., 2018).

In addition to the mRNA regulation, some reports showed a regulatory effect on m^{6}A methylation caused by non-coding RNAs and, in turn, a modulatory role of the generation and function of non-coding RNAs by m^{6}A (for a recent review, see Ma et al., 2019). For instance, m^{6}A is present on circular RNAs (circRNAs) and some authors proposed a cap-independent translation function (Yang et al., 2017; Diallo et al., 2019), while others described m^{6}A recognition by YTHDF2 as a "self" mark versus foreign circRNAs (Chen et al., 2019).

In plants, the decrease of m^{6}A levels in knockdown mutants of *MTA* (Bodi et al., 2012), *FIP37* (Shen et al., 2016) and *VIR* (Růžička et al., 2017), and the mutation of the *reader ECT2* (Wei et al., 2018b) were related to a reduction in the abundance of m^{6}A-targeted transcripts (Shen et al., 2016; Anderson et al., 2018; Wei et al., 2018b; Parker et al., 2020). According to those results, m^{6}A would enhance mRNA stability. In fact, Anderson and co-workers (2018) observed endonucleolytic cleavage around methylation sites in m^{6}A-depleted plants, suggesting that the

presence of methyl groups provides protection to mRNA. Nonetheless, m^{6}A depletion was also described to increase the expression of m^{6}A-targeted mRNAs implied in developmental control (Shen et al., 2016), whereas m^{6}A demethylation activity of ALKBH10B was shown to promote stability of flowering-related genes (Duan et al., 2017). Hopefully, new transcriptome studies will offer us enough indications to draw final conclusions on this matter. Additionally, more and more molecular functions are recently emerging, but many of them need to be deeper studied to be clearly understood. CPSF30 is the 30 kD subunit of the CLEAVAGE AND POLYADENYLATION SPECIFICITY FACTOR involved in pre-mRNA cleavage and 3'end formation (Zhang et al., 2008; Thomas et al., 2012; Bruggeman et al., 2014; Pontier et al., 2019). Two different isoforms, CPSF30-S and CPSF30-L, are produced from the CPSF30 gene, and CPSF30-L is the one that contains a canonical YTH domain of the DC group (Chakrabarti and Hunt, 2015). In fact, FIP37 and CPSF30-L are implied in a (3'UTR m^{6}A)–assisted polyadenylation pathway that safeguards transcriptome integrity at rearranged genomic loci in Arabidopsis (Pontier et al., 2019). Another recent work published in bioRxiv showed that, as found in animals, Arabidopsis primary-microRNAs contain m^{6}A residues and this methylation mechanism might collaborate in miRNAs biogenesis through the interaction of MTA with RNA Pol II and TOUGH, a miRNA biogenesis related factor (Bhat et al., 2019). Furthermore, *in vitro* observations suggested that multiple m^{6}A residues along mitochondrial mRNAs are detrimental for translation, whereas a single modification in the start codon or its proximity may promote the translatability of organellar transcripts (Murik et al., 2019).

4.2.2. Biological functions

According to its molecular functions, m^{6}A seems generally related to the regulation of the state developmental changes and the adaptative responses to external stresses.

In animals, m^{6}A methylation of mRNAs was first described to control the speed of the circadian clock (Fustin et al., 2013). Later, various studies reported its involvement in processes of cellular self-renewal, pluripotency and differentiation, crucial events during embryo development that result in the formation of distinct tissues and organs. For example, null alleles of *writer* components, such as METTL3 and WTAP, lead to embryonic lethality (Fukusumi et al., 2008; Geula et al., 2015), whereas deficiency of ALKBH5, YTHDC1 or YTHDC2 in mice is associated to impaired fertility, suggesting an essential role for m^{6}A in spermatogenesis (Zheng et al., 2013; Hsu et al., 2017; Kasowitz et al., 2018). This hypothesis is reinforced by the fact that YTHDC2 protein is expressed in testes and its absence causes a significant reduction of testes and ovaries

size (Hsu et al., 2017). Moreover, Wojtas et al. (2017) pointed out that YTHDC2 ensures a successful meiosis progression by regulation of m^{6}A-modified mRNAs in the mammalian germline. Additionally, defects in this post-transcriptional gene regulation pathway appear to be related to numerous human diseases, including different types of cancer. In fact, m^{6}A study has facilitated the early diagnosis and treatment of diverse cancers, such as hepatocellular carcinoma or pancreatic, breast, and prostate cancers (Sun et al., 2019).

In Arabidopsis, m^{6}A is known to define plant development at embryonic stage, vegetative growth and flowering. The observation of the embryonic arrest at globular stage in *mta* knockout plants was the first indication of such function (Zhong et al., 2008). Likewise, null alleles of other components that form the *writer* complex are also unable to complete the embryonic development (Zhong et al., 2008; Růžička et al., 2017; Vespa et al., 2004). Interestingly, Shen and coworkers (2016) linked FIP37-mediated m^{6}A methylation with the instability of the mRNAs from the crucial shoot meristem regulator genes, *WUSCHEL* (At2g17950) and *SHOOT MERISTEMLESS* (At1g62360), whose expression avoids the uncontrolled growth of the meristem and the formation of aberrant leaf primordia. Moreover, analysis of knockdown *mta, mtb, fip37* and *vir* in other studies confirmed that m^{6}A depletion causes different developmental defects: delayed growth, atypical organ morphology, loss of apical dominance, defective trichome branching, malfunctioning gravitropic responses and abnormal development of lateral roots and vasculature (Bodi et al., 2012; Vespa et al., 2004; Růžička et al., 2017). In rice, OsFIP and OsMTA2, components of the *writer* complex, are indispensable for sporogenesis (Zhang et al., 2019a) and, in tomato, together with DNA 5-methylcytosine, m^{6}A regulates fruit ripening (Zhou et al., 2019). Furthermore, molecular studies of Arabidopsis plants that lack one or several m^{6}A *readers* established the implication of YTH proteins in some of the phenotypes described in plants defective in *writer* components (Arribas-Hernández et al., 2018; Scutenaire et al., 2018; Wei et al., 2018b). In particular, ECT2, ECT3 and ECT4 are highly expressed at leaf formation sites in the shoot apex and multiple knockout mutants of these three m^{6}A *readers* share *mta* knockdown phenotype (Bodi et al., 2012): slow growth, aberrant leaf, flower and fruit development, and stochastic increase of trichome branch number (Arribas-Hernández et al., 2018, 2020a, 2020b). In that regard, an exhaustive phenotypical study of ECT mutants concluded that these developmental effects are caused by the involvement of the m^{6}A-ECT2/ECT3/ECT4 axis in rapid cell proliferation (Arribas-Hernández, 2020b). Likewise, null alleles of *ECT2* result in a weak increase of trichome branching (Scutenaire et al., 2018; Wei et al., 2018b). On the other hand, ALKBH10B-mediated mRNA demethylation

affects the stability of target transcripts involved in control of flowering time, what reveals the influence of m^{6}A in seasonal plant rhythms (Duan et al., 2017). Similarly, disrupted m^{6}A deposition in *vir* mutant plants produces a lengthening of the circadian period (Parker et al., 2020).

Despite the lack of studies, it seems reasonable to think that, as described for the developmental stage transition control, m^{6}A could also participate in tuning rapid changes in gene expression to respond against stress, like other post-transcriptional gene regulation pathways do (Li et al., 2017). In this sense, there are two indirect proofs that support this hypothesis: (i) the observation that YTH proteins in Arabidopsis and rice are induced by diverse abiotic stresses, such as drought, osmotic stress, heat, cold, salt oxidative and hypoxia, and upon infection with nematodes, bacteria, fungi and viruses (*Cabbage leaf curl virus* and *Turnip mosaic virus*) (Li et al., 2014a; Hu et al., 2019), and that, as stated before, (ii) some m^{6}A *readers* are re-located to stress cytoplasmic granules following heat or osmotic stress (Arribas-Hernández et al., 2018; Scutenaire et al., 2018). Moreover, Anderson and co-workers (2018) reported that salt and osmotic stresses provoke m^{6}A hypermethylation and overexpression of mRNAs involved in adaptative response to those stresses and, conversely, the hypomethylation and downregulation of housekeeping genes. Nonetheless, more sophisticated analysis that use m^{6}A-abrogation mutants to define m^{6}A stoichiometry of stress-related transcripts with and without stress will have to be carried out to get more robust conclusions.

Due to the special interest for the present Thesis work, the role of m^{6}A in response to viral infections and modulating the innate immune response will be deeply analyzed in the following section.

5. m^{6}A modification in animal viral infections

In addition to the roles in regulating biological cellular processes, m^{6}A pathway is implied in viral infections. In fact, more than 40 years ago, methylated adenosines were identified in viruses that replicate in the nucleus, such as *Simian virus 40* (SV40) (Lavi and Shatkin, 1975; Canaani et al., 1979), *Influenza virus* (Krug et al., 1976), *Avian sarcoma virus* (Stoltzfus and Dimock, 1976), *Feline leukemia virus* (Thomason et al., 1976), *Adenovirus* (AV) (Furuichi et al., 1976) and *Herpes simplex virus-1* (HSV-1) (Moss et al., 1977). However, the available technology at that moment did not allow the functional study of this RNA modification. Over the last years, in parallel with

the development of new technologies, several studies try to elucidate the function of m^{6}A in those and other viral infections, although in most of the cases the precise molecular mechanism remains unclear.

In animal virology, elucidation of the m^{6}A-derived mechanisms has become one of the main focus of attention. In general, the most common approach to study viral and cellular m^{6}A epitranscriptomes is to manipulate the cellular m^{6}A machinery – depletion or overexpression of m^{6}A *writers*, *erasers* and *readers* – and to map m^{6}A sites along RNAs using some of the available methodologies (for a recent review, see Linder & Jaffrey, 2019).

5.1. Viral regulation mediated by m^{6}A-modified vRNA

For some viral infections, m^{6}A acts as either a proviral or antiviral signal, while, for others, its presence seems to enhance and inhibit infectivity depending on the methylation context (Fig. 8) (Williams et al., 2019).

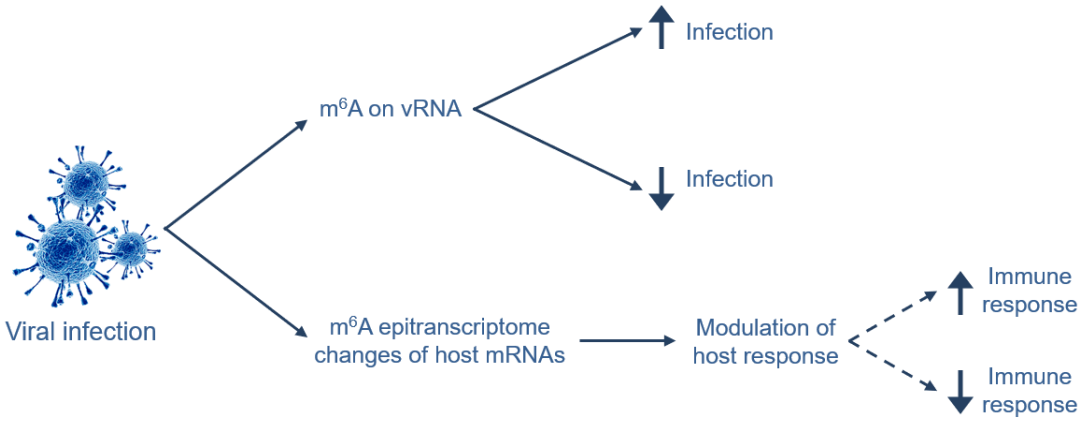

Figure 8. m^{6}A regulation of animal viral infections. *Host machinery may methylate vRNAs, favoring or impairing the infection process. The viral infection might also produce changes on m^{6}A host epitranscriptome, modulating the host response and affecting, for example, genes involved in the immune response.*

5.1.1. Positive m^{6}A-mediated viral regulation

The presence of m^{6}A residues was first found in animal-infecting viruses that replicate in the nucleus and present dsDNA, (-)ssRNA or (+)ssRNA genomes. One of these viruses was IAV, a (-)ssRNA virus that was shown to contain an average of three m^{6}A for each mRNA at first (Krug et al., 1976), although the distribution was observed to be unequal among different IAV transcripts a decade later (Narayan et al., 1987). A more recent work showed that global reduced methylation, caused by a chemical inhibitor or a METTL3 knockdown, leads to the repression of the expression and replication of IAV genes, while overexpression of the YTHDF2 *reader*

produces the opposite effect (Courtney et al., 2017). Additionally, m^{6}A sites along vRNAs (including gRNAs, replication templates or mRNAs) were mapped, finding higher levels of methylation for mRNAs that encode the structural proteins hemagglutinin (HA), neuraminidase (NA), matrix proteins (M1/M2) and nucleoprotein (NP). Finally, the same study described that synonymous mutations of some of the methylated adenosines within HA segment result in the repression of HA mRNA and protein expression. Thus, on the basis of these outcomes, the authors concluded that m^{6}A favors IAV infection (Courtney et al., 2017).

Early studies in the 70s showed that mRNAs transcribed from the dsDNA genome of the polyomavirus SV40 are m^{6}A-modified and that its life cycle is positively regulated by m^{6}A (Canaani et al., 1979; Finkel and Groner, 1983). SV40 life cycle consists of an early and a late phase in which regulatory and structural genes are expressed, respectively. Recently, the specific locations of the m^{6}A sites along SV40 mRNAs were characterized by photo-crosslinking-assisted m^{6}A sequencing, identifying two m^{6}A peaks on early transcripts and 11 on SV40 late transcripts. Besides, the study described that silent mutations of some of those sites on late transcripts decrease viral gene expression and virion production, while m^{6}A-abrogating mutations on early transcripts do not reveal any phenotype. In line with these results, overexpression and inactivation analysis of METTL3 and YTHDF2 genes showed that these proteins enhance lytic replication. Overall, these results led the authors to propose that m^{6}A promotes nuclear export of the late transcripts and, consequently, improves the expression of capsid protein VP1, ultimately enhancing SV40 replication (Tsai et al., 2018). However, the molecular mechanism behind m^{6}A-depending nuclear export of the late transcripts is still unknown.

Herpesviridae is a family of dsDNA viruses whose infection cycle is divided in two phases: the latent infection and the lytic replication, and the transition between the two stages is presumably mediated by changes in the epigenetic marks (Ye, 2017; Uppal et al., 2018). In fact, mRNA from HSV-1, *Human cytomegalovirus*, *Kaposi's sarcoma-associated herpesvirus* (KSHV) and *Epstein-Barr virus* (EBV) were described to undergo m^{6}A methylation (Furuichi et al., 1976; Rubio et al., 2018; Lang et al., 2019). In EBV infection, transcription of the host METTL14 increases during latent infection and is downregulated during lytic infection, suggesting that m^{6}A can participate in promoting latent phase and repressing lytic gene expression. Thereby, viral oncoprotein EBV nuclear antigen 3C (EBNA3C) is upregulated through METTL14-mediated m^{6}A and, in turn, enhances METTL14 transcription and protein stability (Lang et al., 2019). The rest of the methylated members belonging to the *Herpesviridae* family will be discussed in the following sections.

m^{6}A profile of both early and late transcripts of AV (dsDNA) was defined very recently by a mix of two techniques: MeRIP-seq and direct long-read sequencing. Nonetheless, depletion of METTL3 specifically affects the splicing efficiency of only the late transcripts (Price et al., 2019).

RNAs of several retroviruses, such as *Rous sarcoma virus* (RSV), *Murine leukemia virus* (MLV), *Human Immunodeficiency virus-1* (HIV-1) and *Feline leukemia virus*, also include m^{6}A bases. Early studies showed that RSV m^{6}A sites are within RAm^{6}AC motifs (R=G/A) (Beemon and Keith, 1977; Dimock and Stoltzfus, 1977; Kane and Beemon, 1985, 1987) and, more recently, m^{6}A sites were also mapped in MLV genome (Courtney et al., 2019). These studies indicated that m^{6}A plays a positive role for both viral infections. In an early work, it was already found that methylation may modify the splicing of the RSV *Env* transcript (Stoltzfus and Dane, 1982). Likewise, mutations abolishing some m^{6}A sites cause a slightly reduction of viral infectivity, whereas overexpression of YTHDF2 promotes MLV replication (Courtney et al., 2019). HIV-1 data will be discussed in section 5.1.3. (*Mixed m^{6}A-mediated viral regulation*) later on.

In the last years, some viruses that replicate in the cytoplasm – such as *Enterovirus type 71* (EV71) and *Human respiratory syncytial virus* (HRSV) – were observed to be subjected to m^{6}A methylation as well. This discovery opened the debate about the subcellular location of m^{6}A machinery, which might be modified during stresses. In EV71, a non-enveloped (+)ssRNA virus belonging to the *Picornaviridae* family, m^{6}A is present in the vRNAs that encode the P1 region of the capsid protein (VP1-4), the 3D polymerase and the 2C RNA helicase. Point mutations of some of these sites lead to a viral infectivity reduction. Besides, EV71 infection alters the expression patterns of *writers*, *erasers* and *readers*, provoking the nucleocytoplasmic redistribution of METLL3, METLL14, WATP and ALKBH5 and their co-localization with VP1 (Hao et al., 2019). Thereby, it was reported that the viral polymerase 3D interacts with METTL3, which enhances the 3D sumoylation and ubiquitination and, thus, promotes viral replication. This hypothesis agrees with both, the lower viral accumulation observed in METTL3 knockdown mutants and the replication increase observed upon depletion of the FTO *eraser* in Vero cells (Hao et al., 2019). However, although it is evident that YTH proteins modulate viral infection, different outcomes were obtained with distinct cellular types. In Vero cells, YTHDF2 and YTHDF3 seem to play a positive role in EV71 replication, while opposite results were obtained with the knockdown of each YTH protein in RD cells. The authors suggested that these differences may be due to the lack of interferon (IFN) in Vero cells, hinting at a connection between this defense pathway and m^{6}A (Hao et al., 2019). On the other hand, *Poliovirus*, another member of

Picornaviridae family, also contain several post-transcriptional modified bases, including m^{6}A, although their influence in the virus cycle is still unknown (McIntyre et al., 2018).

HRSV is an enveloped (+)ssRNA virus belonging to the *Paramyxoviridae* family and the only described human pathogen of the genus *Pneumovirus*. Most of the mapped m^{6}A sites are located along transcripts of the attachment transmembrane glycoprotein G. Likewise, mutations of some of these bases produce defective replication, gene expression, spread, and virus release in A549 cells, primary well differentiated human airway epithelial cultures and respiratory tract of cotton rats (Xue et al., 2019). Therefore, taken together, these results indicate that m^{6}A favors HRSV infection.

5.1.2. Negative m^{6}A-mediated viral regulation

Conversely, for some viruses, m^{6}A seems to act as a signal that triggers antiviral responses (Fig. 8). Nearly four years ago, m^{6}A residues were found in several (+)ssRNA viruses from the *Flaviviridae* family, which replicate in the cytoplasm: *Hepatitis C virus* (HCV), *Zika virus* (ZIKV), *Dengue virus* (DENV), *Yellow fever virus* and *West Nile virus* (Gokhale et al., 2016; Lichinchi et al., 2016b). The host m^{6}A machinery was found to negatively modulate HCV accumulation without altering RNA replication, as simultaneous depletion of METTL3 and METTL14 leads to an increase of the viral particle production. During infection, YTHDF proteins bind directly to vRNAs and re-localize to lipid droplets, where viral assembly takes place. Additionally, an HCV mutant with abolished m^{6}A sites along its RNA genome presents higher infectivity levels by promoting the interaction between vRNAs and HCV core protein and impairing YTHDF2 binding. Thus, it was proposed that m^{6}A impairs HCV viral assembly, although further studies are required to clarify whether only non-m^{6}A-modified vRNAs are packaged into assembling viral particles (Gokhale et al., 2016). Likewise, Lichinchi et al (2016b) reported that, whereas knockdown mutants of *writers* show an increase of ZIKV infection levels, these are reduced in *eraser* mutants, revealing that m^{6}A negatively regulates this viral infection as well. Moreover, the authors demonstrated that YTHDF1-3 bind to vRNA and silencing of any of these proteins lead to higher viral titers, with YTHDF2 having the utmost effect (Lichinchi et al., 2016b).

5.1.3. Mixed m^{6}A-mediated viral regulation

For some viruses, the mechanisms underlying m^{6}A-dependent regulation seem to draw a much more complex scenario. Both proviral and antiviral cascades are activated depending on m^{6}A position along the vRNA and the stage of the viral cycle that is affected. In contrast to the rest

of m^{6}A-modified retroviruses mentioned above, the results obtained for HIV-1 are more controversial. In 2016, three studies reporting the presence of m^{6}A residues along HIV-1 gRNA and mRNAs were published. According to Lichinchi et al. (2016a), methylation peaks are located in coding and noncoding regions, splicing junctions and splicing regulatory sequences. These authors suggested a positive regulation of HIV cycle induced by the favored binding of HIV-Rev protein to HIV-Rev Response Element RNA (RRE) when two conserved As of the stem loop II region of RRE are methylated. This interaction would promote mRNA nuclear export to the cytoplasm, finally favoring viral replication. Moreover, at the same report, methylation status of RRE RNA was shown to be influenced by m^{6}A enzymes, since knockdown of *METTL3/METTL14* decreases m^{6}A levels of this region, while they are higher in *alkbh5* mutant (Lichinchi et al., 2016a). However, recently, Chu and coworkers (2019) concluded that m^{6}A probably would not importantly modify the structural features of the RNA. Intriguingly, another research group did not identify RRE m^{6}A peaks, but characterized specific m^{6}A sites in the 3'UTR of vRNAs (Kennedy et al., 2016). The authors also found evidence of a positive HIV-1 regulation effect, although mediated via YTHDF proteins recruitment of m^{6}A-containing 3'UTR, what would promote viral translation and replication. On the other hand, a third work described m^{6}A sites in HIV-1 gRNA in the 5' and 3'UTRs as well as *gag* and *rev* genes. The results indicated that m^{6}A methylation of vRNAs favored viral infection, since HIV-1 Gag protein expression was downregulated and upregulated when m^{6}A *writers* or *erasers* were silenced, respectively. On the contrary, in this study the overexpression of YTHDF proteins decreased viral gRNA expression and reverse transcription (RT), impairing HIV-1 infection at this stage (Tirumuru et al., 2016). Some years later, the same research group reported a reduction in the infectivity of two HIV-1 5'UTR m^{6}A sites mutants and described the existence of a complex composed of the YTHDF1-3 proteins and HIV-1 Gag together with viral gRNAs (Lu et al., 2018). Accordingly, Jurczyszak et al. (2020) showed that YTHDF3 proteins are incorporated into HIV-1 particles and suggested that the viral protease cleaves the virion-encapsidated m^{6}A *reader* to reach adequate infectivity levels. Therefore, in view of the above observations, it is well established that HIV-1 transcripts are recognized by YTHDF proteins, but the whole picture is still ill-defined.

As observed for HIV-1, m^{6}A apparently regulates *Hepatitis B virus* (HBV) infection in different ways, depending on the position of the modification along the transcript body. HBV, member of *Hepadnaviridae* family, has a partially dsDNA circular genome and a complex replication cycle. Relaxed circular dsDNA (RC-DNA) genome is released from the viral particle into the nucleus and repaired to form a covalently closed circular DNA. Then, cellular RNA pol II transcribes the pre-

genomic RNA (pgRNA) and subgenomic mRNAs, leading to the synthesis of the viral proteins. The pgRNA is the mRNA for the translation of the polymerase (P) and the capsid subunit, but it is also selectively encapsidated along with P into capsid particles, where it serves as the template for RT to generate RC-DNA. While the 3'UTR of all the transcripts – including pgRNA – share an epsilon stem loop, only the pgRNA 5'UTRs present this structure. Recently, it was reported that all HBV transcripts contain a single m^6A peak within the stem loop at the 3'UTR end, and that the 5'UTR stem loop of pgRNAs has another one. Remarkably, this work indicated that m^6A modification at 5'UTR enhances pgRNA RT, while m^6A sites located in the 3'UTR promotes RNA destabilization. Since YTH depletion leads to a protein expression increase, the authors proposed that the recognition of m^6A in 3'UTR by *reader*s would be responsible of the mentioned destabilization (Imam et al., 2018).

On the other hand, the pattern of m^6A methylation in KSHV changes during the different stages of the viral cycle and between distinct cell types. After entering into host cells, the virus remains in a reversible latent state, in which only a few genes located in the latency-associated region are expressed. Stimuli, such as viral co-infections, hypoxia or oxidative stress, among others, can activate the expression of genes for the transition to the lytic phase. In this phase, an extensive synthesis of viral DNA and proteins is achieved, driving to the assembly and release of viral particles. Besides, lytic replication is also critical for KSHV-induced tumorigenesis. It is well known that lytic ORF50/RTA protein (replication transcription activator, RTA) is a critical lytic switch factor necessary and sufficient to redirect the virus from latency to the lytic state (Purushothaman et al., 2015). Three different reports demonstrated the presence of m^6A in most of the KSHV transcripts and tried to elucidate the role of this modification during the infection. In the first study, the authors suggested a proviral role for m^6A, as knockdown of FTO in B cells enhanced the expression of lytic genes (including ORF50/RTA) and the production of viral particles, and knockdown of METTL3 had the opposite effect. Moreover, they showed that pre-mRNA splicing of ORF50/RTA is regulated by m^6A-binding of YTHDC1 together with serine/arginine-rich splicing factor 3 and 10 (SRSF3, 10) (Ye et al., 2017). In the second report, the results together indicated that m^6A might play different roles depending on the cell-type used for the study. Surprisingly, opposing outcomes were obtained using similar cells than those used in the previous study: knockdown of YTHDF2 and METTL3 in B cells promoted an increase of ORF50/RTA expression (Hesser et al., 2018), while, consistent with Yen et al. (2017), virion production was impaired by the depletion of the same proteins in epithelial cells (iSLK.219 and iSLK.BAC16). However, a third study showed that viral and cellular epitranscriptomes are

conserved among several cell types. According to this report, YTHDF2 would promote the destabilization of viral lytic transcripts, leading to KSHV lytic replication inhibition (Tan et al., 2017). On the other hand, more recently, Baquero-Perez et al. (2019) characterized a new m^6A *reader* protein named SND1, which belongs to the "Royal family", a protein family that recognizes methyl groups in proteins. SND1 binding to m^6A nucleotides on RTA transcript stabilizes the molecule, so depletion of SND1 stops the expression of early-lytic genes. Therefore, although it seems well established that m^6A modulates the ORF50/RTA lytic transactivator, further investigations are required to clarify the discrepancies between the published works.

The contradictions found between studies about m^6A topology along vRNAs are probably due to different infection times evaluated, m^6A detection methodologies and/or cell types. So, it must be kept in mind that the conclusions from a specific study should be limited to the cell line and infection time tested. Interestingly, the apparently inconsistent observations about the m^6A function highlight that several m^6A-mediated strategies could regulate the same infection depending on the viral cycle stage and the m^6A localization (3 or 5'UTR, coding sequences, etc.). Then, we cannot dismiss a context-dependent m^6A role as a general rule during infections, although more investigations thereon will be needed to prove this hypothesis.

Table 1. Proposed mechanism or key available data of m^{6}A-modified viral RNA-mediated regulation for different infections. *(-)ssRNA viruses are in green, (+)ssRNA are in blue and DNA viruses are in gray. For viruses for which m^{6}A presents different effects, positive (+), negative (-) or combined (+/-) regulation is indicated at the beginning of each sentence.*

		Proposed mechanism/main data	References
Proviral regulation	IAV	METTL3-mediated m^{6}A and YTHDF2 promote viral expression. Increased m^{6}A levels in vRNAs that encode structural proteins (HA, NA M, NP).	Courtney et al., 2017
	SV40	METTL3-mediated m^{6}A and, presumably, YTHDF2 triggers nuclear export of the late transcripts, which likely enhances the expression of the capsid protein VP1.	Tsai, Courtney, & Cullen, 2018
	EBV	Viral oncoprotein EBNA3C is upregulated through METTL14-mediated m^{6}A and, in turn, enhances METTL14 transcription and protein stability.	Lang et al., 2019
	AV	METTL3-mediated m^{6}A drives late transcripts splicing.	Price et al., 2019
	RSV	m^{6}A may modify *Env* transcript splicing.	C. Martin Stoltzfus & Dane, 1982
	MLV	The *reader* YTHDF2 promotes viral replication. Mutations that abrogate some m^{6}A sites slightly reduce viral infectivity	Courtney et al., 2019
	EV71	Infection provokes a nucleocytoplasmic redistribution of m^{6}A machinery, colocalizing with VP1. Interaction between viral 3D polymerase and METTL3 would enhance the 3D sumoylation and ubiquitination and, consequently, promote viral infection.	Hao et al., 2019
	HRSV	m^{6}A, mainly present along transcripts of the attachment G protein, favors replication, gene expression, spread and virus release.	Xue et al., 2019
Antiviral regulation	HCV	METTL3/METTL14-mediated m^{6}A would favor the direct binding of YTHDF proteins to vRNA, impairing vRNA-HCV core protein interaction and, thus, virion assembly.	Gokhale et al., 2016
	ZIKV	m^{6}A negatively regulates the infection through YTHDF1-3 binding to vRNA.	Lichinchi et al., 2016b
Mixed regulation	HIV-1	+ METTL3/METTL14- and ALKBH5-regulated m^{6}A levels of HIV-RRE RNA positively modulate the binding of HIV-Rev protein, promoting mRNA nuclear export and favoring viral replication. + Viral translation and replication would be enhanced via YTHDF proteins recruitment by m^{6}A-containing 3'UTR of vRNAs. +/- m^{6}A has positive effects on Gag processing and virus release, but the overexpression of YTHDF1-3 inhibits viral RT. YTHDF1-3 proteins form a complex with HIV-1 Gag and viral gRNAs. - YTHDF3 protein is incorporated into virions, limiting the efficiency of the next round of infection. As counteract, viral protease cleaves the virion-encapsidated YTHDF3.	Lichinchi et al., 2016a Kennedy et al., 2016 Tirumuru et al., 2016; Lu et al., 2018 Jurczyszak et al., 2020
	HBV	m^{6}A at 5'UTR enhances pgRNA RT, while m^{6}A within the 3'UTR of all transcripts promotes RNA destabilization, probably by *readers* recognition.	Imam et al., 2018
	KSHV	+ METTL3-mediated m^{6}A promotes the expression of lytic genes and the production of viral particles, maybe through the action of FTO. m^{6}A-binding of YTHDC1 together with SRSF3 and SRSF10 regulate pre-mRNA splicing of ORF50/RTA (B cells). +/- m^{6}A role depends on the cell type. Proviral in epithelial cells and antiviral in B cells. METTL3-mediated m^{6}A inhibits ORF50/RTA expression, and YTHDF2 is likely implied (B cells). - Viral and cellular epitranscriptomes are conserved among several cell types. YTHDF2 would promote the destabilization of viral lytic transcripts, leading to KSHV lytic replication inhibition. + SND1 binding to m^{6}A residues on RTA transcripts stabilizes the molecule, promoting the expression of early-lytic genes.	Ye et al, 2017 Hesser et al., 2018 Tan et al., 2017 Baquero-Perez et al., 2019

5.2. Indirect m^{6}A-mediated viral regulation

Diverse studies showed that, in response to viral infections, host cells modulate both m^{6}A levels and distribution pattern along their mRNAs (Fig. 8) (for a recent review, see Williams et al., 2019). For most of them, however, the biological consequences of these cellular epitranscriptomic changes remain still unknown. For instance, HIV-1 infection produces an m^{6}A increase in the host mRNAs (Lichinchi et al., 2016a) in a viral replication-independent manner. In fact, increased m^{6}A levels in cellular mRNAs are observed in cells incubated with the envelope protein gp12 and infected with a heat-inactivated HIV-1 or a productive HIV-1 followed by a RT inhibition treatment. Thus, virus attachment, entry and early RT processes can trigger the activation of the m^{6}A deposition in host mRNAs (Tirumuru and Wu, 2019). m^{6}A methylation may constitute an additional layer of host gene expression that participates meaningfully in the transcriptional effects of chronic HIV (Fu et al., 2019). Besides, during the KSHV latent stage, m^{6}A/m^{6}A$_m$ ratio is higher in the 3'UTR and lower in 5'UTR mRNAs in KiSLK infected cells (Tan et al., 2017). On the other hand, Zhang et al. (2020) described m^{6}A changes in host mRNAs after *Bombyx mori nucleopolyhedrovirus* infection, a dsDNA virus that infects silkworms.

Thereby, in addition to directly modulate infections through the presence of m^{6}A on vRNA (Williams et al., 2019), the methylation pathway can also modify host mRNAs processes, such as splicing or stability, and, in turn, drive host response against viral infections. In this sense, the immune system keeps the homeostasis and is the most effective host defense against pathogen invasion in animals. Indeed, diverse studies described the relation between the m^{6}A-dependent innate immune response and viral infections. Zheng et al. (2017) showed that nuclear DEAD-box (DDX) helicases family member DDX46 interacts with ALKBH5 *eraser* to remove m^{6}A methylation from several host antiviral transcripts (Mitochondrial antiviral-signaling and tumor necrosis factor receptor (TNF-R)-associated factor 3 and 6), avoiding their nuclear export and, consequently, decreasing their translation. This phenomenon results in a type I IFN (IFN-I) reduction, and DDX46-ALKBH5 interaction is favored during the infection by *Vesicular stomatitis virus* (VSV), a cytoplasm-replicating (-)ssRNA virus. More recently, Gokhale et al. (2020) showed that *Flaviviridae* infection also provokes m^{6}A changes on host mRNA that, ultimately, modulate infection. Thus, mRNA of RIOK3, a protein kinase that regulates the antiviral innate immune response (Willemsen et al., 2017), presents an extra m^{6}A that promotes its translation in a YTHDF1-dependent manner during viral infection (Gokhale et al., 2020). Furthermore, m^{6}A is involved in IFN-mediated response against DNA viruses as well. Wang et al. (2019b) described that heterogeneous nuclear RNP A2B1 (hnRNPA2B1) recognizes viral DNA in the cell nucleus

during HSV-1 infection, what triggers the activation of the TANK-binding kinase 1–INF regulatory factor 3 (TBK1-IRF3) pathway and initiates IFN-I production. hnRNPA2B1 was proposed to enhance m^6A methylation and, consequently, nuclear exportation and translation of several mRNAs that participate in the IFN-I pathway activation in response to DNA viruses infection. Although Winkler et al. (2019) also reported a negative regulation of the IFN response by direct m^6A methylation of IFN-β mRNAs after infection with diverse viruses (*Human cytomegalovirus*, IAV, AV or VSV), an inactivated virus or dsDNA molecules. Nonetheless, inhibition of IFN signaling do not completely rescue IAV and AV gene expression in METTL3-depleted cells, revealing that IFN signaling is likely only partially responsible of this phenotype (Rubio et al., 2018; Winkler et al., 2019).

Other authors described that m^6A modulates host response against viral infection in an immune response-independent manner. Liu et al. (2019) demonstrated that, in VSV-infected cells, the arginine in position 107 (R107) of ALKBH5 protein is demethylated and, consequently, its enzymatic activity decreases. Therefore, m^6A levels of α-ketoglutarate dehydrogenase (OGDH) mRNA increase and, in turn, its stability and translation are reduced. OGDH is one of the components of the oxoglutarate dehydrogenase complex that participates in citric acid (TCA), lysine degradation and tryptophan metabolism pathways. Reduced OGDH levels negatively affects the synthesis of itaconate – a metabolite produced from *cis*-aconitate in the TCA cycle in macrophages and necessary for viral replication –,ultimately inhibiting viral infection (Liu et al., 2019).

On the other hand, silencing of the *reader* protein YTHDF3 was described to inhibit VSV, HSV-I and *Encephalomyocarditis virus* infections, independently of METTL3-mediated m^6A. Through its interaction with PAB1 and eIF4G2, YTHDF3 collaborates in the negative regulation of the IFN pathway by enhancing FOXO3 translation, a transcriptional repressor of interferon-stimulated genes (ISGs) (Zhang et al., 2019c). Likewise, some RNA-binding proteins, known to be part of SGs and repelled by m^6A-modified RNAs (Arguello et al., 2017; Edupuganti et al., 2017), were described as novel regulators of the IFN response against DENV-serotype 2 (DENV-2). These proteins appear necessary for the translation of several ISGs, and their activity is inhibited through the interaction of a DENV-2 non-coding RNA (Bidet et al., 2014). Conversely, other ISG-encoded RNA-binding proteins selectively recognize m^6A (Arguello et al., 2017; Edupuganti et al., 2017; Shaw et al., 2017), so it is possible that other uncharacterized IFN-induced proteins also affect viral infections by recognition or repelling m^6A modification on viral or cellular transcripts.

6. m^{6}A methylation in plant viral infections: everything is about to be done

First of all, to understand how this post-transcriptional regulation level could influence plant viral infections, it is worth explaining the plant response mechanisms against pathogens (Fig. 9).

To enter cells, animal viruses use cell surface receptors and endocytic pathways, whereas to overcome the rigidity of the cell wall, plant viruses usually take advantage of different biological vectors, such as insects, fungus, nematodes, etc. (Navarro et al., 2019). Plants, unlike vertebrates, do not possess mobile immune cells or an adaptative immune system. Instead, plants employ an array of mechanisms to limit viral infection: immune receptor signaling, hormone-mediated defense, metabolism regulation or gene silencing (Pallas and García, 2011; Calil and Fontes, 2017).

The immune receptor signaling comprises two linked levels to sense and act against pathogenic microorganisms. In the first level, cell surface pattern recognition receptors (PRR) identify microbe-, pathogen- or host-derived damage-associated molecular patterns (MAMPs, PAMPs or DAMPs), provoking the pattern-triggered immunity (PTI) (Nicaise et al., 2017; Han, 2019). In viral infections, Niehl and Heinlein (2019) proposed several scenarios for the perception of dsRNA by plant PRRs. In a second level, effector-triggered immunity (ETI) encompasses intracellular host resistance proteins (encoded by R genes), which recognize effector proteins known as Avirulence factors (Kourelis and Van Der Hoorn, 2018) to activate plant defense responses (Spoel and Dong, 2012). Examples of R genes against plant viruses in Arabidopsis are RCY1 gene against CMV, Tm-1 against *Tomato mosaic virus*, JAX1 against potexviruses, Scmv1 against *Sugarcane mosaic virus* and RTM1/RTM2 against *Tobacco etch virus*. Other R genes described are tobacco N gene against TMV, potato Rx1 and Rx2 genes against *Potato virus X*, rice STV11 gene against *Rice stripe virus*, tomato Ty-1 and Ty-3 genes against *Tomato yellow leaf curl virus*, tomato Sw-5 gene against *Tomato spotted wilt virus* and the I locus in bean against *Bean common mosaic virus* (Calil and Fontes, 2017). This signaling transduction cascade mediated by R proteins is associated with activation of calcium influx and production of reactive oxygen species that, through MAPK kinase signaling, induce the transcription of associated defense genes. Usually, R protein activation causes an hypersensitive response that consists of the programmed cellular death or apoptosis of the infected cells to avoid virus spread (Heath, 2000). ETI can ultimately confer a systemic acquired resistance, which, via production of pathogenesis-related proteins, protects plants from later infections (Hutcheson, 1998). The systemic acquired resistance is

provoked by the transportation from infected to uninfected systemic tissue of mobile immune signals, such as methyl salicylic acid, azelaic acid and glycerol-3-phosphate (Fu and Dong, 2013). Furthermore, recessive resistance genes (r) are specific host factors required for the virus to successfully complete the infection process. Most of the r genes encode translational factors of the 4E and 4G families, and the resistance in this case is due to the presence of a mutated version or to the absence of that factor. Recessive resistance has been described for *Bymo-*, *Carmo-*, *Cucumo-*, *Ipomo-*, *Poty-* and *Sobemovirus* genus (Revers and Nicaise, 2014).

Post-transcriptional gene silencing (PTGS) has been set out as one of the foremost defense mechanisms against invading nucleic acids (Voinnet, 2001). Highly-structured regions of ssRNA viral genomes, double-stranded viral RNAs (dsRNAs) formed during viral replication or bidirectional read-through overlapping mRNAs from DNA viruses are targets of Dicer-like (DCL) endonucleases, resulting in primary viral small interfering RNAs (vsiRNAs) (Voinnet, 2005). vsiRNAs are loaded in AGO proteins and form the RNA-induced silencing complex, which carries out cleavage or translation inhibition of complementary vRNAs (Carbonell and Carrington, 2015). Furthermore, plant RDRs can synthetize new dsRNA from the cleavage fragments of single-stranded vRNAs. In turn, that dsRNA can produce secondary vsiRNAs by DCLs activity, amplifying the antiviral defense (Ding, 2010; Carbonell and Carrington, 2015). In the last years, several authors reported a close relationship between epigenetic modifications – DNA and histone methylation, mainly – involved in the transcriptional gene silencing and plant viral infections (Wang et al., 2019a). The RNA-dependent DNA methylation (RdDM), which was thoroughly described in Arabidopsis (Zhang et al. 2018), is also mediated by siRNAs and produces *de novo* DNA methylation (Matzke and Mosher, 2014). Plant DNA viruses are targeted by RdDM, causing enhanced methylation of viral genome in geminivirus-infected Arabidopsis plants (Raja et al., 2008, 2014; Zhang et al., 2011; Butterbach et al., 2014; Coursey et al., 2018). In addition, Diezma-Navas et al. (2019) described that TRV infection is influenced by DNA methylation (Diezma-Navas et al., 2019). To counteract antiviral RNA silencing, most plant viruses encode proteins with RNA silencing suppressor activity denominated viral suppressors of RNA silencing. These factors can target virtually all steps of the RNA silencing pathway, restricting or even blocking this defense response (Pumplin and Voinnet, 2013; Csorba et al., 2015). The 2b protein of CMV (Hamera et al., 2012; Hui and Shou, 2002), the viral helper component-protease (HC-Pro) of *Potato virus A* (Ivanov et al., 2016) and C2, L2, AL2 and V2 proteins of geminiviruses (Wang et al., 2005, 2019c) are examples of VSR acting in different steps of the silencing pathway (Li and Wang, 2019).

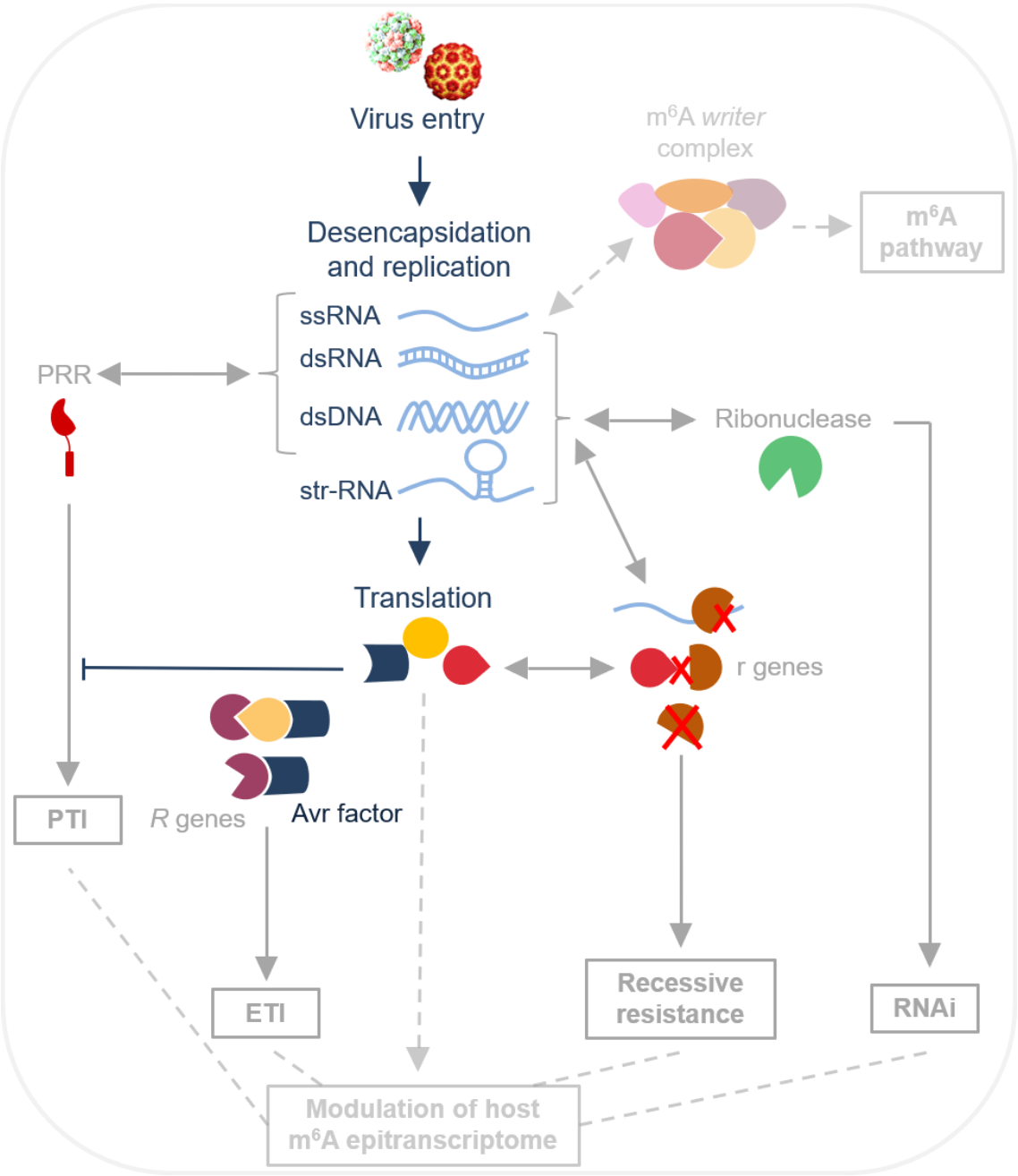

Figure 9. Hypothetical involvement of m^{6}A as part of plant response upon a viral infection. *At first, viral nucleic acids, which can adopt different structures, are perceived by ribonucleases that activate the RNAi. Besides, they might be recognized by PRRs, triggering the PTI. After translation, viral Avr factors might inhibit the PTI and, through direct or indirect interaction with R proteins, provoke the ETI. Furthermore, recessive resistance is conferred by r genes due to the lack of viral nucleic acids or proteins recognition or a deficiency of a negative regulator of the defensive response. In this scenario, m^{6}A pathway might regulate virus accumulation either by direct targeting vRNAs (representing a new and independent defense pathway) and/or through the modulation of the host mRNA epitranscriptome in response to the viral infection, likely affecting the expression of genes involved in any of the other response mechanisms. In dark blue, viral cycle stages; in gray, plant responses. The proposed m^{6}A role is displayed by discontinuous arrowheads and dim colors. str-RNA, structured-RNA.*

Likewise, RNA m^{6}A methylation might represent a novel host-virus interaction mechanism. By methylation of vRNAs and host mRNAs as response to the infection, m^{6}A would act as a host regulatory strategy to control viral growth and/or a viral mechanism to modulate host gene

expression for its own benefit. Unfortunately, despite the fact that most of plant viruses present RNA genomes, the implication of this mechanism in plant viral infections has been scarcely studied. Apart from the work included in this Thesis manuscript (Martínez-Pérez et al., 2017), just a few more references can be found in the literature. According to Li et al. (2018), m^6A levels in *Nicotiana tabacum* mRNAs are lower in TMV infected plants, and the infection induces the expression of a potential *eraser*, orthologous to human ALKBH5, and represses the expression of potential *writers*. Interestingly, some other studies described the presence of AlkB domains in the replicase coding region of some (+)ssRNA plant viruses (Aravind and Koonin, 2001; Martelli et al., 2007), belonging most of them to the *Alphaflexiviridae, Betaflexiviridae* and *Closteroviridae* families. Later, these viral AlkB domains were reported to revert methylation-induced lesions in bacteriophages (Van den Born et al., 2008). In addition, a recent bioinformatic analysis concluded that a region of 150-170 aa forms the viral AlkB functional domain, which has some characteristic residues that are not conserved in the AlkBs from other organisms (Moore and Meng, 2019). Since all these viruses infect perennial plants, the authors suggested that this domain may carry out a counteracting role against the host defense system and it might constitute an evolutionary mechanism to promote long-term survival in this kind of pathosystems. However, *in vitro* and *in vivo* activity assays will be needed to clearly demonstrate their functionality, which might consist on m^6A demethylation.

Thereby, much more studies are required to decipher how m^6A regulation affects plant viral genome/transcripts and host mRNAs fate upon infection, and how it might influence the expression of plant immune factors of the already described pathways, such as R genes or RNA silencing effectors (Fig. 9).

Motivation and objectives

Viruses are obligate parasites that can be found in all living organisms and potentially can cause health problems and economic losses in agriculture and livestock farming. The main pathosystem used in this Thesis is the interaction of *Alfalfa mosaic virus* (AMV) with the model plant *Arabidopsis thaliana*. AMV belongs to the *Alfamovirus* genus, in the *Bromoviridae* family, and affects nearly the worldwide production of alfalfa, causing, moreover, economic losses in important crops, such as potato (*Solanum tuberosum),* tomato (*Solanum lycopersicum*) or soybean (*Glycine max*) (Escriu et al., 2011). AMV genome consists of a tripartite positive-sense single-stranded RNA and its study has significantly contributed to the advance on the knowledge of plant infections caused by RNA viruses (Bol, 2008). Research about AMV has shed light on different important aspects of infection cycles, such as genome activation, viral replication, translation regulation and virus movement.

The starting point of this Thesis was the discovery of the interaction between the coat protein of AMV and an Arabidopsis protein showing similarity with a human RNA demethylase. Modification of the canonical nucleotides can produce RNA structure changes that affect intramolecular interactions or their binding to other factors, including host proteins. Thus, these modifications on mRNAs establish another level of gene expression regulation. One of the most widespread and fundamental modified bases of eukaryotic mRNAs is the N^6-methyladenosine (m^6A), which was found in mRNAs of mammals, insects, plants, yeast and animal-infecting viruses (Liang et al., 2018; Dang et al., 2019). The main eukaryotic methyltransferase (m^6A *writers*) is a highly conserved complex whose composition in plants includes a catalytic core formed by two MTA-70 family proteins (MTA, AT4G10760 and MTB, AT4G09980) and several required factors that compound MT-B subcomplex (Zhong et al., 2008; Shen et al., 2016; Růžička et al., 2017). However, although proteins described as *erasers* are thought to belong to AlkB family, at the beginning of this Thesis, any of them had been functionally characterized in plants (Mielecki et al., 2012). On the other hand, the best characterized m^6A *readers* comprise RNA-binding proteins with a so-called YT521-B homology (YTH) domain (Zhang et al., 2010). These proteins specifically bind m^6A-modified RNAs via a hydrophobic pocket made of aromatic amino acid side chains (Theler et al., 2014) to modulate multiple aspects of RNA metabolism, like pre-mRNA splicing, nuclear export, translation regulation and RNA stability (for recent reviews, see Zaccara et al., 2019 and Arribas-Hernández & Brodersen, 2020). In Arabidopsis, the YTH family is mainly composed of 11 proteins called EVOLUTIONARILY CONSERVED C-TERMINAL REGION proteins 1-11 (ECT1-11), that belong to the subclade YTHDF (Li et al., 2014a). During the course of this Thesis, ECT2, ECT3 and ECT4 were characterized as cytoplasmic m^6A *readers* that have a

crucial function in m^{6}A-dependent control of plant organogenesis (Arribas-Hernández et al., 2018).

Although the m^{6}A mark was already detected in 1975 in viral mRNAs of *Simian Virus 40* (Lavi and Shatkin, 1975), it is only during the last few years, together with the technology development (for a recent review, see Linder & Jaffrey, 2019), when several studies have addressed the function of m^{6}A in multiple animal-infecting virus cycles (Williams et al., 2019). Some authors reported that the presence of m^{6}A residues in viral RNAs from viruses with either RNA or DNA genomes modulates the infection, in some occasions, through the direct binding of YTH proteins to m^{6}A-modified viral RNA. However, none m^{6}A-modified plant virus has been described so far and the potential relevance of this molecular mechanism on plant viral infections remains unknown.

Thus, the main objective of this Thesis work is to decipher the putative role of the m^{6}A methylation mechanism modulating viral infections in plants. To address this global objective, the following three partial objectives were defined:

Objective 1. Characterization of the potential m^{6}A demethylase protein (atALKBH9B) and evaluation of its function in the AMV infection cycle.

Objective 2. Identification of other host m^{6}A machinery components involved in the AMV infection cycle and analysis of the molecular mechanisms behind their implication.

Objective 3. Study of the implication of m^{6}A mechanism in other plant viral infections.

Thus, the characterization of the putative m^{6}A *eraser* (atALKBH9B) and the evaluation of its function in AMV infection is presented in Chapter I, whereas the identification of other m^{6}A host components involved in the life cycle of this virus and the analysis of the molecular mechanisms behind their implication is presented in Chapter II. Studies on the analysis of the involvement of atALKBH9B or other host components regulating m^{6}A modification in other viruses are described in the corresponding chapters.

Chapter I

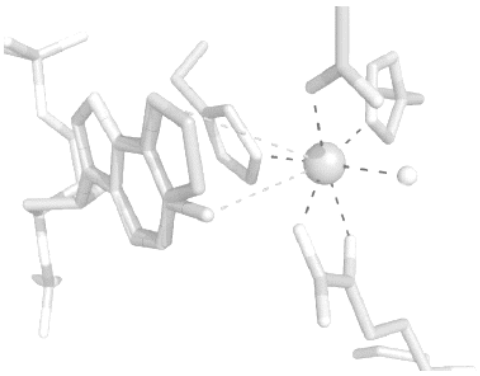

Arabidopsis m^{6}A demethylase activity modulates viral infection of a plant virus and the m^{6}A abundance in its genomic RNAs

Some of the results of this chapter are part of the following publication:

Martínez-Pérez, M., Aparicio, F., López-Gresa, M.P., Bellés, J.M., Sánchez-Navarro, J.A. and Pallás, V. (2017). Arabidopsis m^{6}A demethylase activity modulates viral infection of a plant virus and the m^{6}A abundance in its genomic RNAs. PNAS **114**: 10755–10760.

Abstract

N^6-methyladenosine (m^{6}A) is an internal, reversible nucleotide modification that constitutes an important regulatory mechanism in RNA biology. Unlike mammals and yeast, no component of the m^{6}A cellular machinery has been described in plants at present. m^{6}A has been identified in the genomic RNAs of diverse mammalian viruses and, additionally, viral infection was found to be modulated by the abundance of m^{6}A in viral RNAs. Here we show that the *Arabidopsis thaliana* protein ALKBH9B (At2g17970) is a demethylase that removes m^{6}A from single-stranded RNA molecules *in vitro*. atALKBH9B accumulates in cytoplasmic granules that colocalize with siRNA-bodies and associate to P-bodies, suggesting that atALKBH9B m^{6}A demethylase activity could be linked to mRNA silencing and/or mRNA decay processes. Moreover, we identified the presence of m^{6}A in the RNAs of two members of the *Bromoviridae* family, *Alfalfa mosaic virus* (AMV) and *Cucumber mosaic virus* (CMV), and other two viruses, *Turnip crinkle virus* (TCV) and *Cauliflower mosaic virus* (CaMV). Suppression of atALKBH9B increased the relative abundance of m^{6}A in the AMV genome, but not in CMV genome, correlating with the ability of atALKBH9B to interact (or not) with their coat proteins. Similarly, the demethylation activity of atALKBH9B affected the infectivity of AMV but not of CMV, TCV and CaMV. Our findings suggest that, while atALKBH9B role seems to be specific for AMV, as recently found in animal viruses, m^{6}A modification may represent a plant regulatory strategy to control not only viruses replicating in the nucleus, but also cytoplasm-replicating RNA viruses.

Key words: m^{6}A, demethylase, ALKBH9B, plant virus, coat protein.

Significance

N^6-methyladenosine (m^{6}A) modification has been found to constitute an important regulatory mechanism in RNA biology. Unlike mammals and yeast, no component of the m^{6}A cellular machinery has been described in plants at present. Although the influence of the m^{6}A cellular machinery has been suspected to occur in the plant virus cycle, it has never been proved. Here we have identified the first plant protein with m^{6}A demethylase activity (atALKBH9B) and demonstrate that this protein removes m^{6}A modification from RNA *in vitro*. Remarkably, we found that m^{6}A abundance on the viral genome of *Alfalfa mosaic virus* (AMV) is influenced by atALKBH9B activity and regulates viral infection. This study extends the vast repertoire that plants exploit to control cytoplasm-replicating RNA viruses.

Introduction

N^6-methyladenosine (m^{6}A) is an internal, reversible nucleotide modification present in RNAs of mammals, insects, plants, yeast, and animal viruses that participates in RNA biology through diverse mechanisms such as regulation of mRNA stability (Wang et al., 2014; Xu et al., 2014), translation (Meyer et al., 2015; Wang et al., 2015), nuclear export (Zheng et al., 2013), exon splicing (Zhao et al., 2014), and protein/RNA interactions (Liu et al., 2015).

In mammals, RNA m^{6}A methylation is catalyzed by a polyprotein complex composed of METTL3, METTL14, WTAP, KIAA1429 and several cofactors not yet identified (Liu et al., 2014; Ping et al., 2014; Schwartz et al., 2014). Removal of the m^{6}A is carried out by two RNA demethylases belonging to the AlkB family of non-heme Fe(II)/α-ketoglutarate (α-KG)-dependent dioxygenases, fat mass and obesity-associated protein (FTO) and ALKBH5 (Jia et al., 2011; Zheng et al., 2013). In addition, several proteins (YTHDF1, YTHDF2, YTHDF3, YTHDC, eIF3, and HNRNPC) bind to the m^{6}A-modified mRNAs to control their stability and translation (Fu et al., 2014; Wang et al., 2014; Xu et al., 2014; Xiao et al., 2016).

The internal m^{6}A modification was also found in viral RNAs (vRNAs) of animal viruses that replicate either in the nucleus or in the cytoplasm, representing a mechanism for the regulation of the viral life cycle (Kane and Beemon, 1985; Gokhale et al., 2016; Kennedy et al., 2016; Lichinchi et al., 2016a, 2016b; Tirumuru et al., 2016). Silencing of METTL3/14 decreases HIV-1 replication, whereas depletion of ALKBH5 enhances the export of vRNAs from the nucleus and protein expression, which consequently increases viral replication (Lichinchi et al., 2016a; Tirumuru et al., 2016). However, *Hepatitis C virus* (HCV) and *Zika virus* (ZIKV) infection are positively and negatively regulated by knockdown of METTL3/14 and ALKBH5 or FTO, respectively (Gokhale et al., 2016; Lichinchi et al., 2016b). Further, depletion of YTHDF proteins promotes ZIKV and HCV vRNA expression (Gokhale et al., 2016; Lichinchi et al., 2016b), while in the case of HIV-1, positive (Kennedy et al., 2016) and negative (Tirumuru et al., 2016) effects on HIV-1 vRNA expression were reported. Furthermore, the host machinery that controls m^{6}A methylation detects viral infection and regulates gene expression by modulating the m^{6}A levels of host mRNAs (Lichinchi et al., 2016a, 2016b).

In contrast to mammals, very few studies on the function of m^{6}A have been reported in plants. Transcriptome-wide profiles in *Arabidopsis thaliana* detected this modification in over two-thirds of the mRNAs (Wan et al., 2015). A METTL3 homolog in Arabidopsis (MTA) was identified as a critical factor in plant development (Bodi et al., 2012; Zhong et al., 2008). In addition, the

Arabidopsis FIP37 protein, a plant homolog of WTAP, interacts *in vitro* and *in vivo* with MTA and is essential to mediate m^6A mRNA modification of key shoot meristem genes (Zhong et al., 2008; Shen et al., 2016). However, no demethylase or YTHDF plant activities have been described at present. The Arabidopsis genome contains 13 homologs of *Escherichia coli* AlkB (atALKBH1-10B) (Mielecki et al., 2012). Although their functional characterization has not been reported, a subcellular localization study showed that all of these proteins display a nucleocytoplasmic localization pattern except atALKBH1D, which localizes to the chloroplast as well, and atALKBH9B, which is exclusively cytoplasmic (Mielecki et al., 2012). Interestingly, an AlkB domain was identified in the ORF of the replicase genes from diverse plant viruses. These domains were found to be functional in removing m^1A and m^3C modifications from RNA and DNA *in vitro*, suggesting that the replicase proteins play a role in reversing methylation modifications in the viral genomes (Van den Born et al., 2008).

In this work, we identify a plant protein with m^6A demethylase activity (atALKBH9B) in Arabidopsis and show that the protein interacts with the coat protein (CP) of *Alfalfa mosaic virus* (AMV) in the cell cytoplasm. The AMV genome consists of three single-stranded RNAs of positive sense polarity. RNAs 1 and 2 encode the replicase subunits, whereas RNA 3 encodes the movement protein and serves as a template for the synthesis of nonreplicating subgenomic RNA 4 (sgRNA 4), which encodes the CP (Bol, 2005). The AMV CP localizes to both the nucleus/nucleous and the cytoplasm (Herranz et al., 2012), although viral replication occurs in the cytoplasm, most probably associated with the tonoplast membrane (Ibrahim et al., 2012). We find that an Arabidopsis knockout mutation of atALKBH9B negatively affects virus accumulation and systemic invasion, correlating with increased levels of m^6A of the vRNAs. Our results show that the viral genome methylation state plays a key role in the life cycle of a plant virus.

Results

Arabidopsis atALKBH9B interacts with the CP and the vRNA of AMV. The CP of AMV is a multifunctional protein that participates in replication, translation, viral movement and encapsidation (Bol, 2005; Pallas et al., 2013), which most likely implies that this protein interacts with host factors involved in diverse cellular functions (Balasubramaniam et al., 2014; Aparicio and Pallás, 2017). A yeast two-hybrid (Y2H) screening, using the CP as bait and an Arabidopsis leaf-specific cDNA library as the prey, was performed to identify host proteins that interact with

the AMV CP. Several clones containing part of the atALKBH9B gene (at2g17970) ORF were found to grow on interaction minimal synthetic selective medium (Fig. 1A). To validate the original Y2H screening, the full-length atALKBH9B ORF was fused to the activation domain (pAD plasmid) and transformed into yeast cells expressing the AMV CP fused to the binding domain (pBD plasmid). After growth at 28 °C for 5 d on interaction selective medium, we found that the AMV CP specifically interacted with atALKBH9B but not with the empty pBD vector or the one expressing the Gal4 binding domain fused with lamin (pBD:LAM) (Fig. 1B). To corroborate this interaction, histidine-tagged atALKBH9B (His-atALKBH9B) and the N-terminal fragment of YFP (His-NYFP) were expressed in *E. coli* and purified by Ni-NTA agarose chromatography. Before the elution step, Ni-NTA columns containing his-tagged proteins were incubated with purified AMV virions. Western blot analysis using anti-CP antibody of eluates after incubation with viral particles showed that virions interacted with atALKBH9B but not with NYFP (Fig. 1C). To confirm that the CP–atALKBH9B interaction occurs in planta we used bimolecular fluorescence complementation (BiFC) analysis. Confocal laser scanning microscopy (CLSM) images showed that reconstituted YFP fluorescence formed discrete granules in cells of *Nicotiana benthamiana* infiltrated with atALKBH9B plus AMV CP but not when the host protein was coinfiltrated with the C-terminal fragment of YFP alone (CYFP) (Fig. 1D). Finally, a north-western blot assay demonstrated that atALKBH9B interacts with vRNA, showing that the protein has RNA binding activity (Fig. 1E).

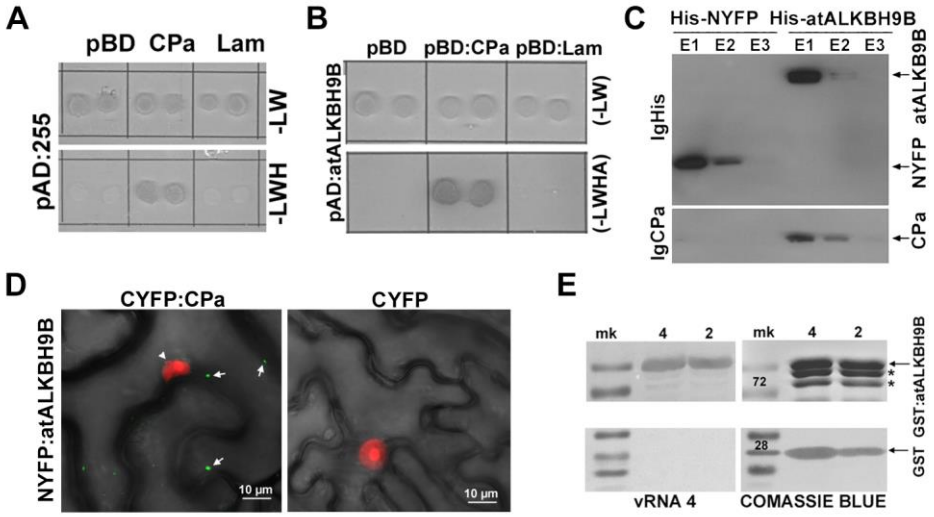

Figure 1. atALKBH9B interacts with the CP of AMV in vitro and in vivo and with the vRNA. (A) *Identification of clones interacting with the AMV CP by Y2H screening of an Arabidopsis cDNA library. After sequencing, these clones corresponded to atALKB9B ORF.* ***(B)*** *Y2H analysis of the interaction between AMV CP and atALKBH9B. Interacting colonies were identified by growth after 5 d on medium lacking leucine, tryptophan, histidine and adenine (–LWHA).* ***(C)*** *Immunoblot analysis of coimmunoprecipitated products after incubation of AMV virions and the histidine-tagged proteins indicated above the figure. Eluted (E1–E3) proteins were detected with antibodies against the His-tag (IgHis) and the CP of AMV (IgCP). The CP was only detected when virions were incubated with His-atALKBH9B.* ***(D)*** *BiFC images of epidermal cells co-infiltrated with the indicated constructs. YFP reconstitution was found to form discrete granules in the cytoplasm (arrows). Fibrillarin fused to the mCherry protein was used to identify the cell nuclei (arrowhead). Pictures are the overlapped images of green, red, and transmitted channels.* ***(E)*** *Analysis of the RNA binding activity*

of atALKBH9B by north-western blot assay. Duplicate membranes with purified GST:atALKBH9B (Upper) or GST proteins (Lower) (4 and 2 µg) were incubated with vRNA 4 (Left) to show the RNA binding activity or stained with Coomassie blue (Right) to confirm the presence of the proteins. Positions of full-length GST and GST:atALKBH9B proteins are indicated by arrows. Asterisks denote truncated GST:atALKBH9B.

Arabidopsis atALKBH9B activity modulates AMV infection. To investigate possible roles for atALKBH9B in virus infection, we searched for T-DNA insertions in *atALKBH9B*. We identified a homozygous T3 line in the Nottingham Arabidopsis Stock Centre (N671317; SALK_015591, ecotype Col-0) with a T-DNA insertion in exon 4 (Fig. 2A). Absence of atALKBH9B mRNA expression was confirmed by RT-PCR with gene-specific primers (Fig. 2B).

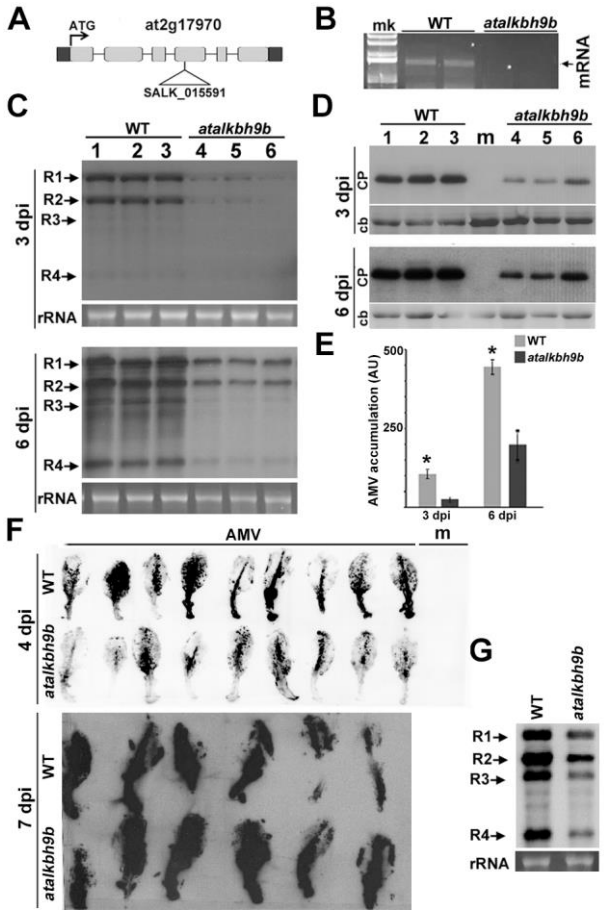

Figure 2. AMV local infection is impaired in atalkbh9b plants. (A) *Annotated genomic atALKBH9B gene structure showing the exons (gray boxes) and location of the T-DNA insertion (SALK_015591).* ***(B)*** *Agarose gel electrophoresis of RT-PCR products produced with specific primers to amplify the full-length mRNA of the atALKBH9B gene from WT and atalkbh9b plants. The position of the mRNA is indicated on the Right.* ***(C and D)*** *Representative northern and western blots from inoculated leaves at 3 and 6 dpi of three WT and atalkbh9b plants. Positions of the vRNAs and CP are indicated on the left. Ethidium bromide and Coomassie blue staining of ribosomal RNAs (rRNA) and total protein extracts (cb, coomassie blue) were used as RNA and protein loading controls.* ***(E)*** *Graphic showing the average of vRNAs accumulation in WT and atalkbh9b mutant. SD values are shown. Asterisks indicate significant differences from the WT (*P<0.05) using Student's t-test (n=3). AU, arbitrary units.* ***(F)*** *Tissue printing of inoculated leaves from WT and atalkbh9b plants at 4 dpi (upper panel) and 7 dpi (bottom panel). m corresponds to mock inoculated plants.* ***(G)*** *Northern blot of inoculated protoplasts from WT and atalkbh9b plants. Positions of the AMV RNAs are indicated on the left. Ethidium bromide staining of rRNA was used as RNA loading control.*

To determine whether reduced levels of atALKBH9B affect virus infection, WT Col-0 and *atalkbh9b* plants were inoculated with AMV viral particles. Total RNA and proteins were extracted and vRNA and CP accumulation were analyzed at 3 and 6 d post-inoculation (dpi) by northern and western blots using a digoxigenin-labelled probe to detect the vRNAs (DigAMV) and a specific anti-CP antibody, respectively. We found that levels of both vRNAs and CP were clearly reduced in *atalkbh9b* compared with WT plants (Fig. 2C-E), indicating that viral accumulation is impaired in *atalkbh9b* plants. Moreover, we addressed an analysis to determine the viral distribution of the virus in leaves. Thus, inoculated leaves from WT and *atalkbh9b* plants

were printed onto nylon membranes at 4 and 7 dpi and AMV RNAs were detected with the corresponding DigAMV probe (Fig. 2F). While most of WT leaves petioles were already infected at 4 dpi, the infection in *atalkbh9b* petioles were not detectable until 7 dpi, suggesting a delay in the viral infection progress in the plant. Next, to evaluate if the infection delay was only caused by restriction in virus movement, or, additionally, the viral replication and/or translation steps were impaired in *atalkbh9b* plants, viral accumulation levels were analyzed in protoplasts. Northern blot analysis of total RNA extracted from AMV inoculated WT and *atalkbh9b* protoplasts showed a lower viral load in the mutant (Fig. 2G), indicating that replication and/or translation processes are also affected by the absence of this protein.

On the other hand, AMV systemic movement was analyzed in two plant organs: roots and floral stems, since seed transmission in the dispersion of this virus is especially important. After total RNA extraction, vRNA load in these tissues was evaluated by northern and dot blot assays (Fig. 3A and B). The results showed that AMV systemic movement is impaired in *atalkbh9b* plants since, while in roots of WT plants the viral invasion was clearly appreciably at 7 dpi, it was almost undetectable in mutant plants (Fig. 3A). Likewise, at 14 dpi, the floral stems were infected only in 9% of *atalkbh9b* plants, while this percentage reached 100% in WT plants (Fig. 3B). Overall, these results indicate that atALKBH9B positively regulates AMV infection, taking part since the first stages of the viral cycle.

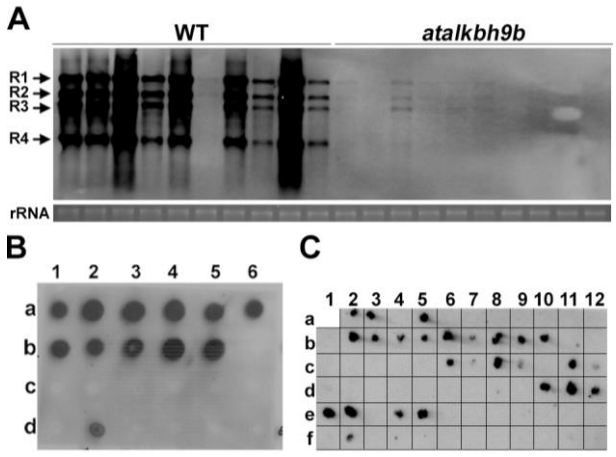

Figure 3. AMV systemic infection is impaired in atalkbh9b plants, but not in the absence of atALKBH9A and/or atALKBH9C. (A) *Northern blot of roots from infected WT and atalkbh9b plants. Positions of the AMV RNAs are indicated on the left. Ethidium bromide staining of rRNA was used as RNA loading control.* ***(B)*** *Dot blot hybridization of floral stems to determine the extent of viral systemic movement. Dots in rows a and b correspond to WT plants; dots in c and d correspond to atalkbh9b plants. Samples b6 and d6 are healthy WT and atalkbh9b plants used as negative controls.* ***(C)*** *Tissue printing of floral stems from infected plants: WT (a2-a5), atalkbh9b (a6-b1 and b11-c5), atalkbh9a (b2-b10), atalkbh9c (c6-c12), atalkbh9a/atalkbh9b (d1-d9), atalkbh9a/atalkbh9c (d10-e5), atalkbh9b/atalkbh9c (e6-f3) and atalkbh9a/atalkbh9b/atalkbh9c (f4-f12).*

Taken into account that in Arabidopsis ALKBH9 members form a specific clade containing atALKBH9A, atALKBH9B and atALKBH9C genes (Fig. 4) (Mielecki et al., 2012), we carried out a

study to check whether atALKBH9A and/or atALKBH9C might be also playing a role in AMV systemic infection. The effect on viral systemic movement of the simple *atalkbh9a, atalkbh9b* and *atalkbh9c*, double *atalkbh9a/atalkbh9b, atalkbh9a/atalkbh9c* and *atalkbh9b/atalkbh9c* and triple *atalkbh9a/atalkbh9b/atalkbh9c* mutants was analyzed by detecting AMV accumulation in floral stems by tissue printing at 12 dpi. As shown in Fig. 3C, the viral systemic movement was impaired only in plants lacking atALKBH9B, indicating that neither atALKBH9A nor atALKBH9C are required for the systemic invasion of the plant.

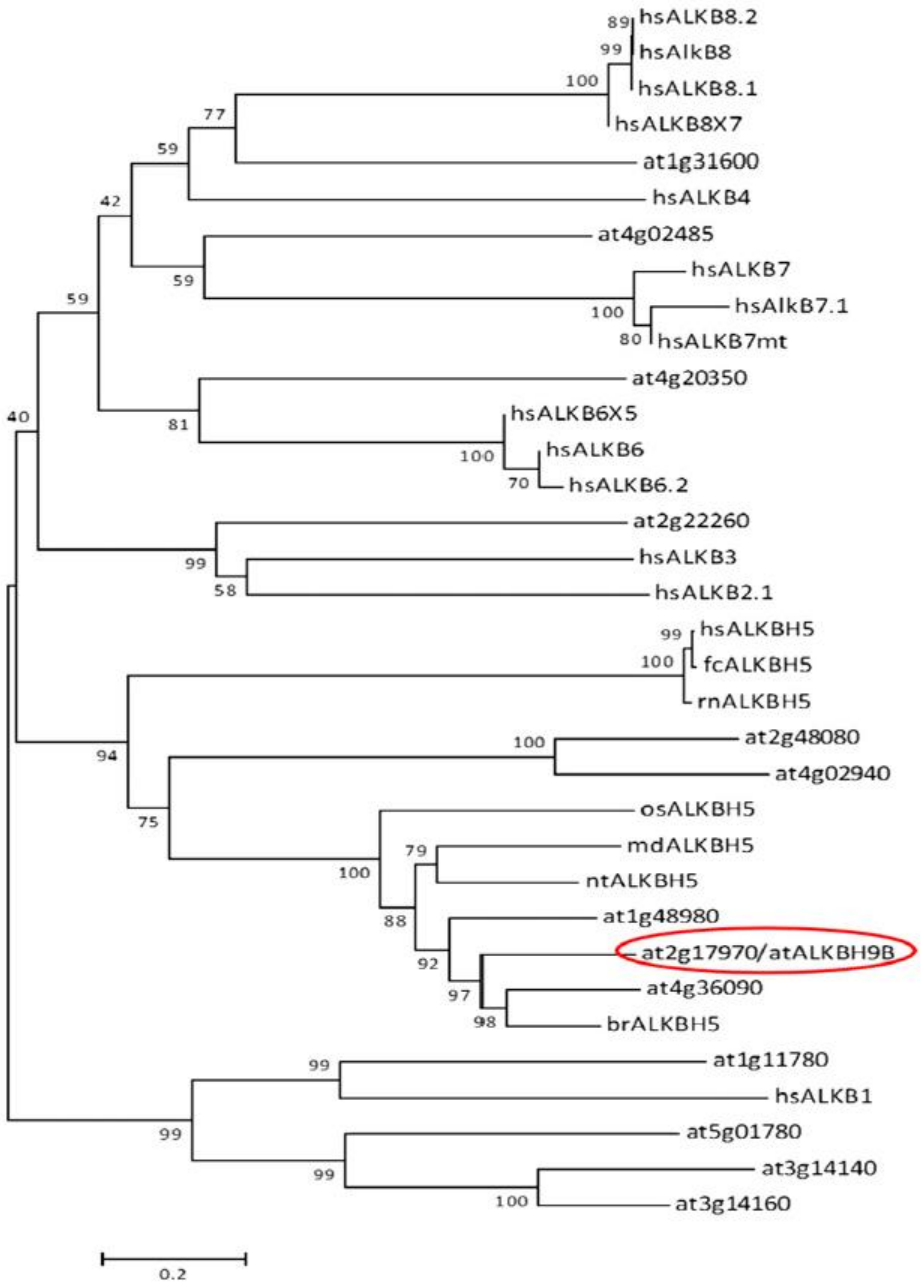

Figure 4. Rootless phylogenetic tree derived from the Clustal Omega analysis between proteins of the AlkB family belonging to different species. *Basic local alignment search (BLAST) web tool (National Center for Biotechnology Information) was used to compare the amino acid sequence of the protein atALKBH9B against a large number of sequences available in the databases. A total of 34 protein sequences were selected with which a multiple alignment was then performed by Clustal Omega (Sievers et al., 2011), available from the European Molecular Biology*

Laboratory–European Bioinformatics Institute website. Finally, using this alignment, a rootless phylogenetic tree was constructed in the MEGA v.6.0 program (Tamura et al., 2013). The minimum evolution method was selected as the statistical method, and the bootstrap (Nei and Saitou, 1987) analysis, with 10,000 replicates, was tested as a phylogeny test. The tree was drawn to scale, with branch lengths in the same units as those of the evolutionary distances used to infer the phylogenetic tree. The evolutionary distances were calculated using the Poisson correction method and they are found in units of number of amino acid substitutions per site. The minimal evolution tree was recorded using the close neighbor interchange (CNI) algorithm at a search level of 1. The neighbor-joining algorithm was used to generate the initial tree. All ambiguous positions were removed for each pair of sequences. A pairwise deletion method was selected for the treatment of gaps. atALKBH9B protein (at2g17970), circled in red, enclosed in a small cluster that encompasses its homologous proteins from other vegetables and this, in turn, in a larger group including the ALKBH5 protein, already described and studied in mammals. The bootstrap values are indicated on each node. At, Arabidopsis thaliana; br, Brassica rapa; fc, Felis catus; hs, Homo sapiens; md, Malus domestica; nt, Nicotiana tomentosiformis; oz, Oryza sativa; and rn, Rattus norvegicus.

atALKBH9B localizes to cytoplasmic bodies. atALKBH9B is one of the 13 homologs of *E. coli* AlkB, and it is the only one that is uniquely located in the cytoplasm (Mielecki et al., 2012). We first performed a sequence similarity analysis, which showed that five Arabidopsis AlkB homologs, including atALKBH9B, grouped in the same branch with human ALKBH5 (Fig. 4). Hence, these proteins might be orthologous to the human protein and other prospective m^6A demethylases. Then, we transiently expressed translational fusions with GFP (GFP:atALKBH9B and atALKBH9B:GFP) by agroinfiltration in *N. benthamiana* leaves to determine more precisely the atALKBH9B subcellular localization. CLSM images showed that atALKBH9B:GFP was localized as a diffuse pattern throughout the cytoplasm, while GFP:atALKBH9B was accumulated in small cytoplasmic granules and filaments (Fig. 5A). It was proposed that m^6A methylation functions in the cytoplasm, serving as a reversible tag to direct mRNAs to processing bodies (P-bodies) (Fu et al., 2014). Moreover, several studies demonstrated that P-bodies dynamically associate with siRNA bodies, and the latter are implicated in post-transcriptional gene silencing (PTGS) through the synthesis of dsRNAs to generate siRNAs (Kumakura et al., 2009; Martínez de Alba et al., 2015). We reasoned that atALKBH9B-forming granules might be related to siRNA and/or P-bodies. To test this hypothesis, we performed colocalization experiments in mock and AMV-infected *N. benthamiana* leaves by co-expressing atALKBH9B with DCP1 (a decapping enzyme located in P-bodies) and SGS3 (a component of siRNA bodies) (Ingelfinger et al., 2002; Kumakura et al., 2009) fused to fluorescent proteins. CLSM images showed that atALKBH9B granules perfectly colocalized with siRNA bodies, whereas ∼40% of the atALKBH9B granules were spatially associated with P-bodies (Fig. 5B). These results suggest that atALKBH9B might be a new component of siRNA bodies and P-bodies.

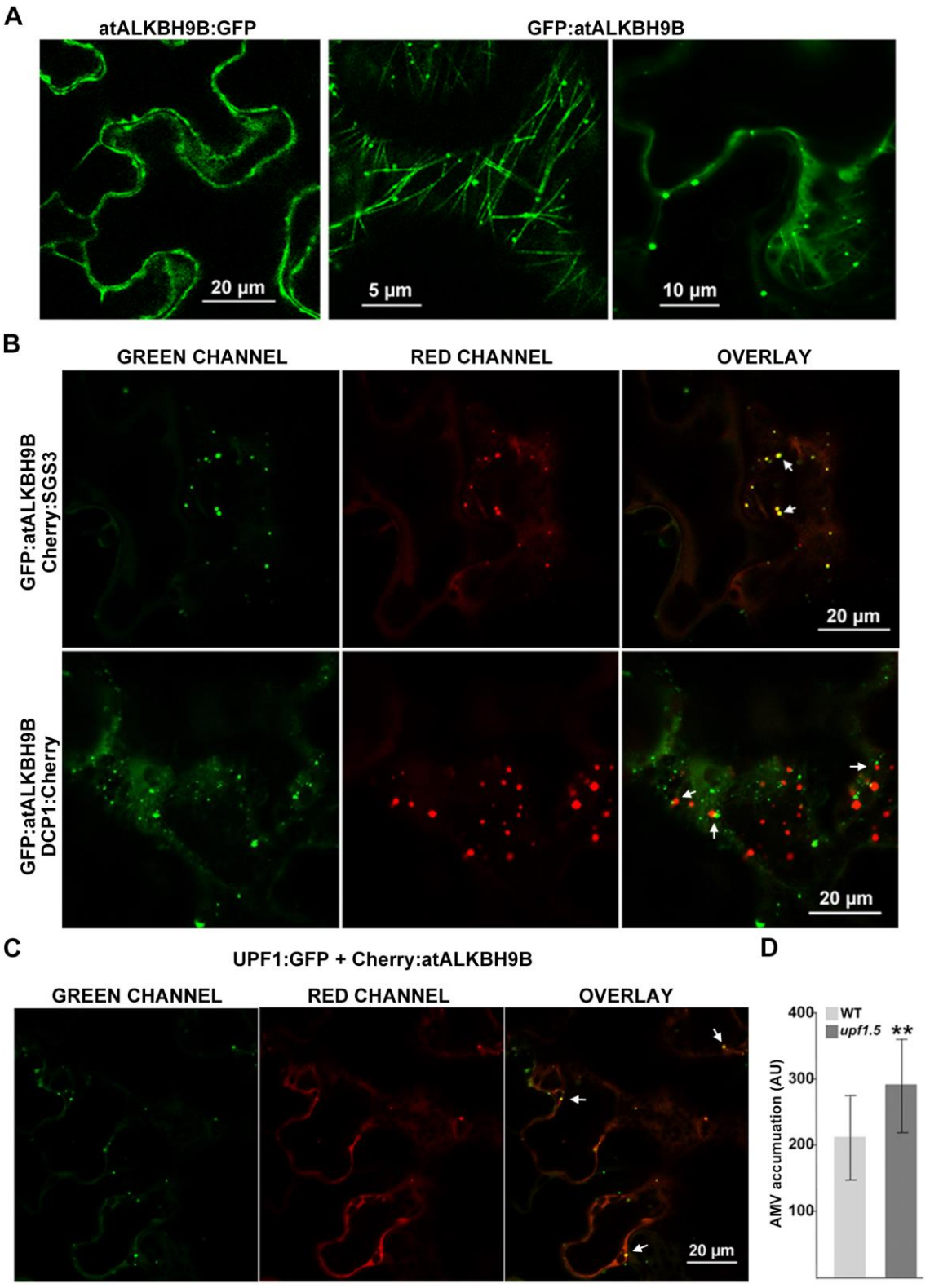

Figure 5. atALKBH9B protein colocalizes with siRNA-bodies/P-bodies components. ***(A)*** *Confocal laser microscope scanning images (CLSM) of N. benthamiana cells agroinfiltrated with the GFP fused to the N- and C-terminal ends of atALKBH9B.* ***(B and C)*** *CLSM images of N. benthamiana leaf epidermal cells co-infiltrated with the DNA constructs indicated above the images. Overlay panels are the superposition of images from the green and red channels. Arrowheads indicate granules with both proteins.* ***(D)*** *vRNAs accumulation in upf1.5 mutant with respect to WT. SD values are shown. Asterisks indicate significant differences from the WT (**P<0.01) using Student's t-test (n=20). AU, arbitrary units.*

Recently, the nonsense-mediated mRNA decay system (NMD) was proposed to work as viral restriction mechanism in plants (Garcia et al., 2014). The regulator of nonsense transcripts 1 (UPF1) is a critical component of this RNA quality control system and was found to be linked to P-bodies (Merai et al., 2013). To shed light on which viral functions might be modulated by m^6A modification, we analyzed the impact of the NMD in AMV infection. Subcellular localization of UPF1 by CLMS showed that the construct atUPF1:GFP also formed cytoplasmic discrete granules colocalizing with mCherry:atALKBH9B (Fig. 5C). Further, the analysis of vRNAs accumulation revealed a significant enhancement in systemic leaves of Arabidopsis *upf1.5* mutant plants (at5g47010; SALK_112922) (Fig. 5C). Moreover, AMV infection do not seem to affect atALKBH9B localization, as the colocalization with SGS3 and the spatial association with DCP1 were also observed in infected tissue (Fig. 6). Altogether, our results suggest that atALKBH9B might be a new component of siRNA bodies and P-bodies and, as found in other plant viruses (Garcia et al., 2014), NMD would restrict AMV infection.

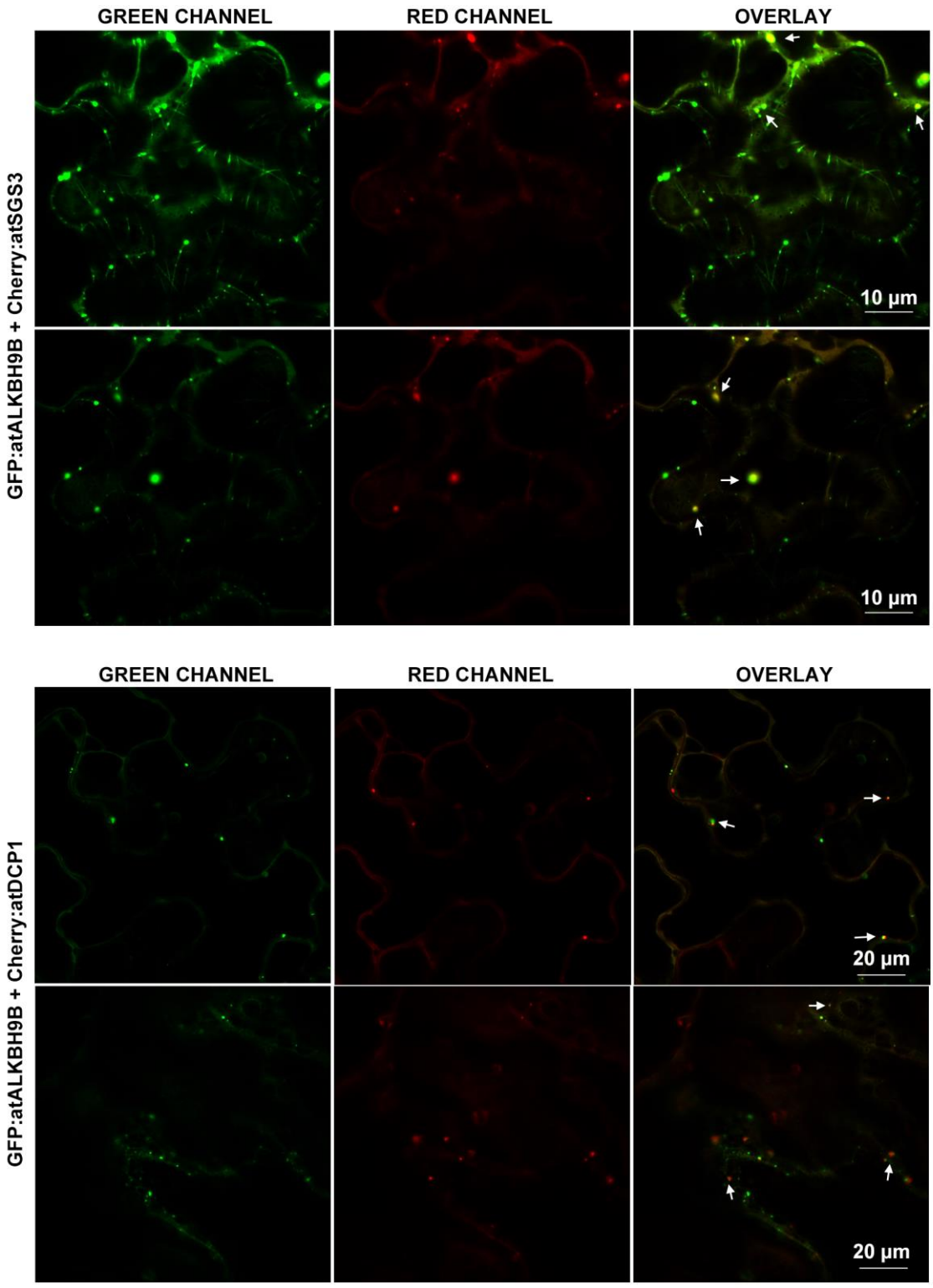

Figure 6. atALKBH9B also colocalizes with siRNA-bodies/P-bodies components in infected tissues. *N. benthamiana leaves were inoculated with AMV viral particles and, 24 h post-infection, were agroinfiltrated with the indicated co-infiltrated DNA constructs indicated above the images. CLSM images were taken 48 h post-infiltration. Overlay panels are the superposition of images from the green and red channels. Arrowheads indicate granules with both proteins.*

atALKBH9B catalyzes m^{6}A demethylation of RNA *in vitro*. To assay the m^{6}A demethylation activity of atALKBH9B, the protein was fused to the glutathione S-transferase (GST) protein (GST:

atALKBH9B) and purified from *E. coli* using the GST purification system. GST:atALKBH9B or GST alone were incubated with a synthetic single-stranded RNA oligonucleotide (ssRNA) with a single specifically incorporated m^{6}A, followed by digestion to nucleosides and ultra-performance liquid chromatography-photodiode detector-quadrupole/time-of-flight–mass spectrometry (UPLC-PDA-TOF-MS) analysis. We found that GST:atALKBH9B almost completely demethylates m^{6}A in the ssRNA substrate (Fig. 7A and B). Therefore, atALKBH9B is the first protein described in plants with ssRNA m^{6}A demethylase activity.

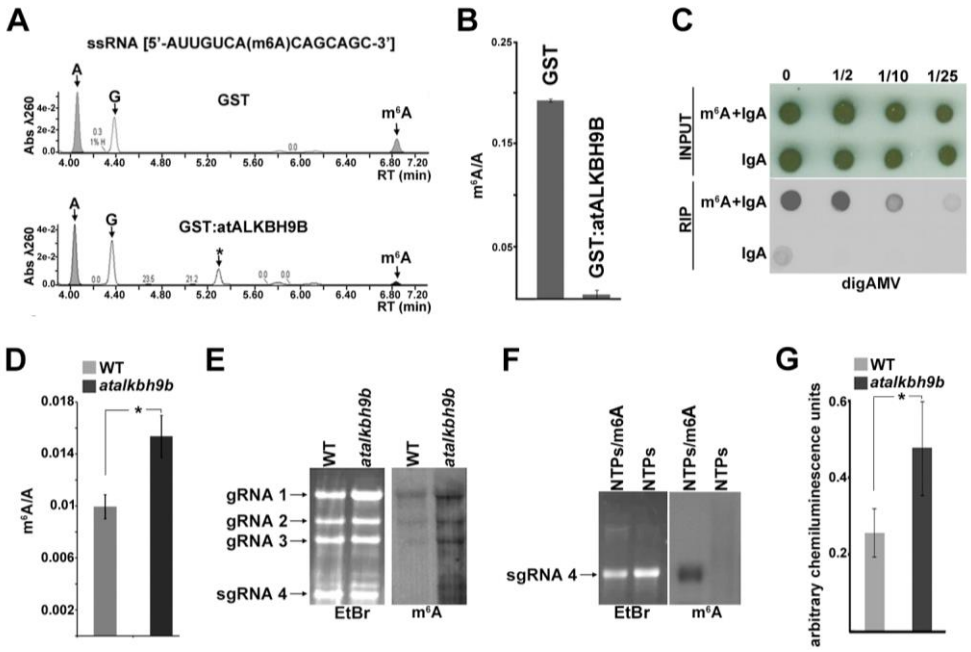

Figure 7. atALKBH9B catalyzes demethylation of m^{6}A in ssRNA in vitro and modulates methylation of vRNAs. (A) *Representative UPLC-PDA-Q/TOF-MS chromatogram showing the retention times of the nucleosides adenosine (A) and N^6-methyladenosine (m^{6}A) after incubation of the m^{6}A-containing ssRNA substrate with GST:atALKBH9B and GST as the negative control. The peak (G) corresponds to the nucleoside guanosine. The peak denoted as (*) could not be unequivocally identified although it was determined to present a molecular weight of 343 with a maximum absorption at 261 nm.* ***(B)*** *Graph representing the demethylation activity in three independent experiments.* ***(C)*** *RIP of vRNAs with a specific anti-m^{6}A antibody. Total RNA extracted from WT plants infected with AMV was incubated with anti-m^{6}A plus IgA or IgA alone. Dilutions of the immunoprecipitated RNAs (indicated on top) were blotted on nylon membranes and the vRNAs were detected with DigAMV.* ***(D–G)*** *Genomic AMV RNAs are m^{6}A hypermethylated in atalkbh9b plants.* ***(D)*** *Graphic showing the average m^{6}A/A ratios obtained by UPLC-Q-Tof-MS after digestion of vRNAs extracted from virions purified from AMV-infected WT and atalkbh9b plants.* ***(E)*** *Representative nylon membrane stained with ethidium bromide (EtBr) and north-western blot with m^{6}A antibody of vRNAs extracted of virions purified from AMV-infected WT and alkbh9b plants. Positions of the genomic AMV RNAs are indicated on the right of EtBr.* ***(F)*** *In vitro transcripts of vRNA 4 obtained with NTPs (non-methylated) or NTPs+m^{6}A (methylated) were used as negative and positive north-western blot controls, respectively.* ***(G)*** *Average ratios of m^{6}A in vRNAs obtained by quantification of three different north-western blots (panel E) from AMV-infected WT and atalkbh9b plants. In B, D, and E error bars represent the SD and asterisks indicate significant differences from the WT (*P<0.05) using Student's t-test (n=3).*

m^{6}A abundance in AMV vRNAs correlates with viral fitness. Given that atALKBH9B has been shown to possess m^{6}A demethylase activity and that its depletion influences AMV infection, we investigated the presence of the m^{6}A modification in AMV vRNAs. Total RNA was purified from Arabidopsis WT AMV-infected plants, and an RNA immunoprecipitation assay (RIP) using the

anti-m^{6}A antibody and immunoglobulin-A was performed to immunoprecipitate the m^{6}A-modified RNAs. Subsequent, hybridization of RIP products with the DigAMV probe clearly detected the presence of the AMV vRNAs (Fig. 7C). These results demonstrate that in Arabidopsis, adenosine residues in the AMV genome become modified to m^{6}A during the infection process.

We next determined whether atALKBH9B depletion in *atalkbh9b* plants modulates m^{6}A levels in the AMV genome. In this case, vRNAs were digested to single nucleosides and the m^{6}A abundance was quantified by UPLC-PDA-Tof-MS. The m^{6}A/adenosine ratio (m^{6}A/A) was reduced ~35% in WT compared with *atalkbh9b* plants (Fig. 7D). In parallel, vRNAs extracted from AMV particles isolated from WT or *atalkbh9b* plants were electrophoresed in agarose gels, transferred to nylon membranes, and immunoblotted using the m^{6}A antibody (Fig. 7E-G). Altogether, these experiments indicate that depletion of atALKBH9B correlates with hypermethylation of the AMV vRNAs.

Finally, we performed a methylated RNA immunoprecipitation sequencing (MeRIP-seq) experiment to map m^{6}A sites within the AMV genome. For this, vRNAs extracted from viral particles isolated from *atalkbh9b* AMV-infected plants were immunoprecipitated with an m^{6}A-specific antibody and RNAs from input, bead-only control and MeRIP-seq samples were used to generate RNA sequence libraries. We identified six discrete peaks distributed along the AMV genome, which contained the common m^{6}A consensus motif (R)RACH (R=A/G, H=A/C/U (Fig. 8).

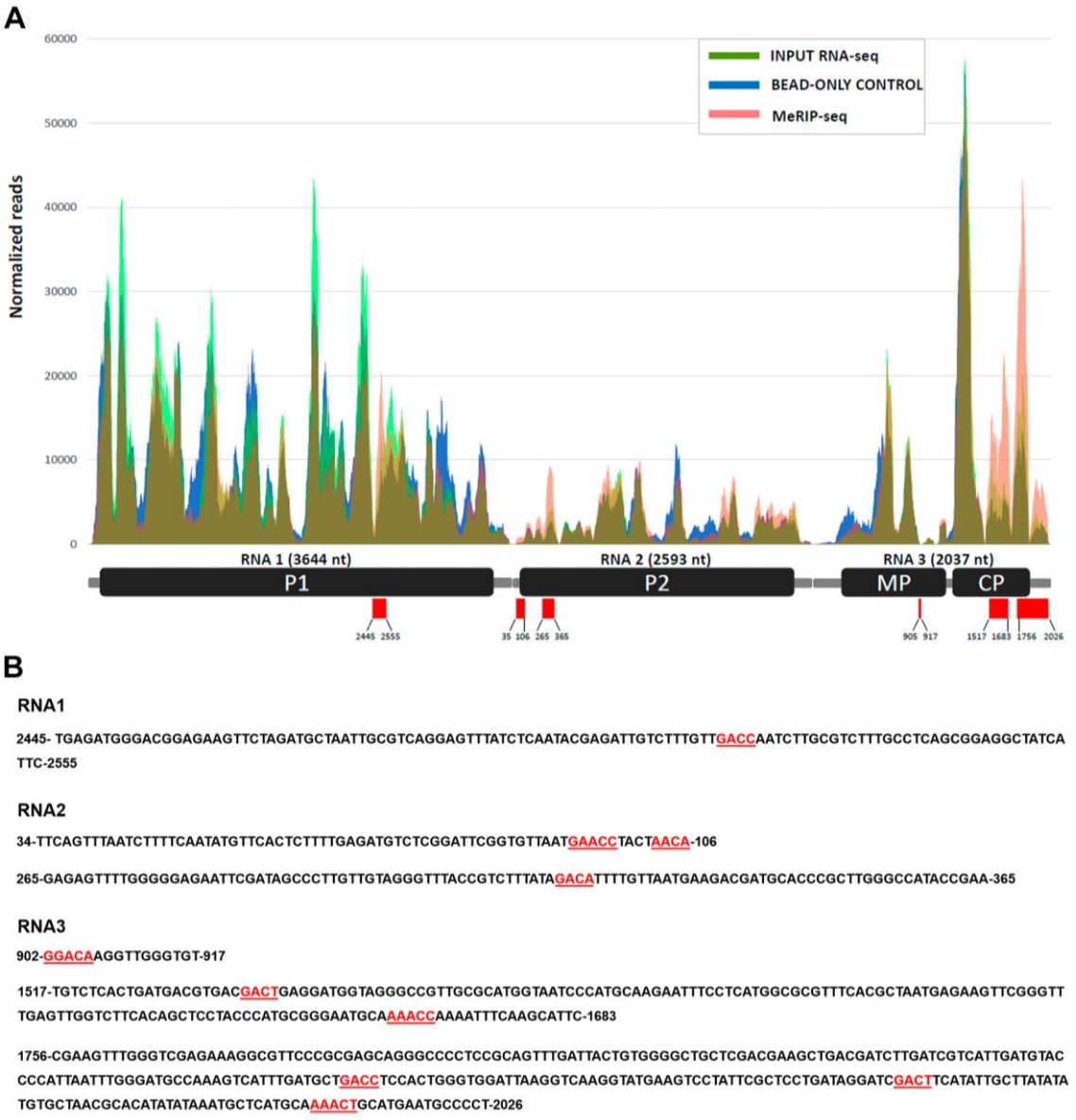

Figure 8. Map of m^{6}A sites within AMV genomic RNAs by MeRIP-seq. (A) *Read coverage of the three RNAs on input RNA-seq (green), bead-only control (blue), and MeRIP-seq (pink). Reads were normalized to the total number of reads mapping to the viral genome. Below, a schematic diagram of the AMV genome is presented. Red rectangles indicate the six m^{6}A peaks identified and numbers show their nucleotide positions in each vRNA.* ***(B)*** *Nucleotide sequence of the six m^{6}A peaks identified, showing in red the consensus motif (R)RACH.*

m^{6}A is present in the genomic RNAs of other viruses. Since m^{6}A appears to regulate AMV infection, we wondered whether other viruses belonging to the *Bromiviridae* family might also be influenced by this modification. So, as representative for this family, we chose *Cucumber mosaic virus* (CMV), the type member of the genus *Cucumovirus*, which infects Arabidopsis. In addition, we selected three other viruses to complete the study: *Tobacco rattle virus* (TRV), *Turnip crinkle virus* (TCV) and *Cauliflower mosaic virus* (CaMV), which belong to *Virgaviridae*, *Tombusviridae* and *Caulimoviridae* families, respectively. RIP from total RNA of WT infected plants using the m^{6}A antibody and hybridization of RIP products with the Dig probes for each virus showed that CMV, TCV and CaMV RNAs were specifically immunoprecipitated with m^{6}A

antibody but not TRV RNAs, indicating that vRNAs of CMV, TCV and CaMV contain m^{6}A (Fig. 9A). Next, we evaluated whether, similar to AMV, atALKBH9B activity might influence viral infectivity of methylated virus, finding that 100% of *alkbh9b* plants were systemically infected by the three viruses (Figure 9B).

In the case of CMV, we also analyzed the presence of m^{6}A in the viral genome contained in viral particles isolated from WT and *atalkbh9b* infected plants. After digestion to single nucleosides, UPLC-PDA-Tof-MS showed no significant differences in the m^{6}A/A ratios in purified vRNAs from WT compared with atALKBH9B plants (Fig. 9C). Therefore, the CMV genome contains m^{6}A, but the methylation levels of vRNAs and viral infection are not regulated by atALKBH9B. We hypothesized that our findings might correlate with a lack of interaction between atALKBH9B and the CMV CP; hence, this interaction was investigated by Y2H analysis. Growth on interaction selective medium of yeast cells co-expressing both proteins showed that the viral protein fails to interact with atALKBH9B *in vivo* (Fig. 9D). CMV CP did not interact with atALKBH9B strongly suggesting that this interaction is an obligate requirement for regulating viral infection. Interestingly, we found that atALKBH9B interacts with the CP of *Prunus necrotic ringspot virus* (PNRSV) (Fig. 9D), a virus that is functionally and phylogenetically closely related to AMV (Sánchez-Navarro et al., 1997; Aparicio et al., 2001). Unfortunately, since Arabidopsis is not a host for PNRSV, we could not assay the virus infectivity in *atalkbh9b* plants. This finding suggests that atALKBH9B may regulate the viral life cycle of other *Bromoviridae* family members.

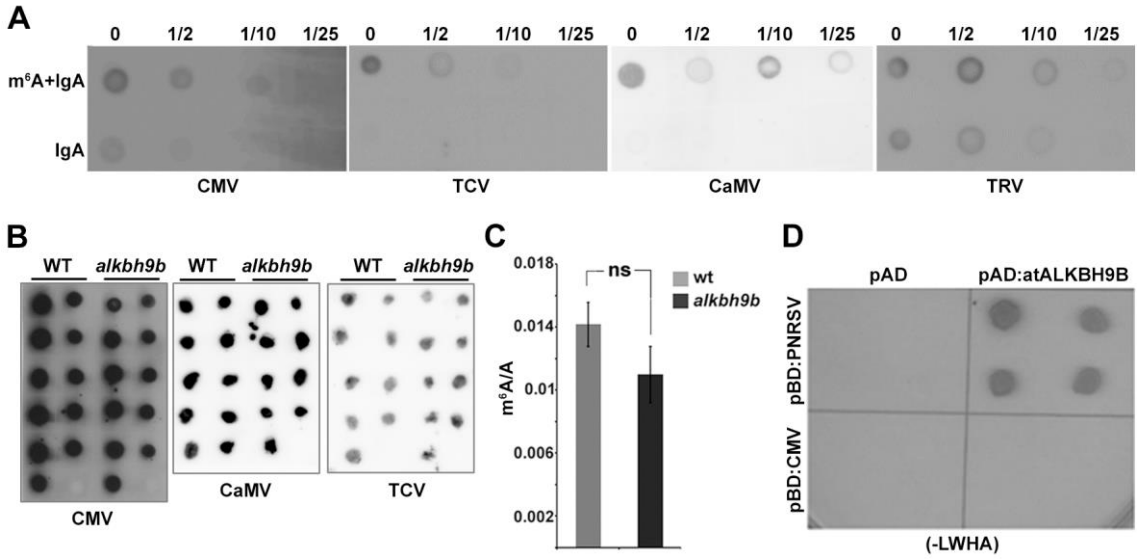

Figure 9. CMV, TCV and CaMV RNAs contain m^{6}A nucleotides. (A) *Detection of m^{6}A in CMV, TCV, CaMV and TRV by RIP of vRNAs with a specific anti-m^{6}A antibody plus IgA or IgA alone. Dilutions of the immunoprecipitated RNAs (indicated on top) were blotted on nylon membranes and vRNAs were detected with Dig probes for each virus.* ***(B)*** *CMV, CaMV and TCV systemic infections are not affected in atalkbh9b plants. Dot-blot hybridization of total RNA (CMV) or direct printing into nylon membranes (TCV and CaMV) of upper floral stems. Negative controls were applied in the right bottom corner of each membrane.* ***(C)*** *Graphic showing the average m^{6}A/A ratios obtained by UPLC-Q-*

Tof-MS after digestion of vRNAs extracted from virions purified from CMV-infected WT and atalkbh9b plants. Error bars represent SD; ns, no significant differences (P > 0.05) from the WT applying Student's t-test (n = 3). ***(D)*** *Yeast two-hybrid analysis of the interaction between CPs of CMV and PNRSV with atALKBH9B. Interacting colonies were identified by growth after 5 d on medium lacking leucine, tryptophan, histidine, and adenine (-LWHA).*

Discussion

In the last few years, m^6A modification has emerged as an important mechanism to regulate mRNA biology (Zheng et al., 2013; Wang et al., 2014; Xu et al., 2014; Zhao et al., 2014; Liu et al., 2015; Wang et al., 2015). Components of this regulatory system (methyltransferases, demethylases and protein effectors) have been identified in mammals and yeast (Fu et al., 2014).

Several recent studies showed that m^6A is also a conserved feature of mRNA in plants (Luo et al., 2014; Wan et al., 2015), and that it plays a critical regulatory role in plant development (Zhong et al., 2008; Bodi et al., 2012; Shen et al., 2016). However, as far as we know, only two components of the methylase complex, MTA and FIP37, have been identified at present (Zhong et al., 2008; Shen et al., 2016). In this work, using a biochemical test, we demonstrate that atALKBH9B possesses m^6A demethylase activity toward single-stranded RNA *in vitro*, and similar to the results of a previous study, we find that this protein localizes exclusively to the cytoplasm (Mielecki et al., 2012). Several studies previously reported the presence of the cellular machinery controlling m^6A methylation in the cytoplasm of mammalian cells (Gokhale et al., 2016; Lichinchi et al., 2016b). Thus, atALKBH9B may be a new component of the cellular machinery controlling m^6A in plant mRNAs, and similar to the situation in mammals, it could take place in the cytoplasm after the export of mRNAs from the nucleus.

A detailed examination showed that atALKBH9B forms discrete granules either in healthy or infected tissues that colocalize with SGS3 and UPF1, and some of these granules presented a spatial association with DCP1. SGS3 is part of siRNA bodies, whereas DPC1 is a component of P-bodies (Ingelfinger et al., 2002; Martínez de Alba et al., 2015) and UPF1 is transported from the cytoplasm to P-bodies by SMG7 (Merai et al., 2013).

In the cytoplasm, binding of different proteins to m^6A mediates host mRNA destination. For instance, binding of YTHDF1 or eIF3 was found to favor mRNA translation (Meyer et al., 2015; Wang et al., 2015), whereas the binding of HNRNPC regulates mRNA degradation (Liu et al., 2015), and YTHDF2 directs m^6A-marked mRNAs to P-bodies for RNA decay (Wang et al., 2015).

RNA turnover in P-bodies and PTGS in siRNA bodies are conserved eukaryotic mechanisms to regulate mRNA integrity that were found to be functionally and spatially associated (Gregory et al., 2008; Martínez de Alba et al., 2015).

Our findings suggest that atALKBH9B m^6A activity might be linked to mRNA silencing and the mRNA decay processes. In this sense, we found that NMD, a surveillance system linked to P-bodies proposed to work as viral restriction mechanism in plants, could act on AMV infection, since UPF1 depletion increased viral accumulation (Garcia et al., 2014).

Recent studies showed that the m^6A machinery modifies the vRNA genomes of several animal viruses belonging to the *Flaviviridae* family, indicating that m^6A modification is a conserved mark that regulates viral infection (Gokhale et al., 2016; Lichinchi et al., 2016b). In this study, we report that adenosines in AMV, CMV, TCV and CaMV RNAs are also modified to m^6A, suggesting that this feature is a conserved phenomenon that can modulate the infection cycles of viruses not only replicating in the nucleus, but also in the cytoplasm of both, mammalian and plant cells. We show that AMV viral cycle was affected in *atalkbh9b* plants, since viral accumulation was reduced in protoplasts and in inoculated leaves, including a delay in the viral invasion towards the petioles. Moreover, the systemic invasion was severely impaired in both, aerial and root tissues. The decrease of the viral load in protoplasts indicates that AMV replication and/or translation steps are affected, at least partially, in *atalkbh9b* plants. Nonetheless, we cannot clearly assign the block of the systemic movement to this decline on the early stages of infectious cycle. A previous study on the infection capability of different AMV mutants showed that mutants with reduced replication rates in protoplast were able to sustain almost WT-like systemic invasion. In contrast, other AMV mutants with replication levels similar to WT in protoplasts showed an impaired systemic movement (Tenllado and Bol, 2000). Thus, it is likely that the viral upload and download in the phloem are also defective in *atalkbh9b* plants. Conversely, atALKBH9A and atALKBH9C are not implied in the systemic movement of this virus, what might be related with their expression pattern and/or their subcellular localization. atALKBH9C is mainly expressed in leaves, but between 70-90% of the protein was found to accumulate in the nucleus, whereas atALKBH9A is virtually undetectable (Duan et al., 2017; Mielecki et al., 2012). In contrast, atALKBH9B is one of the most expressed atALKB genes, mainly in the apical meristem and buds (Duan et al., 2017) and localizes exclusively in the cytoplasm, where AMV replication takes place.

Moreover, AMV genomic RNAs presented higher m^6A levels in *atalkbh9b* plants, providing evidence that m^6A modification negatively affects viral infection. These findings are in

agreement with those recently reported for HCV and ZIKV, in which viral infections are regulated by m^{6}A methylation of their genomic RNAs. Specifically, knockdown of ALKBH5 and FTO increases m^{6}A abundance in the ZIKV genome, negatively affecting the viral titer (Lichinchi et al., 2016b), while depletion of FTO but not ALKBH5 decreases the production of infectious virus (Gokhale et al., 2016). Thus, the host RNA methyltransferase machinery may represent an additional host regulatory mechanism to counter infection by some plant viruses.

Gokhale et al. (2016) proposed that regulation of m^{6}A abundance in genomic RNAs of HCV would allow the virus to replicate at low rates, evading the host immune system and enabling the establishment of persistent infections. In plants, a conserved AlkB domain in the genomes of several single-stranded RNA plant viruses belonging to the *Flexiviridae* family was identified (Bratlie and Drabløs, 2005; Van den Born et al., 2008). Furthermore, a functional characterization analysis showed that these viral AlkB domains repair deleterious RNA genome methylation damage, suggesting that this domain may be biologically relevant in preserving the viability of the viral genome (Van den Born et al., 2008). Interestingly, most of the viruses containing this AlkB domain infect woody or perennial plants, where they have to establish infections that persist for years (Van den Born et al., 2008; Bergua, 2011). In the case of AMV, a similar scenario could occur, since alfalfa (*Medicago sativa*) plants, its natural host, are generally maintained for a minimum of 5 y before the crop is replanted (Bergua, 2011). However, unlike viruses in the *Flexiviridae* family, the AMV genome lacks the Alkb domain, so the virus may have the ability to usurp this host function for its long-term accumulation.

In contrast to AMV, CMV, TCV and CaMV infections were not affected in *atalkbh9b* compared with WT plants. Moreover, m^{6}A abundance in CMV vRNAs was similar in purified virions from *atalkbh9b* and WT plants. Remarkably, the CMV CP did not interact with atALKBH9B *in vivo*. An important difference between AMV and CMV is that, whereas the latter can replicate in the absence of its CP (Ryabov et al., 1999), the CP of AMV is a multifunctional protein that interacts with a variety of host factors and is indispensable for replication and translation (Bol, 2005; Herranz et al., 2012; Ibrahim et al., 2012; Pallas et al., 2013). Thus, it may be possible that the interaction between atALKBH9B and the CP is essential to usurp atALKBH9B activity. But, on the other hand, as mentioned above, the Arabidopsis genome encodes thirteen AlkB orthologous, so a protein different from atALKBH9B could participate in the m^{6}A regulation and/or infection processes of these viruses. In fact, it was reported that depletion of FTO negatively affects HCV infection, while depletion of ALKBH5 has no effect on the HCV cycle (Gokhale et al., 2016).

Finally, we cannot rule out the possibility that m^6A modification does not influence these viral infections *per se*.

Materials and Methods

Y2H screening. Yeast two-hybrid (Y2H) screening performance of Arabidopsis proteins interacting with AMV CP has been previously described (Németh et al., 1998).

Analysis of GST:atALKBH9B-vRNA interaction by north-western assay. Dilutions of GST or GST:ALKBH9B purified proteins were electrophoresed in 12% SDS/PAGE and transferred to PDVF membranes. Membranes were incubated overnight at 4 °C (10 mM Tris·HCl pH 7.5, 1 mM EDTA, 0.1 M NaCl, 0.0005% Triton X). After two washes of 5 min each with the same buffer, membranes were incubated with 20 mL of buffer B (10 mM Tris·HCl pH 7.5, 1 mM EDTA, 0.1 M NaCl) containing 50 ng/µL of the AMV RNA 4 labelled with digoxigenin for 2 h at 25 °C. Then digoxigenin detection procedures were carried out.

Analysis of atALKBH9B-AMV viral particle interaction. Full-length atALKBH9B ORF and the N-terminal part of the yellow fluorescent protein (aminoacids 1–160) were cloned in plasmid pET28a (Novagen) fused in frame with the histidine tag to generate pET28a/His-atALKBH9B and pET28a/His-NYFP. BL21(DE3) *E. coli* cells transformed with the plasmids were grown at 37°C and induced with 1 mM IPTG for 3 h. Cells were resuspended in buffer A (10 mMTris pH 7.5; 150 mMNaCl; 0.5% Triton X-100; 20 mM imidazol). Soluble fractions were incubated with Ni-NTA column (Qiagen) for 1 h at 4 °C. After four washes with buffer A, Ni-NTA columns containing His-atALKBH9B or His-NYFP proteins were incubated with purified AMV virions for 1 h at 4 °C. After three washes with buffer A, protein complexes bound to Ni-NTA columns were eluted with buffer B (10 mM Tris pH 7.5; 150 mM NaCl; 0.5% Triton X-100; 250 mM imidazol). Purified complexes were separated in SDS/PAGE gels and transferred to PDVF membranes in duplicate (Amersham). Western blot analysis using anti-AMV CP (Loewe) or anti-His (Roche) antibodies were conducted following the manufacturer's recommendations.

BiFC and subcellular localization study. atALKBH9B and atUPF1 ORFs were amplified with specific primers designed for cloning using the Gateway System (Invitrogen) and recombined into binary destination vectors expressing the fluorescent proteins mCherry or GFP for subcellular localization studies and the N-terminal part of the YFP for BiFC analysis, following manufacturer recommendations (GFP:atALKBH9B, atALKBH9B:GFP; NYFP:atALKBH9B,

atUPF1:GFP). Plasmid expressing the AMV CP fused to the C-terminal part of the YFP (CYFP:CP) was previously described (Aparicio et al., 2006). All binary vectors were transformed into *Agrobacterium tumefaciens* C58 cells. Cultures were diluted at 0.2 OD600 in infiltration solution (10 mM Mes pH 5.5, 10 mM MgCl2) and infiltrated into 3-wk-old *N. benthamiana* plants. Confocal images were taken at 48 h after agroinfiltration with a Zeiss LSM 780 AxiObserver microscope. All images correspond to single slices of 1.8-µm thickness of epidermal cells. Excitation and emission wavelengths were 488 and 508 nm for GFP, 514 and 527 nm for YFP, and 545 and 572 nm for mCherry.

Plant growth conditions, virus inoculation, and northern blots. Arabidopsis *atalkbh9a atalkbh9c, atalkbh9a/atalkbh9b, atalkbh9a/atalkbh9c, atalkbh9b/atalkbh9c* and *atalkbh9a/atalkbh9b/atalkbh9c* mutants were kindly provide by Dr R. Nadi and Prof J.L. Micoll from Universidad Miguel Hernández (Elche, Alicante). *N. benthamiana* and Arabidopsis plants were grown in 6-cm diameter pots in a growth chamber at 24 °C with a photoperiod of 24 °C-16 h light/20 °C-8 h dark. Plants were mechanically inoculated with purified virions (1 mg/mL) of AMV PV0196 isolate (Plant Virus Collection, DSMZ) in 30 mM sodium phosphate buffer pH 7. Detection of vRNAs was carried out by northern or direct-dot blot analysis. Inoculated leaves (3 or 6 dpi) and upper systemic floral stems (15 dpi) were grounded in liquid nitrogen with mortar and pestle and total RNA was extracted from 0.1 g leaf material using RiboZol reagent protocol (Amresco). A total of 0,5-1 µg of total RNA was denatured by formaldehyde treatment and analyzed by northern blot hybridization. Otherwise, for direct-dot blot analysis, 1 µg of total RNA was directly blotted onto nylon membranes. vRNAs were visualized on blots using digoxigenin-labeled riboprobes to detect the four vRNAs of AMV. Synthesis of the digoxigenin-labeled riboprobes, hybridization, and digoxigenin-detection procedures were carried out as previously described (Pallás et al., 1998). Hybridization intensity signal was measured on files from Fujiflm LAS-3000 Imager using Fujiflm Image Gauge V4.0.

m^{6}A RIP of viral genomic RNAs. Immunoprecipitation of m^{6}A vRNA was performed as previously described (Dominissini et al., 2013). Purified total RNAs (250 µg) from WT or *atalkbh9b* plants were incubated in a final volume of 500 µL with 1× IP buffer [50 mM Tris·HCl 7,4, 150 mM NaCl, 0.5% (vol/vol) Nonidet P-40], 200 U RNasin and 12.5 µg of specific m^{6}A antibody (Synaptic Systems) in rotation for 2 h at 4 °C. Then, 200 µL of recombinant protein A beads in 1× IP buffer were added and additionally incubated in rotation for 2 h at 4 °C. After this, beads were washed four times with 1×IP buffer supplement with RNasin and incubated for 1 hr with vigorous shaking in elution competition buffer [50 mM Tris·HCl, 150 mM NaCl, 0.5% (vol/vol) Nonidet P-40, 200

U RNasin and 6.7 mM m^6A] to elute m^6A containing RNAs. As negative controls the same reactions without specific m^6A antibody were performed. Eluted RNAs and serial dilutions were directly blotted onto nylon membranes and hybridized with DigAMV, DigCMV, DigTCV, DigTRV or DigCaMV probes as described above.

Protoplast isolation and inoculation. Isolation and inoculation of WT and *atalkbh9b* protoplasts were carried out as previously described (Yoo et al., 2007) with some modifications. Well-expanded leaves from 3–week-old plants were chosen and their undersides were slightly rubbed with carborundum. The leaves were incubated on the enzyme solution (20 mM MES (pH 5.7), 1.5% (wt/vol) cellulase R10, 0.4% (wt/vol) macerozyme R10, 0.4 M manitol, 20 mM KCl, 10 mM CaCl2, 1–5 mM β-mercaptoethanol and 0.1% BSA) in the dark for 3 h at room temperature. The enzyme/protoplast solution was diluted with an equal volume of W5 solution (2 mM MES (pH 5.7), 154 mM NaCl, 125 mM CaCl2 and 5 mM KCl) before filtration with miracloth. After that, a sucrose cushion was performed adding approximately 1 mL of 20% sucrose to the bottom of the tube with a pasteur pipette and centrifugated at 800 rpm for 10 minutes. Protoplasts from the interphase were recovered and diluted in 1 volume of W5 and centrifuged at 200 g for 3 min. After removing the supernatant, the protoplasts were resuspended at $2x10^5$ mL^{-1} in W5 solution and kept on ice for 30 min. The supernatant was removed and the protoplast were resuspended at $2x10^5$ mL^{-1} in MMG solution (4 mM MES (pH 5.7), 0.4 M mannitol and 15 mM MgCl2). For the transfection process, 10 µL of vRNA (10–20 µg extracted from AMV virions), 100 µL of protoplasts (10^5 cells) and 110 µL of PEG solution (20–40% (wt/vol) PEG4000, 0.2 M mannitol and 100 mM CaCl2) were gently mixed in a 2-mL microfuge tube and incubated at room temperature for 10 min. To stop the transfection reaction, the samples were diluted with 400–440 µL W5 solution at room temperature and centrifuged at 100g for 2 min. After removing supernatant, protoplasts were resuspended with 1 mL WI (4 mM MES (pH 5.7), 0.5 M mannitol and 20 mM KCl) and incubated at room temperature for 20 h.

Total RNA extraction with RiboZol reagent protocol (Amresco) was carried out to analyze viral accumulation by northern blot analysis.

Tissue printing of inoculated leaves and floral stems. Leaves of 3-weeks old WT and *atalkbh9b* plants were inoculated with AMV virion and directly printed onto a nylon membrane by pressing the lower side as previously described (Más and Pallás, 1995), at 4 or 7 dpi. To analyze AMV systemic invasion in all *atalkbh9* mutant combinations, floral-stems were cut at 12 dpi and directly pressed onto the nylon membranes. Hybridization procedures were carried out as previously described (Pallás et al., 1998).

Viral particle purification and viral genomic RNA purification. Viral particles were purified from inoculated leaves collected at 9 dpi. Leaves were macerated with mortar and pestle in two volumes (wt/vol) of isolation buffer (100 mM K2HPO4; 100 mM ascorbic acid; 20 mM EDTA; pH 7.1). The macerate was filtered through miracloth and mixed with 1/2 volume of butanol-chloroform (1:1). The emulsion was centrifuged at 8,000 × g for 15 min and 1/5 volume of polyethylenglycol (MW 20000) was added to the aqueous phase. After a 15-min incubation in ice, the solution was centrifuged at 8,000 × g for 15 min and supernatants were discarded. Pellets were resuspended with phosphate buffer (10 mM sodium phosphate pH 7, 1 mM EDTA) and Triton X-100 was added at a final concentration of 0.5%. Tubes were incubated for 30 min in ice and centrifuged at 8,000 × g for 5 min. Supernatants were transferred to fresh tubes and centrifuged 76,000 × g for 3 h. For vRNAs purification, pellets were directly resuspended in 1 mL of RiboZol reagent (Amresco) and RNA extraction was carried out following manufacturer recommendations. For vRNAs purification, pellets were directly resuspended in 1 mL of RiboZol reagent (Amresco) and RNA extraction was carried out following manufacturer recommendations.

Purification of atALKBH9B protein and *in vitro* m^{6}A demethylation assays. atALKBH9B was subcloned into pGEX-KG (GE Healthcare Life Sciences) to generate a construct with atALKBH9B fused to the C-terminal part of the GST. GST and GST:atALKBH9B proteins were expressed in BL21 (DE3) *E. coli* cells and purified with glutathione sepharose 4B beads (GE Healthcare Life Sciences) following manufacturer recommendations. All of the protein purification procedures were performed at 4 °C. The m^{6}A demethylase activity assay was performed by incubating 2.5 µg of GST or GST:ALKBH9B proteins and 1 µg of m^{6}A monomethylated ssRNA (Dharmacon, Inc.) oligonucleotide for 3 h at 25 °C in a reaction mixture containing 50 mM of Hepes buffer (pH 7.0), 10 µM α-ketoglutarate, 100 µM L-ascorbic acid ascorbate, 20 µM (NH4)2Fe(SO4)2·6H2O. Finally, reactions were quenched by heating at 95 °C for 10 min.

UPLC-PDA-Tof-MS analysis. For UPLC-PDA-Tof-MS analysis, 10 µg of vRNAs or 1 µg of ssRNA oligonucleotide were digested by incubating for 2 h at 37 °C in 50 µL (final volume) reaction mixture containing 1× buffer C (25 mM Tris pH 8, 2 mM MgCl2, 1 mg/mL; BSA), 10 U Benzonase, 0.002 U phosphodiesterase I and 1.5 U alkaline phosphatase. Then, 5 µL of digested nucleosides was injected into a Micromass Q-TOF spectrometer coupled to an Acquity UPLC-PDA system (Waters) via an electrospray ionization (ESI) interface. Separation was performed on a Waters Acquity BEH C18 column (150 × 2.1 mm i.d., 1.7 µm). During sample running, the mobile phase consisted of 0.1%formic acid in water (phase A), and 0.1% formic acid in acetonitrile (phase B).

The solvent gradient program is conditioned as follows: 100–90% solvent A over the first 20 min, 90–0% solvent A over 10 min, return to the initial 100% A in 5 min, and conditioning at 100% A. The flow rate was 0.4 mL/min and the column and sample temperatures were kept at 40 °C. UV spectra were acquired between 210 and 800 nm with a 1.2-nm resolution and 20 points s−1 sampling rates. The ESI source was operated in positive ionization mode with the capillary and cone voltages at 2.7 kV and 30 V, set at 120 °C and 300 °C. The cone and desolvation gas (nitrogen) flows were 500 l h−1 and 50 l h−1, respectively. The collision energy was set at 5 eV. ESI data acquisition was collected in centroid mode in a full scan range from mass-to-charge ratio [m/z] 50–1,500 at 0.2 s per scan. The mass spectrometer was calibrated using a sodium formate mixture from 200 to 1,500 MW (resolution specification 5,000 FWHM, deviation <5 ppm RMS in the presence of a known lock mass). Leu-enkephalin was used as the lockmass using a LockSpray exact mass ionization source. All data were acquired using Masslynk NT4.1 software (Waters Corp.). The nucleosides were quantified using either the SIR monitoring of 282.1 (m^6A) and 268.1 (adenosine) m/z ratios or the λ 260-nm ratios. Quantification was performed by comparison with the standard curve obtained from authentic nucleoside standards (Sigma-Aldrich) running at the same batch of samples.

MeRip-Seq. Immunoprecipitation of m^6A RNA fragments was performed using 200 µg of purified vRNAs as previously described (Dominissini et al., 2013). Sequencing libraries were prepared from input, bead-only control and m^6A-immunoprecipitated RNAs (MeRip-seq) with TruSeq stranded mRNA Library Preparation kit of Illumina. Libraries were sequenced 2 × 75 base pair reads on the NextSEq. 500 (Illumina) at the Genomic Service Unit (Servicio Central de Apoyo a la Investigación Experimental, Universitat de Valencia). After adapter removal, quality trimming and size filtering with cutadapt, complete paired-end reads longer than 20-bp were mapped to combined *Arabidopsis thaliana* (TAIR10) and AMV genomic RNAs (RefSeq accessions: NC_001495.1, NC_002024.2, and NC_002025.1) using Bowtie2 (Martin, 2011). Only coherently virus-mapped paired reads (50–250 bp mapping distance) were used for subsequent analysis. Search for enriched peaks in the MeRIP-seq sample compared with the input or bead-only control were performed as described previously (Langmead and Salzberg, 2012) with the difference that we calculated the sequencing coverage for every virus genome position using sequence fragments instead of sequence reads (sequence fragments included all of the bases contained between the leftmost and the rightmost base of each paired-end read obtained). For each AMV RNA, nucleotides with differential coverage between input and bead-only control or MeRIP-seq samples were identified using the trimmed mean of M-values (TMM) normalization

and a negative binomial model with the edgeR package (Robinson and Oshlack, 2010). A nucleotide was called positive if the false discovery rate (FDR) was <0.01 and the log2FC was ≥1, and peaks were considered as stretches of more than 10 consecutive positive nucleotides.

ACKNOWLEDGMENTS

We thank L. Corachan for her excellent technical assistance, Dr. Emilio Martinez de Alba and Dr. Christophe Rizenthaler for kindly providing GFP:SGS3 and DCP1:mCherry plasmids, Prof. John W. S. Brown for providing a plasmid containing the ORF of atUPF1, and the Bioinformatics Core Service at the Instituto de Biología Molecular y Celular de Plantas (IBMCP) for the support provided in the data analysis. UPLC-PDAQ/TOF-MS analyses were performed by the Metabolic Analysis Department of the IBMCP. F.A. and M.M.-P. were recipients of Contract RYC-2010-06169 from the Ramón y Cajal Program of the Ministerio de Educación y Ciencia, and Predoctoral Contract FPI-2015-072406 from the Subprograma FPI-MINECO (Formación de Personal Investigador–Ministerio de Economía y Competitividad), respectively. This work was supported by Grant BIO2014-54862-R from the Spanish granting agency Dirección General de Investigación Científica y Técnica and the Prometeo Program (GV2015/010) from the Generalitat Valenciana.

References

Aparicio, F. and Pallás, V. (2017). The coat protein of Alfalfa mosaic virus interacts and interferes with the transcriptional activity of the bHLH transcription factor ILR3 promoting salicylic acid-dependent defence signalling response. Mol. Plant Pathol. **18**: 173–186.

Aparicio, F., Sánchez-Navarro, J.A., Olsthoorn, R.C.L., Pallás, V., and Bol, J.F. (2001). Recognition of cis-acting sequences in RNA 3 of Prunus necrotic ringspot virus by the replicase of Alfalfa mosaic virus. J. Gen. Virol. **82**: 947–51.

Aparicio, F., Sánchez-Navarro, J.A., and Pallás, V. (2006). In vitro and in vivo mapping of the Prunus necrotic ringspot virus coat protein C-terminal dimerization domain by bimolecular fluorescence complementation. J. Gen. Virol. **87**: 1745–50.

Balasubramaniam, M., Kim, B.S., Hutchens-Williams, H.M., and Loesch-Fries, L.S. (2014). The photosystem II oxygen-evolving complex protein PsbP interacts with the coat protein of Alfalfa mosaic virus and inhibits virus replication. Mol. Plant-Microbe Interact. **27**: 1107–1118.

Bergua, M. (2011). El virus del mosaico de la alfalfa (AMV) en España: incidencia y efectos en alfalfa y análisis de la diversidad biológica y genética de poblaciones procedentes de distintos huéspedes. PhD thesis (Universidad Zaragoza/Centro Investig. y Tecnol. Agroaliment. Aragón, Zaragoza, Spain).

Bodi, Z., Zhong, S., Mehra, S., Song, J., Graham, N., Li, H., May, S., and Fray, R.G. (2012).

Adenosine Methylation in Arabidopsis mRNA is Associated with the 3′ End and Reduced Levels Cause Developmental Defects. Front. Plant Sci. **3**: 1–10.

Bol, J.F. (2005). Replication of Alfamo- and Ilarviruses: Role of the Coat Protein. Annu. Rev. Phytopathol. **43**: 39–62.

Bratlie, M.S. and Drabløs, F. (2005). Bioinformatic mapping of AlkB homology domains in viruses. BMC Genomics **6**: 1.

Dominissini, D., Moshitch-Moshkovitz, S., Salmon-Divon, M., Amariglio, N., and Rechavi, G. (2013). Transcriptome-wide mapping of N6-methyladenosine by m 6A-seq based on immunocapturing and massively parallel sequencing. Nat. Protoc. **8**: 176–189.

Duan, H.-C., Wei, L.-H., Zhang, C., Wang, Y., Chen, L., Lu, Z., Chen, P.R., He, C., and Jia, G. (2017). ALKBH10B Is an RNA *N* ^{6} -Methyladenosine Demethylase Affecting Arabidopsis Floral Transition. Plant Cell **29**: 2995–3011.

Fu, Y., Dominissini, D., Rechavi, G., and He, C. (2014). Gene expression regulation mediated through reversible m 6 A RNA methylation. Nat. Rev. Genet. **15**: 293–306.

Garcia, D., Garcia, S., and Voinnet, O. (2014). Nonsense-mediated decay serves as a general viral restriction mechanism in plants. Cell Host Microbe **16**: 391–402.

Gokhale, N.S., McIntyre A.B.R., McFadden M.J., et al. (2016). N6-Methyladenosine in Flaviviridae Viral RNA Genomes Regulates Infection. Cell Host Microbe **20**: 654–665.

Gregory, B.D., O'Malley, R.C., Lister, R., Urich, M.A., Tonti-Filippini, J., Chen, H., Millar, A.H., and Ecker, J.R. (2008). A Link between RNA Metabolism and Silencing Affecting Arabidopsis Development. Dev. Cell **14**: 854–66.

Herranz, M.C., Pallas, V., and Aparicio, F. (2012). Multifunctional roles for the N-terminal basic motif of Alfalfa mosaic virus coat protein: Nucleolar/cytoplasmic shuttling, modulation of RNA-binding activity, and virion formation. Mol. Plant-Microbe Interact. **25**: 1093–103.

Ibrahim, A., Hutchens, H.M., Howard Berg, R., and Sue Loesch-Fries, L. (2012). Alfalfa mosaic virus replicase proteins, P1 and P2, localize to the tonoplast in the presence of virus RNA. Virology **433**: 449–61.

Ingelfinger, D., Arndt-Jovin, D.J., Lührmann, R., and Achsel, T. (2002). The human LSm1-7 proteins colocalize with the mRNA-degrading enzymes Dcp1/2 and Xrnl in distinct cytoplasmic foci. RNA (New York, NY) **8**: 1489–1501.

Jia, G., Fu, Y., Zhao, X., Dai, Q., Zheng, G., Yang, Y., Yi, C., Lindahl, T., Pan, T., Yang, Y.G., and He, C. (2011). N6-Methyladenosine in nuclear RNA is a major substrate of the obesity-associated FTO. Nat. Chem. Biol. **7**: 885–7.

Kane, S.E. and Beemon, K. (1985). Precise localization of m6A in Rous sarcoma virus RNA reveals clustering of methylation sites: implications for RNA processing. Mol. Cell. Biol. **5**: 2298–306.

Kennedy, E.M., Bogerd, H.P., Kornepati, A.V.R., Kang, D., Ghoshal, D., Marshall, J.B., Poling, B.C., Tsai, K., Gokhale, N.S., Horner, S.M., and Cullen, B.R. (2016). Posttranscriptional m6A Editing of HIV-1 mRNAs Enhances Viral Gene Expression. Cell Host Microbe **19**: 675–685.

Kumakura, N., Takeda, A., Fujioka, Y., Motose, H., Takano, R., and Watanabe, Y. (2009). SGS3 and RDR6 interact and colocalize in cytoplasmic SGS3/RDR6-bodies. FEBS Lett. **583**: 1261–6.

Langmead, B. and Salzberg, S.L. (2012). Fast gapped-read alignment with Bowtie 2. Nat. Methods **9**: 357–9.

Lichinchi, G., Gao, S., Saletore, Y., Gonzalez, G.M., Bansal, V., Wang, Y., Mason, C.E., and Rana, T.M. (2016a). Dynamics of the human and viral m(6)A RNA methylomes during HIV-1 infection of T cells. Nat. Microbiol. **1**: 16011.

Lichinchi, G., Zhao, B.S., Wu, Y., Lu, Z., Qin, Y., He, C., and Rana, T.M. (2016b). Dynamics of Human and Viral RNA Methylation during Zika Virus Infection. Cell Host Microbe **20**: 666–673.

Liu, J., Yue, Y., Han, D. et al. (2014). A METTL3-METTL14 complex mediates mammalian nuclear

RNA N6-adenosine methylation. Nat. Chem. Biol. **10**: 93–5.

Liu, N., Dai, Q., Zheng, G., He, C., Parisien, M., and Pan, T. (2015). N6 -methyladenosine-dependent RNA structural switches regulate RNA-protein interactions. Nature **518**: 560–564.

Luo, G.Z., Macqueen, A., Zheng, G., Duan, H., Dore, L.C., Lu, Z., Liu, J., Chen, K., Jia, G., Bergelson, J., and He, C. (2014). Unique features of the m6A methylome in Arabidopsis thaliana. Nat. Commun. **28**: 5630.

Martin, M. (2011). Cutadapt removes adapter sequences from high-throughput sequencing reads. EMBnet.journal **24**: 1138–43.

Martínez de Alba, A.E., Moreno, A.B., Gabriel, M., Mallory, A.C., Christ, A., Bounon, R., Balzergue, S., Aubourg, S., Gautheret, D., Crespi, M.D., Vaucheret, H., and Maizel, A. (2015). In plants, decapping prevents RDR6-dependent production of small interfering RNAs from endogenous mRNAs. Nucleic Acids Res. **43**: 2902–2913.

Más, P. and Pallás, V. (1995). Non-isotopic tissue-printing hybridization: a new technique to study long-distance plant virus movement. J. Virol. Methods **52**: 317–26.

Merai, Z., Benkovics, A.H., Nyiko, T., Debreczeny, M., Hiripi, L., Kerenyi, Z., Kondorosi, E., and Silhavy, D. (2013). The late steps of plant nonsense-mediated mRNA decay. Plant J. **73**: 50–62.

Meyer, K.D., Patil, D.P., Zhou, J., Zinoviev, A., Skabkin, M.A., Elemento, O., Pestova, T. V., Qian, S.B., and Jaffrey, S.R. (2015). 5′ UTR m6A Promotes Cap-Independent Translation. Cell **163**: 999–1010.

Mielecki, D., Zugaj, D., Muszewska, A., Piwowarski, J., Chojnacka, A., Mielecki, M., Nieminuszczy, J., Grynberg, M., and Grzesiuk, E. (2012). Novel AlkB dioxygenases-alternative models for in silico and in vivo studies. PLoS One **7**: e30588.

Nei, M. and Saitou, N. (1987). The neighbor-joining method: a new method for reconstructing phylogenetic trees. Mol. Biol. Evol. **4**: 406–25.

Németh, K., Salchert K., Putnoky P. et al. (1998). Pleiotropic control of glucose and hormone responses by PRL1, a nuclear WD protein, in Arabidopsis. Genes Dev.

Pallas, V., Aparicio, F., Herranz, M.C., Sanchez-Navarro, J.A., and Scott, S.W. (2013). The Molecular Biology of Ilarviruses. Adv. Virus Res. **87**: 139–81.

Pallás, V., Más, P., and Sánchez-Navarro, J.A. (1998). Detection of Plant RNA Viruses by Nonisotopic Dot-Blot Hybridization. Methods Mol Biol **81**: 461–8.

Ping, X.L., Sun, B., Wang, L. et al. (2014). Mammalian WTAP is a regulatory subunit of the RNA N6-methyladenosine methyltransferase. Cell Res. **24**: 177–89.

Robinson, M.D. and Oshlack, A. (2010). A scaling normalization method for differential expression analysis of RNA-seq data. Genome Biol. **11**: R25.

Ryabov, E. V., Roberts, I.M., Palukaitis, P., and Taliansky, M. (1999). Host-specific cell-to-cell and long-distance movements of cucumber mosaic virus are facilitated by the movement protein of groundnut rosette virus. Virology **260**: 98–108.

Sánchez-Navarro, J.A., Reusken, C.B.E.M., Bol, J.F., and Pallás, V. (1997). Replication of alfalfa mosaic virus RNA 3 with movement and coat protein genes replaced by corresponding genes of Prunus necrotic ringspot ilarvirus. J. Gen. Virol. **78**: 3171–6.

Schwartz, S., Mumbach M.R., Jovanovic M. et al. (2014). Perturbation of m6A writers reveals two distinct classes of mRNA methylation at internal and 5′ sites. Cell Rep. **8**: 284–96.

Shen, L., Liang, Z., Gu, X., Chen, Y., Teo, Z.W.N., Hou, X., Cai, W.M., Dedon, P.C., Liu, L., and Yu, H. (2016). N 6 -Methyladenosine RNA Modification Regulates Shoot Stem Cell Fate in Arabidopsis. Dev. Cell **38**: 186–200.

Sievers, F., Wilm, A., Dineen, D., Gibson, T.J., Karplus, K., Li, W., Lopez, R., McWilliam, H., Remmert, M., Söding, J., Thompson, J.D., and Higgins, D.G. (2011). Fast, scalable generation of high-quality protein multiple sequence alignments using Clustal Omega. Mol. Syst. Biol. **7**: 539.

Tamura, K., Stecher, G., Peterson, D., Filipski, A., and Kumar, S. (2013). MEGA6: Molecular evolutionary genetics analysis version 6.0. Mol. Biol. Evol. **30**: 2725–9.

Tenllado, F. and Bol, J.F. (2000). Genetic dissection of the multiple functions of alfalfa mosaic virus coat protein in viral RNA replication, encapsidation, and movement. Virology **268**: 29–40.

Tirumuru, N., Zhao, B.S., Lu, W., Lu, Z., He, C., and Wu, L. (2016). N6-methyladenosine of HIV-1 RNA regulates viral infection and HIV-1 Gag protein expression. Elife **5**: e15528.

Van den Born, E., Omelchenko, M. V., Bekkelund, A., Leihne, V., Koonin, E. V., Dolja, V. V., and Falnes, P.O. (2008). Viral AlkB proteins repair RNA damage by oxidative demethylation. Nucleic Acids Res. **36**: 5451–5461.

Wan, Y., Tang, K., Zhang, D., Xie, S., Zhu, X., Wang, Z., and Lang, Z. (2015). Transcriptome-wide high-throughput deep m6A-seq reveals unique differential m6A methylation patterns between three organs in Arabidopsis thaliana. Genome Biol. **16**: 272.

Wang, X. Lu, Z., Gomez, A. et al. (2014). N 6-methyladenosine-dependent regulation of messenger RNA stability. Nature **505**: 117–120.

Wang, X., Zhao, B.S., Roundtree, I.A., Lu, Z., Han, D., Ma, H., Weng, X., Chen, K., Shi, H., and He, C. (2015). N6-methyladenosine modulates messenger RNA translation efficiency. Cell **161**: 1388–1399.

Xiao, W., Adhikari S., Dahal U. et al. (2016). Nuclear m6A Reader YTHDC1 Regulates mRNA Splicing. Mol. Cell **61**: 507–19.

Xu, C., Wang, X., Liu, K., Roundtree, I.A., Tempel, W., Li, Y., Lu, Z., He, C., and Min, J. (2014). Structural basis for selective binding of m6A RNA by the YTHDC1 YTH domain. Nat. Chem. Biol. **10**: 927–929.

Yoo, S.D., Cho, Y.H., and Sheen, J. (2007). Arabidopsis mesophyll protoplasts: A versatile cell system for transient gene expression analysis. Nat. Protoc. **2**: 1565–72.

Zhao, X., Yang, Y., Sun, B. et al. (2014). FTO-dependent demethylation of N6-methyladenosine regulates mRNA splicing and is required for adipogenesis. Cell Res. **24**: 1403–19.

Zheng, G., Dahl J.A., Niu Y. et al. (2013). ALKBH5 Is a Mammalian RNA Demethylase that Impacts RNA Metabolism and Mouse Fertility. Mol. Cell **49**: 18–29.

Zhong, S., Li, H., Bodi, Z., Button, J., Vespa, L., Herzog, M., and Fray, R.G. (2008). MTA Is an Arabidopsis Messenger RNA Adenosine Methylase and Interacts with a Homolog of a Sex-Specific Splicing Factor. Plant Cell Online **20**: 1278–1288.

Chapter II

The Arabidopsis m^{6}A *readers* ECT2, ECT3 and ECT5 restrict infection of *Alfalfa mosaic virus*

Part of the work included in this chapter was performed in Prof. Peter Brodersen's laboratory (University of Copenhagen, Denmark).

Abstract

Methylation of *N*^{6}-adenosine (m^{6}A) is a post-transcriptional modification that influences the fate of their RNA targets, mainly through the binding of m^{6}A *readers*. In a previous work, we identified the presence of m^{6}A in the RNAs of several plant viruses and found that the relative abundance of m^{6}A in *Alfalfa mosaic virus* (AMV) RNAs regulates viral infectivity. Furthermore, we showed that the demethylase activity of atALKBH9B modulates this viral regulation process, probably via its interaction with the AMV CP. Here we report the upregulation of some m^{6}A machinery genes after AMV infection and analyze the involvement of Arabidopsis m^{6}A *readers* in the infection cycle of plant viruses. Consistent with the previously observed m^{6}A-dependent antiviral effect, we find that, in Arabidopsis plants, the absence of ECT2/ECT3/ECT5 module promotes the systemic infection of two members of the *Bromoviridae* family, AMV and *Cucumber mosaic virus* (CMV). Furthermore, an ECT2 point mutant specifically defective in m^{6}A recognition loses wild type antiviral activity, suggesting that this effect, at least for ECT2, relies in the capability of the *reader* protein to interact with m^{6}A sites. Immunoprecipitation experiments in transgenic plants expressing either WT or point mutant ECT2 corroborate the *in vivo* interaction of this reader protein with AMV m^{6}A-RNAs through its m^{6}A binding site.

Key words: m^{6}A, viral RNA, ECTs, plant viral infections, AMV, readers.

Significance

Methylation of *N*^{6}-adenosine (m^{6}A) has emerged as a regulator of many fundamental aspects of RNA biology. Recent reports have empathized the key role of this post-transcriptional modification in the infection cycle of an increasing number of mammalian viruses. However, research about m^{6}A in plant viruses is in their infancy and we are now beginning to understand the regulatory mechanisms of this modification. The m^{6}A modification state of an RNA depends on the action of two key enzymes with opposing functions, methyltransferases (*writers*) and demethylases (*erasers*), and on a class of proteins that can specifically recognize m^{6}A-containing RNAs (*readers*). Here, we show, for the first time, that the Arabidopsis *readers* ECT2, ECT3 and ECT5 have a profound impact in the infection cycle of a plant virus through their capability to interact to m^{6}A-containing viral RNAs. Our results definitively establish this RNA modification as a critical regulatory mechanism for a plant RNA virus and open the possibility that it can be extrapolated to other virus-host interactions.

Introduction

N^6-methyladenosine (m^{6}A) is one of the most prevalent covalently modified bases in eukaryotic mRNAs (Liang et al., 2018). It has been found in mRNAs of several viruses and different organisms, including mammals, insects, plants and yeast (Yang et al., 2018; Dang et al., 2019).

The m^{6}A methylation state of an RNA depends on the action of two key enzymes with opposite functions: methyltransferases (*writers*) and demethylases (*erasers*) (Liang et al., 2018; Balacco and Soller, 2019; Lesbirel and Wilson, 2019; Zaccara et al., 2019). The discovery of *erasers* opened a debate on the reversibility of m^{6}A methylation, but there is no clear consensus on this issue yet (Ke et al., 2017; Meyer and Jaffrey, 2017; Rosa-Mercado et al., 2017; Darnell et al., 2018; Wei et al., 2018a; Shi et al., 2019). In turn, like any other chemical modification, m^{6}A could affect protein structure and/or generate a binding site for proteins termed *readers* that can specifically recognize m^{6}A-modified RNAs. m^{6}A *readers* modulate multiple aspects of RNA metabolism, such as pre-mRNA splicing, nuclear export, translation regulation and RNA stability (for recent reviews, see Zaccara et al., 2019 and Arribas-Hernández & Brodersen, 2020).

Unlike in mammals, research about m^{6}A in plants is in their infancy and we are now beginning to understand the regulatory mechanisms of this modification. The major *writer* complex, highly conserved among several species, comprises a catalytic core formed by two MTA-70 family proteins (MTA, AT4G10760 and MTB, AT4G09980) and the MT-B subcomplex, compounded of several necessary factors, like FKBP12 interacting protein 37 (FIP37, AT3G54170), VIRILIZER (VIR, AT3G05680) and the E3 ubiquitin ligase HAKAI (AT5G01160) (Zhong et al., 2008; Shen et al., 2016; Růžička et al., 2017). As in all other eukaryotic organisms investigated so far, this complex methylates sites matching the degenerate consensus motif (R)RACH (R=A/G, H=A/C/U) (Luo et al., 2014; Wan et al., 2015; Shen et al., 2016; Duan et al., 2017; Wang et al., 2017; Miao et al., 2020; Parker et al., 2020). Proteins described as *erasers* belong to the AlkB family of Fe(II)- and α-ketoglutarate-dependent dioxygenases (Van den Born et al., 2009). In Arabidopsis, the AlkB family is composed of 13 proteins, but the demethylation activity has so far only been demonstrated experimentally for atALKBH9B and atALKBH10B (Mielecki et al., 2012; Martínez-Pérez et al., 2017; Duan et al., 2017). On the other hand, the best characterized m^{6}A *readers* are proteins that contain a so-called YT521-B homology (YTH) RNA binding domain (Imai et al., 1998; Zhang et al., 2010; Liao et al., 2018). In mammals, three different YTH families are described: YTHDF (YTHDF1-3), YTHDC1 and YTHDC2 (Liao et al., 2018). Human YTHDFs are modular proteins that have a N-terminal part with several P/Q/N-rich patches, predicted to constitute

intrinsically disordered regions (IDR) that function as regulatory elements (Wang et al., 2014), and a C-terminal YTH domain, which recognizes m^{6}A via a hydrophobic pocket made of aromatic amino acid side chains (Theler et al., 2014; Patil et al., 2018). YTHDF proteins were proposed to act together in the cytoplasm to influence the translation and stability of m^{6}A-modified mRNAs. Thus, whereas YTHDF1 would promote protein production (Wang et al., 2015), YTHDF2 would accelerate the decay of m^{6}A-modified transcripts (Wang et al., 2014), and YTHDF3 would facilitate mRNAs translation in synergy with YTHDF1 and affect methylated-mRNA decay mediated by YTHDF2 (Shi et al., 2017). However, a very recent study reported that YTHDF1-3 recognize the same m^{6}A-modified mRNAs and act together in mRNA degradation proportionally to the number of m^{6}A residues (Zaccara and Jaffrey, 2020). While twelve YTH-domain containing genes were identified in rice (osYTH1-12), in Arabidopsis, the YTH family is composed of 13 proteins: EVOLUTIONARILY CONSERVED C-TERMINAL REGION proteins 1-11 (ECT1-11), At4g11970 and the CLEAVAGE AND POLYADENYLATION SPECIFICITY FACTOR 30 (CPSF30). ECT1-11 belong to YTHDF clade, whereas CPSF30 and At4g11970 cluster into YTHDC group (Li et al., 2014a; Scutenaire et al., 2018). ECT2, ECT3 and ECT4 were described as m^{6}A *readers* that play redundant roles in m^{6}A-dependent control of developmental timing and leaf morphogenesis (Arribas-Hernández et al., 2018) and, accordingly, ECT2 and ECT3 are highly expressed at leaf formation sites in the shoot apex. In addition, several studies described stochastic defects in control of branch numbers in epidermal hairs (trichomes) in *ect2* mutants (Arribas-Hernández et al., 2018; Scutenaire et al., 2018; Wei et al., 2018b), a process in which ECT3 has an equivalent, yet seemingly not completely redundant, function (Arribas-Hernández et al., 2018). Sequence homology analysis found that the residues implicated in RNA and m^{6}A binding of human YTHDF proteins are highly conserved in Arabidopsis ECT1-4 proteins, including the three tryptophan residues homologous to those that form the m^{6}A binding aromatic cage (Arribas-Hernández et al., 2018). Moreover, mutational studies of these tryptophan residues demonstrated that integrity of this aromatic cage is required for ECT2 binding to m^{6}A-modified RNAs (Scutenaire et al., 2018) and for ECT2 and ECT3 function *in vivo* (Arribas-Hernández et al., 2018). Regarding the subcellular localization of these proteins, ECT1 shows a predominant nuclear localization (Ok et al., 2005), whereas ECT2, ECT3 and ECT4 were described as cytoplasmic proteins (Arribas-Hernández et al., 2018), although seemingly nuclear localization of ECT2 were also reported (Scutenaire et al., 2018; Wei et al., 2018b). Interestingly, heat and osmotic stresses trigger the accumulation of ECT2, ECT3 and ECT4 in cytosolic foci different to P-bodies that, in the case of ECT2, were identified as stress granules (SGs) (Arribas-Hernández et al., 2018; Scutenaire et al., 2018).

Although m^{6}A mark was already detected in viral mRNAs of *Simian virus 40* (SV40) in 1975 (Lavi and Shatkin, 1975), its function in multiple viral cycles was not addressed until the last few years (for a recent review, see Williams, Gokhale, & Horner, 2019). m^{6}A was found in viral RNAs (vRNAs) from mammalian viruses with RNA and DNA genomes, and direct binding of YTH proteins to RNAs from some of these viruses, such as *Hepatitis C* (HCV), *Zika virus* (ZIKV) or *Human immunodeficiency virus-1* (HIV-1), were observed (Gokhale et al., 2016; Kennedy et al., 2016; Lichinchi et al., 2016b). Intriguingly, this modification seems to regulate the viral infections in different ways (Pereira-Montecinos et al., 2017; Dang et al., 2019). For example, whereas the overexpression of YTHDF2 increases the replication of *Influenza A virus* (IAV) (Courtney et al., 2017), the depletion of any YTHDF protein positively affects ZIKV replication and HCV particle production (Gokhale et al., 2016). In addition, conflicting results were reported for some viruses. For HIV-1, several studies showed that binding of YTHDF1–3 proteins to viral m^{6}A sites can lead to reduced viral infection by blocking reverse transcription (RT) (Tirumuru et al., 2016; Lu et al., 2018), while others suggested that YTH proteins mainly stimulate viral replication (Lichinchi et al., 2016a), transcription and translation (Kennedy et al., 2016). Some of these discrepancies could be due to methodological reasons – different m^{6}A detection techniques or viral infection time span evaluated –, but it is also likely that other factors contribute to define m^{6}A function. For instance, during Hepatitis B infection, binding of YTHs to m^{6}A at the 5'-UTR epsilon loop of the pre-genomic RNA enhances viral RT, but binding to m^{6}A sites located at 3'-UTR promotes RNA destabilization (Imam et al., 2018).

In plant viruses, there are far fewer examples of the involvement of m^{6}A in infection cycles. m^{6}A levels of *Nicotiana tabacum* plants mRNAs were shown to increase during infection with *Tobacco mosaic virus* (TMV) and, additionally, a potential *eraser*, orthologous to human ALKBH5, and all the potential *writers* were induced and repressed, respectively, respect to healthy plants (Li et al., 2018). Remarkably, other studies reported the presence of AlkB domains in some positive single-stranded RNA ((+)ssRNA) viruses of *Alphaflexiviridae, Betaflexiviridae* and Closteroviridae families (Martelli et al., 2007) that revert methylation-induced lesions in bacteriophages (Aravind and Koonin, 2001; Van den Born et al., 2008). Later, through bioinformatic analysis, this AlkB functional domain was delimited to a 150-170 amino acids region with some characteristic residues, which are not conserved in AlkB proteins from other organisms (Moore and Meng, 2019). Nonetheless, additional *in vitro* and *in vivo* activity assays will be required to prove their putative m^{6}A demethylation activity.

In this work, we analyze the role of several Arabidopsis m^{6}A *readers* in the infection by *Alfalfa mosaic virus* (AMV). This virus belongs to the *Bromoviridae* family (Bujarski et al., 2019) and, like all members of this family, its genome consists of three (+)ssRNAs. RNAs 1 and 2 encode the replicase subunits, whereas RNA 3 encodes the movement protein and serves as a template for the synthesis of the non-replicating subgenomic RNA 4 (sgRNA 4), which encodes the coat protein (CP) (Krab et al., 2005). AMV, together with ilarviruses, is the only virus that requires the presence of CP or sgRNA 4 in the inoculum to initiate the infection, a process known as "genome activation" (Bol, 2005; Pallas et al., 2013). Thus, AMV CP is a multifunctional protein involved in the regulation of translation of vRNAs, and in cell-to-cell and systemic movement of the virus (Herranz et al., 2012). In the previous chapter, we described that AMV contains several m^{6}A sites scattered along the three genomic RNAs, and its CP acts to recruit the host m^{6}A *eraser* atALKBH9B to reduce the m^{6}A content in vRNAs. This demethylation is key for viral infectivity, because AMV systemic spread towards the floral stems is severely hampered in at*alkbh9b* plants (Martínez-Pérez et al., 2017). Here, we show for the first time the involvement of m^{6}A *reader*s in the infection cycle of a plant virus. In Arabidopsis plants, the absence of ECT2/ECT3/ECT5 module promotes the systemic infection of AMV and *Cucumber mosaic virus* (CMV), another member of the *Bromoviridae* family. Furthermore, we find that an ECT2 point mutant specifically defective in m^{6}A recognition loses wild type antiviral activity and that ECT2 can be cross-linked to AMV RNA *in vivo*. These observations suggest that ECT2 may exert its antiviral effect by direct interaction with m^{6}A bases contained within vRNAs.

Results

AMV-induced differential expression of mRNAs encoding components of m^{6}A machinery. Viral infections cause significant alterations in the expression of host mRNAs as a consequence of two reciprocal effects: (i) viral manipulation of the host environment to increase pathogenicity and (ii) defense responses activated by the host to fend off the virus (Pallas and García, 2011; Rodrigo et al., 2012). To understand how Arabidopsis responds to AMV infection, we performed mRNA-seq analysis of AMV-infected tissues. Young, emerging rosette leaves were chosen for this analysis, since our main objective was the evaluation of the expression changes for m^{6}A mechanism components, which were shown to be mostly expressed in tissues with high cell division rates (Zhong et al., 2008; Arribas-Hernández et al., 2018). Differential expression analysis showed that 2611 genes were significantly upregulated ($\log_2$FC≥1; FC, fold change),

whereas only 194 genes were downregulated ($log_2FC \leq -1$) because of AMV infection (Fig. 1A). Most of these genes encode proteins localized in the nucleus, plasma membrane and chloroplasts, and are known to encode protein-, DNA- or RNA-binding proteins, including some components of the m^6A machinery (Fig. 1B). The levels of mRNAs encoding three components of the methylation complex – MTA, MTB and VIRILIZER – were upregulated by the infection, whereas the levels of mRNAs encoding potential m^6A *erasers* did not substantially change (Fig. 1C). Among the possible *reader* proteins containing YTH domains, only ECT5 showed a significant overexpression. In contrast, the previously described as functional m^6A *readers* ECT2, ECT3 and ECT4 (Arribas-Hernández et al., 2018) were not drastically deregulated, although ECT2 and ECT3 have log_2FC values around 0,5 (0,6 and 0,4, respectively) with p-values in the order of 10^{-6}-10^{-7}, which could mean a slightly upregulation (Fig. 1C). The overexpressed m^6A machinery factors, ECT5, MTA, MTB and VIR, were selected as representative genes to validate the RNA-seq experiment. Thereby, the RT-qPCR analysis corroborated the upregulation of these four genes following AMV infection (Fig. 1D).

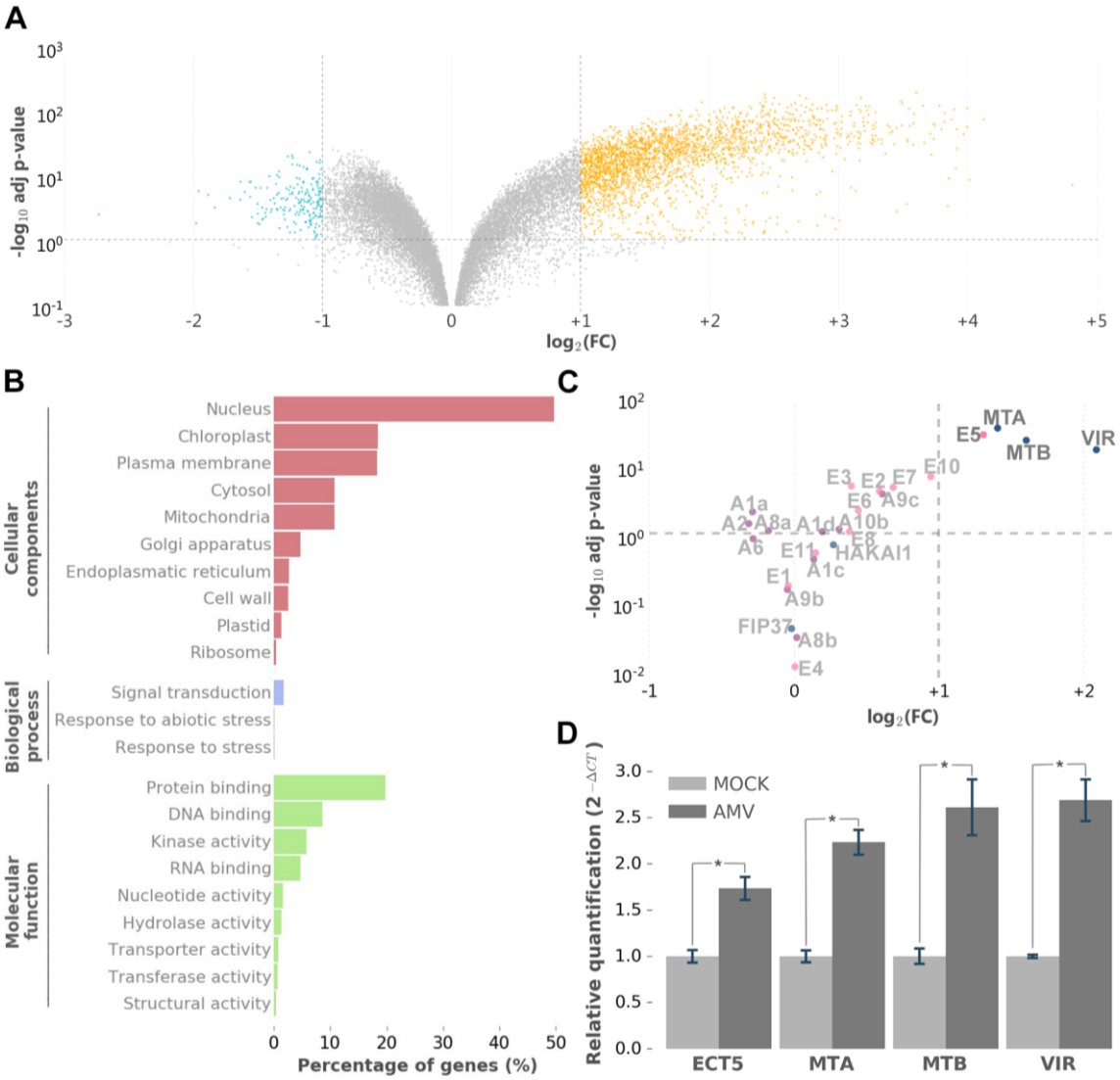

Figure 1. Changes on Arabidopsis transcriptome induced by AMV infection. (A) *Volcano plot depicting the distribution of nearly 18000 unique genes (minimum expression of 1 read per kilobase million, RPKM) in response to AMV infection. Upregulated genes ($log_2FC \geq 1$) are in yellow and downregulated genes ($log_2FC \leq -1$) are in blue, being the accepted adjusted p-value≤0,05.* ***(B)*** *Gene ontology (GO) analysis result of the genes significantly deregulated.* ***(C)*** *Volcano plot showing only genes implied in m^{6}A mechanism. A1-10, ALKBH1-10; E1-11, ECT1-11.* ***(D)*** *Sequencing validation by RT-qPCR of four upregulated m^{6}A genes in three biological replicates. Error bars represent the standard error of the mean (SEM). Asterisks indicate p-value<0,05 applying Student's t-test for ΔCt mean values (n=3).*

AMV infection is promoted in m^{6}A *readers* mutants. Recent studies showed that m^{6}A binding activity of the YTHDF proteins ECT2, ECT3 and ECT4 are required for normal development of Arabidopsis plants (Arribas-Hernández et al., 2018). To check whether the described m^{6}A *readers* are involved in the AMV infection process, Arabidopsis WT Col-0 and *ect2, ect3* or *ect4* single knockout plants were inoculated with viral particles (Annex I). Northern blots of systemic tissue at 7 days post-inoculation (dpi) did not show consistent differences in viral accumulation of the single mutants respect to WT plants (data not shown), so we hypothesized that it may be due to the partial functional redundancy of these proteins, an observation previously described in the context of organogenesis (Arribas-Hernández et al., 2018; 2020). Therefore, we carried

out the same experiment using the double *ect2-1/ect3-1, ect2-1/ect4-2*, *ect3-1/ect4-2* and the triple *ect2-1/ect3-1/ect4-2* mutant lines (described by Arribas-Hernández et al., 2018) (Annex I), and analyzed viral accumulation in inoculated leaves at 3 dpi and in systemic tissue at 7 dpi. As it can be observed, AMV titers did not change in the inoculated leaves (Fig. 2A and 2B) but were noticeable higher in the systemic tissue (Fig. 2C and 2D) of all mutants compared with WT. Clearly, the most appreciable differences in viral accumulation were observed in double mutants lacking ECT2, whereas these differences were not significant in *ect3-1/ect4-2*. Thus, while ECT2 may have a more essential role in the viral infection, ECT4 seems to have a minor participation in this process. Hence, in spite of the fact that *ect2-1/ect3-1/ect4-2* showed the highest viral accumulation, we decided to use the *ect2-1/ect3-1* mutant in the following experiments, since the triple mutation causes a more pronounced developmental phenotype in Arabidopsis plants (Arribas-Hernández et al., 2018). On top of this, the differences of viral systemic load between WT and *ect2/ect3* were confirmed using another independent transgenic line, *ect2-3/ect3-2* (Fig. S1).

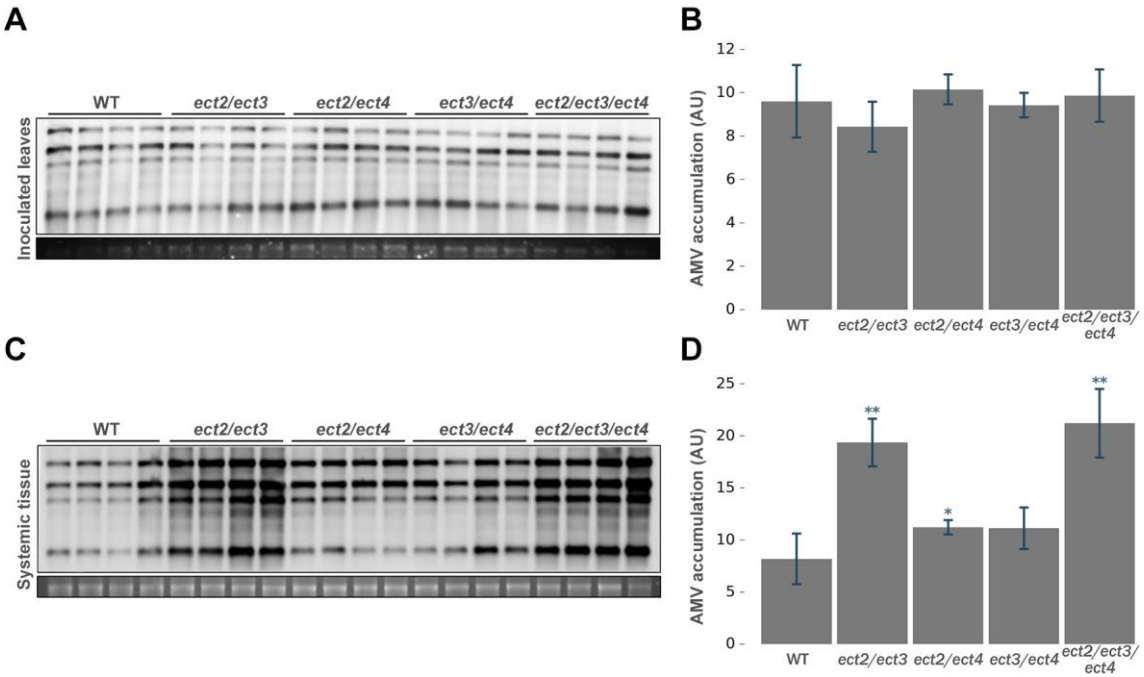

Figure 2. AMV accumulation analysis in ECT2/3/4 mutants compared to WT plants. (A and C) *Representative northern blot from inoculated leaves at 3 dpi (A) and from systemic aerial tissue at 7 dpi (C) of WT and double and triple ECT2/3/4 mutants (genotypes are indicated on the top of each northern blot). vRNA 1-4 were detected by specific Dig-labelled probes and ethidium bromide of ribosomal RNAs (rRNAs) was used as RNA loading control. Each sample corresponds to a mix of three plants. (**B and D)** Graphics showing the quantification of panels A (B) and C (D). Error bars corresponds to standard deviations (SD) values. Asterisks indicate significant differences from the WT (*p-value < 0,05 and ** p-value <0,01) using the Student's t-test (n = 4). AU, arbitrary units.*

Development and characterization of *ECT5* mutants. Since *ECT5* was the most highly induced ECT by AMV infection, we also tested the possible involvement of this gene in antiviral defense.

We identified a T-DNA line homozygous for an insertion in exon 5 (N653489; SALK_131549, ecotype Col-0), that we named *ect5-1* (Fig. 3A). Presence of the T-DNA was confirmed by PCR, showing that this transgenic line is homozygous for the insertion. Furthermore, we analyzed ECT5 mRNA levels in WT and mutant backgrounds by RT-PCR to amplify the full-length ECT5 mRNA and we found that *ect5-1* mutant does not produce any stable full-length mRNA (Fig. 3B). In parallel, since the *ECT2* (AT3G13460) and *ECT5* (AT3G13060) chromosomal loci are closely linked (~205 kb apart) (Fig. 3C), we next used CRISPR (clustered regularly interspaced short palindromic repeats)/Cas9 to engineer *ECT5* deletions directly in the *ect2-1* and *ect2-1/ect3-1* backgrounds (Arribas-Hernández et al., 2018) to obtain a set of double (*ect2-1/ect5-2* and *ect2-1/ect5-3)* and triple mutants (*ect2-1/ect3-1/ect5-4* and *ect2-1/ect3-1/ect5-5*), each containing independent deletions in the *ECT5* gene (Fig. 3A and Annex I and II). In this case, *ect2-1* and *ect2-1/ect3-1* plants were transformed with two sgRNAs following a previously described protocol (Tsutsui and Higashiyama, 2017). Except a slightly reduction of the flowering stem growth, *ect5* and *ect2/ect5* plants do not present any other clear developmental defect compared to WT, whereas the triple mutant *ect2/ect3/ect5* shares the developmental phenotype of *ect2/ect3*, already described by Arribas-Hernández et al. (2018) (Fig. 3D).

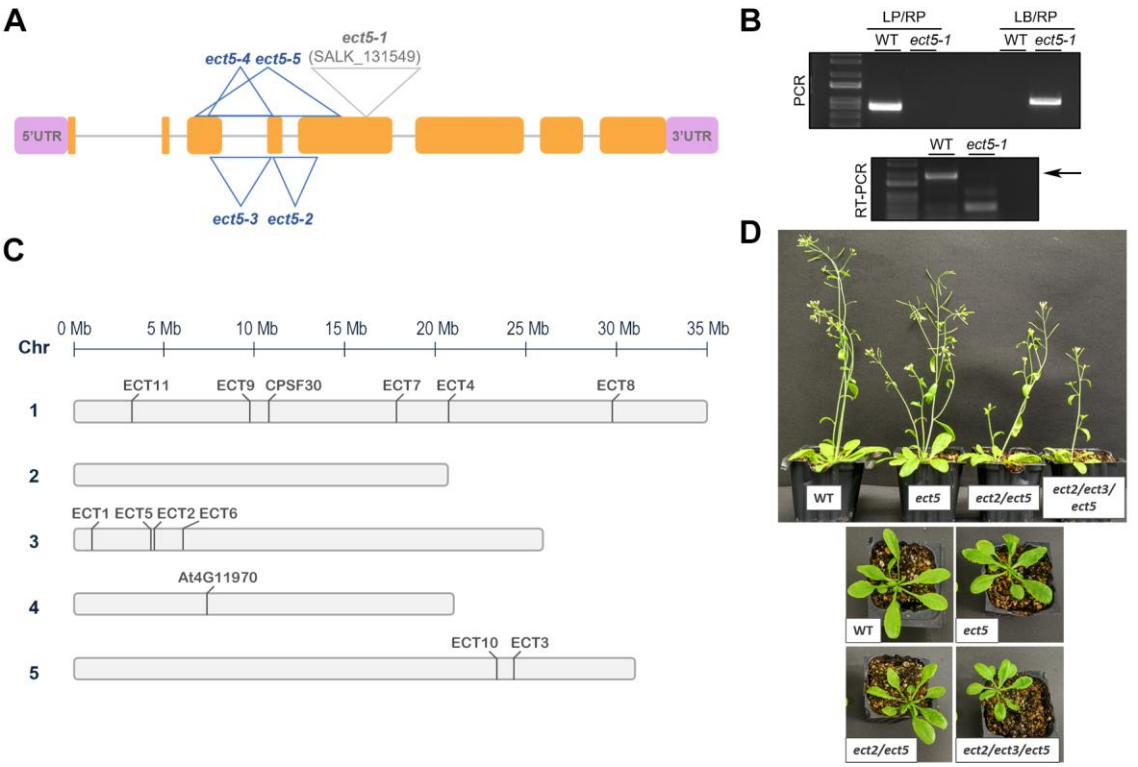

Figure 3. Construction and genotyping of ECT5 Arabidopsis mutant plants. (A) *Annotated genomic ECT5 gene structure (AT3G13060.2) showing the exons (orange boxes), location of the T-DNA insertion (SALK_131549) in ect5-1 mutant (in grey) and deletions constructed by CRISPR/Cas9 (in blue).* ***(B)*** *ect5-1 genotyping confirmation. Agarose gels electrophoresis images of the PCR and RT-PCR products produced with specific primers (Annex III) to corroborate the presence of the T-DNA (upper panel) and the full-length mRNA (bottom panel) of the ECT5 gene from WT and ect5-1*

plants. The position of the full-length mRNA is indicated on the right. LP and RP, left and right genomic primer; LB, left border primer of the T-DNA insertion. ***(C)*** *Schematic physical map indicating the position of the YTH gene loci on the 5 chromosomes (Chr) of Arabidopsis thaliana. Mb, mega base pairs.* ***(D)*** *Representative pictures of 23 days-old plants showing the phenotypes of each ect5 mutant compared to WT.*

Implication of ECT5 on AMV infection. To determine the potential role of ECT5 in the AMV infection cycle, vRNAs levels in inoculated and systemic leaves were quantified by northern blot in all the *ect5* mutants and WT plants. As with single *ect2*, *ect3* and *ect4* null alleles, the absence of *ECT5* alone did not cause significant changes in viral titers, neither in inoculated nor in systemic tissue (Fig. 4). Likewise, despite the increase of AMV load, the variation found in double and triple mutants compared to WT in the inoculated leaves was not statistically significant (Fig. 4A and 4B). In contrast, the systemic accumulation of AMV was significantly higher in *ect2/ect5* and *ect2/ect3/ect5* compared to WT plants (Fig. 4C and 4D). Results shown in Figure 4 correspond to *ect2-1/ect5-2* and *ect2-1/ect3-1/ect5-4,* but similar results were obtained with *ect2-1/ect5-3* and *ect2-1/ect3-1/ect5-5* lines (Fig. S2).

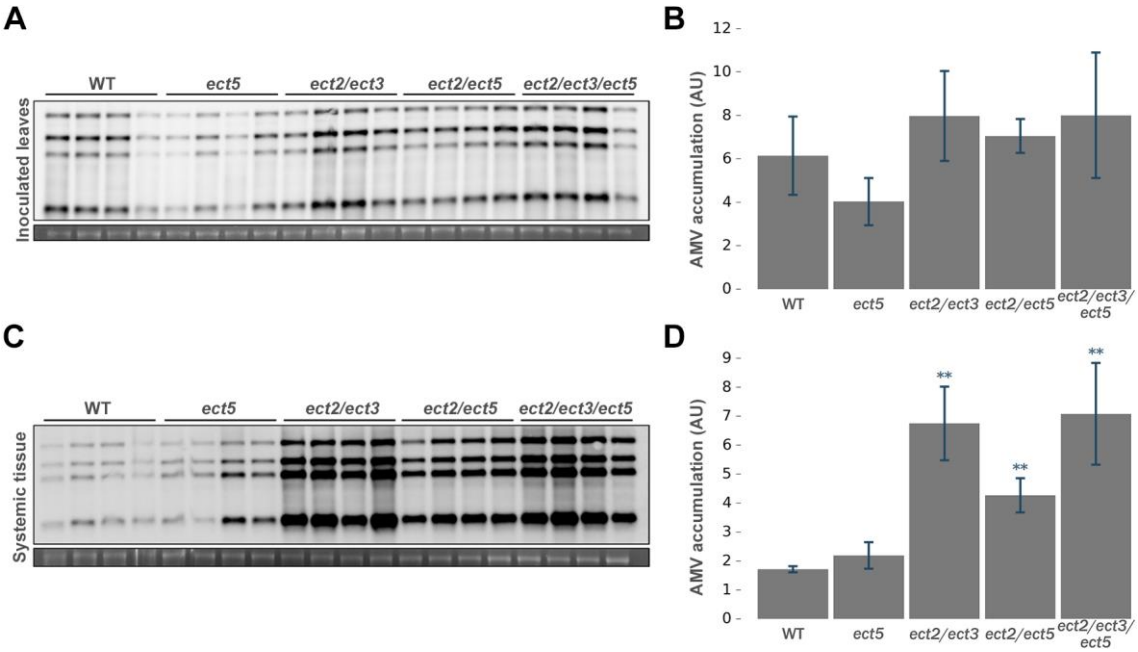

Figure 4. ECT5 is implied in AMV infection cycle. (A and C) *Representative northern blot from inoculated leaves at 3 dpi (A) and systemic aerial tissue at 7 dpi (C) of WT and ECT5 mutants described in Fig.3 (genotypes are indicated on the top of each northern blot). vRNA 1-4 were detected by specific Dig-labelled probes and ethidium bromide of rRNAs was used as RNA loading control. Each sample corresponds to a pool of two plants. (**B and D)** Graphics showing the quantification of panels A (B) and C (D). The experiment was carried out with the two ect2/ect5 and ect2/ect3/ect5 mutant lines, obtaining similar results (Fig. S2). Error bars correspond to SD values. Asterisks indicate significant differences from the WT (**p-value<0,01) using the Student's t-test (n=4). AU, arbitrary units.*

Taken together, the observations that *ECT5* is induced during AMV infection and that the infectivity of AMV is increased in knockouts of *ECT2, ECT3* and/or *ECT5* indicate that these m^{6}A *readers* restrict AMV infection. Two broad scenarios could explain this effect. First, mutation of *ECT* genes could deregulate key host housekeeping pathways leading to an altered

developmental and cellular state, more favorable to viral replication, compared with WT. We consider this first possibility to be unlikely, because it would be expected that these altered host pathways correlate with phenotypical changes and *ect2/ect5,* in contrast to *ect2/ect3*, does not exhibit any observable developmental phenotype effect, yet shows robust increase in AMV titers upon infection compared to WT. Alternatively, keeping in mind that at least *ECT5* expression is induced in AMV-infected plants, we consider a more plausible scenario that ECT2/3/5 function as immune effector genes restricting viral infection either by shaping host m^6A RNA expression and/or via direct binding to m^6A-modified vRNAs. To experimentally corroborate this last hypothesis, we next analyzed whether m^6A-binding activity of ECT2 is required for its antiviral effect and the putative direct recognition of m^6A-modified vRNAs by ECT2.

A functional ECT2 m^6A-binding site is required to restrict AMV accumulation. Tryptophan residues that form the aromatic cage are essential for high-affinity binding ability of ECTs to m^6A-containing RNAs (Li et al., 2014b, 2018; Xu et al., 2014, 2015; Zhu et al., 2014; Arribas-Hernández et al., 2018). Consequently, substitution of the tryptophan residue at position 464 by an alanine (W464A) makes the fusion protein $ECT2^{W464A}$:mCherry to fail rescuing *ect2-1/ect3-1/ect4-2* mutant phenotype (Arribas-Hernández et al., 2018). We used complementation lines in the *ect2-1/ect3-1* background expressing the fusion proteins ECT2:mCherry (E2mCh plants) or $ECT2^{W464A}$:mCherry ($E2^{w}$mCh plants) (Annex I) to check the requirement of a fully intact m^6A binding site in ECT2 for AMV infectivity. Viral accumulation was analyzed in systemic tissue from two different E2mCh and $E2^{w}$mCh lines and northern blots revealed that AMV levels in E2mCh complemented lines were similar to WT plants, whereas it clearly increased in $E2^{w}$mCh lines, resembling *ect2-1/ect3-1* infection levels (Fig. 5A, upper and lower panels). Moreover, this complementation effect could also be observed at phenotypical level. As shown in Figure 5B, plants lacking a functional ECT2 protein showed a clear growth defect consisting in a reduction of fresh weight, and, remarkably, AMV infection produced a slightly fresh weight reduction only in *ect2-1/ect3-1* mutant and in $E2^{w}$Ch complemented lines respect to the MOCK inoculated plants. Overall, our results suggest that ECT2 requires a fully functional m^6A binding site to modulate AMV infection, but, at that time, it was still unknown whether ECT2 directly recognizes m^6A-modified vRNAs.

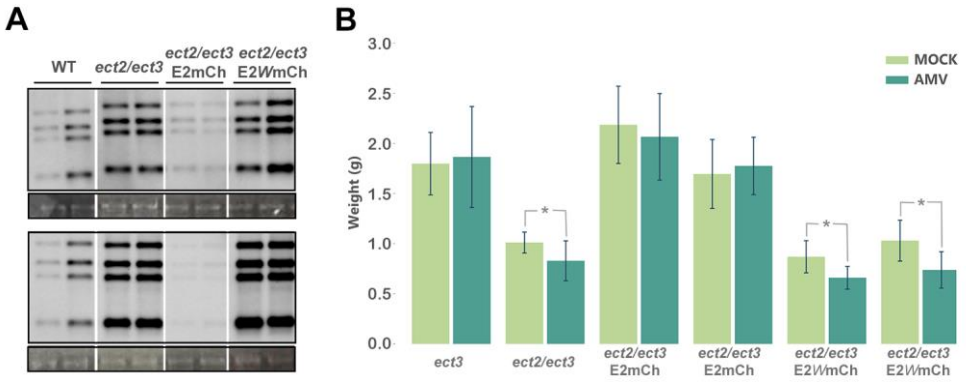

Figure 5. Infection phenotype is rescued when ect2/ect3 mutant is complemented with E2mCh, but not with E2^{w}mCh. (A) *Representative northern blot from systemic tissue at 7 dpi of WT, ect2/ect3 and two complemented E2mCh or E2^{w}mCh independent transgenic lines (upper and lower panels). vRNA 1-4 were detected by specific Dig-labelled probes and ethidium bromide of rRNAs was used as RNA loading control. Each sample corresponds to a pool of three plants.* ***(B)*** *Graphic showing the differences of fresh weight (grams, g) between MOCK (healthy) and AMV-infected plants for each genotype. Error bars corresponds to SD values. Asterisks indicate significant differences from the WT (*p-value<0,05) using Student's t-test (n=8).*

ECT2 directly interacts with vRNAs *in vivo*. We next addressed the possible recognition of m^{6}A-modified vRNAs by ECT2. Transgenic lines expressing 3xHA:ECT2 (HA:E2) or 3xHA:ECT2^{W464A} (HA:E2^{W}) in the *ect2-1* background (Annex I) were inoculated with AMV. To stabilize RNA-protein interactions *in vivo*, a cross-link step was performed by applying Ultra-Violet (UV) light to entire plants and HA:ECT2-RNA complexes were immunoprecipitated (IP) using an anti-HA antibody (Fig. 6A). The presence of AMV RNAs in input mock (M) and infected (A) samples was evaluated by northern blot analysis (Fig. 6B), whereas a western blot using an anti-HA antibody and a dot blot analysis were carried out to detect the presence of HA:ECT2 and vRNAs in the IP samples, respectively (Fig. 6C and 6D). Although approximately the same quantity of HA:ECT2 was detected in the input and IP extracts for all the samples (Fig. 6C), vRNAs were detected in *ect2-1* plants complemented with HA:E2, but not in HA:E2^{W} plants, suggesting that ECT2 interacts directly with AMV m^{6}A-RNAs *in vivo* through its m^{6}A binding site (Fig. 6D, last square denoted by an arrowhead).

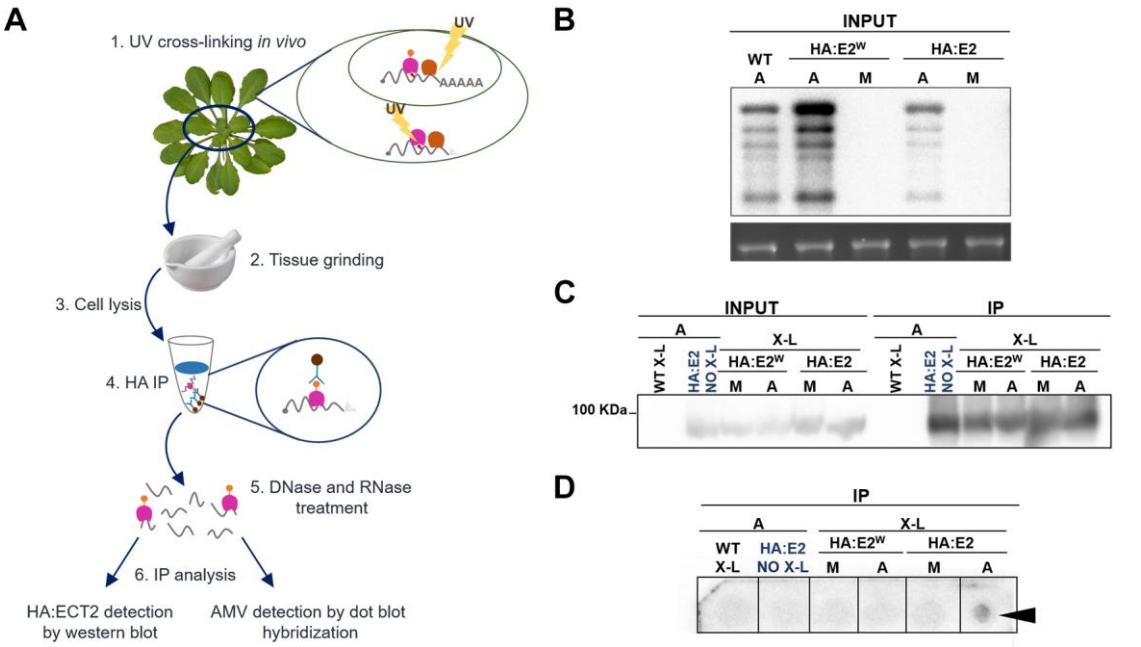

Figure 6. In vivo interaction between ECT2 and AMV RNAs. (A) *Schematic diagram showing ECT2-vRNA immunoprecipitation (IP) protocol.* ***(B)*** *Northern blot from input samples used for the IP assay. vRNA 1-4 were detected by specific Dig-labelled probes and ethidium bromide of rRNAs was used as RNA loading control.* ***(C)*** *Western blot from input and IP samples to detect HA:E2 and HA:E2^{W} proteins using an anti-HA antibody.* ***(D)*** *Dot blot using specific radioactively labelled probes to detect AMV RNAs from IP samples. X-L, cross-link; M, MOCK; A, AMV.*

In principle, *in vivo* association between ECT2 and vRNA would indicate that *readers* directly modulate m^{6}A-modified vRNAs. Hence, the loss of ECT function could revert the partial resistance against AMV observed in *atalkbh9b* plants, which is apparently caused by the viral hypermethylation. In other words, it would be expected that, in the absence of the effector proteins, the methylation of vRNAs would not significantly affect the infection process. To test this hypothesis, we analyzed the viral titers in the quadruple mutant *atalkbh9b/ect2/ect3/ect4* obtained from *atalkbh9b* x *ect2/ect3/ect4* cross (Annex I). Remarkably, northern blot analysis of systemic tissue at 7 dpi showed that knockout of the module *ECT2/3/4* in the *atalkbh9b* background recovers the WT phenotype against AMV infection, although viral accumulation levels were lower than in *ect2/ect3/ect4* plants (Fig. 7).

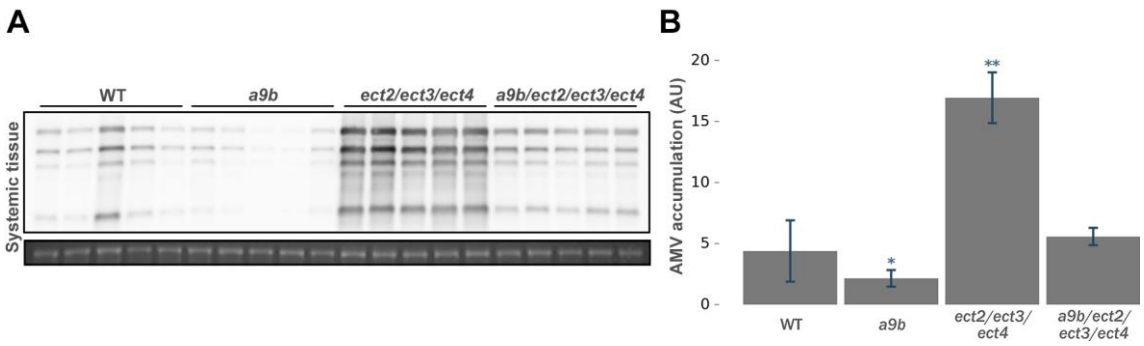

Figure 7. Knockout of ECT2/3/4 module in atalkbh9b background recovers WT susceptibility against AMV infection. ***(A)*** *Northern blot from aerial systemic tissue at 7 dpi. Genotypes are indicated on the top of each northern blot. a9b,*

atalkbh9b. vRNA 1-4 were detected by specific Dig-labelled probes and ethidium bromide of rRNAs was used as RNA loading control. ***(B)*** *Graphic showing the quantification of panel A. Error bars correspond to SD values. Asterisks indicate significant differences from the WT (**p-value<0,05 and *p-value<0,1) using the Student's t-test (n=5). AU, arbitrary units.*

ECT5 may localize in cytoplasmic loci, and ECT2/5 interact with atALKBH9B. Subcellular localization of ECT2, ECT3 and ECT4 were previously described as cytoplasmic, occasionally showing some granule formation (Arribas-Hernández et al., 2018; Scutenaire et al., 2018). In order to increase our knowledge on the subcellular pattern of Arabidopsis ECTs, we addressed the analysis of ECT5 subcellular location by transient expression of translational fusions with GFP (GFP:ECT5 and ECT5:GFP) in agroinfiltrated *Nicotiana benthamiana* leaves. Confocal laser scan microscope (CLSM) images show different localization patterns depending on the position of the fused GFP in ECT5 protein. Thus, GFP:ECT5 fusion protein displayed a cytoplasmic diffuse pattern, whilst ECT5:GFP, in addition to this cytoplasmic pattern, formed unidentified granules and aggregates of different size (Fig. 8A).

Bearing in mind that AMV CP directly interacts with the demethylase atALKBH9B (Martínez-Pérez et al., 2017), we wondered whether the CP could establish also direct interactions with m^{6}A *readers* to facilitate the formation of virus-m^{6}A effector complexes. Thus, CP and ECT2 or ECT5 were fused to the N-terminal and C-terminal parts of the GFP, respectively (NGFP:CP, CGFP:ECT2, CGFP:ECT5 and ECT5:CGFP) (Figure 8B). Bimolecular Fluorescence Complementation (BiFC) assay revealed that GFP luminescence was not reconstituted in cells of *N. benthamiana* infiltrated with CP plus ECT5 or ECT2 (Fig. 8B). Interestingly, both ECT proteins interacted with atALKBH9B (Fig. 8B), indicating that different m^{6}A machinery players might form protein complexes.

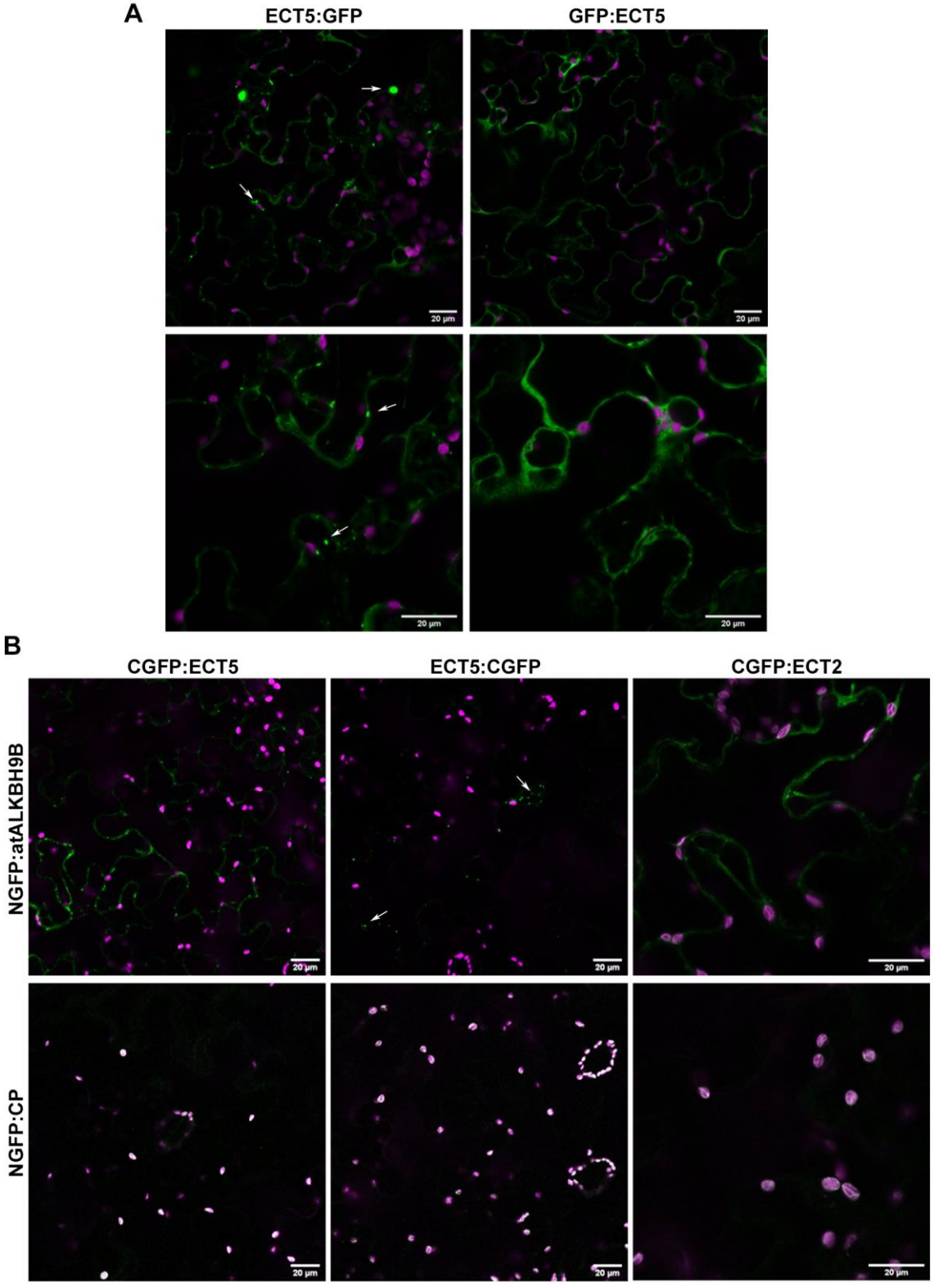

Figure 8. Subcellular localization of ECT5 and interactions between m^{6}A mechanism components. *Confocal laser scanning microscope (CLSM) images of N. benthamiana leaf epidermal cells infiltrated with the DNA constructs indicated above the images. Pictures are the overlay of the green and chlorophyll (in violet) channels.* ***(A)*** *Subcellular localization of the fusion protein ECT5:GFP and GFP:ECT5. Granules formed by ECT5:GFP are indicated by arrows.* ***(B)*** *BiFC assay of CGFP:ECT5, ECT5:CGFP or CGFP:ECT2 with NGFP:ALKBH9B or NGFP:CP$_{AMV}$. Granules formed by atALKBH9B-ECT5 interaction are indicated by arrows.*

Effect of the ECT2/ECT3/ECT5 module in other viral infections. Taken together, our observations suggest that AMV infection is regulated by ECT2/ECT3/ECT5 module through, at least, the interaction between ECT2 and the m^{6}A residues along the AMV genome. To analyze whether this antiviral effect is specific of AMV or, by contrast, it is a more general mechanism, we checked the viral fitness for the systemic invasion of CMV in double *ect2/ect3, ect2/ect5* and triple *ect2/ect3/ect5* mutants. Due to the fact that, in Arabidopsis, CMV moves to the upper systemic tissues faster than AMV, we analyzed viral accumulation in systemic aerial tissue at 4 and 7 dpi. Although the effect was more evident at 4 dpi, the absence of ECT2 and ECT3 and/or ECT5 increased the host susceptibility to CMV accumulation at both times, suggesting that the implication of ECT2/ECT3/ECT5 module may not be an exclusively trait of AMV (Fig. 9). Results shown in Figure 8 correspond to *ect2-1/ect5*-3 and *ect2-1/ect3-1/ect5*-4, but similar results were obtained at 4 dpi using *ect2-1/ect5-2* and *ect2-1/ect3-1/ect5-5* lines (Fig. S3). Further studies using other not phylogenetically related viruses are required to determine whether these m^{6}A *readers* can be part of a broad plant regulatory strategy to control viral infections in plants.

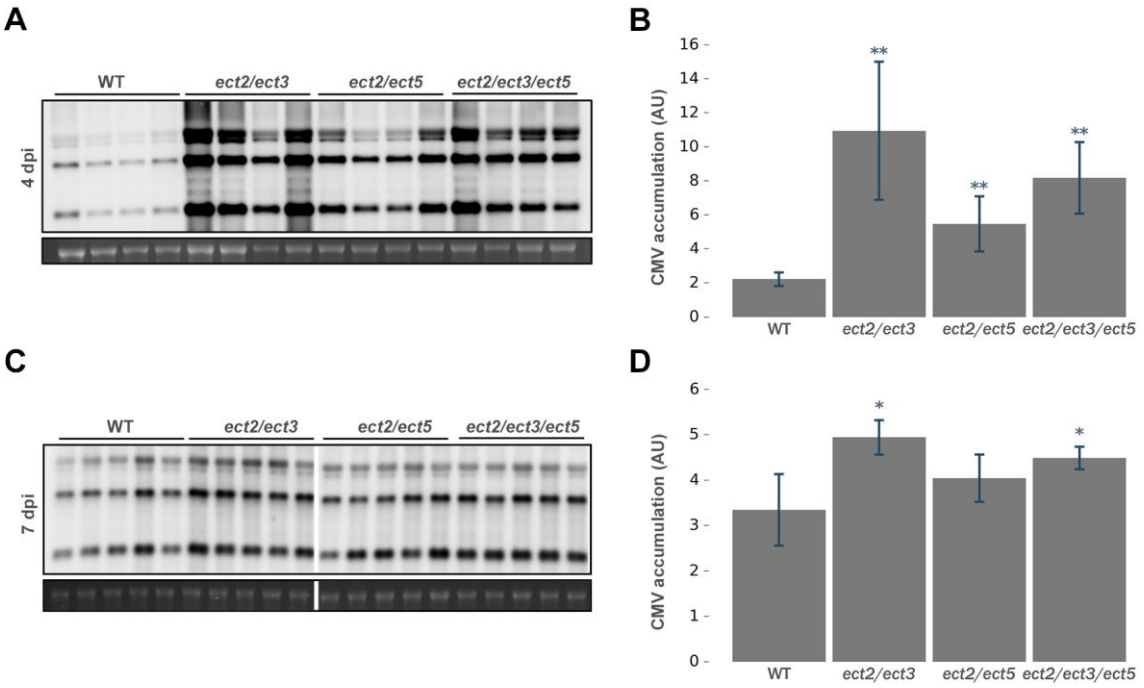

Figure 9. ECT2/3/5 module is also implied in CMV infection cycle. (A and C) *Representative northern blots from aerial systemic tissue at 4 dpi (A) and 7 dpi (C). Genotypes are indicated on the top of each northern blot. vRNA 1-4 were detected by specific Dig-labelled probes and ethidium bromide of rRNAs was used as RNA loading control.* ***(B and D)*** *Graphics showing the quantification of panel A (B) and C (D). Error bars of the quantification graphics corresponds to SD values. Asterisks indicate significant differences from the WT (**p-value<0,01 and *p-value<0,05) using the Student's t-test (n=4). The experiment at 4 dpi was carried out with the two ect2/ect5 and ect2/ect3/ect5 mutant lines, obtaining comparable results (Fig. S3). AU, arbitrary units.*

Discussion

In the previous chapter, we reported that, as found in animal viruses, plant m^{6}A-mediated regulatory mechanism influences the infection process of a plant RNA virus. We described the presence of m^{6}A in the AMV genome and hypothesized that overaccumulation of this mark in vRNAs negatively affects the viral process. The absence of the *eraser* atALKBH9B induces an increase of m^{6}A levels in the AMV genome and dramatically affects the capability of the virus to systemically invade the plant. These observations prompted us to propose that m^{6}A may play an important role in the infection cycle of plant viruses (Martínez-Pérez et al., 2017). Therefore, the main goal of the present work was to identify regulatory components of the m^{6}A pathway involved in viral infections and to comprehend the molecular mechanism governing this process.

To identify responsive m^{6}A components, we performed a high-throughput transcriptome sequencing analysis of young, emerging rosette leaves of Arabidopsis AMV-infected plants, since some of the host m^{6}A regulatory effectors are mostly expressed in tissues with high cell division rates (Zhong et al., 2008; Arribas-Hernández et al., 2018). AMV infection in Arabidopsis leads to the upregulation of 2611 genes in comparison to 194 downregulated ones. Although the set of genes differentially expressed are in general unique for each virus-host interaction, finding a larger number and diversity of upregulated than downregulated genes seems to be a common feature, probably reflecting the induction of the plant metabolism caused by the viral infection (Postnikova and Nemchinov, 2012). Moreover, according to the GO analysis presented here, the majority of these deregulated genes encode proteins that localized in the nucleus and chloroplast, and are defined as protein- and DNA- or RNA-binding factors. In this sense, it is worth noting that AMV CP is a multifunctional protein with a nucleocytoplasmic localization and, in fact, it was found to interfere with the activity and function of transcription factors and chloroplast-targeted proteins, key regulators in plant development, senescence and defense response (Herranz et al., 2012; Balasubramaniam et al., 2014; Aparicio and Pallás, 2017).

The mRNA-seq analysis reported that methylation complex subunits MTA, MTB and VIRILIZER and the potential m^{6}A *reader* ECT5 were upregulated, whereas any of the potential demethylase proteins substantially changed their expression, which may be reflecting an activation of the m^{6}A pathway in response to AMV infection. Remarkably, ECT5, together with ECT9 and ECT10, would be expected to possess 10-fold higher affinity towards m^{6}A RNA than the rest of ECT proteins due to an aspartate substitution by an asparagine (Xu et al., 2015; Scutenaire et al., 2018). Interestingly, a study comparing the Arabidopsis transcriptome in response to 11 plant

viruses pointed out that MTA, HAKAI1, ECT5 and ECT6 are deregulated upon infection with at least one virus, whereas ECT3 deregulation is a common response against all viruses (Postnikova and Nemchinov, 2012). This suggests that m^{6}A could constitute a general response of plants against viral infection or a general viral strategy to modulate host cellular machinery.

Reinforcing this hypothesis, the lack of ECT2 and ECT3 or ECT5 leads to an increase of the viral titer in the systemic tissue, indicating that these m^{6}A *readers* are negatively regulating AMV infection. The necessity of mutating at least two of these genes to perceive a pronounced effect is presumably due to their previously reported partial functional redundancy (Arribas-Hernández et al., 2018; 2020). The greatest effects observed occur in the double mutants *ect2/ect3* and *ect2/ect5*, and triple mutants *ect2/ect3/ect4* and *ect2/ect3/ect5*, while, although favored, the rise of the systemic viral load was much more modest with the knockout combinations *ect2/ect4* and *ect3/ect4*, especially in the latest. Our observations suggest that ECT2 plays the most relevant role among the evaluated ECTs in AMV infection, since the double mutants lacking ECT2 presented the highest systemic viral titers, while ECT4 seems to be less relevant for AMV infection. Interestingly, CMV infection levels were also increased when ECT2 and ECT3 or ECT5 were absent, suggesting that m^{6}A mechanism would not likely be exclusive for AMV, but influence other viral pathogens. Future analyses using other viruses will clarify whether these m^{6}A *readers* are part of a more general plant regulatory strategy to control viral infections.

Moreover, m^{6}A binding ability of ECT2 seems to be essential for the plant response to AMV, as the complementation of ECT2 activity in the double mutant *ect2/ect3* rescued the WT viral susceptibility, whereas ECT2^{W464A} mutant protein, which cannot recognize m^{6}A, did not. The role of m^{6}A *readers* as regulators of viral infection has been also described in mammalian viruses during the last years (Williams et al., 2019). Depletion of YTHDF proteins were found to enhance viral replication of HIV-1 (Tirumuru et al., 2016; Jurczyszak et al., 2020) and ZIKV (Lichinchi et al., 2016b), virus particle formation of HCV (Gokhale et al., 2016) and viral mRNA stability and protein expression of *Hepatitis B virus* (HBV) (Imam et al., 2018). Conversely, YTHDF proteins were found to have positive effects on HIV-1 Gag processing and virus release (Tirumuru et al., 2016), and to enhance viral translation and replication via its binding to m^{6}A-sites located at the 3'UTR region of the vRNas (Kennedy et al., 2016). Thereby, YTH proteins and m^{6}A modification in general may play either anti or proviral roles depending on its position along the viral genome or the viral stage. For instance, the position of the modification appears to be crucial for HBV, as m^{6}A presence at 5'UTR on the viral pregenomic RNA (pgRNA) enhances reverse transcription,

while m^{6}A sites located in the 3'UTR promotes RNA destabilization (Imam et al., 2018). It could be related with the observations demonstrating that, besides YTHs-mediated regulation, m^{6}A may act as secondary structure switch caused by weaker m^{6}A-U than A-U base pairs (Kierzek and Kierzek, 2003; Liu et al., 2015). Thus, we cannot discard the possibility of that the presence of m^{6}A nucleotides has different consequences for AMV infection. Although ECT proteins are presumably implied in the recognition of these residues along the viral genome, it is also possible that, for example, in other positions, they may produce secondary structure changes in the vRNAs that interfere with its binding properties in some stages of the infection cycle.

Furthermore, it is important to note that some authors found evidence relating an effect of host mRNA m^{6}A-mediated regulation with viral accumulation. In animals, m^{6}A was described to indirectly modulate host defense in an immune response-independent manner (Liu et al., 2019), and to, direct or indirectly, regulate interferon pathway after infection with either RNA or DNA viruses (Zheng et al., 2017; Rubio et al., 2018; Wang et al., 2019; Winkler et al., 2019; Gokhale et al., 2020). Thus, according to these studies, the implication of the ECT proteins in the AMV infection could be a consequence of the regulation of endogenous genes, maybe including defense-related factors, via m^{6}A binding. Nonetheless, our results advocate a direct interaction between ECT2 and AMV RNAs, pointing out that ECT proteins exert repression of viral infectivity via, at least partially, direct binding to m^{6}A-modified vRNAs. While ECT2 pulled down vRNAs, ECT2^{W464A} failed to interact with vRNAs and was incapable to complement the susceptibility phenotype of the double mutant *ect2/ect3*. The observation that AMV accumulation in the quadruple knockout *atalkbh9b/ect2/ect3/ect4* is comparable to WT but still lower than *ect2/ect3/ect4* plants suggests that there are other ECTs (different from ECT2/3/4) that process m^{6}A-modified vRNA. The development of a quintuple mutant that includes *ECT5* will probably offer a more conclusive result. Besides, as it was mentioned above, other ECT-independent m^{6}A functions may affect AMV infection, which would also justify the effect of the viral hypermethylation observed in *atalkbh9b/ect2/ect3/ect4* plants.

Interestingly, we found that ECT5 forms aggregates in different sized foci when overexpressed by agroinfiltration. Recently, ECT2, ECT3 and ECT4 were described to form similar punctuate foci after heat and osmotic stress that, in the case of ECT2, were identified as SGs (Arribas-Hernández et al., 2018; Scutenaire et al., 2018). SGs are sites where viral mRNAs/proteins are hijacked to decrease replication and/or to act as antiviral signaling cores (Lloyd, 2013). In fact, animal-infecting viruses have developed strategies to avoid their formation, to promote their disassembly and/or to modify their structure, recruiting and taking advantage of their

components (Zhang et al., 2019b). Likewise, diverse studies suggested that m^{6}A poly-methylated mRNAs could act as scaffold for YTHDF proteins, allowing the formation of cytoplasmic granules through interactions between their IDRs (Fu and Zhuang, 2019; Gao et al., 2019; Ries et al., 2019) and, remarkably, like mammal YTDHF proteins, ECT2 was proved to also have the ability of undergoing gel-like phase *in vitro* (Arribas-Hernández et al., 2018). Therefore, it is tempting to speculate that m^{6}A poly-methylated AMV RNAs would act as scaffold for the ECT proteins that, at the same way that it was shown in mammalian cells, would form SGs, decreasing viral translation and replication rates. At the same time, as an acquired evolutive system, the virus would usurp the atALKBH9B function to remove the excess of m^{6}A from its genome and avoid ECT sequestration, resembling the strategy of woody plants-infecting viruses that incorporate an AlkB domain as part of their replicase (Moore and Meng, 2019). As previously suggested, it might constitute an evolutionary mechanism to promote host and, consequently, viral survival during long-term-infections (Moore and Meng, 2019). Nevertheless, further experiments will have to be carried out to demonstrate the validity of this hypothesis.

On the other hand, our results suggest that ECT2 and ECT5 may interact with the demethylase atALKBH9B, pointing out to a crosstalk among the different effectors of m^{6}A regulatory mechanism. It is in line with another recent observation: a mass spectrometry analysis of a co-immunoprecipitation experiment using ECT2:mCherry as bait revealed the co-purification of other m^{6}A methylation machinery components, including atALKBH10B (Tankmar, 2019). Considering the opposite effect of ECT2/5 and atALKBH9B (Martínez-Pérez et al., 2017) on AMV infection, it should be kept in mind an inhibitor role between *readers* and *erasers* as a plausible function of these interactions, although more studies are needed to verify and disclose the meaning of this phenomenon.

In summary, here we demonstrate for the first time the involvement of m^{6}A *reader*s in the infection cycles of plant viruses, apparently through its capability to interact to m^{6}A-containing vRNAs. Remarkably, the observed antiviral effects for the *reader*s are consistent with the previously proviral effects observed for the *eraser* atALKBH9B in the same pathosystem, reinforcing the homeostatic nature of the m^{6}A regulatory mechanism in the viral infection cycle. Our results definitively establish this RNA modification as a critical regulatory mechanism for a plant RNA virus and open the possibility that it can be extrapolated to other virus-host interactions.

Materials and methods

RNA differential expression analysis between Arabidopsis Col-0 WT MOCK and AMV samples. 3-weeks Arabidopsis Col-0 WT plants were inoculated with PE buffer (30 mM sodium phosphate buffer, pH 7) (MOCK plants) or AMV PV0196 isolate (Plant Virus Collection, DSMZ) viral particles in PE. The experiment consisted of three biological replicates (8 individual plants/replicate) of MOCK and AMV WT inoculated plants. Tissue from the young, emerging rosette leaves were harvested at 8 dpi and grounded in liquid nitrogen with mortar and pestle. Total RNA was extracted from 0.1 g leaf material using EXTRAzol reagent protocol (Blirt; Gdańsk, Poland) and treated with DNase I for 30 min at 37ºC. Generation and sequencing of the cDNA libraries were performed by the Genomic Service (SCSIE) of the Universidad de Valencia. Six TruSeq Stranded cDNA libraries (three for healthy and three for AMV infected plants) were sequenced by non-paired end sequencing (75 bp) in a NextSeq 550 (Illumina; San Diego, California, USA). The bioinformatic analysis was carried out by the Bioinformatic Service of IBMCP. DESeq2 package was the tool used for the differential expression analysis and a threshold of 1RPMK was applied.

Quantitative reverse-transcription PCR (qPCR). cDNA was obtained by reverse transcription (RT) of the same DNase-treated total RNA samples used for NextSeq. Four µl of the reaction containing DNA-free RNA were mixed with 0.5 µg (1 µl) of oligo(dT)18 (ThermoFisher Scientific; Waltham, Massachusetts, USA), denatured for 5 min at 65ºC and added to a total of 20 µl of first-strand cDNA synthesis reaction containing 1 U of RevertAid H Minus Reverse Transcriptase, 0.5 U of Ribolock, 4 mM dNTP mix and 1x RT buffer (ThermoFisher Scientific; Waltham, Massachusetts, USA). The RT reaction proceeded at 42°C for 1 hour, followed by 10 min at 70°C to deactivate the enzyme. qPCR reactions consisted of 5 µl of Maxima SYBR Green qPCR Master Mix (2x) (ThermoFisher Scientific; Waltham, Massachusetts, USA) mixed with 0.5 µl of the cDNA prepared as described above and the appropriate primers (Annex III) in 0.3 µM final concentration each, to reach a total volume of 10 µl. The reactions were monitored in real time in a Bio-Rad CFX ConnectTM thermal cycler, and expression analysis was performed calculating the relative quantification (RQ) values respect to the endogenous genes (F-BOX and PDF2) (Lilly et al., 2011) of three biological replicates. Student's *t*-test was applied to ΔCt values for statistical analysis.

Plant growth conditions, virus inoculation, and northern blot analysis. Source and background of each *Arabidopsis thaliana* (Columbia-0) transgenic line is described in Annex I. Plants were grown in 6 cm diameter pots in a growth chamber at 24°C with a photoperiod of 24°C-16 h

light/20°C-8 h dark. The mechanical inoculations of 18-21 days old plants were carried out using carborundum and purified virions (1 mg/mL) of AMV PV0196 in PE buffer or sap extracts of CMV Fyn isolate infected tissue. Next, detection of vRNAs was performed by northern blot analysis. Inoculated leaves and systemic aerial tissue were harvested at the corresponding dpi. Tissues were grounded in liquid nitrogen with mortar and pestle and total RNA was extracted, following EXTRAzol reagent protocol (Blirt; Gdańsk, Poland), from 0.1 g leaf material. For northern blots, 500 ng of total RNA was denatured by formaldehyde treatment and after agarose gel electrophoresis in MOPS buffer, RNAs were transferred to positively charged nylon membranes (Roche; Basel, Switzerland) by capillarity in SSC buffer as previously described (Sambrook et al., 1988) and hybridized with digoxigenin-labeled riboprobes to detect AMV or CMV RNA 1, RNA 2, RNA 3 and sgRNA 4. Synthesis of the digoxigenin-labeled riboprobes, hybridization, and digoxigenin-detection procedures were performed as previously described (Pallás et al., 1998). Hybridization intensity signal was measured on files from Fujiflm LAS-3000 Imager using Fujiflm Image Gauge V4.0.

Generation of Arabidopsis CRISPR/Cas9 transgenic lines. Arabidopsis lines carrying CRISPR/Cas9-mediated gene knockout were generated using the pKAMA-ITACHI Red (pKIR1.1) vector as it was previously described (Tsutsui and Higashiyama, 2017) with some modifications. A simply adaptable single guide RNA (sgRNA) leads Cas9 endonucleases to target its complementary sequence, generating a DNA double-strand break (DSB) within a specific genomic sequence. The repair mechanisms are not completely efficient and often result in mutations (Lieber, 2010). In summary, different primers (Annex III) were designed inside the ORF of ECT5 (AT3G13060), searching for protospacer adjacent motif (PAM) sequences (NGG), to work as single guide RNAs (sgRNAs) and ligations of the hybridized DNA oligomers with vector, previously digested with AarI enzyme, were performed. *Agrobacterium tumefaciens* GV3101 was transformed with the resulting vectors and cultures expressing two different sgRNAs were used to generate Arabidopsis stable transgenic lines by floral dip transformation (Clough and Bent, 1998) in *ect2-1* and *ect2-1/ect3-1* backgrounds. Selection of T1 transgenic plants was carried out by hygromycin resistance and a first assortment of Cas9-free T2 seeds was performed by absence of red fluoresce. Final genotyping by PCR with specific primers (Annex III) was realized from T2 plants and confirmed in T3 transformants. Finally, an RT-PCR with specific primers (Annex III) of total RNA extraction from plants of selected lines and the sequencing of the cDNA products verified the non-frameshift mutations (Annex II).

Analysis of ECT2-RNA$_{AMV}$ interaction. Three independent *Arabidopsis* transgenic lines expressing 3xHA:ECT2 or 3xHA:ECT2^{W464A} in the *ect2-1* background (Annex I) were inoculated with buffer or AMV particles at 16 days after germination as described before. At 7 dpi, inoculated plants were irradiated with 254 nm Ultra-Violet (UV) light at a dose of 2000 mJ/cm^2 to cross-link RNA-protein interactions *in vivo*. Then, for each sample, tissue from the young, emerging rosette leaves of the three lines were mixed and ground in liquid nitrogen with mortar and pestle. The following steps were adapted from a previously described "individual-nucleotide resolution UV cross-linking and immunoprecipitation" (iCLIP) protocol (Meyer et al., 2017). Thus, grounded tissue were mixed with 1.5 V of cell lysis buffer previously heated at 66ºC for 10 sec (50 mM Tris-HCl, pH 7.5, 150 mM NaCl, 4 mM $MgCl_2$, 0.25% Igepal CA-630, 1% SDS, 0.25% sodium deoxycholate, 5 mM DTT, Complete Protease Inhibitor (Roche; Basel, Switzerland), 1 mM phenylmethylsulfonyl fluorid (Sigma-Aldrich; Darmstadt, Germany) and 1 mM Plant Protease Inhibitor (Sigma-Aldrich; Darmstadt, Germany)) and tubes were shaken at 1500 rpm and 40ºC until homogenization (the samples should be still cold) and immediately placed in ice. After a centrifugation of 15 min at 4ºC, the supernatants were transferred to new tubes containing previously washed αHA-3F10 beads (Roche; Basel, Switzerland) and incubated for 1h at 4ºC with constant rotation to capture RNA-protein complexes. After this, four washing steps for 10 min with 1 mL of cooled RIP-washing buffer (50 mM Tris-HCl, pH 7.5, 500 mM NaCl, 4 mM $MgCl_2$, 0.5% Igepal CA-630, 1% SDS, 0.5% sodium deoxycholate, 2 M urea, 2 mM DTT, Complete Protease Inhibitor) and two with 1 ml of original iCLIP buffer (20 mM Tris-HCl pH 7.4, 10 mM $MgCl_2$ and 0.2% Tween 20) (König et al., 2010) were carried out at 4ºC with constant rotation. Next, beads were incubated for 10 min at 37 °C with 2 µL Turbo DNase (ThermoFisher Scientific; Waltham, Massachusetts, USA) and 5 µL of 1/3000 dilution RNase I (Ambion; Waltham, Massachusetts, USA) to degrade nucleic acids not bounded to HA:ECT2 proteins and finally the reaction was stopped by incubating the tubes on ice for 3 min. After two additional washes with original iCLIP buffer, beads were resuspended with 20 µL of 2xLDS and immediately incubated at 95ºC for 10 min. To analyze the presence of AMV RNAs in the immunoprecipitated samples, 3 µL of each sample were directly applied on a nylon membrane. After blotting, RNAs were UV-crosslinked to positively charged nylon membranes. After fixing the RNAs with UV light, the membrane was incubated with PerfectHybTM Plus Hybridization buffer (Sigma-Aldrich; Darmstadt, Germany) at 58ºC for 20 min. Then, a mixture of radioactively labelled probes to detect AMV RNA 1, RNA 2, RNA 3 and sgRNA 4 were added for hybridization overnight at 58ºC with constant rotation. Probes were synthesized using the Prime-a-Gene (Promega; Madison, USA) kit and denatured (5 min at 95ºC) before incubation with the membrane. After

hybridization and washing (two washes for 20 min with 2x SSC 0.1% SDS followed by two washes for 20 min with 0.1x SSC 0.1% SDS, both at 58ºC), the membrane was exposed to a phosphor screen for image analysis.

BiFC assay and subcellular localization study. BiFC assays were carried out essentially as previously described (Aparicio et al., 2006). ECT5 ORF (AT3G13060.2), ECT2 (AT3G13460.1), AMV CP and atALKBH9B (AT2G17970.1) ORFs were amplified with specific primers (Annex III) for cloning with appropriate restriction enzymes in a modified pSK vector. This vector contains an expression cassette containing a duplicated CAMV 35S promoter and the N- or C-terminal part of GFP (NGFP or CGFP) with a multicloning site either at the N- or C-terminal part of the split GFP parts. Thus, 35S:CGFP:ECT5, 35S:ECT5:CGFP, 35S:CGFP:ECT2, 35S:NGFP:ALKBH9B, 35S:NGFP:CP_{AMV} and 35S:NYFP:ALKBH9B fusion protein cassettes were generated and subsequently cloned in the binary vector pMOG using appropriate restriction enzyme sites. ECT5 ORF (AT3G13060.2) was amplified with specific primers (Annex III) designed for cloning using the Gateway System (Invitrogen; Waltham, Massachusetts, USA) and recombined into binary destination vectors expressing GFP following manufacturer recommendations. Thus, GFP:ECT5 and ECT5:GFP fusion protein were generated for localization analysis. All binary vectors were transformed into *Agrobacterium tumefaciens* C58 cells. Cultures were diluted at 0,3 OD600 in infiltration solution (10 mM Mes pH 5.5, 10 mM MgCl2) and infiltrated into 3-week-old *N. benthamiana* plants. Confocal images were taken at 48 h after agroinfiltration with a confocal laser microscope Zeiss LSM 780 AxiObserver. All images correspond to single slices of 1.8-µm thickness of epidermal cells. Excitation and emission wavelengths were 488 and 508 nm for GFP.

ACKNOWLEDGMENTS

We thank L. Corachan for her excellent technical assistance, and J. Rato, D. Torrent-Silla and the Bioinformatics Core Service at the Instituto de Biología Molecular y Celular de Plantas (IBMCP) for the support provided in the data analysis. M.M.-P. was recipient of a Predoctoral Contract FPI-2015-072406 from the Subprograma FPI-MINECO (Formación de Personal Investigador–Ministerio de Economía y Competitividad). This work was supported by Grant BIO2017–88321-R from the Spanish Agencia Estatal de Investigación (AEI) and Fondo Europeo de Desarrollo Regional (FEDER). Part of this work was carried out in Prof. Brodersen's lab at the University of Copenhagen (Denmark) thanks to a FEBS (Federation of European Biochemical Societies) Short-Term Fellowship.

References

Aparicio, F. and Pallás, V. (2017). The coat protein of Alfalfa mosaic virus interacts and interferes with the transcriptional activity of the bHLH transcription factor ILR3 promoting salicylic acid-dependent defence signalling response. Mol. Plant Pathol. **18**: 173–186.

Aparicio, F., Sánchez-Navarro, J.A., and Pallás, V. (2006). In vitro and in vivo mapping of the Prunus necrotic ringspot virus coat protein C-terminal dimerization domain by bimolecular fluorescence complementation. J. Gen. Virol. **87**: 1745–50.

Aravind, L. and Koonin, E. V. (2001). The DNA-repair protein AlkB, EGL-9, and leprecan define new families of 2-oxoglutarate- and iron-dependent dioxygenases. Genome Biol. **2**: research0007.

Arribas-Hernández, L., Bressendorff, S., Hansen, M.H., Poulsen, C., Erdmann, S., and Brodersen, P. (2018). An m ^{6} A-YTH Module Controls Developmental Timing and Morphogenesis in Arabidopsis. Plant Cell **30**: 952–967.

Arribas-Hernández, L. and Brodersen, P. (2020). Occurrence and Functions of m6A and Other Covalent Modifications in Plant mRNA. Plant Physiol. **182**: 79–96.

Balacco, D.L. and Soller, M. (2019). The m6A Writer: Rise of a Machine for Growing Tasks. Biochemistry **58**: 363–378.

Balasubramaniam, M., Kim, B.S., Hutchens-Williams, H.M., and Loesch-Fries, L.S. (2014). The photosystem II oxygen-evolving complex protein PsbP interacts with the coat protein of Alfalfa mosaic virus and inhibits virus replication. Mol. Plant-Microbe Interact. **27**: 1107–1118.

Bol, J.F. (2005). Replication of Alfamo- and Ilarviruses: Role of the Coat Protein. Annu. Rev. Phytopathol. **43**: 39–62.

Bujarski, J., Gallitelli, D., García-Arenal, F., Pallás, V., Palukaitis, P., Krishna Reddy, M., and Wang, A. (2019). ICTV virus taxonomy profile: Bromoviridae. J. Gen. Virol. **100**: 1206–1207.

Clough, S.J. and Bent, A.F. (1998). Floral dip: A simplified method for Agrobacterium-mediated transformation of Arabidopsis thaliana. Plant J. **16**: 735–743.

Courtney, D.G., Kennedy, E.M., Dumm, R.E., Bogerd, H.P., Tsai, K., Heaton, N.S., and Cullen, B.R. (2017). Epitranscriptomic Enhancement of Influenza A Virus Gene Expression and Replication. Cell Host Microbe **22**: 377–86.

Dang, W., Xie, Y., Cao, P., Xin, S., Wang, J., Li, S., Li, Y., and Lu, J. (2019). N6-Methyladenosine and Viral Infection. Front. Microbiol. **10**: 1–12.

Darnell, R.R., Shengdong, K.E., and Darnell, J.E. (2018). Pre-mRNA processing includes N6 methylation of adenosine residues that are retained in mRNA exons and the fallacy of "RNA epigenetics." RNA **24**: 262–267.

Duan, H.-C., Wei, L.-H., Zhang, C., Wang, Y., Chen, L., Lu, Z., Chen, P.R., He, C., and Jia, G. (2017). ALKBH10B Is an RNA *N* ^{6} -Methyladenosine Demethylase Affecting Arabidopsis Floral Transition. Plant Cell **29**: 2995–3011.

Fu, Y. and Zhuang, X. (2019). m6A-binding YTHDF proteins promote stress granule formation by modulating phase separation of stress granule proteins. bioRxiv: doi: https://doi.org/10.1101/694455.

Gao, Y., Pei, G., Li, D., Li, R., Shao, Y., Zhang, Q.C., and Li, P. (2019). Multivalent m6A motifs promote phase separation of YTHDF proteins. Cell Res. **29**: 767–769.

Gokhale, N.S., McIntyre A.B.R., McFadden M.J. et al. (2016). N6-Methyladenosine in Flaviviridae Viral RNA Genomes Regulates Infection. Cell Host Microbe **20**: 654–665.

Gokhale, N.S., McIntyre, A.B.R., Mattocks, M.D., Holley, C.L., Lazear, H.M., Mason, C.E., and Horner, S.M. (2020). Altered m6A Modification of Specific Cellular Transcripts Affects Flaviviridae Infection. Mol. Cell **77**: 542–555.

Herranz, M.C., Pallas, V., and Aparicio, F. (2012). Multifunctional roles for the N-terminal basic

motif of Alfalfa mosaic virus coat protein: Nucleolar/cytoplasmic shuttling, modulation of RNA-binding activity, and virion formation. Mol. Plant-Microbe Interact. **25**: 1093–103.

Imai, Y., Matsuo, N., Ogawa, S., Tohyama, M., and Takagi, T. (1998). Cloning of a gene, YT521, for a novel RNA splicing-related protein induced by hypoxia/reoxygenation. Mol. Brain Res. **53**: 33–40.

Imam, H., Khan, M., Gokhale, N.S., McIntyre, A.B.R., Kim, G.-W., Jang, J.Y., Kim, S.-J., Mason, C.E., Horner, S.M., and Siddiqui, A. (2018). N6 -methyladenosine modification of hepatitis B virus RNA differentially regulates the viral life cycle . Proc. Natl. Acad. Sci. **115**: 8829–8834.

Jurczyszak, D., Zhang, W., Terry, S.N., Kehrer, T., Bermúdez González, M.C., McGregor, E., Mulder, L.C.F., Eckwahl, M.J., Pan, T., and Simon, V. (2020). HIV protease cleaves the antiviral m6A reader protein YTHDF3 in the viral particle. PLoS Pathog.: https://doi.org/10.1371/journal.ppat.1008305.

Ke, S., Pandya-Jones, A., Saito, Y., Fak, J.J., Vågbø, C.B., Geula, S., Hanna, J.H., Black, D.L., Darnell, J.E., and Darnell, R.B. (2017). m6A mRNA modifications are deposited in nascent pre-mRNA and are not required for splicing but do specify cytoplasmic turnover. Genes Dev. **31**: 990–1006.

Kennedy, E.M., Bogerd, H.P., Kornepati, A.V.R., Kang, D., Ghoshal, D., Marshall, J.B., Poling, B.C., Tsai, K., Gokhale, N.S., Horner, S.M., and Cullen, B.R. (2016). Posttranscriptional m6A Editing of HIV-1 mRNAs Enhances Viral Gene Expression. Cell Host Microbe **19**: 675–685.

Kierzek, E. and Kierzek, R. (2003). The thermodynamic stability of RNA duplexes and hairpins containing N6-alkyladenosines and 2-methylthio-N6-alkyladenosines. Nucleic Acids Res. **31**: 4472–80.

König, J., Zarnack, K., Rot, G., Curk, T., Kayikci, M., Zupan, B., Turner, D.J., Luscombe, N.M., and Ule, J. (2010). ICLIP reveals the function of hnRNP particles in splicing at individual nucleotide resolution. Nat. Struct. Mol. Biol. **17**: 909–915.

Krab, I.M., Caldwell, C., Gallie, D.R., and Bol, J.F. (2005). Coat protein enhances translational efficiency of Alfalfa mosaic virus RNAs and interacts with the eIF4G component of initiation factor eIF4F. J. Gen. Virol. **86**: 1841–49.

Lavi, S. and Shatkin, A.J. (1975). Methylated simian virus 40-specific RNA from nuclei and cytoplasm of infected BSC-1 cells. Proc. Natl. Acad. Sci. **72**: 2012–2016.

Lesbirel, S. and Wilson, S.A. (2019). The m 6 A-methylase complex and mRNA export. Biochim. Biophys. Acta - Gene Regul. Mech. **1862**: 319–328.

Li, D., Zhang, H., Hong, Y., Huang, L., Li, X., Zhang, Y., Ouyang, Z., and Song, F. (2014a). Genome-Wide Identification, Biochemical Characterization, and Expression Analyses of the YTH Domain-Containing RNA-Binding Protein Family in Arabidopsis and Rice. Plant Mol. Biol. Report. **32**: 1169–86.

Li, F., Zhao, D., Wu, J., and Shi, Y. (2014b). Structure of the YTH domain of human YTHDF2 in complex with an m6A mononucleotide reveals an aromatic cage for m6A recognition. Cell Res. **24**: 1490–92.

Li, Z., Shi, J., Yu, L., Zhao, X., Ran, L., Hu, D., and Song, B. (2018). N 6 -methyl-adenosine level in Nicotiana tabacum is associated with tobacco mosaic virus. Virol. J. **15**: 1–10.

Liang, Z., Geng, Y., and Gu, X. (2018). Adenine Methylation: New Epigenetic Marker of DNA and mRNA. Mol. Plant **11**: 1219–1221.

Liao, S., Sun, H., and Xu, C. (2018). YTH Domain: A family of N6-methyladenosine (m6A) readers. Genomics Proteomics Bioinforma. **16**: 99–107.

Lichinchi, G., Gao, S., Saletore, Y., Gonzalez, G.M., Bansal, V., Wang, Y., Mason, C.E., and Rana, T.M. (2016a). Dynamics of the human and viral m(6)A RNA methylomes during HIV-1 infection of T cells. Nat. Microbiol. **1**: 16011.

Lichinchi, G., Zhao, B.S., Wu, Y., Lu, Z., Qin, Y., He, C., and Rana, T.M. (2016b). Dynamics of Human and Viral RNA Methylation during Zika Virus Infection. Cell Host Microbe **20**: 666–

673.

Lieber, M.R. (2010). The Mechanism of Double-Strand DNA Break Repair by the Nonhomologous DNA End-Joining Pathway. Annu. Rev. Biochem. **79**: 181–211.

Lilly, S.T., Drummond, R.S.M., Pearson, M.N., and MacDiarmid, R.M. (2011). Identification and validation of reference genes for normalization of transcripts from virus-infected Arabidopsis thaliana. Mol. Plant-Microbe Interact. **24**: 294–304.

Liu, N., Dai, Q., Zheng, G., He, C., Parisien, M., and Pan, T. (2015). N6 -methyladenosine-dependent RNA structural switches regulate RNA-protein interactions. Nature **518**: 560–564.

Liu, Y., You, Y., Lu, Z., Yang, J., Li, P., Liu, L., Xu, H., Niu, Y., and Cao, X. (2019). N 6 -methyladenosine RNA modification–mediated cellular metabolism rewiring inhibits viral replication. Science. **365**: 1171.

Lloyd, R.E. (2013). Regulation of stress granules and P-bodies during RNA virus infection. Wiley Interdiscip. Rev. RNA **4**: 317–331.

Lu, W., Tirumuru, N., Gelais, C.S., Koneru, P.C., Liu, C., Kvaratskhelia, M., He, C., and Wu, L. (2018). N 6 -Methyladenosine– binding proteins suppress HIV-1 infectivity and viral production. J. Biol. Chem. **293**: 12992–13005.

Luo, G.Z., Macqueen, A., Zheng, G., Duan, H., Dore, L.C., Lu, Z., Liu, J., Chen, K., Jia, G., Bergelson, J., and He, C. (2014). Unique features of the m6A methylome in Arabidopsis thaliana. Nat. Commun. **28**: 5630.

Martelli, G.P., Adams, M.J., Kreuze, J.F., and Dolja, V. V. (2007). Family Flexiviridae : A Case Study in Virion and Genome Plasticity. Annu. Rev. Phytopathol. **45**: 73–100.

Martínez-Pérez, M., Aparicio, F., López-Gresa, M.P., Bellés, J.M., Sánchez-Navarro, J.A., and Pallás, V. (2017). *Arabidopsis* m ^{6} A demethylase activity modulates viral infection of a plant virus and the m ^{6} A abundance in its genomic RNAs. Proc. Natl. Acad. Sci. **114**: 10755–10760.

Meyer, K., Köster, T., Nolte, C., Weinholdt, C., Lewinski, M., Grosse, I., and Staiger, D. (2017). Adaptation of iCLIP to plants determines the binding landscape of the clock-regulated RNA-binding protein AtGRP7. Genome Biol. **18**: 1–22.

Meyer, K.D. and Jaffrey, S.R. (2017). Rethinking m 6 A Readers, Writers, and Erasers . Annu. Rev. Cell Dev. Biol. **33**: 319–342.

Miao, Z., Zhang, T., Qi, Y., Song, J., Han, Z., and Ma, C. (2020). Evolution of the RNA N6-Methyladenosine Methylome Mediated by Genomic Duplication. Plant Physiol.: DOI: https://doi.org/10.1104/pp.19.00323.

Mielecki, D., Zugaj, D., Muszewska, A., Piwowarski, J., Chojnacka, A., Mielecki, M., Nieminuszczy, J., Grynberg, M., and Grzesiuk, E. (2012). Novel AlkB dioxygenases-alternative models for in silico and in vivo studies. PLoS One **7**: e30588.

Moore, C. and Meng, B. (2019). Prediction of the molecular boundary and functionality of novel viral AlkB domains using homology modelling and principal component analysis. J. Gen. Virol. **100**: 691–703.

Ok, S.H., Jeong, H.J., Bae, J.M., Shin, J.S., Luan, S., and Kim, K.N. (2005). Novel CIPK1-associated proteins in Arabidopsis contain an evolutionarily conserved C-terminal region that mediates nuclear localization. Plant Physiol. **139**: 138–50.

Pallas, V., Aparicio, F., Herranz, M.C., Sanchez-Navarro, J.A., and Scott, S.W. (2013). The Molecular Biology of Ilarviruses. Adv. Virus Res. **87**: 139–81.

Pallas, V. and García, J.A. (2011). How do plant viruses induce disease? Interactions and interference with host components. J. Gen. Virol. **92**: 2691–705.

Pallás, V., Más, P., and Sánchez-Navarro, J.A. (1998). Detection of Plant RNA Viruses by Nonisotopic Dot-Blot Hybridization. Methods Mol Biol **81**: 461–8.

Parker, M.T., Knop, K., Sherwood, A. V., Schurch, N.J., Mackinnon, K., Gould, P.D., Hall, A.J., Barton, G.J., and Simpson, G.G. (2020). Nanopore direct RNA sequencing maps the

complexity of Arabidopsis mRNA processing and m6A modification. Elife **9**: e49658.

Patil, D.P., Pickering, B.F., and Jaffrey, S.R. (2018). Reading m6A in the Transcriptome: m6A-Binding Proteins. Trends Cell Biol. **28**: 113–127.

Pereira-Montecinos, C., Valiente-Echeverría, F., and Soto-Rifo, R. (2017). Epitranscriptomic regulation of viral replication. Biochim. Biophys. Acta - Gene Regul. Mech. **1860**: 460–471.

Postnikova, O.A. and Nemchinov, L.G. (2012). Comparative analysis of microarray data in Arabidopsis transcriptome during compatible interactions with plant viruses. Virol. J. **29**: 101.

Ries, R.J., Zaccara, S., Klein, P., Olarerin-George, A., Namkoong, S., Pickering, B.F., Patil, D.P., Kwak, H., Lee, J.H., and Jaffrey, S.R. (2019). m6A enhances the phase separation potential of mRNA. Nature **571**: 424–8.

Rodrigo, G., Carrera, J., Ruiz-Ferrer, V., del Toro, F.J., Llave, C., Voinnet, O., and Elena, S.F. (2012). A meta-analysis reveals the commonalities and differences in arabidopsis thaliana response to different viral pathogens. PLoS One **7**: e40526.

Rosa-Mercado, N.A., Withers, J.B., and Steitz, J.A. (2017). Settling the m6A debate: Methylation of mature mRNA is not dynamic but accelerates turnover. Genes Dev. **31**: 957–8.

Rubio, R.M., Depledge, D.P., Bianco, C., Thompson, L., and Mohr, I. (2018). RNA m6A modification enzymes shape innate responses to DNA by regulating interferon β. Genes Dev. **32**: 1472–1484.

Růžička, K., Zhang, M., Campilho, A. et al. (2017). Identification of factors required for m6A mRNA methylation in Arabidopsis reveals a role for the conserved E3 ubiquitin ligase HAKAI. New Phytol. **215**: 157–172.

Sambrook, J., Maniatis, T., and Fritsch, E.F. (1988). Molecular Cloning : a laboratory manual. 2nd edition. Cold Spring Harb. ,New York.

Scutenaire, J., Deragon, J.-M., Jean, V., Benhamed, M., Raynaud, C., Favory, J.-J., Merret, R., and Bousquet-Antonelli, C. (2018). The YTH Domain Protein ECT2 Is an m 6 A Reader Required for Normal Trichome Branching in Arabidopsis. Plant Cell **30**: 986–1005.

Shen, L., Liang, Z., Gu, X., Chen, Y., Teo, Z.W.N., Hou, X., Cai, W.M., Dedon, P.C., Liu, L., and Yu, H. (2016). N 6 -Methyladenosine RNA Modification Regulates Shoot Stem Cell Fate in Arabidopsis. Dev. Cell **38**: 186–200.

Shi, H., Wang, X., Lu, Z., Zhao, B.S., Ma, H., Hsu, P.J., Liu, C., and He, C. (2017). YTHDF3 facilitates translation and decay of N 6-methyladenosine-modified RNA. Cell Res. **27**: 315–328.

Shi, H., Wei, J., and He, C. (2019). Where, When, and How: Context-Dependent Functions of RNA Methylation Writers, Readers, and Erasers. Mol. Cell **74**: 640–50.

Tankmar, M.D. (2019). Functional Analysis of Arabidopsis m6A Readers. Faculty of Science. Masther Thesis. University of Copenhagen (Denmark).

Theler, D., Dominguez, C., Blatter, M., Boudet, J., and Allain, F.H.T. (2014). Solution structure of the YTH domain in complex with N6-methyladenosine RNA: A reader of methylated RNA. Nucleic Acids Res. **42**: 13911–13919.

Tirumuru, N., Zhao, B.S., Lu, W., Lu, Z., He, C., and Wu, L. (2016). N6-methyladenosine of HIV-1 RNA regulates viral infection and HIV-1 Gag protein expression. Elife **5**: e15528.

Tsutsui, H. and Higashiyama, T. (2017). PKAMA-ITACHI vectors for highly efficient CRISPR/Cas9-mediated gene knockout in Arabidopsis thaliana. Plant Cell Physiol. **58**: 46–56.

Van den Born, E., Bekkelund, A., Moen, M.N., Omelchenko, M. V., Klungland, A., and Falnes, P. (2009). Bioinformatics and functional analysis define four distinct groups of AlkB DNA-dioxygenases in bacteria. Nucleic Acids Res. **37**: 7124–36.

Van den Born, E., Omelchenko, M. V., Bekkelund, A., Leihne, V., Koonin, E. V., Dolja, V. V., and Falnes, P.O. (2008). Viral AlkB proteins repair RNA damage by oxidative demethylation. Nucleic Acids Res. **36**: 5451–5461.

Wan, Y., Tang, K., Zhang, D., Xie, S., Zhu, X., Wang, Z., and Lang, Z. (2015). Transcriptome-wide high-throughput deep m6A-seq reveals unique differential m6A methylation patterns

between three organs in Arabidopsis thaliana. Genome Biol. **16**: 272.

Wang, L., Wen, M., and Cao, X. (2019). Nuclear hnRNPA2B1 initiates and amplifies the innate immune response to DNA viruses. Science. **365**: eaav0758.

Wang, X., Lu, Z., Gomez, A. et al. (2014). N 6-methyladenosine-dependent regulation of messenger RNA stability. Nature **505**: 117–120.

Wang, X., Zhao, B.S., Roundtree, I.A., Lu, Z., Han, D., Ma, H., Weng, X., Chen, K., Shi, H., and He, C. (2015). N6-methyladenosine modulates messenger RNA translation efficiency. Cell **161**: 1388–1399.

Wang, Z., Tang, K., Zhang, D., Wan, Y., Wen, Y., Lu, Q., and Wang, L. (2017). High-throughput m6A-seq reveals RNA m6A methylation patterns in the chloroplast and mitochondria transcriptomes of Arabidopsis thaliana. PLoS One **12**: e0185612.

Wei, J., Liu, F., Lu, Z. et al. (2018a). Differential m 6 A, m 6 A m , and m 1 A Demethylation Mediated by FTO in the Cell Nucleus and Cytoplasm. Mol. Cell **71**: 973–85.

Wei, L.-H., Song, P., Wang, Y., Lu, Z., Tang, Q., Yu, Q., Xiao, Y., Zhang, X., Duan, H.-C., and Jia, G. (2018b). The m 6 A Reader ECT2 Controls Trichome Morphology by Affecting mRNA Stability in Arabidopsis. Plant Cell **30**: 968–85.

Williams, G.D., Gokhale, N.S., and Horner, S.M. (2019). Regulation of Viral Infection by the RNA Modification N6 -Methyladenosine. Annu. Rev. Virol. **6**: 235–53.

Winkler, R., Gillis, E., Lasman, L. et al. (2019). m 6 A modification controls the innate immune response to infection by targeting type I interferons. Nat. Immunol. **20**: 173–182.

Xu, C., Liu, K., Ahmed, H., Loppnau, P., Schapira, M., and Min, J. (2015). Structural basis for the discriminative recognition of N6-Methyladenosine RNA by the human YT521-B homology domain family of proteins. J. Biol. Chem. **290**: 24902–24913.

Xu, C., Wang, X., Liu, K., Roundtree, I.A., Tempel, W., Li, Y., Lu, Z., He, C., and Min, J. (2014). Structural basis for selective binding of m6A RNA by the YTHDC1 YTH domain. Nat. Chem. Biol. **10**: 927–929.

Yang, Y., Hsu, P.J., Chen, Y.S., and Yang, Y.G. (2018). Dynamic transcriptomic m6A decoration: Writers, erasers, readers and functions in RNA metabolism. Cell Res. **28**: 616–624.

Zaccara, S. and Jaffrey, S.R. (2020). A Unified Model for the Function of YTHDF Proteins in Regulating m6A-Modified mRNA. Cell **181**: 1582–95.

Zaccara, S., Ries, R.J., and Jaffrey, S.R. (2019). Reading, writing and erasing mRNA methylation. Nat. Rev. Mol. Cell Biol. **20**: 608–24.

Zhang, Q., Sharma, N.R., Zheng, Z.M., and Chen, M. (2019). Viral Regulation of RNA Granules in Infected Cells. Virol. Sin. **34**: 175–91.

Zhang, Z., Theler, D., Kaminska, K.H., Hiller, M., De La Grange, P., Pudimat, R., Rafalska, I., Heinrich, B., Bujnick, J.M., Allain, F.H.T., and Stamm, S. (2010). The YTH domain is a novel RNA binding domain. J. Biol. Chem. **285**: 14701–14710.

Zheng, Q., Hou, J., Zhou, Y., Li, Z., and Cao, X. (2017). The RNA helicase DDX46 inhibits innate immunity by entrapping m 6 A-demethylated antiviral transcripts in the nucleus. Nat. Immunol. **18**: 1094–1103.

Zhong, S., Li, H., Bodi, Z., Button, J., Vespa, L., Herzog, M., and Fray, R.G. (2008). MTA Is an Arabidopsis Messenger RNA Adenosine Methylase and Interacts with a Homolog of a Sex-Specific Splicing Factor. Plant Cell Online **20**: 1278–1288.

Zhu, T., Roundtree, I.A., Wang, P., Wang, X., Wang, L., Sun, C., Tian, Y., Li, J., He, C., and Xu, Y. (2014). Crystal structure of the YTH domain of YTHDF2 reveals mechanism for recognition of N6-methyladenosine. Cell Res. **24**: 1493–6.

ANNEX I

List of A. thaliana mutant lines employed in this work. *All the lines used as genetic background were defined by Arribas-Hernández et al. (2018). Superscripts indicate if the transgene was described by Arribas-Hernández et al. (2018) ([1]) or it is used for the first time in this work ([2]).*

Mutant lines	Genetic background	Transgene	Source of the mutant line
ect2-1	WT	T-DNA (SALK_002225) [(1)]	1
ect3-1	WT	T-DNA (SALK_077502) [(1)]	1
ect4-2	WT	T-DNA (GK_241H02) [(1)]	1
ect5-1	WT	T-DNA (SALK_131549) [(2)]	2
ect2-3	WT	T-DNA (GK_132F02)[(1)]	1
ect3-2	WT	T-DNA (GABIseq_487H12)[(1)]	1
ect2-3/ect3-2	*ect2-3* x *ect3-2*	-	1
ect2-1/ect3-1	*ect2-1* x *ect3-1*	-	1
ect2-1/ect4-2	*ect2-1* x *ect4-2*	-	1
ect3-1/ect4-2	*ect3-1* x *ect4-2*	-	1
ect2-1/ect5-2	*ect2-1*	Deletion CRISPR/Cas9 [(2)]	2
ect2-1/ect5-3	*ect2-1*	Deletion CRISPR/Cas9 [(2)]	2
ect2-1/ect3-1/ect4-2	*ect2-1/ect3-1* x *ect4-2*	-	1
atalkbh9b/ ect2-1/ect3-1/ect4-2	*atalkbh9b x ect2-1/ect3-1/ect4-2*	-	2
ect2-1/ect3-1/ect5-4	*ect2-1/ect3-1*	Deletion CRISPR/Cas9 [(2)]	2
ect2-1/ect3-1/ect5-5	*ect2-1/ect3-1*	Deletion CRISPR/Cas9 [(2)]	2
ect2-1/ect3-1 ECT2^{W464A}:mCherry	*ect2-1/ect3-1*	ECT2^{W464A}:mCherry [(1)]	2
ect2-1/ect3-1 ECT2:mCherry	*ect2-1/ect3-1*	ECT2:mCherry [(1)]	2
ect2-1 3xHA-ECT2^{W464A}	*ect2-1*	3xHA-ECT2^{W464A} [(1)]	2
ect2-1 3xHA-ECT2	*ect2-1*	3xHA-ECT2 [(1)]	2

ANNEX II. Deletions *ECT5* CRISPR/Cas9 mutants

ANNEX III. List of oligonucleotides

qPCR	ECT5_qPCR_F	AGGCAGCAAAGAAGCAGTCA
	ECT5_qPCR_R	CCAGACCCGGTCAGACGTAA
	MTA_qPCR_F	CGGATCCACCATGGGACATT
	MTA_qPCR_R	AAGCTCCAAACATTCACGGC
	MTB_qPCR_F	GTACTGTGTTTCAGCGTTCC
	MTB_qPCR_R	TTCTGAGTCGAACCATAAGGAG
	VIR_qPCR_F	ACGCAAGTCCAGCCTTACTATCAC
	VIR_qPCR_R	CGGTCACTTAATAGAGCCTGAATGG
ect5 genotyping	LPect5-1	TGGACACGGTTCTTTCTCATC
	RPect5-1	TGATCAAATCAGGTTGGCTTC
CRISPR/Cas9 RNA guides	sgRNA_ECT5.1F	ATTGAAGTGTCCGGCAAAATCAC
	sgRNA_ECT5.1R	AAACGTGATTTTGCCGGACACTT
	sgRNA_ECT5.2F	ATTGTGAAAACCCCACAGGCGAA
	sgRNA_ECT5.2R	AAACTTCGCCTGTGGGGTTTTCA
	sgRNA_ECT5.3F	ATTGGGCAAGGGACTTGCTGCAG
	sgRNA_ECT5.3R	AAACCTGCAGCAAGTCCCTTGCC
CRISPR/Cas9 genotyping	C9_ECT5g_F	GCAGACTGTCCCGGCAAAC
	C9_ECT5g_R	CGGGCTGAGTTGGAGAAGTAA
	C9(LA)_ECT5-F	CTATGTTGGGGAGCCAGG
	C9(LA)_ECT5-R	GCTGGTAATACGGTGATGC
ECT5 ORF cloning	ECT5_GW_F	GGGGACCACTTTGTACAAGAAAGCTGGGTActagttggattgaccagaag
	ECT5_GW_Rstop	GGGGACCACTTTGTACAAGAAAGCTGGGTActagttggattgaccagaag
	ECT5_GW_R	GGGGACCACTTTGTACAAGAAAGCTGGGTAgttggattgaccagaagag
	ECT5_Fw	GGTCTCcCATGGCAACGACTCAATCACAC
	ECT5_Rv_STOP	GGTCTCgCTAGTTGGATTGACCAGAAGAG
	ECT5_Rv	GGTCTCgCTAgcGTTGGATTGACCAGAAGAGAC
ECT2 ORF cloning	ECT2_F	AAACCATGGCTACCGTTGCTCCTCCTG
	ECT2_R	AAAGCTAGCTTAGCAACCATTTGCCACGCTAGC
atALKBH9B ORF cloning	ALKBH9B_F	AACCATGGAAAACGATCCATTTC
	ALKBH9B_R	AAAGCTAGCTTAACCGTAGTTTCTTCTAC
CP_{AMV} ORF cloning	CP_{AMV}_F	AAACCATGGGTTCTTCACAAAAGAAAG
	CP_{AMV}_R	AAAAGCTAGCTCATTGACGATCAAGATCGTC

Supplementary figures

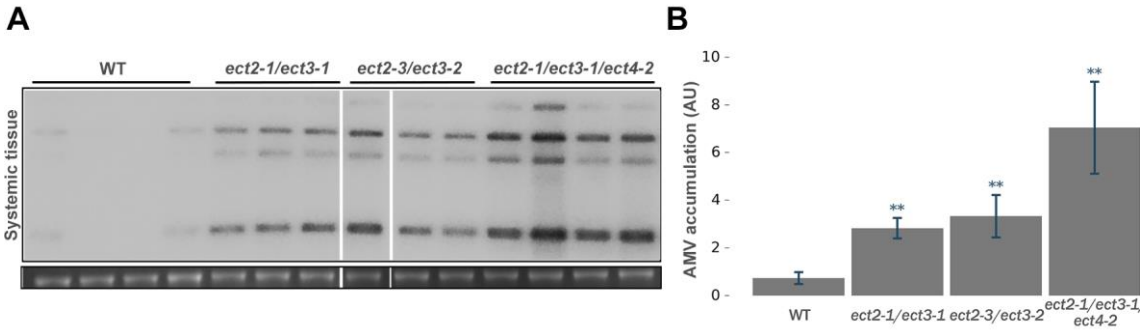

Figure S1. AMV accumulation analysis in ECT2/3/4 mutants compared to WT plants. (A) *Representative northern blot from systemic aerial tissue at 6 dpi of WT and double (ect2-1/ect3-1 and ect2-3/ect3-2 lines) and triple ECT2/3/4 mutants (genotypes are indicated on the top of each northern blot). vRNA 1-4 were detected by specific Dig-labelled probes and ethidium bromide of rRNAs was used as RNA loading control. (**B)** Graphic showing the quantification of panel A. Error bars corresponds to SD values. Asterisks indicate significant differences from the WT (*p-value < 0,05 and ** p-value <0,01) using the Student's t-test. AU, arbitrary units.*

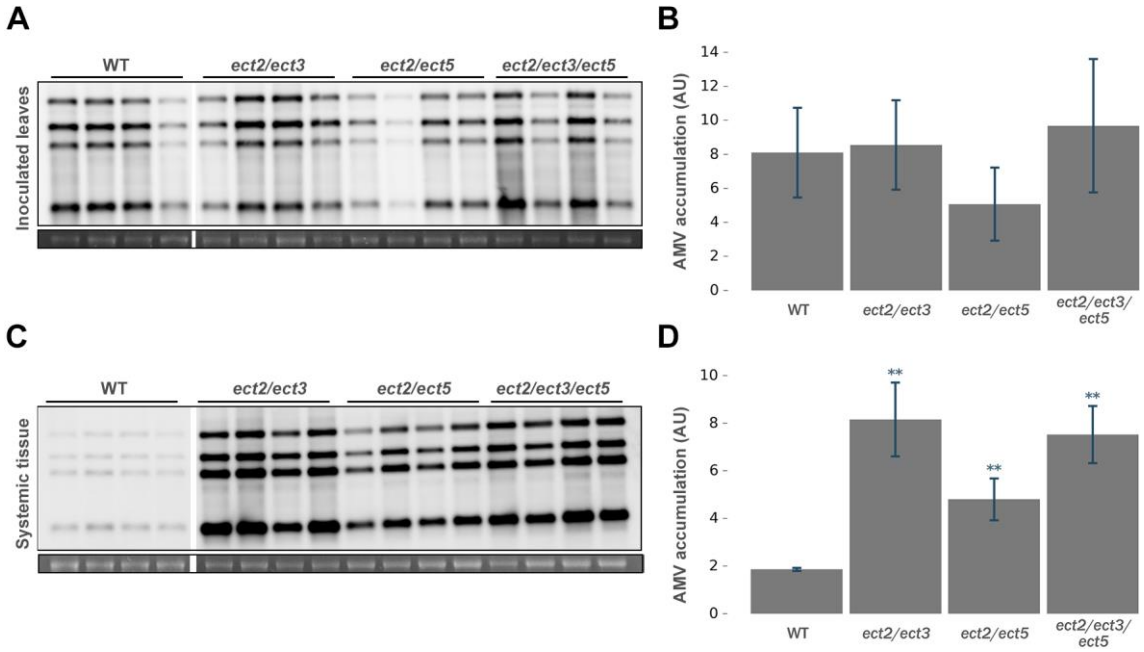

Figure S2. ECT5 is implied in AMV infection cycle. (A and C) *Representative northern blot from inoculated leaves at 3 dpi (A) and systemic aerial tissue at 7 dpi (C) of WT and ECT5 mutants described in Fig.3 (genotypes are indicated on the top of each northern blot). vRNA 1-4 were detected by specific Dig-labelled probes and ethidium bromide of rRNAs was used as RNA loading control. Each sample corresponds to a pool of two plants. (**B and D)** Graphics showing the quantification of panels A (B) and C (D). The lines used for this experiment were ect2-1/ect5-3 and ect2-1/ect3-1/ect5-5. Error bars correspond to standard deviations (SD) values. Asterisks indicate significant differences from the WT (**p-value<0,01) using the Student's t-test (n=4). AU, arbitrary units.*

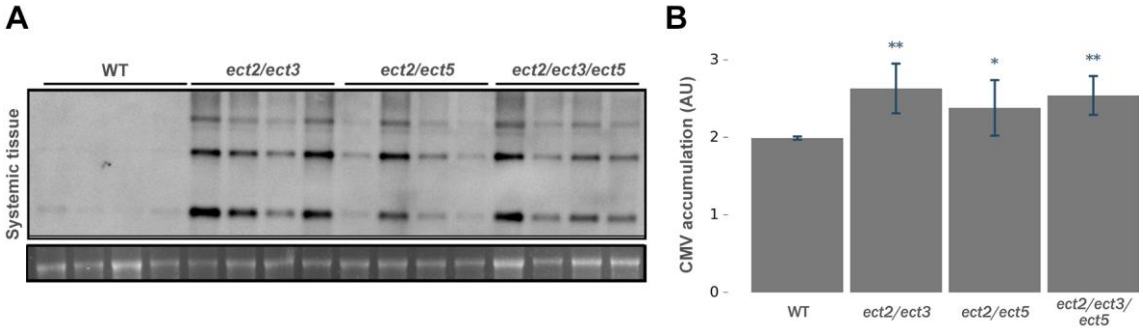

Figure S3. ECT2/3/5 module is also implied in CMV infection cycle. (A) *Representative northern blot from aerial systemic tissue at 4 dpi. Genotypes are indicated on the top of each northern blot (ect2-1/ect5-2 and ect2-1/ect3-1/ect5-5 lines). vRNA 1-4 were detected by specific Dig-labelled probes and ethidium bromide of rRNAs was used as RNA loading control.* ***(B)*** *Graphic showing the quantification of panel A. Error bars of the quantification graphics corresponds to SD values. Asterisks indicate significant differences from the WT (**p-value<0,01 and *p-value<0,05) using the Student's t-test (n=4). AU, arbitrary units.*

General discussion

As indicated throughout this manuscript, adenosine methylation at nitrogen-6 position (m^6A) has recently emerged as a new critical level of gene expression by regulating the fate of the modified transcripts (Zaccara et al., 2019; Arribas and Brodersen, 2020). m^6A *writers* and *erasers* define the methylation state of an RNA, whereas m^6A *reader*s specifically recognize this modification and can modulate the activity and half-life of diverse RNAs. Although m^6A was revealed as a key regulatory mechanism for different plant developmental processes (Arribas-Hernández et al., 2018), its potential involvement in the infection process of any plant pathogen had not been described. Hence, the main goal of this Thesis has been to unravel how m^6A methylation mechanism influences plant viral infections. A brief discussion about the most important discoveries and contributions that this work adds to our knowledge in the field of host-virus interactions is presented below.

AMV infection is regulated by the m^6A methylation machinery, including the first described protein with m^6A demethylation capability in plants. The transcriptomic analysis presented in this Thesis reveals that AMV infection modulates the expression of m^6A machinery in Arabidopsis**.** Thus, in AMV infected cells, m^6A pathway seems to be induced, since some methylation complex subunits (MTA, MTB and VIRILIZER) and the potential m^6A *reader* ECT5 are overexpressed, while none of the putative *erasers* considerably varies their expression. It is remarkable that ECT5, together with ECT9 and ECT10, presents a substitution of an aspartate by asparagine in the helix α1 within the YTH domain with respect to the rest of ECTs (Scutenaire et al., 2018). Interestingly, a mutational study on the m^6A recognition function of this domain found that a YTHDF1 mutant that contains this substitution showed 16-fold higher affinity towards m^6A-modified RNA (Xu et al., 2015). Other viral infections were previously reported to deregulate the expression of diverse ECTs and/or components that comprise the *writer* complex (Postnikova and Nemchinov, 2012), suggesting that m^6A methylation may constitute either a general antiviral plant response or a common viral mechanism to manipulate host transcriptome. Moreover, this work demonstrates that AMV RNAs become m^6A methylated during infection in Arabidopsis plants and that diverse components of the host m^6A regulation pathway are implied in several viral infections. In this line, the first plant protein with m^6A demethylation activity has been described and characterized here. The Arabidopsis protein atALKBH9B demethylates m^6A-modified single-stranded RNA *in vitro* and its activity correlates with m^6A levels of AMV in infected plants, since vRNAs are hypermethylated in *atalkbh9b* plants. Therefore, it is reasonable to propose atALKBH9B as one component of the cellular machinery monitoring m^6A levels in host RNAs. Interestingly, the CP of AMV interacts with atALKBH9B (see

below the proposed model to explain this interaction). It is worth mentioning that, during the development of this work, several other factors implied in this molecular mechanism have been identified by other authors (Introduction, Fig. 5), including the *eraser* atALKBH10B, which affects the Arabidopsis flowering process (Duan et al., 2017).

Remarkably, we observed that AMV infection is impaired in *atalkbh9b* and enhanced in *ect2/ect3/ect5* Arabidopsis plants. These opposite effects induced by the *eraser* and the *readers* in the same pathosystem emphasize the homeostatic nature of the m^6A methylation mechanism as a regulatory pathway in viral infections. Conversely, neither atALKBH9A nor atALKBH9C seem to participate in AMV infection, what might be related to the low expression of atALKBH9A and to the mostly nuclear localization of atALKBH9C (Mielecki et al., 2012; Duan et al., 2017). atALKBH9B, however, presents two exclusive features among the atALKB proteins: it localizes exclusively in the cytoplasm, where AMV replication occurs, and is one of the most expressed atALKB genes, mainly in buds and apical meristem (Duan et al., 2017). The absence of atALKBH9B affects, at least partially, AMV replication and/or translation steps, as the decrease of the viral titer observed in *atalkbh9b* vs WT plants is clearly appreciable in protoplasts. In addition, viral load in inoculated leaves is also lower in *atalkbh9b* plants and there is a delay in the viral invasion towards the petioles in Arabidopsis mutants compared to WT. However, the drastic block of the systemic infection towards the floral stems caused by the lack of *atALKBH9B* (only 9% of the inoculated plants were systemically infected) could not be exclusively due to reduced viral replication/translation functions. In fact, it was previously shown that reduced AMV replication rates does not necessarily affect the viral titer of the systemic tissue (Tenllado and Bol, 2000). On the other hand, the higher viral accumulation in systemic tissue in *ect2/ect3* and *ect2/ect5* plants indicates that these m^6A *readers* are negatively regulating AMV cycle. It is worth noting that at least two of these genes must be absent to observe a clear effect, likely due to their previously reported partial functional redundancy (Arribas-Hernández et al., 2018; 2020). The results presented here reveal that ECT4 has the minor implication, while ECT2 seems to be the most important among the assayed ECT proteins in AMV infection, since the highest systemic viral titers are observed for double mutants lacking ECT2.

AMV infection is regulated by m^6A levels on vRNAs through direct interactions of the m^6A machinery components. It cannot be distinctly ruled out that mutations of the m^6A pathway components could lead to an altered developmental and cellular state that modifies the susceptibility of the mutant plants against the virus compared with WT. Nevertheless, the observation that *atalkbh9b* and *ect2/ect5* mutants do not exhibit any observable developmental

phenotype effect weakens this hypothesis. On the other hand, ECT2/3/5 may act as defense effector genes that impair viral infection by manipulating host gene expression and not by a direct recognition of m^{6}A-modified vRNAs. In fact, in animal-infecting viruses, there are some lines of evidence indicating that m^{6}A mechanism modulates host defense in an immune response-independent manner (Liu et al., 2019), and by direct or indirect regulation of the IFN pathway after viral infections (Zheng et al., 2017; Rubio et al., 2018; Wang et al., 2019; Winkler et al., 2019; Gokhale et al., 2020). However, there are some arguments favoring the hypothesis that m^{6}A machinery components regulate AMV infection directly through m^{6}A accumulation and recognition on vRNAs. First, AMV infection seems to be related to m^{6}A levels along vRNAs that, in turn, depends on the atALKBH9B function, since, as mentioned above, AMV RNAs from *atalkbh9b* plants exhibit higher methylation rates. In fact, atALKBH9B binds to AMV RNAs, which could be facilitated by the CP-atALKBH9B interaction. This agrees with results found in several studies with animal-infecting viruses, in which viral infections are regulated by m^{6}A methylation of their genomic RNAs. For instance, knockdown of ALKBH5 or FTO increases m^{6}A levels in the ZIKV genome and negatively affects the viral infection (Lichinchi et al., 2016b). Secondly, findings of this Thesis suggest that viral impairment carried out by ECT proteins is, at least partially, mediated by m^{6}A-modified vRNAs direct binding. Unlike ECT2:mCherry, ECT2^{W464A}:mCherry mutant protein, which is incapable of recognizing m^{6}A, does not revert the susceptibility phenotype of *ect2/ect3* against the virus. This finding demonstrates that m^{6}A binding capability of ECT2 is critical for its role in AMV infection. Moreover, according to the IP results, ECT2 binds vRNAs *in vivo*, whereas ECT2^{W464A} does not, pointing to a direct interaction between ECT2 and AMV RNAs through m^{6}A recognition. Likewise, in the last years, multiple examples of viral modulation triggered by m^{6}A *readers* were described for mammalian viruses (for a recent review, see Williams et al., 2019). Remarkably, depending on the viral stage and/or the position along the viral genome, the presence of m^{6}A or the function of YTH proteins may have a positive or negative effect on viral fitness (Imam et al., 2018). It can be expected that the potential impact on the secondary structure triggered by m^{6}A presence and even other RNA-binding proteins contribute to these apparently opposite effects (Kierzek and Kierzek, 2003; Liu et al., 2015). Thus, it should be kept in mind that m^{6}A residues may have different consequences for AMV infection and, depending on the context, it could also produce secondary structure variations that affect other interactors.

m^{6}A methylation may constitute a general modulatory mechanism for plant viral infections. Interestingly, evaluation of other plant viruses carried out in this work indicates that plant m^{6}A-

mediated regulatory mechanism may affect the infection processes of several viruses. Thus far, CMV RNAs have been confirmed to contain m^6A residues, and our analysis of TCV and CaMV also suggest that these viruses are m^6A methylated. Other experimental approaches will be carried out to unequivocally corroborate this observation. These results highlight that m^6A methylation could be a conserved feature that drive infection processes of plant viruses replicating in either nucleus or cytoplasm, as found with mammalian viruses. Furthermore, likewise AMV, CMV infection levels are increased in *ect2/ect5* and *ect2/ect3* compared to WT plants, suggesting that the involvement of m^6A *readers* would influence other plant viruses. However, in contrast to AMV, neither differences on m^6A accumulation levels in CMV RNAs compared to WT plants, nor CMV, TCV and CaMV systemic infection block of floral stems are observed in *atalkbh9b* plants. Nonetheless, we cannot rule out the possibility that any of the other twelve AlkB orthologous of Arabidopsis could participate in the m^6A regulation and/or infection processes of these viruses. For instance, it was reported that depletion of FTO negatively affects HCV infection, while depletion of ALKBH5 has no effect on the life cycle of this virus (Gokhale et al., 2016). Thus, our results definitively reinforce the hypothesis of m^6A as a new critical regulatory mechanism in plant viral infections.

Link between m^6A machinery components, cytoplasmic granules and viral infections. atALKBH9B was found to localize exclusively in the cytoplasm (Mielecki et al., 2012) and here, a more detailed subcellular location study shows that this protein forms discrete cytoplasmic granules colocalizing with SGS3, component of siRNA bodies, and UPF1, NMD factor (Merai et al., 2013; Martínez de Alba et al., 2015). Additionally, some of these granules presented a spatial association with DCP1, a component of P-bodies (Ingelfinger et al., 2002) (Fig. 1 and Introduction, Fig.4). These outcomes suggest that atALKBH9B activity is related to mRNA silencing and decay processes, a premise reinforced by the observation that UPF1 depletion increased AMV accumulation. Interestingly, the m^6A *readers* ECT2, ECT3 and ECT4 also form similar punctuate foci after heat and somatic stress that, in the case of ECT2, were identified as SGs (Arribas-Hernández et al., 2018; Scutenaire et al., 2018). In line with that, this Thesis shows that ECT5 forms aggregates of varying sizes when overexpressed by agroinfiltration, which is probably a kind of stressful process for the plant. Several studies showed that as a result of the phase separation, proteins containing low-complexity amino acid sequences, like mammalian YTHDF, can form fibrils or hydrogels *in vitro* and in cells. This condensation is enhanced in presence of poly-m^6A methylated mRNAs, since they act as scaffolds for the interaction among the low-complexity domains. Thereby, m^6A-modified RNA/YTHDF complexes undergo

segregation into different phase-separated compartments, such as SGs or P-bodies (Fu and Zhuang, 2019; Gao et al., 2019; Ries et al., 2019), where mRNAs are subjected to specific foci regulation (for recent reviews in animals and plants, see Zaccara et al., 2019 and Arribas-Hernández and Brodersen, 2020, respectively). Reinforcing this hypothesis, mRNA/YTHDF2 complexes were reported to localize in P-bodies (Wang et al., 2014) and Arabidopsis ECT2 was also shown to have the ability of undergoing phase separation *in vitro* forming gel-like condensates (Arribas-Hernández et al., 2018). Furthermore, it is well known the existence of a crosstalk between viral infections and SGs components in both animals and plants (Zhang et al., 2019; Xu et al., 2020). Evading SG formation, enhancing their disassembly and/or varying their structure to hijack their components and take advantage of their functions are some of the evolved strategies developed by viruses, possibly to avoid the translational arrest and, thus, the viral restriction. Therefore, here, it is proposed that the interaction between Arabidopsis ECT proteins and poly-methylated AMV RNAs, as previously shown in mammalian cells, would lead to the formation of RNA granules such as SGs, reducing viral translation and replication rates.

Molecular m^{6}A-dependent regulation model for AMV infection in Arabidopsis. As mentioned in the introduction, the CP is a multifunctional protein that binds multiple host components and acquires a special importance for AMV and ilarviruses: CP binding to the 3'UTR switches the stem-loop structure of this region to a pseudo-knotted conformation changing the translatability of the vRNAs to a replication-competent form (Bol, 2005; Pallas et al., 2013). In this Thesis, a new additional role for the CP of AMV linked to the host m^{6}A methylation mechanism is suggested. Remarkably, the CP of AMV and PNRSV, a member of the *Ilarvirus* genus that does not infect Arabidopsis, interact with atALKBH9B *in vivo*, whereas CP of CMV does not. Thus, we hypothesize that the CP-atALKBH9B interaction is indispensable to usurp atALKBH9B activity, what would explain that neither CMV m^{6}A ratio nor infection levels are affected in *atalkbh9b*. Figure 1 illustrates the proposed molecular m^{6}A-dependent regulation model of AMV cycle. After entry in the cell and the subsequent uncoating, CP dimers remain bound to the vRNAs to facilitate viral protein translation through the interaction of the CP with the initiation factor eIF4F. Then, genomic RNAs are targeted to vacuolar membranes where viral factories are formed (Introduction, Fig. 3B) (Bol, 2008). An unidentified m^{6}A methyltransferase would cause methylation along vRNAs. After recognition of m^{6}A poly-methylated vRNAs, ECTs would form RNA granules, likely SGs, via the interaction among their IDRs, most probably causing vRNA translation arrest. Moreover, since atALKBH9B colocalizes with siRNA bodies and NMD factors, vRNAs might be also brought to these granules, but there is no evidence about that so far. To counteract the cell response, the virus would usurp the atALKBH9B function, through its

interaction with the CP, to remove the excess of m^{6}A from its genome and avoid ECTs sequestration, enhancing viral accumulation. Furthermore, the presence of m^{6}A nucleotides along the 3'UTR of the AMV RNAs could potentially disturb its structural organization affecting the CP binding and/or the 3'UTR conformational switch required for competent viral replication and translation.

Interestingly, BiFC analysis carried out in this Thesis reveals an interaction of atALKBH9B with Arabidopsis ECT2 and ECT5, which is in line with a recent observation showing that the *eraser* atALKBH10B was enriched after ECT2:mCherry immunoprecipitation (Tankmar, 2019). These preliminary results advocate an auto-regulatory system in which *readers* and *erasers* would inhibit the action of each other to adjust the cell mRNA fate. The opposite effects that ECT2/3/5 and atALKBH9B exert on AMV infection support this hypothesis (Fig. 1). Further analysis will decipher the details of this cross-talk mechanism and the direction of this inhibition. At the same time, infection would lead to a competition between the CP and the ECTs for the atALKBH9B hijack.

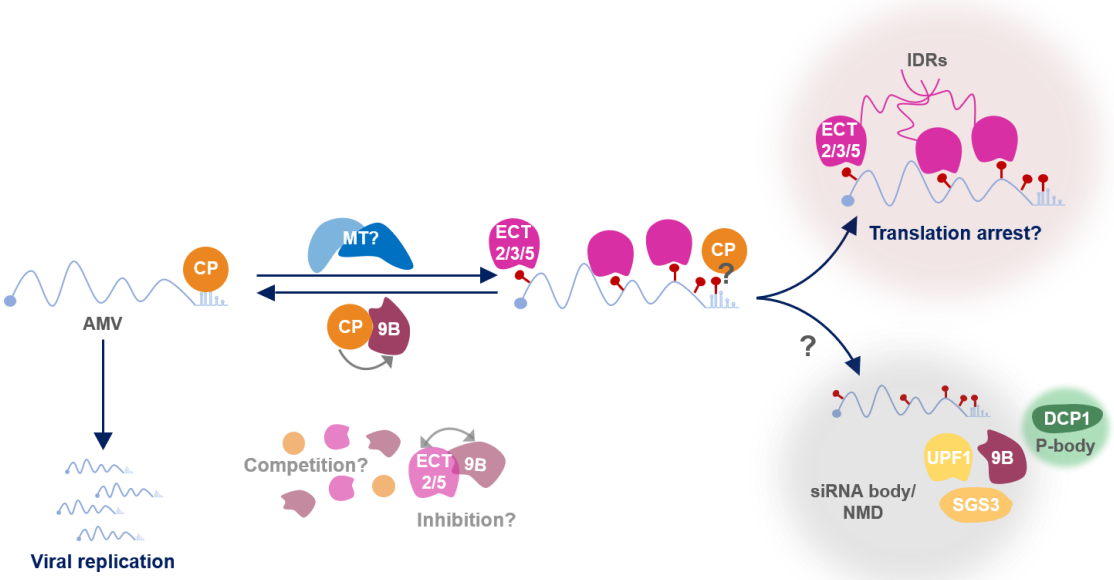

Figure 1. Schematic representation of the hypothetical model of m^{6}A-mediated AMV regulation in Arabidopsis. *vRNAs would be methylated by an unidentified m^{6}A methyltransferase. ECT2, ECT3 and ECT5 would recognize the m^{6}A poly-methylated vRNAs and the interaction among their IDRs would undergo phased separation that favor the localization of m^{6}A-modified vRNAs to RNA granules. These could be SGs, where vRNA would be translationally repressed. vRNAs might be also brought to siRNA bodies, where atALKBH9B has been found. In turn, AMV CP would hijack the atALKBH9B to demethylate the vRNAs and avoid ECTs sequestration, enhancing the viral replication. However, CP would have to compete with the ECTs for the atALKBH9B binding, since ECT2 and ECT5 interact to atALKBH9B, maybe to inhibit the action of each other. Moreover, m^{6}A might potentially affect the CP binding to the 3'UTR of viral RNAs. m^{6}A residues are represented as red circles; AMV, Alfalfa mosaic virus; CP, capsid protein; ECT, EVOLUTIONARILY CONSERVED C-TERMINAL REGION; 9b, atALKBH9B; IDR, intrinsically disordered regions; MT, unidentified m^{6}A methyltransferase complex. See main text for details.*

Relation between m^{6}A methylation mechanism and long-term infections. It seems clear that m^{6}A modification is conserved among animal and plant viruses, advocating an evolutionarily established host-virus interaction mechanism. Curiously, slower replication rates were related to persistent infections via a dodging of the immune system in HCV chronic pathology (Bocharov et al., 2004). In this line, Gokhale et al. (2016) proposed that the modulation of m^{6}A levels in genomic RNAs of HCV could constitute a mechanism to make the virus to replicate at low rates and, thus, allow the setting up of persistent infections. Remarkably, several RNA plant viruses belonging to the *Flexiviridae* family contain a conserved AlkB domain inserted in the coding region of their replicases (Bratlie and Drabløs, 2005; Martelli et al., 2007; Van den Born et al., 2008). A functional characterization of these domains found that they may be biologically important, since they repair RNA methylation damage (Van den Born et al., 2008). Outstandingly, most of these viruses infect woody or perennial plants and it was proposed that AlkB domains might have been acquired to promote long-term survival of these RNA viruses (Moore and Meng, 2019). Likewise, alfalfa plants, the natural host of AMV, are usually kept in the field around five years before sewing new seeds to regenerate the crop (Bergua, 2011; Escriu et al., 2011). These seeds are typically collected from their previous crops by farmers, and AMV transmission studies of alfalfa in Spain reported infection rates up to 80% in 3-4 years old plants (Escriu et al., 2011). Thus, this agricultural practice leads to the infection maintaining over the years. On the other hand, AMV genome lacks Alkb domain, so the virus may need to usurp this function from the host to accumulate for long-term periods. In this scenario, it is tempting to speculate that m^{6}A may act as an evolutionarily acquired control mechanism to reach an equilibrium between infection and host survival that would lead to the establishment of long-term infections (Fig. 2). Nonetheless, further experiments will have to be perform to demonstrate the validity of this hypothesis.

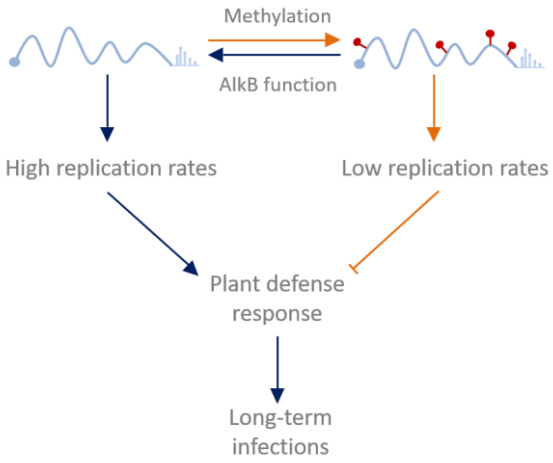

Figure 2. Scheme for a hypothetical viral strategy for long-term infections. *m^{6}A residues are represented as red circles.*

Conclusions

1. atALKBH9B is the first protein with m^{6}A demethylation *in vitro* capability described in plants. Accordingly, m^{6}A/A ratio on AMV RNAs is increased in *atalkbh9b* infected plants, suggesting that viral RNAs would be targets of this *eraser*. Moreover, atALKBH9B forms discrete granules colocalizing with siRNA bodies and NMD factors, and presents a spatial association with P-bodies, suggesting that its activity is related to the mRNA silencing and decay processes. Furthermore, atALKBH9B interacts with the CP of AMV, although the actual biological significance of this interaction remains unclear.

2. Components of the m^{6}A methylation complex, MTA, MTB, VIR, and a potential m^{6}A *reader*, ECT5, are upregulated in Arabidopsis AMV-infected plants, indicating that m^{6}A pathway is induced upon viral infection.

3. Altogether, the results reported in this Thesis indicate that m^{6}A methylation status of the viral RNAs has a profound impact in the AMV infection. Replication and/or translation processes are impaired in *atalkbh9b* plants, whereas systemic movement to the floral stems is practically blocked. On the contrary, lack of the ECT2/ECT3/ECT5 *reader* module increases the systemic infection of AMV. The antiviral effect of ECT2 seems to be derived from its direct binding to the m^{6}A-modified viral RNAs, as an ECT2 mutant protein defective in m^{6}A recognition loses wild type antiviral activity and is unable to pull down AMV RNAs *in vivo*.

4. In addition to AMV, CMV and, in default of reinforcing the observations presented here, TCV and CaMV RNAs have been found to contain m^{6}A residues. Thus, as found in animal-infecting viruses, m^{6}A methylation of viral RNAs during the infection process could be a widespread phenomenon for plant viruses. Likewise, the m^{6}A *reader*-dependent regulation may be a general cross-talk mechanism between hosts and viruses, as CMV infection levels are also increased when ECT2/ECT3 and ECT2/ECT5 activities are absent. Nevertheless, atALKBH9B-dependent viral modulation seems to be specific for AMV, since no effect was observed in *atalkbh9b* plants infected with CMV, TCV or CaMV compared to WT. Since CMV CP, unlike AMV CP, does not interact with atALKBH9B, this interaction might be critical to hijack atALKBH9B function.

5. The observation that ECT5 forms aggregates of different sizes when overexpressed by agroinfiltration is in line with previous results reported by others indicating that ECT2 can localize to stress granules and undergo gel-like phase *in vitro*. As found for mammalian YTH proteins, these outcomes might be explained by assuming that the interaction between ECTs

and poly-methylated viral RNAs would promote the formation of SGs and, consequently, reduce viral translation and replication rates.

6. The results obtained in this Thesis have allowed us to propose a working model to explain the m^6A-dependent regulation for AMV infection in Arabidopsis plants.

References

Anders, M., Chelysheva, I., Goebel, I., Trenkner, T., Zhou, J., Mao, Y., Verzini, S., Qian, S.B., and Ignatova, Z. (2018). Dynamic m6a methylation facilitates mRNA triaging to stress granules. Life Sci. Alliance **1**: e201800113.

Anderson, P. and Kedersha, N. (2008). Stress granules: the Tao of RNA triage. Trends Biochem. Sci. **33**: 141–50.

Anderson, S.J., Kramer, M.C., Gosai, S.J., Yu, X., Vandivier, L.E., Nelson, A.D.L., Anderson, Z.D., Beilstein, M.A., Fray, R.G., Lyons, E., and Gregory, B.D. (2018). N6-Methyladenosine Inhibits Local Ribonucleolytic Cleavage to Stabilize mRNAs in Arabidopsis. Cell Rep. **25**: 1146–1157.

Ansel-McKinney, P., Scott, S.W., Swanson, M., Ge, X., and Gehrke, L. (1996). A plant viral coat protein RNA binding consensus sequence contains a crucial arginine. EMBO J. **15**: 5077–84.

Aparicio, F. and Pallás, V. (2017). The coat protein of Alfalfa mosaic virus interacts and interferes with the transcriptional activity of the bHLH transcription factor ILR3 promoting salicylic acid-dependent defence signalling response. Mol. Plant Pathol. **18**: 173–186.

Aparicio, F., Sánchez-Navarro, J.A., Olsthoorn, R.C.L., Pallás, V., and Bol, J.F. (2001). Recognition of cis-acting sequences in RNA 3 of Prunus necrotic ringspot virus by the replicase of Alfalfa mosaic virus. J. Gen. Virol. **82**: 947–51.

Aparicio, F., Sánchez-Navarro, J.A., and Pallás, V. (2006). In vitro and in vivo mapping of the Prunus necrotic ringspot virus coat protein C-terminal dimerization domain by bimolecular fluorescence complementation. J. Gen. Virol. **87**: 1745–50.

Aparicio, F., Vilar, M., Perez-Payá, E., and Pallás, V. (2003). The coat protein of prunus necrotic ringspot virus specifically binds to and regulates the conformation of its genomic RNA. Virology **313**: 213–23.

Aravind, L. and Koonin, E. V. (2001). The DNA-repair protein AlkB, EGL-9, and leprecan define new families of 2-oxoglutarate- and iron-dependent dioxygenases. Genome Biol. **2**: research0007.

Arguello, A.E., Deliberto, A.N., and Kleiner, R.E. (2017). RNA Chemical Proteomics Reveals the N6-Methyladenosine (m6A)-Regulated Protein-RNA Interactome. J. Am. Chem. Soc. **139**: 17249–52.

Arribas-Hernández, L., Bressendorff, S., Hansen, M.H., Poulsen, C., Erdmann, S., and Brodersen, P. (2018). An m ^{6} A-YTH Module Controls Developmental Timing and Morphogenesis in Arabidopsis. Plant Cell **30**: 952–967.

Arribas-Hernández, L. and Brodersen, P. (2020a). Occurrence and Functions of m6A and Other Covalent Modifications in Plant mRNA. Plant Physiol. **182**: 79–96.

Arribas-Hernández, L., Simonini, S., Hansen, M.H., Botterweg, E., Bressendorff, S., Dong, Y., Østergaard, L. and Brodersen, P. (2020b). Recurrent requirement for the m6A-ECT2/ECT3/ECT4 axis in the control of cell proliferation during plant organogenesis. Development. doi: 10.1242/dev.189134.

Bailey, A.S., Batista, P.J., Gold, R.S., Grace Chen, Y., de Rooij, D.G., Chang, H.Y., and Fuller, M.T. (2017). The conserved RNA helicase YTHDC2 regulates the transition from proliferation to differentiation in the germline. Elife **6**: e26116.

Balacco, D.L. and Soller, M. (2019). The m6A Writer: Rise of a Machine for Growing Tasks. Biochemistry **58**: 363–378.

Balasubramaniam, M., Kim, B.S., Hutchens-Williams, H.M., and Loesch-Fries, L.S. (2014). The photosystem II oxygen-evolving complex protein PsbP interacts with the coat protein of Alfalfa mosaic virus and inhibits virus replication. Mol. Plant-Microbe Interact. **27**: 1107–1118.

Baquero-Perez, B., Antanaviciute, A., Yonchev, I.D., Carr, I.M., Wilson, S.A., and Whitehouse, A. (2019). The tudor SND1 protein is an m6a RNA reader essential for replication of kaposi's sarcoma-associated herpesvirus. Elife **8**: e47261.

Beckham, C.J. and Parker, R. (2008). P Bodies, Stress Granules, and Viral Life Cycles. Cell Host Microbe **3**: 206–12.

Beemon, K. and Keith, J. (1977). Localization of N6-methyladenosine in the Rous sarcoma virus genome. J. Mol. Biol. **113**: 165–79.

Beijerinck, M.W. (1898). Concerning a contagium vivum fluidum as cause of the Spot Disease of Tobacco leaves. Verh. der K. Akad. van Wet. te Amsterdam **65**: 3–21.

Bergua, M. (2011). El virus del mosaico de la alfalfa (AMV) en España: incidencia y efectos en alfalfa y análisis de la diversidad biológica y genética de poblaciones procedentes de distintos huéspedes. PhD thesis (Universidad Zaragoza/Centro Investig. y Tecnol. Agroaliment. Aragón, Zaragoza, Spain).

Berlivet, S., Scutenaire, J., Deragon, J.M., and Bousquet-Antonelli, C. (2019). Readers of the m 6 A epitranscriptomic code. Biochim. Biophys. Acta - Gene Regul. Mech. **1862**: 329–342.

Bhasin, H. and Hülskamp, M. (2017). ANGUSTIFOLIA, a plant homolog of CtBP/BARS localizes to stress granules and regulates their formation. Front. Plant Sci. **8**: 1004.

Bhat, S.S., Bielewicz, D., Grzelak, N., Gulanicz, T., Bodi, Z., Szewc, L., Bajczyk, M., Dolata, J., Smolinski, D.J., Fray, R.G., Jarmolowski, A., and Szweykowska-Kulinska, Z. (2019). mRNA adenosine methylase (MTA) deposits m6A on pri-miRNAs to modulate miRNA biogenesis in Arabidopsis thaliana. bioRxiv: https://doi.org/10.1101/557900.

Bidet, K., Dadlani, D., and Garcia-Blanco, M.A. (2014). G3BP1, G3BP2 and CAPRIN1 Are Required for Translation of Interferon Stimulated mRNAs and Are Targeted by a Dengue Virus Non-coding RNA. PLoS Pathog. **10**: e1004242.

Boccaletto, P., MacHnicka, M.A., Purta, E., Pitkowski, P., Baginski, B., Wirecki, T.K., De Crécy-Lagard, V., Ross, R., Limbach, P.A., Kotter, A., Helm, M., and Bujnicki, J.M. (2018). MODOMICS: A database of RNA modification pathways. 2017 update. Nucleic Acids Res. **46**: D303–D307.

Bocharov, G., Ludewig, B., Bertoletti, A., Klenerman, P., Junt, T., Krebs, P., Luzyanina, T., Fraser, C., and Anderson, R.M. (2004). Underwhelming the Immune Response: Effect of Slow Virus Growth on CD8+-T-Lymphocyte Responses. J. Virol. **78**: 2247–54.

Bodi, Z., Zhong, S., Mehra, S., Song, J., Graham, N., Li, H., May, S., and Fray, R.G. (2012). Adenosine Methylation in Arabidopsis mRNA is Associated with the 3′ End and Reduced Levels Cause Developmental Defects. Front. Plant Sci. **3**: 1–10.

Bokar, J.A., Rath-Shambaugh, M.E., Ludwiczak, R., Narayan, P., and Rottman, F. (1994). Characterization and partial purification of mRNA N6-adenosine methyltransferase from HeLa cell nuclei: Internal mRNA methylation requires a multisubunit complex. J. Biol. Chem. **269**: 17697–17704.

Bokar, J.A., Shambaugh, M.E., Polayes, D., Matera, A.G., and Rottman, F.M. (1997). Purification and cDNA cloning of the AdoMet-binding subunit of the human mRNA (N6-adenosine)-methyltransferase. RNA **3**: 1233–47.

Bol, J.F. (2003). Alfalfa mosaic virus: Coat protein-dependent initiation of infection. Mol. Plant Pathol. **4**: 1–8.

Bol, J.F. (2008). Alfalfa Mosaic Virus. In Encyclopedia of Virology.

Bol, J.F. (2005). Replication of Alfamo- and Ilarviruses: Role of the Coat Protein. Annu. Rev. Phytopathol. **43**: 39–62.

Bol, J.F., Van Vloten-Doting, L., and Jaspars, E.M.J. (1971). A functional equivalence of top component a RNA and coat protein in the initiation of infection by alfalfa mosaic virus. Virology **46**: 73–85.

Bratlie, M.S. and Drabløs, F. (2005). Bioinformatic mapping of AlkB homology domains in viruses. BMC Genomics **6**: 1.

Bruggeman, Q., Garmier, M., de Bont, L., Soubigou-Taconnat, L., Mazubert, C., Benhamed, M., Raynaud, C., Bergounioux, C., and Delarue, M. (2014). The polyadenylation factor subunit CLEAVAGE AND POLYADENYLATION SPECIFICITY FACTOR30: A key factor of programmed

cell death and a regulator of immunity in arabidopsis. Plant Physiol. **165**: 732–46.

Bujarski, J., Gallitelli, D., García-Arenal, F., Pallás, V., Palukaitis, P., Krishna Reddy, M., and Wang, A. (2019). ICTV virus taxonomy profile: Bromoviridae. J. Gen. Virol. **100**: 1206–1207.

Butterbach, P., Verlaan, M.G., Dullemans, A., Lohuis, D., Visser, R.G.F., Bai, Y., and Kormelink, R. (2014). Tomato yellow leaf curl virus resistance by Ty-1 involves increased cytosine methylation of viral genomes and is compromised by cucumber mosaic virus infection. Proc. Natl. Acad. Sci. U. S. A. **111**: 12942–7.

Calil, I.P. and Fontes, E.P.B. (2017). Plant immunity against viruses: Antiviral immune receptors in focus. Ann. Bot. **119**: 711–23.

Canaani, D., Kahana, C., Lavi, S., and Groner, Y. (1979). Identification and mapping of N6-methyladenosine containing sequences in simian virus 40 RNA. Nucleic Acids Res. **6**: 2879–99.

Carbonell, A. and Carrington, J.C. (2015). Antiviral roles of plant ARGONAUTES. Curr. Opin. Plant Biol. **27**: 111–7.

Chakrabarti, M. and Hunt, A.G. (2015). CPSF30 at the interface of alternative polyadenylation and cellular signaling in plants. Biomolecules **5**: 1151–68.

Chen, J., Noueiry, A., and Ahlquist, P. (2001). Brome Mosaic Virus Protein 1a Recruits Viral RNA2 to RNA Replication through a 5' Proximal RNA2 Signal. J. Virol. **75**: 3207–19.

Chen, S.-C. and Olsthoorn, R.C.L. (2010). In Vitro and In Vivo Studies of the RNA Conformational Switch in Alfalfa Mosaic Virus. J. Virol. **84**: 1423–9.

Chen, Y.G., Chen, R., Ahmad, S., Verma, R., Kasturi, S.P., Amaya, L., Broughton, J.P., Kim, J., Cadena, C., Pulendran, B., Hur, S., and Chang, H.Y. (2019). N6-Methyladenosine Modification Controls Circular RNA Immunity. Mol. Cell **76**: 96–109.

Chicois, C., Scheer, H., Garcia, S., Zuber, H., Mutterer, J., Chicher, J., Hammann, P., Gagliardi, D., and Garcia, D. (2018). The UPF1 interactome reveals interaction networks between RNA degradation and translation repression factors in Arabidopsis. Plant J. **96**: 119–32.

Choe, J., Lin, S., Zhang, W. et al. (2018). mRNA circularization by METTL3–eIF3h enhances translation and promotes oncogenesis. Nature **561**: 556–60.

Choi, J., Kim, B.S., Zhao, X., and Loesch-Fries, S. (2003). The importance of alfalfa mosaic virus coat protein dimers in the initiation of replication. Virology **305**: 44–9.

Chu C.-C., Liu B., Plangger R., Kreutz C., Al-Hashimi H.M. (2019). m6A minimally impacts the structure, dynamics, and Rev ARM binding properties of HIV-1 RRE stem IIB. PLoS ONE **14**: e0224850.

Clancy, M.J. (2002). Induction of sporulation in Saccharomyces cerevisiae leads to the formation of N6-methyladenosine in mRNA: a potential mechanism for the activity of the IME4 gene. Nucleic Acids Res. **30**: 4509–18.

Clough, S.J. and Bent, A.F. (1998). Floral dip: A simplified method for Agrobacterium-mediated transformation of Arabidopsis thaliana. Plant J. **16**: 735–743.

Conti, G., Zavallo, D., Venturuzzi, A.L., Rodriguez, M.C., Crespi, M., and Asurmendi, S. (2017). TMV induces RNA decay pathways to modulate gene silencing and disease symptoms. Plant J. **89**: 73–84.

Coursey, T., Regedanz, E., and Bisaro, D.M. (2018). Arabidopsis RNA Polymerase V Mediates Enhanced Compaction and Silencing of Geminivirus and Transposon Chromatin during Host Recovery from Infection. J. Virol. **92**: e01320-17.

Courtney, D.G., Chalem, A., Bogerd, H.P., Law, B.A., Kennedy, E.M., Holley, C.L., and Cullen, B.R. (2019). Extensive epitranscriptomic methylation of A and C residues on murine leukemia virus transcripts enhances viral gene expression. MBio **10**: e01209-19.

Courtney, D.G., Kennedy, E.M., Dumm, R.E., Bogerd, H.P., Tsai, K., Heaton, N.S., and Cullen, B.R. (2017). Epitranscriptomic Enhancement of Influenza A Virus Gene Expression and Replication. Cell Host Microbe **22**: 377–86.

Csorba, T., Kontra, L., and Burgyán, J. (2015). Viral silencing suppressors: Tools forged to fine-

tune host-pathogen coexistence. Virology **479**–**480**: 85–103.

Culver, J.N. and Padmanabhan, M.S. (2007). Virus-Induced Disease: Altering Host Physiology One Interaction at a Time. Annu. Rev. Phytopathol. **45**: 221–43.

Dang, W., Xie, Y., Cao, P., Xin, S., Wang, J., Li, S., Li, Y., and Lu, J. (2019). N6-Methyladenosine and Viral Infection. Front. Microbiol. **10**: 1–12.

Darnell, R.R., Shengdong, K.E., and Darnell, J.E. (2018). Pre-mRNA processing includes N6 methylation of adenosine residues that are retained in mRNA exons and the fallacy of "RNA epigenetics." RNA **24**: 262–267.

Desrosiers, R., Friderici, K., and Rottman, F. (1974). Identification of methylated nucleosides in messenger RNA from Novikoff hepatoma cells. Proc. Natl. Acad. Sci. U. S. A. **71**: 3971–5.

Diallo, L.H., Tatin, F., David, F., Godet, A.C., Zamora, A., Prats, A.C., Garmy-Susini, B., and Lacazette, E. (2019). How are circRNAs translated by non-canonical initiation mechanisms? Biochimie **164**: 45–52.

Díaz-Ruiz, J.R. and Moreno, R. (1972). Symptomatologic, Morphologic and Ultrastructural Characteristics of a Strain of Alfalfa Mosaic Virus Found in Spain. Microbiol Esp **25**: 127–40.

Diezma-Navas, L., Pérez-González, A., Artaza, H., Alonso, L., Caro, E., Llave, C., and Ruiz-Ferrer, V. (2019). Crosstalk between epigenetic silencing and infection by tobacco rattle virus in Arabidopsis. Mol. Plant Pathol. **20**: 1439–52.

Dimock, K. and Stoltzfus, C.M. (1977). Sequence Specificity of Internal Methylation in B77 Avian Sarcoma Virus RNA Subunits. Biochemistry **16**: 471–8.

Ding, S.W. (2010). RNA-based antiviral immunity. Nat. Rev. Immunol. **10**: 632–44.

Dominissini, D., Moshitch-Moshkovitz, S., Salmon-Divon, M., Amariglio, N., and Rechavi, G. (2013). Transcriptome-wide mapping of N6-methyladenosine by m 6A-seq based on immunocapturing and massively parallel sequencing. Nat. Protoc. **8**: 176–189.

Dominissini, D., Moshitch-Moshkovitz, S., Schwartz, S., Salmon-Divon, M., Ungar, L., Osenberg, S., Cesarkas, K., Jacob-Hirsch, J., Amariglio, N., Kupiec, M., Sorek, R., and Rechavi, G. (2012). Topology of the human and mouse m6A RNA methylomes revealed by m6A-seq. Nature **485**: 201–206.

Dougherty, J.D., White, J.P., and Lloyd, R.E. (2011). Poliovirus-Mediated Disruption of Cytoplasmic Processing Bodies. J. Virol. **85**: 64–75.

Du, H., Zhao, Y., He, J., Zhang, Y., Xi, H., Liu, M., Ma, J., and Wu, L. (2016). YTHDF2 destabilizes m 6 A-containing RNA through direct recruitment of the CCR4-NOT deadenylase complex. Nat. Commun. **7**: 1–11.

Duan, H.-C., Wei, L.-H., Zhang, C., Wang, Y., Chen, L., Lu, Z., Chen, P.R., He, C., and Jia, G. (2017). ALKBH10B Is an RNA N^6-Methyladenosine Demethylase Affecting Arabidopsis Floral Transition. Plant Cell **29**: 2995–3011.

Edupuganti, R.R., Geiger S., Lindeboom R.G.H., et al. (2017). N6-methyladenosine (m6A) recruits and repels proteins to regulate mRNA homeostasis. Nat. Struct. Mol. Biol. **24**: 870–8.

Encyclopædia Britannica. Encyclopædia Britannica Online. Encyclopædia Britannica, 2011. Web. 26 Jan. 2011. <http://www.britannica.com/EBchecked/topic/423842/obligate-parasite>.

Escriu, F., Vidal, M.B., Arteaga, M.L., and Vargas-Mainar, M.E. (2011). Síntomas, dispersión y daños del virus del mosaico de la alfalfa. Vida Rural **322**: 48–52.

Fedeles, B.I., Singh, V., Delaney, J.C., Li, D., and Essigmann, J.M. (2015). The AlkB family of Fe(II)/α-ketoglutarate-dependent dioxygenases: Repairing nucleic acid alkylation damage and beyond. J. Biol. Chem. **290**: 20734–42.

Finkel, D. and Groner, Y. (1983). Methylations of adenosine residues (m6A) in pre-mRNA are important for formation of late simian virus 40 mRNAs. Virology **131**: 409–25.

Fontaine, K.A., Leon, K.E., Khalid, M.M., Tomar, S., Jimenez-Morales, D., Dunlap, M., Kaye, J.A., Shah, P.S., Finkbeiner, S., Krogan, N.J., and Ott, M. (2018). The cellular NMD pathway restricts zika virus infection and is targeted by the viral capsid protein. MBio **9**: e02126-18.

Fros, J.J., Domeradzka, N.E., Baggen, J., Geertsema, C., Flipse, J., Vlak, J.M., and Pijlman, G.P. (2012). Chikungunya Virus nsP3 Blocks Stress Granule Assembly by Recruitment of G3BP into Cytoplasmic Foci. J. Virol. **86**: 10873–9.

Fu, Y., Dominissini, D., Rechavi, G., and He, C. (2014). Gene expression regulation mediated through reversible m 6 A RNA methylation. Nat. Rev. Genet. **15**: 293–306.

Fu, Y. and Zhuang, X. (2019). m6A-binding YTHDF proteins promote stress granule formation by modulating phase separation of stress granule proteins. bioRxiv: doi: https://doi.org/10.1101/694455.

Fu, Y., Zorman, B., Sumazin, P., Sanna, P.P., and Repunte-Canonigo, V. (2019). Epitranscriptomics: Correlation of N 6 -methyladenosine RNA methylation and pathway dysregulation in the hippocampus of HIV transgenic rats. PLoS One **14**: 1–16.

Fu, Z.Q. and Dong, X. (2013). Systemic Acquired Resistance: Turning Local Infection into Global Defense. Annu. Rev. Plant Biol. **64**: 839–63.

Fukusumi, Y., Naruse, C., and Asano, M. (2008). Wtap is required for differentiation of endoderm and mesoderm in the mouse embryo. Dev. Dyn. **237**: 618–29.

Furuichi, Y., Morgan, M., Shatkin, A.J., and Darnell, J.E. (1976). The Methylation of Adenovirus-Specific Nuclear and Cytoplasmic RNA. Nucleic Acids Res. **3**: 749–65.

Fustin, J.M., Doi, M., Yamaguchi, Y., Hida, H., Nishimura, S., Yoshida, M., Isagawa, T., Morioka, M.S., Kakeya, H., Manabe, I., and Okamura, H. (2013). RNA-methylation-dependent RNA processing controls the speed of the circadian clock. Cell **155**: 793–806.

Gao, Y., Pei, G., Li, D., Li, R., Shao, Y., Zhang, Q.C., and Li, P. (2019). Multivalent m6A motifs promote phase separation of YTHDF proteins. Cell Res. **29**: 767–769.

Garcia-Campos, M.A., Edelheit, S., Toth, U. et al. (2019). Deciphering the "m6A Code" via Antibody-Independent Quantitative Profiling. Cell **178**: 731–47.

Garcia, D., Garcia, S., and Voinnet, O. (2014). Nonsense-mediated decay serves as a general viral restriction mechanism in plants. Cell Host Microbe **16**: 391–402.

Gergerich, R.C. and Dolja, V. V. (2006). Introduction to Plant Viruses, the Invisible Foe. Plant Heal. Instr.: DOI: 10.1094/PHI-I-2006-0414-01.

Geula, S., Moshitch-Moshkovitz, S., Dominissini, D. et al. (2015). m6A mRNA methylation facilitates resolution of naïve pluripotency toward differentiation. Science. **347**: 1002–6.

Gokhale, N.S., McIntyre, A.B.R., McFadden, M.J. et al. (2016). N6-Methyladenosine in Flaviviridae Viral RNA Genomes Regulates Infection. Cell Host Microbe **20**: 654–665.

Gokhale, N.S., McIntyre, A.B.R., Mattocks, M.D., Holley, C.L., Lazear, H.M., Mason, C.E., and Horner, S.M. (2020). Altered m6A Modification of Specific Cellular Transcripts Affects Flaviviridae Infection. Mol. Cell **77**: 542–555.

Gregory, B.D., O'Malley, R.C., Lister, R., Urich, M.A., Tonti-Filippini, J., Chen, H., Millar, A.H., and Ecker, J.R. (2008). A Link between RNA Metabolism and Silencing Affecting Arabidopsis Development. Dev. Cell **14**: 854–66.

Guogas, L.M., Laforest, S.M., and Gehrke, L. (2005). Coat Protein Activation of Alfalfa Mosaic Virus Replication Is Concentration Dependent. J. Virol. **79**: 5752–61.

Gutierrez-Beltran, E., Moschou, P.N., Smertenko, A.P., and Bozhkov, P. V. (2015). Tudor staphylococcal nuclease links formation of stress granules and processing bodies with mRNA catabolism in arabidopsis. Plant Cell **27**: 926–43.

Hamera, S., Song, X., Su, L., Chen, X., and Fang, R. (2012). Cucumber mosaic virus suppressor 2b binds to AGO4-related small RNAs and impairs AGO4 activities. Plant J. **69**: 104–15.

Han, G.Z. (2019). Origin and evolution of the plant immune system. New Phytol. **222**: 70–83.

Hao, H., Hao, S., Chen, H., Chen, Z., Zhang, Y., Wang, J., Wang, H., Zhang, B., Qiu, J., Deng, F., and Guan, W. (2019). N 6 -methyladenosine modification and METTL3 modulate enterovirus 71 replication. Nucleic Acids Res. **47**: 362–374.

Hartmann, A.M., Nayler, O., Schwaiger, F.W., Obermeier, A., and Stamm, S. (1999). The interaction and colocalization of Sam68 with the splicing-associated factor YT521-B in

nuclear dots is regulated by the Src family kinase p59(fyn). Mol. Biol. Cell **10**: 3909–26.

Haussmann, I.U., Bodi, Z., Sanchez-Moran, E., Mongan, N.P., Archer, N., Fray, R.G., and Soller, M. (2016). M6 A potentiates Sxl alternative pre-mRNA splicing for robust Drosophila sex determination. Nature **540**: 301–304.

He, B., Fajolu, O.L., Wen, R.-H., and Hajimorad, M.R. (2010). Seed Transmissibility of Alfalfa mosaic virus in Soybean. Plant Heal. Prog.: doi:10.1094/PHP-2010-1227-01-BR.

Heath, M.C. (2000). Hypersensitive response-related death. Plant Mol. Biol. **44**: 321–34.

Herranz, M.C., Pallas, V., and Aparicio, F. (2012). Multifunctional roles for the N-terminal basic motif of Alfalfa mosaic virus coat protein: Nucleolar/cytoplasmic shuttling, modulation of RNA-binding activity, and virion formation. Mol. Plant-Microbe Interact. **25**: 1093–103.

Herranz, M.C., Sanchez-Navarro, J.A., Saurí, A., Mingarro, I., and Pallás, V. (2005). Mutational analysis of the RNA-binding domain of the Prunus necrotic ringspot virus (PNRSV) movement protein reveals its requirement for cell-to-cell movement. Virology **339**: 31–41.

Hesser, C.R., Karijolich, J., Dominissini, D., He, C., and Glaunsinger, B.A. (2018). N6-methyladenosine modification and the YTHDF2 reader protein play cell type specific roles in lytic viral gene expression during Kaposi's sarcoma-associated herpesvirus infection. PLoS Pathog. **14**: 1–23.

Hipper, C., Brault, V., Ziegler-Graff, V., and Revers, F. (2013). Viral and cellular factors involved in phloem transport of plant viruses. Front. Plant Sci. **4**: 154.

Holley, R.W., Apgar, J., Everett, G.A., Madison, J.T., Marquisee, M., Merrill, S.H., Penswick, J.R., and Zamir, A. (1965). Structure of a ribonucleic acid. Science. **147**: 1462–5.

Horiuchi, K., Kawamura, T., Iwanari, H., Ohashi, R., Naito, M., Kodama, T., and Hamakubo, T. (2013). Identification of Wilms' tumor 1-associating protein complex and its role in alternative splicing and the cell cycle. J. Biol. Chem. **288**: 33292–302.

Houwing, C.J. and Jaspars, E.M.J. (1986). Coat protein blocks the in vitro transcription of the virion RNAs of the alfalfa mosaic virus. FEBS Lett **209**: 284–8.

Hsu, P.J., Zhu, Y., Ma, H. et al. (2017). Ythdc2 is an N6 -methyladenosine binding protein that regulates mammalian spermatogenesis. Cell Res. **27**: 1115–1127.

Hu, J., Manduzio, S., and Kang, H. (2019). Epitranscriptomic RNA methylation in plant development and abiotic stress responses. Front. Plant Sci. **10**: 500.

Huang, H., Weng, H., Zhou, K. et al. (2019). Histone H3 trimethylation at lysine 36 guides m6A RNA modification co-transcriptionally. Nature **567**: 414–419.

Huang, M., Jongejan, L., Zheng, H., Zhang, L., and Bol, J.F. (2001). Intracellular localization and movement phenotypes of Alfalfa mosaic virus movement protein mutants. Mol. Plant-Microbe Interact. **14**: 1063–74.

Hubstenberger, A., Courel, M., Bénard, M. et al. (2017). P-Body Purification Reveals the Condensation of Repressed mRNA Regulons. Mol. Cell **68**: 144–157.

Hui, S.G. and Shou, W.D. (2002). A viral protein inhibits the long range signaling activity of the gene silencing signal. EMBO J. **21**: 398–407.

Hutcheson, S.W. (1998). CURRENT CONCEPTS OF ACTIVE DEFENSE IN PLANTS. Annu. Rev. Phytopathol. **36**: 59–90.

Ibrahim, A., Hutchens, H.M., Howard Berg, R., and Sue Loesch-Fries, L. (2012). Alfalfa mosaic virus replicase proteins, P1 and P2, localize to the tonoplast in the presence of virus RNA. Virology **433**: 449–61.

ICTV (2017). Virus taxonomy: the classification and nomenclature of viruses. The online (10th) report of the ICTV.: https://talk.ictvonline.org/ictv-reports/ictv_onli.

Imai, Y., Matsuo, N., Ogawa, S., Tohyama, M., and Takagi, T. (1998). Cloning of a gene, YT521, for a novel RNA splicing-related protein induced by hypoxia/reoxygenation. Mol. Brain Res. **53**: 33–40.

Imam, H., Khan, M., Gokhale, N.S., McIntyre, A.B.R., Kim, G.-W., Jang, J.Y., Kim, S.-J., Mason, C.E., Horner, S.M., and Siddiqui, A. (2018). N6 -methyladenosine modification of hepatitis

B virus RNA differentially regulates the viral life cycle . Proc. Natl. Acad. Sci. **115**: 8829–8834.

Ingelfinger, D., Arndt-Jovin, D.J., Lührmann, R., and Achsel, T. (2002). The human LSm1-7 proteins colocalize with the mRNA-degrading enzymes Dcp1/2 and Xrnl in distinct cytoplasmic foci. RNA (New York, NY) **8**: 1489–1501.

Ivanov, K.I., Eskelin, K., Bašic, M., De, S., Lõhmus, A., Varjosalo, M., and Mäkinen, K. (2016). Molecular insights into the function of the viral RNA silencing suppressor HCPro. Plant J. **85**: 30–45.

Iwanowski, D. (1892). Concerning the mosaic disease of the tobacco plant. St Petersb Acad Imp Sci Bul **35**: 67–70.

Jia, G., Fu, Y., Zhao, X., Dai, Q., Zheng, G., Yang, Y., Yi, C., Lindahl, T., Pan, T., Yang, Y.G., and He, C. (2011). N6-Methyladenosine in nuclear RNA is a major substrate of the obesity-associated FTO. Nat. Chem. Biol. **7**: 885–7.

Jones, R.A.C. (2016). Future Scenarios for Plant Virus Pathogens as Climate Change Progresses. Adv. Virus Res. **95**: 87–147.

Jones, R.A.C. (2014). Plant virus ecology and epidemiology: Historical perspectives, recent progress and future prospects. Ann. Appl. Biol. **164**: 320–347.

Jones, R.A.C. and Naidu, R.A. (2019). Global Dimensions of Plant Virus Diseases: Current Status and Future Perspectives. Annu. Rev. Virol. **6**: 387–409.

Jouannet, V., Moreno, A.B., Elmayan, T., Vaucheret, H., Crespi, M.D., and Maizel, A. (2012). Cytoplasmic Arabidopsis AGO7 accumulates in membrane-associated siRNA bodies and is required for ta-siRNA biogenesis. EMBO J. **31**: 1704–13.

Jungfleisc, J., Blasco-Moreno, B., and Díez, J. (2016). Use of cellular decapping activators by positive-strand RNA viruses. Viruses: doi: 10.3390/v8120340.

Jurczyszak, D., Zhang, W., Terry, S.N., Kehrer, T., Bermúdez González, M.C., McGregor, E., Mulder, L.C.F., Eckwahl, M.J., Pan, T., and Simon, V. (2020). HIV protease cleaves the antiviral m6A reader protein YTHDF3 in the viral particle. PLoS Pathog.: https://doi.org/10.1371/journal.ppat.1008305.

Kan, L., Grozhik, A.V., Vedanayagam, J. et al. (2017). The m 6 A pathway facilitates sex determination in Drosophila. Nat. Commun. **8**: 15737.

Kane, S.E. and Beemon, K. (1987). Inhibition of methylation at two internal N6-methyladenosine sites caused by GAC to GAU mutations. J. Biol. Chem. **262**: 3422–7.

Kane, S.E. and Beemon, K. (1985). Precise localization of m6A in Rous sarcoma virus RNA reveals clustering of methylation sites: implications for RNA processing. Mol. Cell. Biol. **5**: 2298–306.

Kasowitz, S.D., Ma, J., Anderson, S.J., Leu, N.A., Xu, Y., Gregory, B.D., Schultz, R.M., and Wang, P.J. (2018). Nuclear m6A reader YTHDC1 regulates alternative polyadenylation and splicing during mouse oocyte development. PLoS Genet. **14**: e1007412.

Kasteel, D.T.J., Van Der Wel, N.N., Jansen, K.A.J., Goldbach, R.W., and Van Lent, J.W.M. (1997). Tubule-forming capacity of the movement proteins of alfalfa mosaic virus and brome mosaic virus. J. Gen. Virol. **78**: 2089–93.

Ke, S., Alemu, E.A., Mertens, C., et al. (2015). A majority of m6A residues are in the last exons, allowing the potential for 3′ UTR regulation. Genes Dev. **29**: 2037–53.

Ke, S., Pandya-Jones, A., Saito, Y., Fak, J.J., Vågbø, C.B., Geula, S., Hanna, J.H., Black, D.L., Darnell, J.E., and Darnell, R.B. (2017). m6A mRNA modifications are deposited in nascent pre-mRNA and are not required for splicing but do specify cytoplasmic turnover. Genes Dev. **31**: 990–1006.

Kennedy, E.M., Bogerd, H.P., Kornepati, A.V.R., Kang, D., Ghoshal, D., Marshall, J.B., Poling, B.C., Tsai, K., Gokhale, N.S., Horner, S.M., and Cullen, B.R. (2016). Posttranscriptional m6A Editing of HIV-1 mRNAs Enhances Viral Gene Expression. Cell Host Microbe **19**: 675–685.

Khaperskyy, D.A., Hatchette, T.F., and McCormick, C. (2012). Influenza A virus inhibits

cytoplasmic stress granule formation. FASEB J. **26**: 1629–39.

Kierzek, E. and Kierzek, R. (2003). The thermodynamic stability of RNA duplexes and hairpins containing N6-alkyladenosines and 2-methylthio-N6-alkyladenosines. Nucleic Acids Res. **31**: 4472–80.

Kim, J., Kim, Y., Yeom, M., Kim, J.H., and Nam, H.G. (2008). FIONA1 is essential for regulating period length in the Arabidopsis circadian clock. Plant Cell **20**: 307–19.

Knorr, D.A. (1983). Effects of a Necrosis-Inducing Isolate of Alfalfa Mosaic Virus on Stand Loss in Tomatoes. Phytopathology **73**: 1554–8.

Knuckles, P., Lence, T., Haussmann, I.U. et al. (2018). Zc3h13/Flacc is required for adenosine methylation by bridging the mRNA-binding factor RbM15/spenito to the m6 a machinery component Wtap/Fl(2)d. Genes Dev. **32**: 415–429.

König, J., Zarnack, K., Rot, G., Curk, T., Kayikci, M., Zupan, B., Turner, D.J., Luscombe, N.M., and Ule, J. (2010). ICLIP reveals the function of hnRNP particles in splicing at individual nucleotide resolution. Nat. Struct. Mol. Biol. **17**: 909–915.

Kourelis, J. and Van Der Hoorn, R.A.L. (2018). Defended to the nines: 25 years of resistance gene cloning identifies nine mechanisms for R protein function. Plant Cell **30**: 285–99.

Krab, I.M., Caldwell, C., Gallie, D.R., and Bol, J.F. (2005). Coat protein enhances translational efficiency of Alfalfa mosaic virus RNAs and interacts with the eIF4G component of initiation factor eIF4F. J. Gen. Virol. **86**: 1841–49.

Krapp, S., Greiner, E., Amin, B., Sonnewald, U., and Krenz, B. (2017). The stress granule component G3BP is a novel interaction partner for the nuclear shuttle proteins of the nanovirus pea necrotic yellow dwarf virus and geminivirus abutilon mosaic virus. Virus Res. **227**: 6–14.

Kretschmer, J., Rao, H., Hackert, P., Sloan, K.E., Höbartner, C., and Bohnsack, M.T. (2018). The m6A reader protein YTHDC2 interacts with the small ribosomal subunit and the 5′-3′ exoribonuclease XRN1. RNA **24**: 1339–50.

Krug, R.M., Morgan, M.A., and Shatkin, A.J. (1976). Influenza viral mRNA contains internal N6-methyladenosine and 5′-terminal 7-methylguanosine in cap structures. J. Virol. **20**: 45–53.

Kumakura, N., Takeda, A., Fujioka, Y., Motose, H., Takano, R., and Watanabe, Y. (2009). SGS3 and RDR6 interact and colocalize in cytoplasmic SGS3/RDR6-bodies. FEBS Lett. **583**: 1261–6.

Laliberté, J.-F. and Zheng, H. (2014). Viral Manipulation of Plant Host Membranes. Annu. Rev. Virol. **1**: 237–59.

Lang, F., Singh, R.K., Pei, Y., Zhang, S., Sun, K., and Robertson, E.S. (2019). EBV epitranscriptome reprogramming by METTL14 is critical for viral-associated tumorigenesis. PLoS Pathog. **15**: e1007796. doi.

Langmead, B. and Salzberg, S.L. (2012). Fast gapped-read alignment with Bowtie 2. Nat. Methods **9**: 357–9.

Lavi, S. and Shatkin, A.J. (1975). Methylated simian virus 40-specific RNA from nuclei and cytoplasm of infected BSC-1 cells. Proc. Natl. Acad. Sci. **72**: 2012–2016.

Lence, T., Akhtar, J., Bayer, M., Schmid, K., Spindler, L., Ho, C.H., Kreim, N., Andrade-Navarro, M.A., Poeck, B., Helm, M., and Roignant, J.Y. (2016). M6A modulates neuronal functions and sex determination in Drosophila. Nature **540**: 242–7.

Lesbirel, S. and Wilson, S.A. (2019). The m 6 A-methylase complex and mRNA export. Biochim. Biophys. Acta - Gene Regul. Mech. **1862**: 319–328.

Li, D., Zhang, H., Hong, Y., Huang, L., Li, X., Zhang, Y., Ouyang, Z., and Song, F. (2014a). Genome-Wide Identification, Biochemical Characterization, and Expression Analyses of the YTH Domain-Containing RNA-Binding Protein Family in Arabidopsis and Rice. Plant Mol. Biol. Report. **32**: 1169–86.

Li, F. and Wang, A. (2019). RNA-Targeted Antiviral Immunity: More Than Just RNA Silencing. Trends Microbiol. **27**: 792–805.

Li, F. and Wang, A. (2018). RNA decay is an antiviral defense in plants that is counteracted by viral RNA silencing suppressors. PLoS Pathog. **14**: e1007228.

Li, F., Zhao, D., Wu, J., and Shi, Y. (2014b). Structure of the YTH domain of human YTHDF2 in complex with an m6A mononucleotide reveals an aromatic cage for m6A recognition. Cell Res. **24**: 1490–92.

Li, S., Castillo-González, C., Yu, B., and Zhang, X. (2017). The functions of plant small RNAs in development and in stress responses. Plant J. **90**: 654–70.

Li, Z., Shi, J., Yu, L., Zhao, X., Ran, L., Hu, D., and Song, B. (2018). N 6 -methyl-adenosine level in Nicotiana tabacum is associated with tobacco mosaic virus. Virol. J. **15**: 1–10.

Liang, Z., Geng, Y., and Gu, X. (2018). Adenine Methylation: New Epigenetic Marker of DNA and mRNA. Mol. Plant **11**: 1219–1221.

Liao, S., Sun, H., and Xu, C. (2018). YTH Domain: A family of N6-methyladenosine (m6A) readers. Genomics Proteomics Bioinforma. **16**: 99–107.

Lichinchi, G., Gao, S., Saletore, Y., Gonzalez, G.M., Bansal, V., Wang, Y., Mason, C.E., and Rana, T.M. (2016a). Dynamics of the human and viral m(6)A RNA methylomes during HIV-1 infection of T cells. Nat. Microbiol. **1**: 16011.

Lichinchi, G., Zhao, B.S., Wu, Y., Lu, Z., Qin, Y., He, C., and Rana, T.M. (2016b). Dynamics of Human and Viral RNA Methylation during Zika Virus Infection. Cell Host Microbe **20**: 666–673.

Lieber, M.R. (2010). The Mechanism of Double-Strand DNA Break Repair by the Nonhomologous DNA End-Joining Pathway. Annu. Rev. Biochem. **79**: 181–211.

Lilly, S.T., Drummond, R.S.M., Pearson, M.N., and MacDiarmid, R.M. (2011). Identification and validation of reference genes for normalization of transcripts from virus-infected Arabidopsis thaliana. Mol. Plant-Microbe Interact. **24**: 294–304.

Lin, S., Choe, J., Du, P., Triboulet, R., and Gregory, R.I. (2016). The m6A Methyltransferase METTL3 Promotes Translation in Human Cancer Cells. Mol. Cell **62**: 335–45.

Linder, B., Grozhik, A. V., Olarerin-George, A.O., Meydan, C., Mason, C.E., and Jaffrey, S.R. (2015). Single-nucleotide-resolution mapping of m6A and m6Am throughout the transcriptome. Nat. Methods **12**: 767–72.

Linder, B. and Jaffrey, S.R. (2019). Discovering and mapping the modified nucleotides that comprise the epitranscriptome of mrna. Cold Spring Harb. Perspect. Biol. **11**: a032201.

Liu, J., Yue, Y., Han, D. et al. (2014). A METTL3-METTL14 complex mediates mammalian nuclear RNA N6-adenosine methylation. Nat. Chem. Biol. **10**: 93–5.

Liu, J., Liu, J., Cui, X. et al. (2018). VIRMA mediates preferential m6A mRNA methylation in 3'UTR and near stop codon and associates with alternative polyadenylation. Cell Discov. **4**: https://doi.org/10.1038/s41421-018-0019-0.

Liu, J., Dou, X., Chen, C., Chen, C., Liu, C., Michelle Xu, M., Zhao, S., Shen, B., Gao, Y., Han, D., and He, C. (2020). N6-methyladenosine of chromosome-associated regulatory RNA regulates chromatin state and transcription. Science. **367**: 580–6.

Liu, N., Dai, Q., Zheng, G., He, C., Parisien, M., and Pan, T. (2015). N6 -methyladenosine-dependent RNA structural switches regulate RNA-protein interactions. Nature **518**: 560–564.

Liu, N., Zhou, K.I., Parisien, M., Dai, Q., Diatchenko, L., and Pan, T. (2017). N6-methyladenosine alters RNA structure to regulate binding of a low-complexity protein. Nucleic Acids Res. **45**: 6051–6063.

Liu, Y., You, Y., Lu, Z., Yang, J., Li, P., Liu, L., Xu, H., Niu, Y., and Cao, X. (2019). N 6 -methyladenosine RNA modification–mediated cellular metabolism rewiring inhibits viral replication. Science. **365**: 1171.

Lloyd, R.E. (2013). Regulation of stress granules and P-bodies during RNA virus infection. Wiley Interdiscip. Rev. RNA **4**: 317–331.

Lu, W., Tirumuru, N., Gelais, C.S., Koneru, P.C., Liu, C., Kvaratskhelia, M., He, C., and Wu, L.

(2018). N 6 -Methyladenosine– binding proteins suppress HIV-1 infectivity and viral production. J. Biol. Chem. **293**: 12992–13005.

Luo, G.Z., Macqueen, A., Zheng, G., Duan, H., Dore, L.C., Lu, Z., Liu, J., Chen, K., Jia, G., Bergelson, J., and He, C. (2014). Unique features of the m6A methylome in Arabidopsis thaliana. Nat. Commun. **28**: 5630.

Luo, J.H., Wang, Y., Wang, M., Zhang, L.Y., Peng, H.R., Zhou, Y.Y., Jia, G.F., and He, Y. (2020). Natural Variation in RNA m6A Methylation and Its Relationship with Translational Status. Plant Physiol. **182**: 332–44.

Luo, Y., Na, Z., and Slavoff, S.A. (2018). P-Bodies: Composition, Properties, and Functions. Biochemistry **57**: 2424–31.

Ma, S., Chen, C., Ji, X., Liu, J., Zhou, Q., Wang, G., Yuan, W., Kan, Q., and Sun, Z. (2019). The interplay between m6A RNA methylation and noncoding RNA in cancer. J. Hematol. Oncol. **12**: 121.

Ma, X., Nicole, M.C., Meteignier, L.V., Hong, N., Wang, G., and Moffett, P. (2015). Different roles for RNA silencing and RNA processing components in virus recovery and virus-induced gene silencing in plants. J. Exp. Bot. **66**: 919–32.

Mäkinen, K., Lõhmus, A., and Pollari, M. (2017). Plant RNA regulatory network and RNA granules in virus infection. Front. Plant Sci. **8**: 2093.

Marsh, L.E., Pogue, G.P., and Hall, T.C. (1989). Similarities among plant virus (+) and (-) RNA termini imply a common ancestry with promoters of eukaryotic tRNAs. Virology **172**: 415–27.

Martelli, G.P., Adams, M.J., Kreuze, J.F., and Dolja, V. V. (2007). Family Flexiviridae : A Case Study in Virion and Genome Plasticity. Annu. Rev. Phytopathol. **45**: 73–100.

Martin, M. (2011). Cutadapt removes adapter sequences from high-throughput sequencing reads. EMBnet.journal **24**: 1138–43.

Martinez-Gil, L., Sanchez-Navarro, J.A., Cruz, A., Pallas, V., Perez-Gil, J., and Mingarro, I. (2009). Plant Virus Cell-to-Cell Movement Is Not Dependent on the Transmembrane Disposition of Its Movement Protein. J. Virol. **83**: 5535–43.

Martínez-Pérez, M., Aparicio, F., López-Gresa, M.P., Bellés, J.M., Sánchez-Navarro, J.A., and Pallás, V. (2017). *Arabidopsis* m ^{6} A demethylase activity modulates viral infection of a plant virus and the m ^{6} A abundance in its genomic RNAs. Proc. Natl. Acad. Sci. **114**: 10755–10760.

Martínez de Alba, A.E., Moreno, A.B., Gabriel, M., Mallory, A.C., Christ, A., Bounon, R., Balzergue, S., Aubourg, S., Gautheret, D., Crespi, M.D., Vaucheret, H., and Maizel, A. (2015). In plants, decapping prevents RDR6-dependent production of small interfering RNAs from endogenous mRNAs. Nucleic Acids Res. **43**: 2902–2913.

Más, P. and Pallás, V. (1995). Non-isotopic tissue-printing hybridization: a new technique to study long-distance plant virus movement. J. Virol. Methods **52**: 317–26.

Matzke, M.A. and Mosher, R.A. (2014). RNA-directed DNA methylation: An epigenetic pathway of increasing complexity. Nat. Rev. Genet. **15**: 394–408.

Mauer, J., Luo X., Blanjoie A. et al. (2017). Reversible methylation of m 6 A m in the 5′ cap controls mRNA stability. Nature **541**: 371–375.

Mauer, J., Sindelar, M., Despic, V., Guez, T., Hawley, B.R., Vasseur, J.J., Rentmeister, A., Gross, S.S., Pellizzoni, L., Debart, F., Goodarzi, H., and Jaffrey, S.R. (2019). FTO controls reversible m 6 Am RNA methylation during snRNA biogenesis. Nat. Chem. Biol. **15**: 340–347.

McIntyre, W., Netzband, R., Bonenfant, G., Biegel, J.M., Miller, C., Fuchs, G., Henderson, E., Arra, M., Canki, M., Fabris, D., and Pager, C.T. (2018). Positive-sense RNA viruses reveal the complexity and dynamics of the cellular and viral epitranscriptomes during infection. Nucleic Acids Res. **46**: 5776–91.

Merai, Z., Benkovics, A.H., Nyiko, T., Debreczeny, M., Hiripi, L., Kerenyi, Z., Kondorosi, E., and Silhavy, D. (2013). The late steps of plant nonsense-mediated mRNA decay. Plant J. **73**: 50–

62.

Meyer, K., Köster, T., Nolte, C., Weinholdt, C., Lewinski, M., Grosse, I., and Staiger, D. (2017). Adaptation of iCLIP to plants determines the binding landscape of the clock-regulated RNA-binding protein AtGRP7. Genome Biol. **18**: 1–22.

Meyer, K.D. and Jaffrey, S.R. (2017). Rethinking m 6 A Readers, Writers, and Erasers . Annu. Rev. Cell Dev. Biol. **33**: 319–342.

Meyer, K.D., Patil, D.P., Zhou, J., Zinoviev, A., Skabkin, M.A., Elemento, O., Pestova, T. V., Qian, S.B., and Jaffrey, S.R. (2015). 5′ UTR m6A Promotes Cap-Independent Translation. Cell **163**: 999–1010.

Meyer, K.D., Saletore, Y., Zumbo, P., Elemento, O., Mason, C.E., and Jaffrey, S.R. (2012). Comprehensive analysis of mRNA methylation reveals enrichment in 3′ UTRs and near stop codons. Cell **149**: 1635–46.

Miao, Z., Zhang, T., Qi, Y., Song, J., Han, Z., and Ma, C. (2020). Evolution of the RNA N6-Methyladenosine Methylome Mediated by Genomic Duplication. Plant Physiol.: DOI: https://doi.org/10.1104/pp.19.00323.

Mielecki, D., Zugaj, D., Muszewska, A., Piwowarski, J., Chojnacka, A., Mielecki, M., Nieminuszczy, J., Grynberg, M., and Grzesiuk, E. (2012). Novel AlkB dioxygenases-alternative models for in silico and in vivo studies. PLoS One **7**: e30588.

Moore, C. and Meng, B. (2019). Prediction of the molecular boundary and functionality of novel viral AlkB domains using homology modelling and principal component analysis. J. Gen. Virol. **100**: 691–703.

Moreno, A. and Fereres, A. (2012). Virus Diseases in Lettuce in the Mediterranean Basin. Adv. Virus Res. **84**: 247–88.

Moss, B., Gershowitz, A., Stringer, J.R., Holland, L.E., and Wagner, E.K. (1977). 5′-Terminal and internal methylated nucleosides in herpes simplex virus type 1 mRNA. J. Virol. **23**: 234–9.

Murik, O., Chandran, S.A., Nevo-Dinur, K., Sultan, L.D., Best, C., Stein, Y., Hazan, C., and Ostersetzer-Biran, O. (2019). Topologies of N6-adenosine methylation (m6A) in land plant mitochondria and their putative effects on organellar gene expression. Plant J. **101**: 1269–86.

Narayan, P., Ayers, D.F., Rottman, F.M., Maroney, P.A., and Nilsen, T.W. (1987). Unequal distribution of N6-methyladenosine in influenza virus mRNAs. Mol. Cell. Biol. **7**: 1572–5.

Navarro, J.A., Sanchez-Navarro, J.A., and Pallas, V. (2019). Key checkpoints in the movement of plant viruses through the host. Adv. Virus Res. **104**: 1–64.

Nechushtai, R., Conlan, A.R., Harir, Y. et al. (2012). Characterization of Arabidopsis NEET reveals an ancient role for NEET proteins in iron metabolism. Plant Cell **24**: 2139–54.

Neeleman, L., Olsthoorn, R.C.L., Linthorst, H.J.M., and Bol, J.F. (2002). Translation of a nonpolyadenylated viral RNA is enhanced by binding of viral coat protein or polyadenylation of the RNA. Proc. Natl. Acad. Sci. **98**: 14286–14291.

Nei, M. and Saitou, N. (1987). The neighbor-joining method: a new method for reconstructing phylogenetic trees. Mol. Biol. Evol. **4**: 406–25.

Németh, K., Salcher,t K., Putnoky, P. et al. (1998). Pleiotropic control of glucose and hormone responses by PRL1, a nuclear WD protein, in Arabidopsis. Genes Dev.

Nichols, J.L. and Welder, L. (1981). Nucleotides adjacent to N6-methyladenosine in maize poly(A)-containing RNA. Plant Sci. Lett. **21**: 75–81.

Niehl, A. and Heinlein, M. (2019). Perception of double-stranded RNA in plant antiviral immunity. Molecular plant pathology, **20**, 1203–1210.

Ok, S.H., Jeong, H.J., Bae, J.M., Shin, J.S., Luan, S., and Kim, K.N. (2005). Novel CIPK1-associated proteins in Arabidopsis contain an evolutionarily conserved C-terminal region that mediates nuclear localization. Plant Physiol. **139**: 138–50.

Olsthoorn, R.C.L. and Bol, J.F. (2002). Role of an Essential Triloop Hairpin and Flanking Structures in the 3′ Untranslated Region of Alfalfa Mosaic Virus RNA in In Vitro Transcription. J. Virol.

76: 8747–56.

Olsthoorn, R.C.L., Mertens, S., Brederode, F.T., and Bol, J.F. (1999). A conformational switch at the 3' end of a plant virus RNA regulates viral replication. EMBO J. **18**: 4856–4864.

Pallás, V. (2007). En el límite de la vida. Un siglo de virus. La Voz de Galicia.

Pallas, V., Aparicio, F., Herranz, M.C., Sanchez-Navarro, J.A., and Scott, S.W. (2013). The Molecular Biology of Ilarviruses. Adv. Virus Res. **87**: 139–81.

Pallas, V. and García, J.A. (2011). How do plant viruses induce disease? Interactions and interference with host components. J. Gen. Virol. **92**: 2691–705.

Pallás, V., Más, P., and Sánchez-Navarro, J.A. (1998). Detection of Plant RNA Viruses by Nonisotopic Dot-Blot Hybridization. Methods Mol Biol **81**: 461–8.

Panas, M.D., Varjak, M., Lulla, A., Eng, K.E., Merits, A., Hedestam, G.B.K., and McInerney, G.M. (2012). Sequestration of G3BP coupled with efficient translation inhibits stress granules in Semliki Forest virus infection. Mol. Biol. Cell **23**: 4701–12.

Park, O.H., Ha, H., Lee, Y., Boo, S.H., Kwon, D.H., Song, H.K., and Kim, Y.K. (2019). Endoribonucleolytic Cleavage of m6A-Containing RNAs by RNase P/MRP Complex. Mol. Cell **74**: 494–507.

Parker, M.T., Knop, K., Sherwood, A. V., Schurch, N.J., Mackinnon, K., Gould, P.D., Hall, A.J., Barton, G.J., and Simpson, G.G. (2020). Nanopore direct RNA sequencing maps the complexity of Arabidopsis mRNA processing and m6A modification. Elife **9**: e49658.

Patil, D.P., Chen, C.K., Pickering, B.F., Chow, A., Jackson, C., Guttman, M., and Jaffrey, S.R. (2016). M6 A RNA methylation promotes XIST-mediated transcriptional repression. Nature **537**: 369–373.

Patil, D.P., Pickering, B.F., and Jaffrey, S.R. (2018). Reading m6A in the Transcriptome: m6A-Binding Proteins. Trends Cell Biol. **28**: 113–127.

Peiro, A., Izquierdo-Garcia, A.C., Sanchez-Navarro, J.A., Pallas, V., Mulet, J.M., and Aparicio, F. (2014). Patellins 3 and 6, two members of the Plant Patellin family, interact with the movement protein of Alfalfa mosaic virus and interfere with viral movement. Mol. Plant Pathol. **15**: 881–91.

Pendleton, K.E., Chen, B., Liu, K., Hunter, O. V., Xie, Y., Tu, B.P., and Conrad, N.K. (2017). The U6 snRNA m6A Methyltransferase METTL16 Regulates SAM Synthetase Intron Retention. Cell **169**: 824–835.

Pereira-Montecinos, C., Valiente-Echeverría, F., and Soto-Rifo, R. (2017). Epitranscriptomic regulation of viral replication. Biochim. Biophys. Acta - Gene Regul. Mech. **1860**: 460–471.

Perry, R.P. and Kelley, D.E. (1974). Existence of methylated messenger RNA in mouse L cells. Cell **1**: 37–42.

Ping, X.L., Sun, B., Wang, L. et al. (2014). Mammalian WTAP is a regulatory subunit of the RNA N6-methyladenosine methyltransferase. Cell Res. **24**: 177–89.

Pontier, D., Picart, C., El Baidouri, M. et al. (2019). The m6A pathway protects the transcriptome integrity by restricting RNA chimera formation in plants. Life Sci. Alliance **2**: e201900393.

Postnikova, O.A. and Nemchinov, L.G. (2012). Comparative analysis of microarray data in Arabidopsis transcriptome during compatible interactions with plant viruses. Virol. J. **29**: 101.

Price, A.M., Hayer, K.E., McIntyre, A.B.R., Gokhale, N.S., Fera, A.N. Della, Mason, C.E., Horner, S.M., Wilson, A.C., Depledge, D.P., and Weitzman, M.D. (2019). Direct RNA sequencing reveals m6A modifications on adenovirus RNA are necessary for efficient splicing. bioRxiv: doi: https://doi.org/10.1101/865485.

Pumplin, N. and Voinnet, O. (2013). RNA silencing suppression by plant pathogens: Defence, counter-defence and counter-counter-defence. Nat. Rev. Microbiol. **11**: 745–60.

Purushothaman, P., Uppal, T., and Verma, S.C. (2015). Molecular biology of KSHV lytic reactivation. Viruses **7**: 116–53.

Raja, P., Jackel, J.N., Li, S., Heard, I.M., and Bisaro, D.M. (2014). Arabidopsis Double-Stranded

RNA Binding Protein DRB3 Participates in Methylation-Mediated Defense against Geminiviruses. J. Virol. **88**: 2611–22.

Raja, P., Sanville, B.C., Buchmann, R.C., and Bisaro, D.M. (2008). Viral Genome Methylation as an Epigenetic Defense against Geminiviruses. J. Virol. **82**: 8997–9007.

Rampey, R.A., Woodward, A.W., Hobbs, B.N., Tierney, M.P., Lahner, B., Salt, D.E., and Bartel, B. (2006). An arabidopsis basic helix-loop-helix leucine zipper protein modulates metal homeostasis and auxin conjugate responsiveness. Genetics **174**: 1841–57.

Reagan, B.C. and Burch-Smith, T.M. (2020). Viruses reveal the secrets of plasmodesmal cell biology. Mol. Plant-Microbe Interact. **33**: 26–39.

Reichel, M., Liao, Y., Rettel, M., Ragan, C., Evers, M., Alleaume, A.M., Horos, R., Hentze, M.W., Preiss, T., and Millar, A.A. (2016). In planta determination of the mRNA-binding proteome of arabidopsis etiolated seedlings. Plant Cell **28**: 2435–52.

Revers, F. and Nicaise, V. (2014). Plant Resistance to Infection by Viruses. eLS: doi:10.1002/9780470015902.a0000757.pub2.

Ries, R.J., Zaccara, S., Klein, P., Olarerin-George, A., Namkoong, S., Pickering, B.F., Patil, D.P., Kwak, H., Lee, J.H., and Jaffrey, S.R. (2019). m6A enhances the phase separation potential of mRNA. Nature **571**: 424–8.

Robinson, M.D. and Oshlack, A. (2010). A scaling normalization method for differential expression analysis of RNA-seq data. Genome Biol. **11**: R25.

Rodrigo, G., Carrera, J., Ruiz-Ferrer, V., del Toro, F.J., Llave, C., Voinnet, O., and Elena, S.F. (2012). A meta-analysis reveals the commonalities and differences in arabidopsis thaliana response to different viral pathogens. PLoS One **7**: e40526.

Roost, C., Lynch, S.R., Batista, P.J., Qu, K., Chang, H.Y., and Kool, E.T. (2015). Structure and thermodynamics of N6-methyladenosine in RNA: A spring-loaded base modification. J. Am. Chem. Soc. **137**: 2107–15.

Rosa-Mercado, N.A., Withers, J.B., and Steitz, J.A. (2017). Settling the m6A debate: Methylation of mature mRNA is not dynamic but accelerates turnover. Genes Dev. **31**: 957–8.

Roundtree, I.A., Luo, G.-Z., Zhang, Z. et al. (2017). YTHDC1 mediates nuclear export of N6-methyladenosine methylated mRNAs. Elife **6**: 1–28.

Rubio, R.M., Depledge, D.P., Bianco, C., Thompson, L., and Mohr, I. (2018). RNA m6A modification enzymes shape innate responses to DNA by regulating interferon β. Genes Dev. **32**: 1472–1484.

Růžička, K., Zhang, M., Campilho, A. et al. (2017). Identification of factors required for m6A mRNA methylation in Arabidopsis reveals a role for the conserved E3 ubiquitin ligase HAKAI. New Phytol. **215**: 157–172.

Ryabov, E. V., Roberts, I.M., Palukaitis, P., and Taliansky, M. (1999). Host-specific cell-to-cell and long-distance movements of cucumber mosaic virus are facilitated by the movement protein of groundnut rosette virus. Virology **260**: 98–108.

Sambrook, J., Maniatis, T., and Fritsch, E.F. (1988). Molecular Cloning : a laboratory manual. 2nd edition. Cold Spring Harb. ,New York.

Samira, R., Li, B., Kliebenstein, D., Li, C., Davis, E., Gillikin, J.W., and Long, T.A. (2018). The bHLH transcription factor ILR3 modulates multiple stress responses in Arabidopsis. Plant Mol. Biol. **97**: 297–309.

Samson, L. and Cairns, J. (1977). A new pathway for DNA repair in Escherichia coli. Nature **267**: 281–3.

Sánchez-Navarro, J.A. and Bol, J.F. (2001). Role of the Alfalfa mosaic virus movement protein and coat protein in virus transport. Mol. Plant-Microbe Interact. **14**: 1051–62.

Sánchez-Navarro, J.A., Herranz, M.C., Pallás, V. (2006) Cell-to-cell movement of Alfalfa mosaic virus can be mediated by the movement proteins of Ilar-, bromo-, cucumo-, tobamo- and comoviruses and does not require virion formation. Virology **346**: 66-73.

Sánchez-Navarro, J.A., Reusken, C.B.E.M., Bol, J.F., and Pallás, V. (1997). Replication of alfalfa

mosaic virus RNA 3 with movement and coat protein genes replaced by corresponding genes of Prunus necrotic ringspot ilarvirus. J. Gen. Virol. **78**: 3171–6.

Schwartz, S., Agarwala, S.D., Mumbach, M.R. et al. (2013). High-Resolution mapping reveals a conserved, widespread, dynamic mRNA methylation program in yeast meiosis. Cell **155**: 1409–21.

Schwartz, S., Mumbach, M.R., Jovanovic, M. et al. (2014). Perturbation of m6A writers reveals two distinct classes of mRNA methylation at internal and 5′ sites. Cell Rep. **8**: 284–96.

Schweingruber, C., Rufener, S.C., Zünd, D., Yamashita, A., and Mühlemann, O. (2013). Nonsense-mediated mRNA decay - Mechanisms of substrate mRNA recognition and degradation in mammalian cells. Biochim. Biophys. Acta - Gene Regul. Mech. **1829**: 612–23.

Scutenaire, J., Deragon, J.-M., Jean, V., Benhamed, M., Raynaud, C., Favory, J.-J., Merret, R., and Bousquet-Antonelli, C. (2018). The YTH Domain Protein ECT2 Is an m 6 A Reader Required for Normal Trichome Branching in Arabidopsis . Plant Cell **30**: 986–1005.

Seo, J.K. and Kim, K.H. (2016). Long-distance movement of viruses in plants. Curr. Res. Top. Plant Virol. **1**: 314–7.

Sepúlveda R, P., Larraín S, P., Quiroz E, C., Rebufel A, P., and Graña S, F. (2005). Identificación e Incidencia de Virus en Pimiento en la Zona Centro Norte de Chile y su Asociación con Vectores. Agric. Técnica **65**: 235–45.

Shaw, A.E., Hughes, J., Gu, Q., Behdenna, A., Singer, J.B., Dennis, T., Orton, R.J., Varela, M., Gifford, R.J., Wilson, S.J., and Palmarini, M. (2017). Fundamental properties of the mammalian innate immune system revealed by multispecies comparison of type I interferon responses. PLoS Biol. **15**: e2004086.

Shen, L., Liang, Z., Gu, X., Chen, Y., Teo, Z.W.N., Hou, X., Cai, W.M., Dedon, P.C., Liu, L., and Yu, H. (2016). N 6 -Methyladenosine RNA Modification Regulates Shoot Stem Cell Fate in Arabidopsis. Dev. Cell **38**: 186–200.

Sheth, U. and Parker, R. (2006). Targeting of Aberrant mRNAs to Cytoplasmic Processing Bodies. Cell **125**: 1095–109.

Shi, H., Wang, X., Lu, Z., Zhao, B.S., Ma, H., Hsu, P.J., Liu, C., and He, C. (2017). YTHDF3 facilitates translation and decay of N 6-methyladenosine-modified RNA. Cell Res. **27**: 315–328.

Shi, H., Wei, J., and He, C. (2019). Where, When, and How: Context-Dependent Functions of RNA Methylation Writers, Readers, and Erasers. Mol. Cell **74**: 640–50.

Sievers, F., Wilm, A., Dineen, D., Gibson, T.J., Karplus, K., Li, W., Lopez, R., McWilliam, H., Remmert, M., Söding, J., Thompson, J.D., and Higgins, D.G. (2011). Fast, scalable generation of high-quality protein multiple sequence alignments using Clustal Omega. Mol. Syst. Biol. **7**: 539.

Sommer, S., Lavi, U., and Darnell, J.E. (1978). The absolute frequency of labeled N-6-methyladenosine in HeLa cell messenger RNA decreases with label time. J. Mol. Biol. **124**: 487–99.

Spoel, S.H. and Dong, X. (2012). How do plants achieve immunity? Defence without specialized immune cells. Nat. Rev. Immunol. **12**: 89–100.

Stoltzfus, C.M. and Dane, R.W. (1982). Accumulation of Spliced Avian Retrovirus mRNA Is Inhibited in S-Adenosylmethionine-Depleted Chicken Embryo Fibroblasts. J. Virol. **42**: 918–31.

Stoltzfus, C.M. and Dimock, K. (1976). Evidence of methylation of B77 avian sarcoma virus genome RNA subunits. J. Virol. **18**: 586–95.

Su, L.W., Chang, S.H., Li, M.Y., Huang, H.Y., Jane, W.N., and Yang, J.Y. (2013). Purification and biochemical characterization of Arabidopsis At-NEET, an ancient iron-sulfur protein, reveals a conserved cleavage motif for subcellular localization. Plant Sci. **213**: 46–54.

Sun, T., Wu, R., and Ming, L. (2019). The role of m6A RNA methylation in cancer. Biomed. Pharmacother. **112**: 108613.

Tamura, K., Stecher, G., Peterson, D., Filipski, A., and Kumar, S. (2013). MEGA6: Molecular evolutionary genetics analysis version 6.0. Mol. Biol. Evol. **30**: 2725–9.

Tan, B., Liu, H., Zhang, S., Da Silva, S.R., Zhang, L., Meng, J., Cui, X., Yuan, H., Sorel, O., Zhang, S.W., Huang, Y., and Gao, S.J. (2017). Viral and cellular N 6 -methyladenosine and N 6 ,2′-O-dimethyladenosine epitranscriptomes in the KSHV life cycle. Nat. Microbiol. **3**: 108–20.

Tankmar, M.D. (2019). Functional Analysis of Arabidopsis m6A Readers. Faculty of Science. Masther Thesis. University of Copenhagen (Denmark).

Tenllado, F. and Bol, J.F. (2000). Genetic dissection of the multiple functions of alfalfa mosaic virus coat protein in viral RNA replication, encapsidation, and movement. Virology **268**: 29–40.

Theler, D., Dominguez, C., Blatter, M., Boudet, J., and Allain, F.H.T. (2014). Solution structure of the YTH domain in complex with N6-methyladenosine RNA: A reader of methylated RNA. Nucleic Acids Res. **42**: 13911–13919.

Thomas, P.E., Wu, X., Liu, M., Gaffney, B., Ji, G., Li, Q.Q., and Hunt, A.G. (2012). Genome-wide control of polyadenylation site choice by CPSF30 in arabidopsis. Plant Cell **24**: 4376–88.

Thomason, A.R., Brian, D.A., Velicer, L.F., and Rottman, F.M. (1976). Methylation of high-molecular-weight subunit RNA of feline leukemia virus. J. Virol. **20**: 123–32.

Tirumuru, N. and Wu, L. (2019). HIV-1 envelope proteins up-regulate N 6 -methyladenosine levels of cellular RNA independently of viral replication. J. Biol. Chem. **294**: 3249–60.

Tirumuru, N., Zhao, B.S., Lu, W., Lu, Z., He, C., and Wu, L. (2016). N6-methyladenosine of HIV-1 RNA regulates viral infection and HIV-1 Gag protein expression. Elife **5**: e15528.

Tsai, K., Courtney, D.G., and Cullen, B.R. (2018). Addition of m6A to SV40 late mRNAs enhances viral structural gene expression and replication. PLoS Pathog. **14**: 1–23.

Tsutsui, H. and Higashiyama, T. (2017). PKAMA-ITACHI vectors for highly efficient CRISPR/Cas9-mediated gene knockout in Arabidopsis thaliana. Plant Cell Physiol. **58**: 46–56.

Tsuzuki, M., Motomura, K., Kumakura, N., and Takeda, A. (2017). Interconnections between mRNA degradation and RDR-dependent siRNA production in mRNA turnover in plants. J. Plant Res. **130**: 211–26.

Tutucci, E., Vera, M., Biswas, J., Garcia, J., Parker, R., and Singer, R.H. (2018). An improved MS2 system for accurate reporting of the mRNA life cycle. Nat. Methods **15**: 81–9.

Uppal, T., Sarkar, R., Dhelaria, R., and Verma, S.C. (2018). Role of pattern recognition receptors in KSHV infection. Cancers (Basel). **10**: 85.

Valkonen, J.P.T., Pehu, E., and Watanabe, K. (1992). Symptom expression and seed transmission of alfalfa mosaic virus and potato yellowing virus (SB-22) in Solanum brevidens and S. etuberosum. Potato Res. **35**: 403–10.

Van den Born, E., Bekkelund, A., Moen, M.N., Omelchenko, M. V., Klungland, A., and Falnes, P. (2009). Bioinformatics and functional analysis define four distinct groups of AlkB DNA-dioxygenases in bacteria. Nucleic Acids Res. **37**: 7124–36.

Van den Born, E., Omelchenko, M. V., Bekkelund, A., Leihne, V., Koonin, E. V., Dolja, V. V., and Falnes, P.O. (2008). Viral AlkB proteins repair RNA damage by oxidative demethylation. Nucleic Acids Res. **36**: 5451–5461.

Van Der Heijden, M.W., Carette, J.E., Reinhoud, P.J., Haegi, A., and Bol, J.F. (2001). Alfalfa Mosaic Virus Replicase Proteins P1 and P2 Interact and Colocalize at the Vacuolar Membrane. J. Virol. **75**: 1879–87.

Van Der Vossen, E.A. g., Neeleman, L., and Bol, J.F. (1993). Role of the 5′ leader sequence of alfalfa mosaic virus RNA 3 in replication and translation of the viral RNA. Nucleic Acids Res. **21**: 1361–7.

Van Der Vossen, E.A.G. and Bol, J.F. (1996). Analysis of Cis-acting elements in the 5′ leader sequence of alfalfa mosaic virus RNA 3. Virology **220**: 539–43.

Van Der Vossen, E.A.G., Neeleman, L., and Bol, J.F. (1994). Early and late functions of alfalfa mosaic virus coat protein can be mutated separately. Virology **202**: 891–903.

Van Der Wel, N.N., Goldbach, R.W., and M. Van Lent, J.W. (1998). The movement protein and coat protein of alfalfa mosaic virus accumulate in structurally modified plasmodesmata. Virology **244**: 322–29.

Van Pelt-Heerschap, H., Verbeek, H., Willem Slot, J., and Van Vloten-Doting, L. (1987). The location of coat protein and viral RNAs of alfalfa mosaic virus in infected tobacco leaves and protoplasts. Virology **160**: 297–300.

Van Tran, N., Ernst, F., Hawley, B. R., Zorbas, C., Ulryck, N., Hackert, P., Bohnsack, K. E., Bohnsack, M. T., Jaffrey, S. R., Graille, M., & Lafontaine, D. (2019). The human 18S rRNA m6A methyltransferase METTL5 is stabilized by TRMT112. Nucleic Acids Res. **47**: 7719–33.

Vespa, L., Vachon, G., Berger, F., Perazza, D., Faure, J.D., and Herzog, M. (2004). The immunophilin-interacting protein AtFIP37 from arabidopsis is essential for plant development and is involved in trichome endoreduplication. Plant Physiol. **134**: 1283–92.

Voinnet, O. (2005). Induction and suppression of RNA silencing: Insights from viral infections. Nat. Rev. Genet. **6**: 206–20.

Voinnet, O. (2001). RNA silencing as a plant immune system against viruses. Trends Genet. **17**: 449–59.

Wan, Y., Tang, K., Zhang, D., Xie, S., Zhu, X., Wang, Z., and Lang, Z. (2015). Transcriptome-wide high-throughput deep m6A-seq reveals unique differential m6A methylation patterns between three organs in Arabidopsis thaliana. Genome Biol. **16**: 272.

Wang, C., Wang, C., Zou, J., Yang, Y., Li, Z., and Zhu, S. (2019a). Epigenetics in the plant–virus interaction. Plant Cell Rep. **38**: 1031–1038.

Wang, H., Buckley, K.J., Yang, X., Buchmann, R.C., and Bisaro, D.M. (2005). Adenosine Kinase Inhibition and Suppression of RNA Silencing by Geminivirus AL2 and L2 Proteins. J. Virol. **79**: 7410–8.

Wang, L., Wen, M., and Cao, X. (2019b). Nuclear hnRNPA2B1 initiates and amplifies the innate immune response to DNA viruses. Science. **365**: eaav0758.

Wang, X., Lu, Z., Gomez, A. et al. (2014). N 6-methyladenosine-dependent regulation of messenger RNA stability. Nature **505**: 117–120.

Wang, X., Zhao, B.S., Roundtree, I.A., Lu, Z., Han, D., Ma, H., Weng, X., Chen, K., Shi, H., and He, C. (2015). N6-methyladenosine modulates messenger RNA translation efficiency. Cell **161**: 1388–1399.

Wang, Y., Wu, Y., Gong, Q. et al. (2019c). Geminiviral V2 Protein Suppresses Transcriptional Gene Silencing through Interaction with AGO4. J. Virol. **93**: e01675-18.

Wang, Z., Tang, K., Zhang, D., Wan, Y., Wen, Y., Lu, Q., and Wang, L. (2017). High-throughput m6A-seq reveals RNA m6A methylation patterns in the chloroplast and mitochondria transcriptomes of Arabidopsis thaliana. PLoS One **12**: e0185612.

Warda, A.S., Kretschmer, J., Hackert, P., Lenz, C., Urlaub, H., Höbartner, C., Sloan, K.E., and Bohnsack, M.T. (2017). Human METTL16 is a N 6 -methyladenosine (m 6 A) methyltransferase that targets pre-mRNAs and various non-coding RNAs. EMBO Rep. **18**: 2004–14.

Wei, J., Liu, F., Lu, Z. et al. (2018a). Differential m 6 A, m 6 A m , and m 1 A Demethylation Mediated by FTO in the Cell Nucleus and Cytoplasm. Mol. Cell **71**: 973–85.

Wei, L.-H., Song, P., Wang, Y., Lu, Z., Tang, Q., Yu, Q., Xiao, Y., Zhang, X., Duan, H.-C., and Jia, G. (2018b). The m 6 A Reader ECT2 Controls Trichome Morphology by Affecting mRNA Stability in Arabidopsis. Plant Cell **30**: 968–85.

Weimer, J.L. (1931). Alfalfa mosaic. Phytopathology **21**: 122–3.

White, J.P., Cardenas, A.M., Marissen, W.E., and Lloyd, R.E. (2007). Inhibition of Cytoplasmic mRNA Stress Granule Formation by a Viral Proteinase. Cell Host Microbe **2**: 295–305.

Wilkinson, F.L., Holaska, J.M., Zhang, Z., Sharma, A., Manilal, S., Holt, I., Stamm, S., Wilson, K.L., and Morris, G.E. (2003). Emerin interacts in vitro with the splicing-associated factor, YT521-B. Eur. J. Biochem. **270**: 2459–66.

Willemsen, J., Wicht, O., Wolanski, J.C. et al. (2017). Phosphorylation-Dependent Feedback Inhibition of RIG-I by DAPK1 Identified by Kinome-wide siRNA Screening. Mol. Cell **65**: 403–15.

Williams, G.D., Gokhale, N.S., and Horner, S.M. (2019). Regulation of Viral Infection by the RNA Modification N6 -Methyladenosine. Annu. Rev. Virol. **6**: 235–53.

Winkler, R., Gillis, E., Lasman, L. et al. (2019). m 6 A modification controls the innate immune response to infection by targeting type I interferons. Nat. Immunol. **20**: 173–182.

Wojtas, M.N., Pandey, R.R., Mendel, M., Homolka, D., Sachidanandam, R., and Pillai, R.S. (2017). Regulation of m6A Transcripts by the 3'→5' RNA Helicase YTHDC2 Is Essential for a Successful Meiotic Program in the Mammalian Germline. Mol. Cell **68**: 374–87.

Wu, B., Su, S., Patil, D.P., Liu, H., Gan, J., Jaffrey, S.R., and Ma, J. (2018). Molecular basis for the specific and multivariant recognitions of RNA substrates by human hnRNP A2/B1. Nat. Commun. **9**: 420.

Xiang, Y., Laurent, B., Hsu, C.H. et al. (2017). RNA m6 A methylation regulates the ultraviolet-induced DNA damage response. Nature **543**: 573–6.

Xiao, W. , Adhikari, S., Dahal, U. et al. (2016). Nuclear m6A Reader YTHDC1 Regulates mRNA Splicing. Mol. Cell **61**: 507–19.

Xu, C., Liu, K., Ahmed, H., Loppnau, P., Schapira, M., and Min, J. (2015). Structural basis for the discriminative recognition of N6-Methyladenosine RNA by the human YT521-B homology domain family of proteins. J. Biol. Chem. **290**: 24902–24913.

Xu, C., Wang, X., Liu, K., Roundtree, I.A., Tempel, W., Li, Y., Lu, Z., He, C., and Min, J. (2014). Structural basis for selective binding of m6A RNA by the YTHDC1 YTH domain. Nat. Chem. Biol. **10**: 927–929.

Xu, M., Mazur, M.J., Tao, X., and Kormelink, R. (2020). Cellular RNA hubs: Friends and foes of plant viruses. Mol. Plant-Microbe Interact. **33**: 40–54.

Xue, M., Zhao, B.S., Zhang, Z., et al. (2019). Viral N 6-methyladenosine upregulates replication and pathogenesis of human respiratory syncytial virus. Nat. Commun. **10**: 4595.

Yang, Y., Fan, X., Mao, M. et al. (2017). Extensive translation of circular RNAs driven by N 6 -methyladenosine. Cell Res. **27**: 626–41.

Yang, Y., Hsu, P.J., Chen, Y.S., and Yang, Y.G. (2018). Dynamic transcriptomic m6A decoration: Writers, erasers, readers and functions in RNA metabolism. Cell Res. **28**: 616–624.

Ye, F. (2017). RNA N6-Adenosine Methylation (m6A) Steers Epitranscriptomic Control of Herpesvirus Replication. Inflamm. Cell Signal. **4**: e1604.

Ye, F., Chen, E.R., and Nilsen, T.W. (2017). Kaposi's Sarcoma-Associated Herpesvirus Utilizes and Manipulates RNA N 6 -Adenosine Methylation To Promote Lytic Replication. J. Virol. **91**: e00466-17.

Yoo, S.D., Cho, Y.H., and Sheen, J. (2007). Arabidopsis mesophyll protoplasts: A versatile cell system for transient gene expression analysis. Nat. Protoc. **2**: 1565–72.

Zaccara, S. and Jaffrey, S.R. (2020). A Unified Model for the Function of YTHDF Proteins in Regulating m6A-Modified mRNA. Cell **181**: 1582–95.

Zaccara, S., Ries, R.J., and Jaffrey, S.R. (2019). Reading, writing and erasing mRNA methylation. Nat. Rev. Mol. Cell Biol. **20**: 608–24.

Zhang, F., Zhang, Y.C., Liao, J.Y., Yu, Y., Zhou, Y.F., Feng, Y.Z., Yang, Y.W., Lei, M.Q., Bai, M., Wu, H., and Chen, Y.Q. (2019a). The subunit of RNA n6-methyladenosine methyltransferase OsFIP regulates early degeneration of microspores in rice. PLoS Genet. **15**: e1008120.

Zhang, J., Addepalli, B., Yun, K.Y., Hunt, A.G., Xu, R., Rao, S., Li, Q.Q., and Falcone, D.L. (2008). A polyadenylation factor subunit implicated in regulating oxidative signaling in Arabidopsis thaliana. PLoS One **3**: e2410.

Zhang, Q., Sharma, N.R., Zheng, Z.M., and Chen, M. (2019b). Viral Regulation of RNA Granules in Infected Cells. Virol. Sin. **34**: 175–91.

Zhang, X., Zhang, Y., Dai, K. et al. (2020). N6-Methyladenosine Level in Silkworm Midgut/Ovary Cell Line Is Associated With Bombyx mori Nucleopolyhedrovirus Infection. Front. Microbiol. **10**: 2988.

Zhang, Y., Wang, X., Zhang, X., Wang, J., Ma, Y., Zhang, L., and Cao, X. (2019c). RNA-binding protein YTHDF3 suppresses interferon-dependent antiviral responses by promoting FOXO3 translation. Proc. Natl. Acad. Sci. U. S. A. **116**: 976–81.

Zhang, Z., Chen, H., Huang, X. et al. (2011). BSCTV C2 attenuates the degradation of SAMDC1 to suppress DNA methylation-mediated gene silencing in Arabidopsis. Plant Cell **23**: 273–88.

Zhang, Z., Theler, D., Kaminska, K.H., Hiller, M., De La Grange, P., Pudimat, R., Rafalska, I., Heinrich, B., Bujnick, J.M., Allain, F.H.T., and Stamm, S. (2010). The YTH domain is a novel RNA binding domain. J. Biol. Chem. **285**: 14701–14710.

Zhao, X., Yang, Y., Sun, B. et al. (2014). FTO-dependent demethylation of N6-methyladenosine regulates mRNA splicing and is required for adipogenesis. Cell Res. **24**: 1403–19.

Zheng, G., Dahl, J.A., Niu, Y. et al. (2013). ALKBH5 Is a Mammalian RNA Demethylase that Impacts RNA Metabolism and Mouse Fertility. Mol. Cell **49**: 18–29.

Zheng, H., Wang, G., and Zhang, L. (1997). Alfalfa mosaic virus movement protein induces tubules in plant protoplasts. Mol. Plant-Microbe Interact. **10**: 1010–14.

Zheng, Q., Hou, J., Zhou, Y., Li, Z., and Cao, X. (2017). The RNA helicase DDX46 inhibits innate immunity by entrapping m 6 A-demethylated antiviral transcripts in the nucleus. Nat. Immunol. **18**: 1094–1103.

Zhong, S., Li, H., Bodi, Z., Button, J., Vespa, L., Herzog, M., and Fray, R.G. (2008). MTA Is an Arabidopsis Messenger RNA Adenosine Methylase and Interacts with a Homolog of a Sex-Specific Splicing Factor. Plant Cell Online **20**: 1278–1288.

Zhou, L., Tian, S., and Qin, G. (2019). RNA methylomes reveal the m6A-mediated regulation of DNA demethylase gene SlDML2 in tomato fruit ripening. Genome Biol. **20**: 156.

Zhu, T., Roundtree, I.A., Wang, P., Wang, X., Wang, L., Sun, C., Tian, Y., Li, J., He, C., and Xu, Y. (2014). Crystal structure of the YTH domain of YTHDF2 reveals mechanism for recognition of N6-methyladenosine. Cell Res. **24**: 1493–6.